THE DETERMINATION BY X-RAY DIFFRACTION METHODS OF THE CRYSTAL AND MOLECULAR STRUCTURES OF SOME CO-ORDINATION COMPOUNDS

A study of the stereochemistry of pentaco-ordination

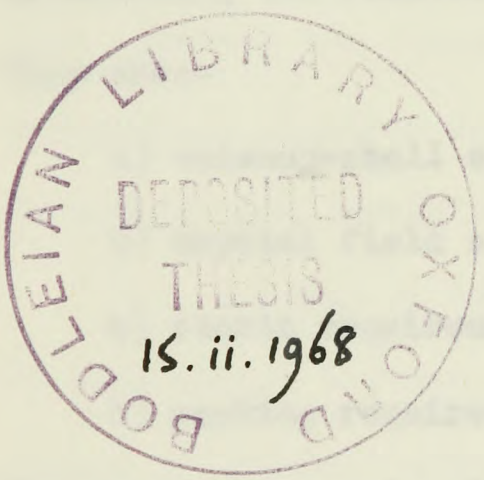

A thesis submitted for the Degree of Doctor of Philosophy in the University of Oxford.

October, 1967

T. L. Blundell
Brasenose College

ABSTRACT

This dissertation is concerned with the stereochemical problem of pentaco-ordination.

The early theoretical work of Pauling, Daudel and Bucher and Linnett gave conflicting predictions about the relative stabilities of the square pyramid and the trigonal bipyramid, and offered no explanation for the many distortions from these idealised geometries observed in pentaco-ordinate complexes. Due to the unsatisfactory description given by these rather simple theories alone, several workers have recently suggested other factors which they consider important in determining the relative stabilities of the possible geometries. They are:-

a) valency-shell electron-pair repulsions

b) crystal field stabilization energy

c) steric requirements of the ligand

d) packing requirements in the crystal

The crystal and molecular structures of four complexes have been analysed by X-ray diffraction techniques in order to gain further information about the relative importances of these factors in determining the stereochemistry of pentaco-ordinate complexes.

The complexes studied have the following molecular formulae:-

a) $(TTAS)Ag\text{-}Co(CO)_4$ [TTAS = methyl-bis (o-dimethyl arsinophenyl) arsine]

b) $[Pd(TPAS)Cl]ClO_4.C_6H_6$ {TPAS = o-phenylene bis-(o-dimethyl arsinophenyl-methyl arsine)}

c) $[Co(QP)Cl]BPh_4$ {QP = tris (o-diphenyl phosphinophenyl) phosphine}

d) $[TlMe_2 1,10\text{phen}]ClO_4$

These complexes have between twenty-four and eighty-five atoms per asymmetric unit. Their X-ray analyses have been confused both by over-determination (of the phases) in b) and d) and by underdetermination in c) . Thus the normal procedures of heavy-atom structure analysis - data processing, the solution of Patterson functions by analytical and superposition methods, Fourier methods and least squares refinement - have involved the study of badly resolved and also in c) pseudo-symmetrical electron density maps, and have been supplemented by the following work involving relatively new techniques.

(i) A study of intensity statistics has been carried out in order to distinguish between any triclinic, monoclinic or orthorhombic space groups of crystals containing several heavy atoms which may be in any combination of special positions. A one-step computer programme has been written to calculate the absolute scale and overall temperature factor, to calculate normalised structure factors and to carry out various probability tests including N(z), N(F) and the calculation of theoretical and observed higher moments. A critical discussion of these methods is given.

(ii) The successful use of the anomalous dispersion technique of Raman and Ramachandran in the X-ray analysis of $[Co(QP)Cl]BPh_4$ is described. A comparison of the phases obtained with those from refinement by Fourier methods is included, and suggestions are made concerning the general use of this technique.

(iii) An attempt to refine phases by the tangent formula in the early stages of the structure analysis of $[Co(QP)Cl]BPh_4$ and the computer programmes written for this purpose are described.

All computer programmes have been written in C-autocode with sections in KDF.9 user code. In each case the overall strategy of the programme is fully discussed, and flow diagrams are given describing the tactics used in detail.

The structure analyses have given final reliability factors of 0.08 to 0.11.

The results of the structure analyses are briefly as follows.

The molecular structure of $(TTAS)Ag\text{-}Co(CO)_4$ shows the cobalt has a distorted trigonal bipyramidal co-ordination, with the silver-cobalt single-bond in the apical position and the equatorial carbonyl groups bent towards the silver atom. An explanation for this stereochemistry in terms of valency-shell electron-pair repulsions is suggested. The stabilization resulting from rehybridisation and consequent decrease of non-bonding electron repulsions, and also the importance of inter-molecular contacts are discussed.

The crystal structure of $[Pd(TPAS)Cl]ClO_4.C_6H_6$ has clathrated benzene molecules with a square pyramidal co-ordination palladium atom. The chlorine occupies a basal plane position, the palladium and four basal atoms are closely coplanar and the apical bond is considerably longer than the basal plane bonds. No oxygen atom from the perchlorate ion is within 3.5Å of the palladium atom, and no hydrogen atom of the ligand occupies the sixth co-ordination position to make the co-ordination octahedral. The preferred stereochemistry is described in terms of crystal field stabilisation.

The distorted trigonal bipyramidal co-ordination of cobalt in $[Co(QP)Cl]BPh_4$ is not due to steric requirements of the ligand. The large distortion from trigonal symmetry giving one equatorial angle of 137.2° is attributed to a Jahn Teller effect.

$[TlMe_2(1,10\text{-phen})]ClO_4$ is not pentaco-ordinate. The thallium has a co-ordination best described as pentagonal bipyramidal with one equatorial position vacant. The perchlorate ions are weakly bidentate giving rise to a polymeric structure in the crystal. The rationale of this structure, attributed to important packing requirements, and also the non-linear thallium dimethyl group are discussed.

To conclude, it appears that in some pentaco-ordinate complexes one of the factors discussed in this thesis may clearly be most important in determining the geometry but the preferred stereochemistry will usually result from a delicate balance of several factors.

ACKNOWLEDGEMENTS

I wish to thank Professor H. M. Powell for his help, advice, and encouragement.

I am grateful to Professor R. Nyholm and Dr. A. T. Phillip of University College, London, to Professor I. R. Beattie of Southampton University and Dr. L. M. Venanzi of the Inorganic Laboratory, Oxford, for their close co-operation in preparing suitable complexes for my study of pentaco-ordination.

For advice and assistance with computing problems, I would particularly like to thank Mr. O. J. R. Hodder, and I am grateful to Dr. J. B. Wilford and Mr. P. Murray Rust for many helpful discussions.

I thank Mrs. J. Bennett and Mr. F. Welch for technical assistance and Miss A. Martin for typing this thesis. Finally, I am very grateful to my wife for help with some of the diagrams and for encouragement at all times.

I acknowledge a Research Studentship from the Science Research Council and a Senior Hulme Scholarship at Brasenose College.

CONTENTS

PART I

THE STEREOCHEMICAL PROBLEM OF PENTACO-ORDINATION

CHAPTER I

Introduction

For many years, pentaco-ordinate complexes were considered unstable because their geometry must lack a centre of symmetry. This identification of a lack of high symmetry with a lack of stability caused chemists and crystallographers alike to overlook many stable pentaco-ordinate complexes. However, recently Nyholm,[1] Gillespie, Venanzi,[2] Powell[3] and others have presented convincing evidence of the stability of these unsymmetrical geometries, and many chemists and crystallographers are now actively involved in investigating pentaco-ordinate stereochemistries.[4]

Of course, the idea that nature is highly symmetrical has long been a dominant influence in the formation of scientific hypotheses. In many cases, this belief has been beneficial to the advancement of scientific knowledge, but in others the desire to find a symmetrical model to explain natural phenomena has retarded progress of science. This side has manifested itself in early objections to the helio-centric cosmology of Aristarchus, in Plato's atomistic theory of the elements, and in religious opposition to Kepler's laws concerning the elliptic orbits of the planets. More recently it held up the development of ideas concerning the secondary structure of poly-peptides, on which crystallographers other than Linus Pauling tried to force a highly symmetrical screw axis. The lack of interest in

pentaco-ordinate stereochemistry for such a time must surely be yet a further manifestation of this desire to find nature symmetrical.

However, like the unsymmetrical α-helix, the pentaco-ordinate stereochemistries have proved to be not only very stable, but also a fascinating and rewarding topic for study. Nevertheless, despite the increased interest in pentaco-ordination, the stereochemical problem has not yet been resolved.

For pentaco-ordination there are two possible idealised geometries. These are the square pyramid and the trigonal bipyramid, and they are represented in Figure 1.1. The square pyramid is drawn on its side in order to emphasise its close resemblance to the trigonal bipyramid. The stereochemical problem is this. First, which of the two idealised geometries will be assumed in co-ordination complexes, and, secondly, if the idealised geometries are not assumed, what will be the nature of the distortions from them? Chemists and crystallographers require general working rules which will enable them to predict the preferred geometry of any pentaco-ordinate complex.

The different attempts to provide a general theoretical model for this co-ordination form an historical introduction to the problem. In 1939, Linus Pauling[5] predicted on the basis of the valence-bond theory that the square pyramidal arrangement would be of "little significance" while Daudel and Bucher[6] a few years later concluded that it would be the most favourable geometry when 'les electrons 'd' de valence sont

Figure 1.1

Possible pentaco-ordinate stereochemistries

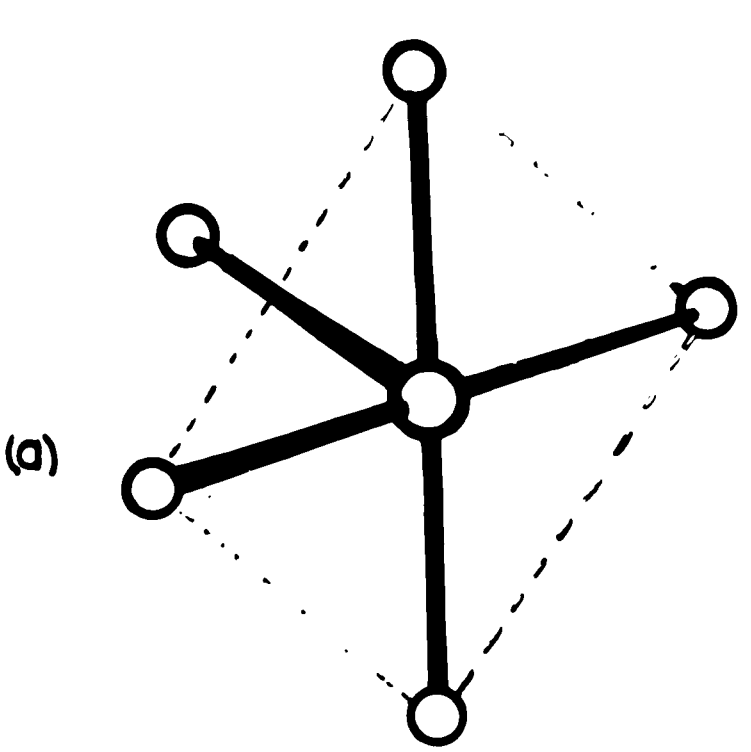
(a)

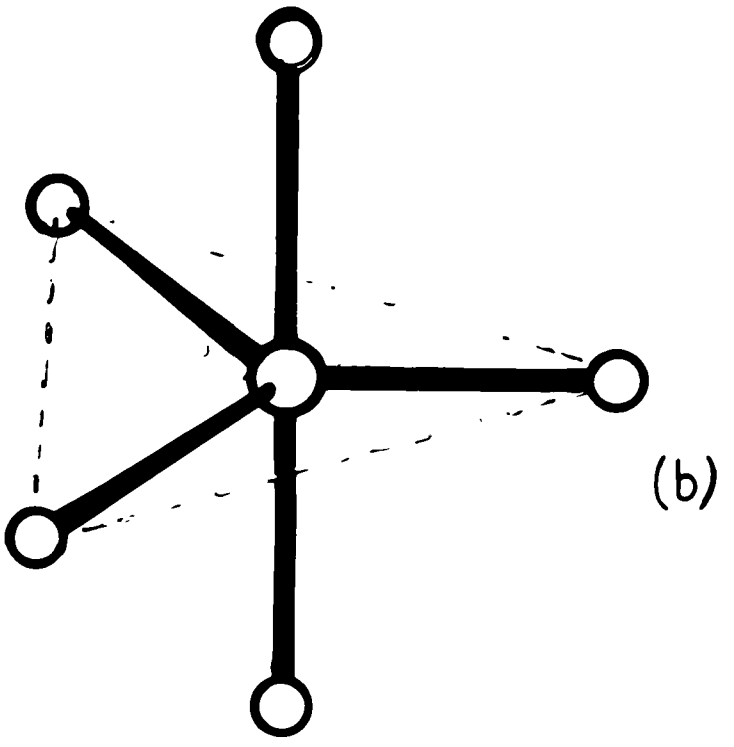
(b)

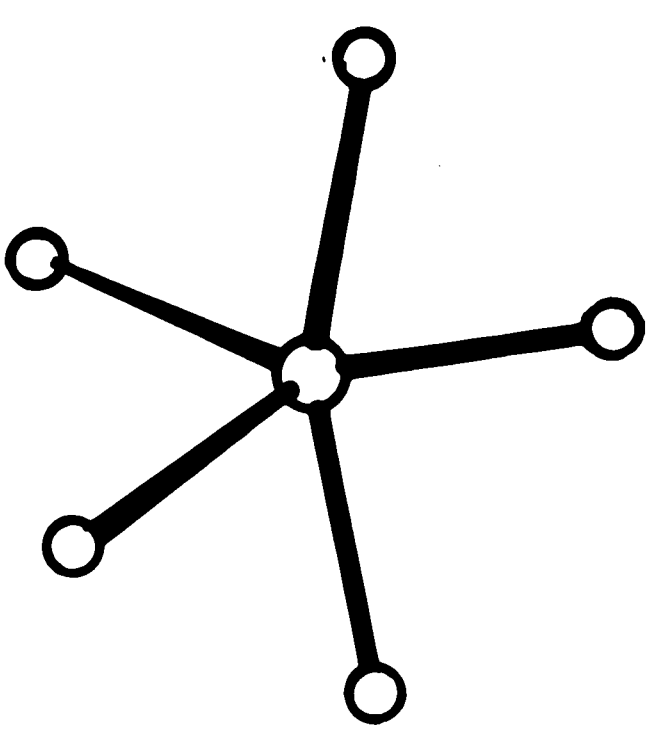
(c)

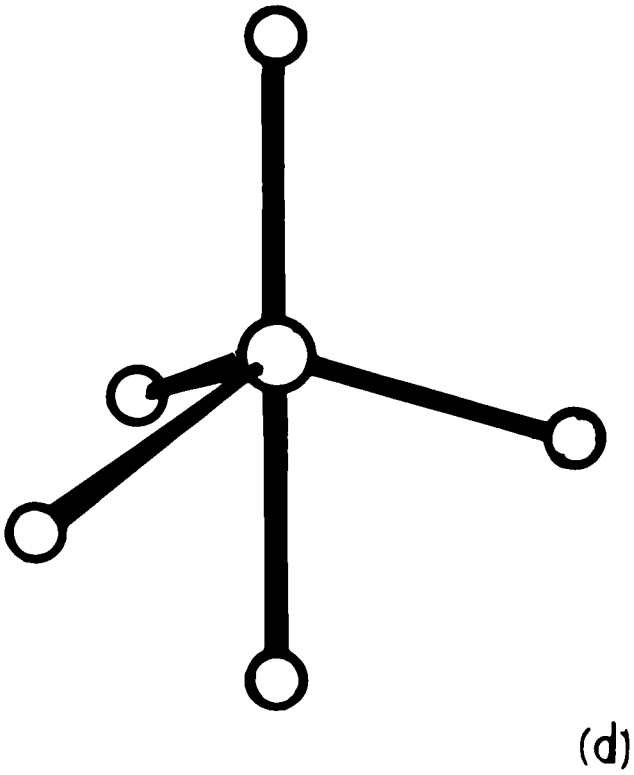
(d)

sous-jacents'. These authors used unorthogonalised orbitals. In 1956, Linnett[7] published a paper agreeing with Pauling's prediction of the greater stability for the trigonal bipyramidal geometry. However, even where these different approaches predict the same preferred stereochemistry, the characterisation of the bonding is different. Moreover, no correlation between the calculated strength of bonding in the square pyramid and the trigonal bipyramid, and their relative stabilities appears to have been discovered. The theories often predict the wrong relative strengths of the equatorial and apical bonds. For instance, the valence-bond theory leads to the conclusion that the equatorial bonds will be weaker and, therefore, longer than the axial bonds of a trigonal bipyramid. This is not observed. Finally, these theories give no explanation for the many distortions from idealised geometry that are observed in pentaco-ordinate complexes.

In an attempt to explain these anomalies, various authors have recently suggested factors they consider important in determining the relative stabilities of the possible geometries.

The most important of these appear to be:-

(a) valency-shell electron-pair repulsions [8]

(b) crystal field stabilisation energy effects [9]

(c) steric requirements of the ligands [2,3]

(d) packing requirements of the complex in the crystal.

At the present time, there is insufficient evidence concerning

the importance of these factors. Further, there has been some confusion in the literature and many authors have chosen to ignore the suggestions. These publications will be considered more fully in the final discussion in this thesis.

This thesis concerns the structure analyses (by X-ray diffraction methods) of four complexes, which were chosen to give information about the relative importance of these factors in determining the stereochemistry of pentaco-ordination. Each complex was chosen to emphasise one of the factors, but their interplay is the dominant theme in the thesis. The complexes are introduced in the relevant discussion of the factors listed above.

8

a) Valency-shell electron-pair repulsions:-

The valency-shell electron-pair repulsion approach is associated with four names: Sedgewick, Powell, Nyholm and Gillespie. The preferred geometry of co-ordination is derived by presupposing that the bonding electron-pairs are placed in orbitals as far apart as possible, so that repulsions between the electrons in different orbitals are minimised. Only then are orbitals that will give good overlap considered.

For pentaco-ordination this is best achieved with the trigonal biprymidal geometry. The metal orbitals $\underline{d}_{z}2$, $\underline{s}$, $\underline{p}_{x}$, $\underline{p}_{y}$, and $\underline{p}_{z}$ can then be used to overlap with the ligand orbitals. This stereochemistry is found in PCl_5.

Slightly less stable than the trigonal bipyramid is the square pyramid with the angle between the apical and the basal plane bonds slightly greater than 90° (Figure 1c) which is found in many copper complexes with oxygen and nitrogen ligands.[4] Least stable of all is the regular square pyramid with the basal bonds and the metal atom coplanar.

In the trigonal bipyramid, the bonds are not equivalent. Closer examination of the bonding pair interactions shows that the equatorial bonds are different from the axial ones. The axial bonding electron-pairs have three bonds at right-angles to them whereas the equatorial bonds have two at right-angles and two at 120°. Now as soon as charge clouds interact they repel each other with forces which increase greatly in proportion to a high power of the reciprocal of the distance between the electrons. In fact, there is much greater repulsion due to two electron pairs at right angles than two at 120°. Moreover, according to Gillespie,[8] the repulsion due to two electron pairs at 120° to a bond is less than that of one at 90°. Therefore, as far as these interactions are concerned the equatorial electron pairs of a trigonal bipyramid are more stabilised than the axial ones. This, it has been suggested is the reason for the shorter equatorial bonds in PCl_5. The importance of bonding electron-pair repulsions between bonds in the same co-ordination sphere would be increased if the bonds are covalent rather than ionic, and multiple bonded rather than single bonded. The fact that trigonal bipyramidal $Fe(CO)_5$,[10]

$[Co(NCCH_3)_5]^+$,[11] $Pt(SnCl_3)_5^{3-}$,[12] and $Co(CO)_3(PPh_3)(C_2F_4H)$[13] all contain several strongly multiple bonding ligands is consistent with this idea.

The complexes, triphenylphosphinegold-cobalt tetracarbonyl[14] and methyl-bis(o-dimethylarsinophenyl)arsino-silver cobalt-tetracarbonyl[15] are relevant to this point. Each has a five co-ordinate cobalt atom with one metal-metal and four metal-carbonyl bonds in the co-ordination sphere. They would probably be trigonal bipyramidal if the effect of bonding electron-pair repulsions were important.

Chemical and spectroscopic evidence[15] indicate that these molecules have $\underline{C}_{3\underline{v}}$ symmetry. The structures are shown diagrammatically in Figure 1.2. The crystal structure of triphenylphosphinegold-cobalt tetracarbonyl was analysed by X-ray diffraction methods by the author as his research project for Part II of the Oxford Chemistry Degree. The crystal structure of (TTAS)Ag-$Co(CO)_4$ has now been determined.

The investigations were carried out in order to confirm the chemical and spectroscopic results which are consistent with the dominance of electron-pair repulsion effects, and to investigate distortions from $\underline{C}_{3\underline{v}}$ symmetry which are not distinguished by spectroscopic methods. The structures had the added interest of an unusual metal-metal bond.

b) Crystal field stabilisation energy:-

A gaseous metal ion has five degenerate d orbitals. In a field

Fig. 1.2 a) Triphenylphosphorus-gold-cobalt-tetracarbonyl

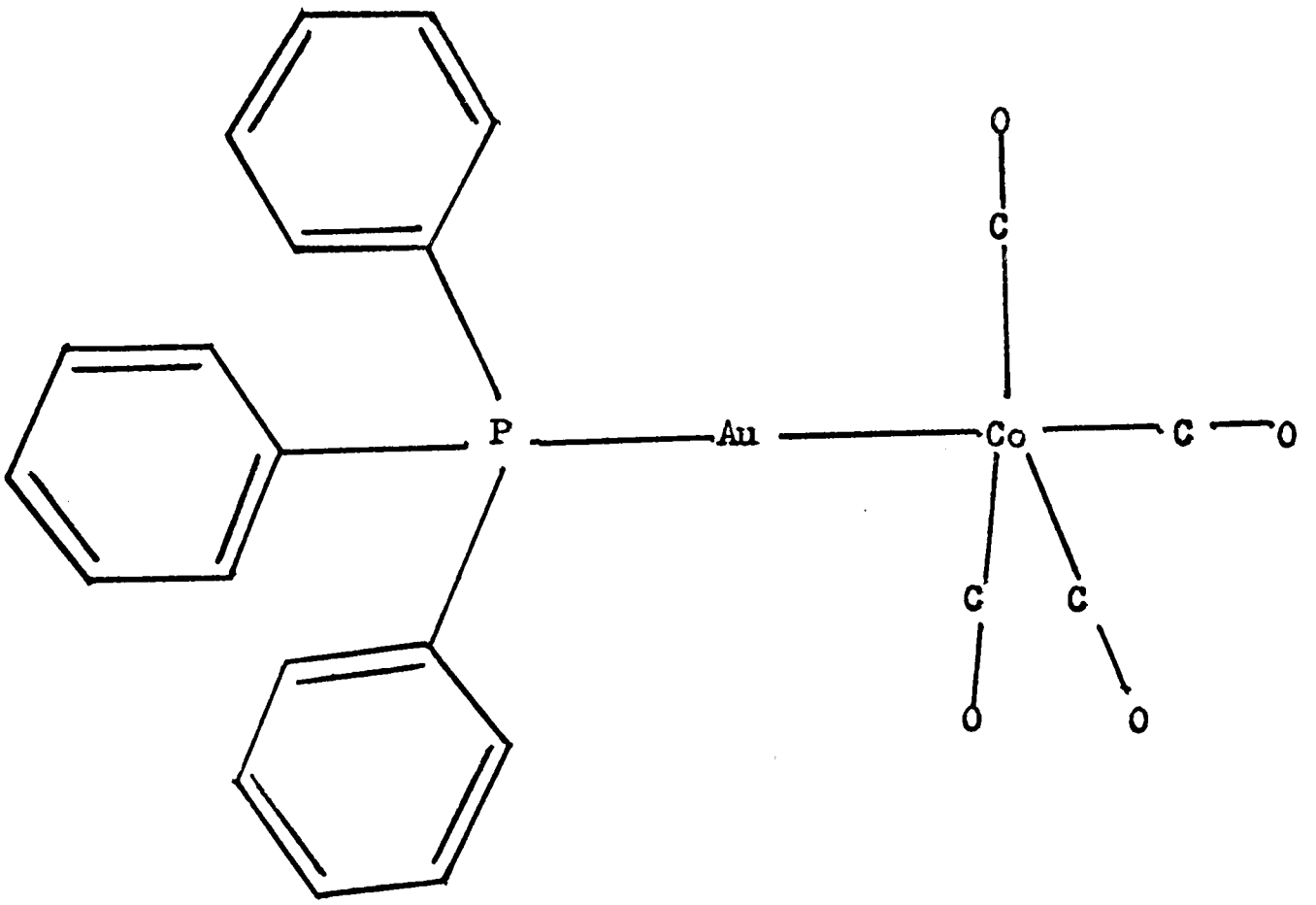

Fig. 1.2 b) Triarsine-silver-cobalt-tetracarbonyl

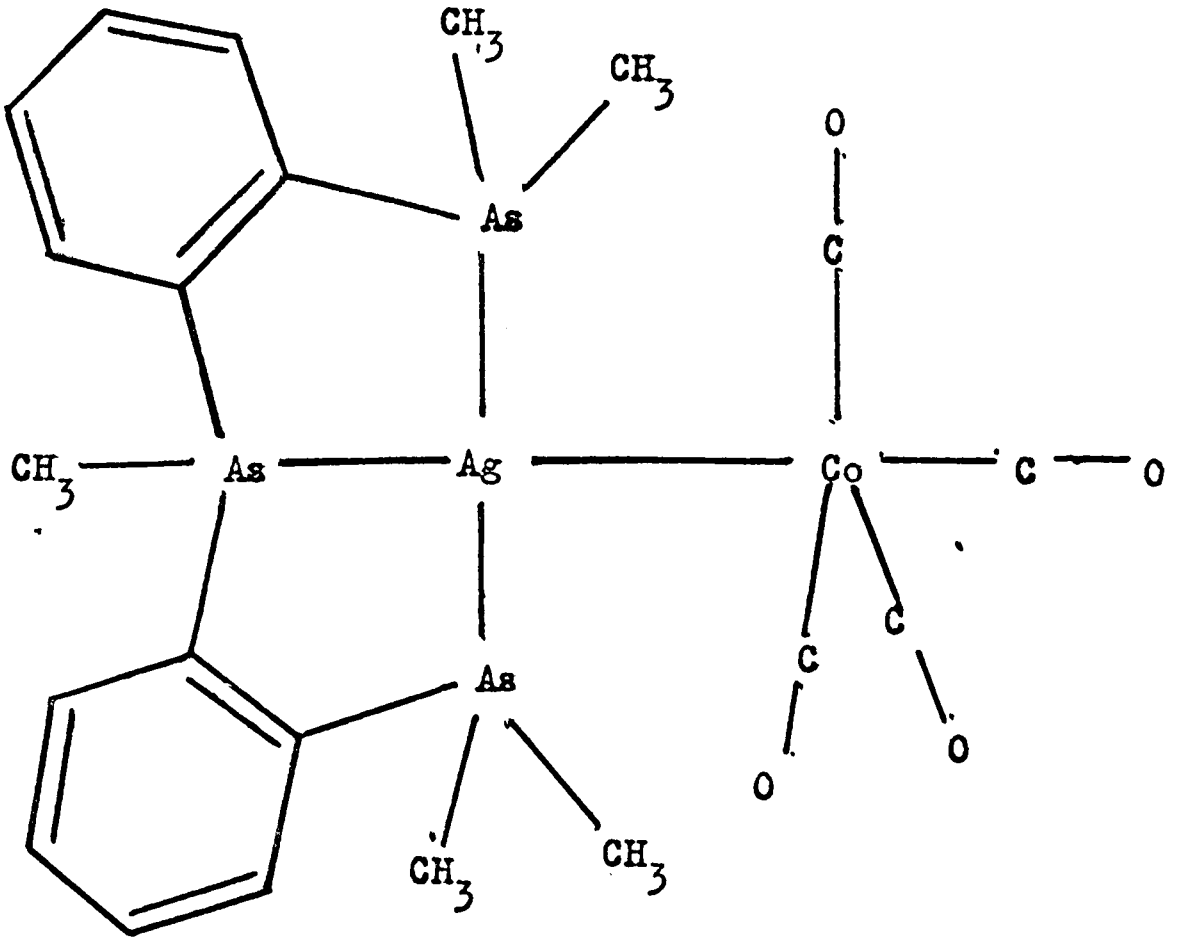

due to the electronic charges or dipoles of ligands at the apices of a square pyramid or a trigonal bipyramid, the orbitals are no longer degenerate, but some are stabilised relative to others. The crystal field stabilisation energy resulting from partially filling these d orbitals is different for the trigonal bipyramid and square pyramid. It is an important factor in determining the relative stabilities of the two idealised geometries for the transition metals.

The energies of the d orbitals in a crystal field may be predicted by use of a combined quantum mechanical and electrostatic model. A set of Slater type d wave functions are assumed, and first order perturbation theory for degenerate orbitals is used to calculate the new energies and wave functions produced by the electric field of the ligands, which are idealised as point charges or dipoles. Energy levels in terms of one or more radial parameters (B_0, B_2, B_4 after Ballhausen)[16] are given.

For the square pyramid, these are:-

$$E_{(d_{z^2})} = \mu f^2 8/45(4B_o - 4/7B_2 + 3/7B_4) + \mu_z f^2 8/45(B_o + 2/7B_2 + 2/7B_4)$$

$$E_{(d_{x^2-y^2})} = \mu f^2 8/45(4B_o + 4/7B_2 + 19/21B_4) + \mu_z f^2 8/45(B_o - 2/7B_2 + 1/21B_4)$$

$$E_{(d_{xy})} = \mu f^2 8/45(4B_o + 4/7B_2 - 16/21B_4) + \mu_z f^2 8/45(B_o - 2/7B_2 + 1/21B_4)$$

$$E_{(d_{xz}, d_{yz})} = \mu f^2 8/45(4B_o - 2/7B_2 - 2/7B_4) + \mu_z f^2 8/45(B_o + 1/7B_2 - 4/21B_4)$$

where μ is the dipole moment of the basal plane ligands, which are assumed to be equivalent, and μ_z is the dipole of the apical ligand.

For the trigonal bipyramidal geometry the energy levels are:-

$$E_{(d_{x^2-y^2}, d_{xy})} = \mu f^2 8/45(3B_o + 3B_2/7 + 3B_4/56) + \mu_z f^2 8/45(2B_o - \tfrac{4}{7}B_2 + \tfrac{2}{21}B_4)$$

$$E_{(d_{xz}, d_{yz})} = \mu f^2 8/45(3B_o - 3B_2/14 - 3B_4/14) + \mu_z f^2 8/45(2B_o + 2B_2/7 - 8B_4/21)$$

$$E_{(d_{z2})} = \mu f^2 8/45(3B_o - 3B_2/7 + 9B_4/28) + \mu_z f^2 8/45(2B_o + 4B_2/7 + 4B_4/7)$$

The square pyramidal geometry has four orbitals, one of which is doubly degenerate, while the trigonal bipyramid has three energy levels with two doubly degenerate.

If $\mu = \mu_z$, and if $B_2 = 2B_4$ approximately, these expressions may be simplified as follows:-

For the square pyramid:

$$E_{(d_{x^2-y^2})} = K\mu(5B_o + 32/21B_4)$$

$$E_{(d_{z2})} = K\mu(5B_o + 3/21B_4)$$

$$E_{(d_{xy})} = K\mu(5B_o - 3/21B_4)$$

$$E_{(d_{xz}, d_{yz})} = K\mu(5B_o - 16/21B_4)$$

For the trigonal bipyramid:

$$E_{(d_{z2})} = K\mu(5B_o + 33/28B_4)$$

$$E_{(d_{xy}, d_{x^2-y^2})} = K\mu(5B_o - 23/168B_4)$$

$$E_{(d_{xz}, d_{yz})} = K\mu(5B_o - 19/42B_4)$$

where K is a constant that depends on the distance of the ligand from the ion.

These energy levels[9] are plotted in Figure 1.3(a). Both cases consist of a group of orbitals which are low in energy, and one orbital

Fig. 1.3

CRYSTAL FIELD STABILISATION FOR FIVE CO-ORDINATE COMPLEXES

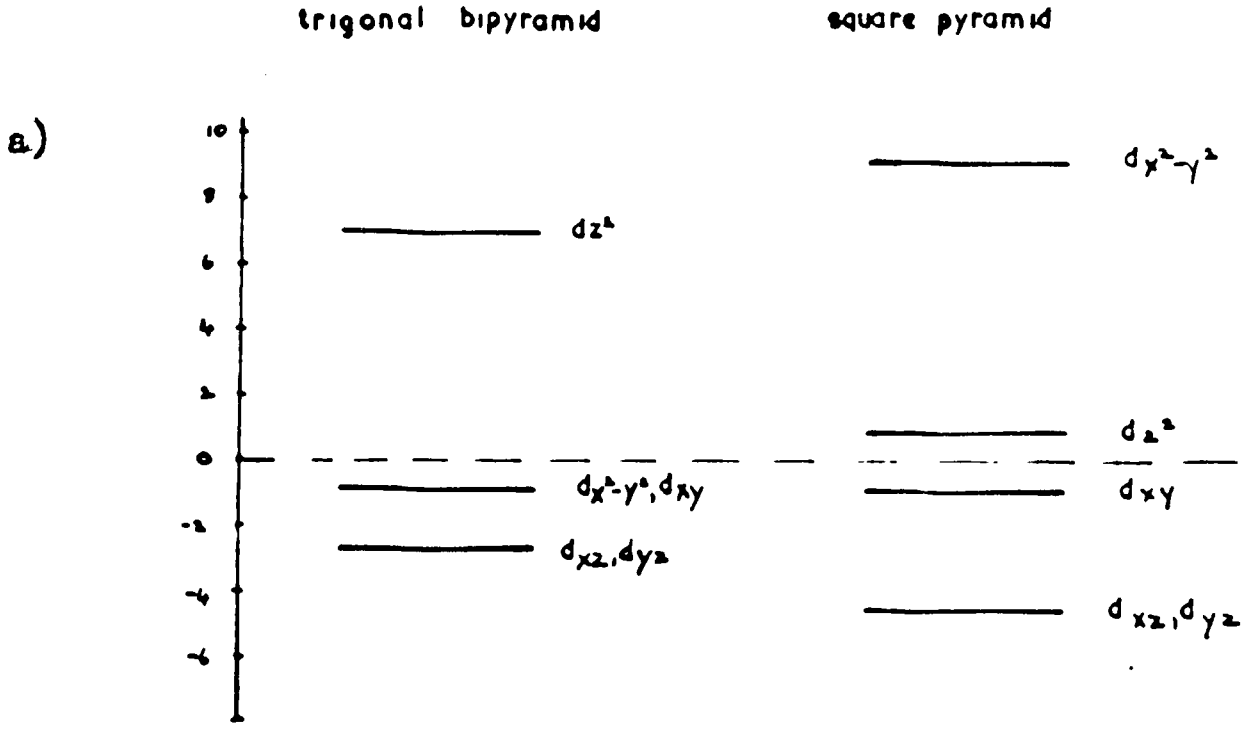

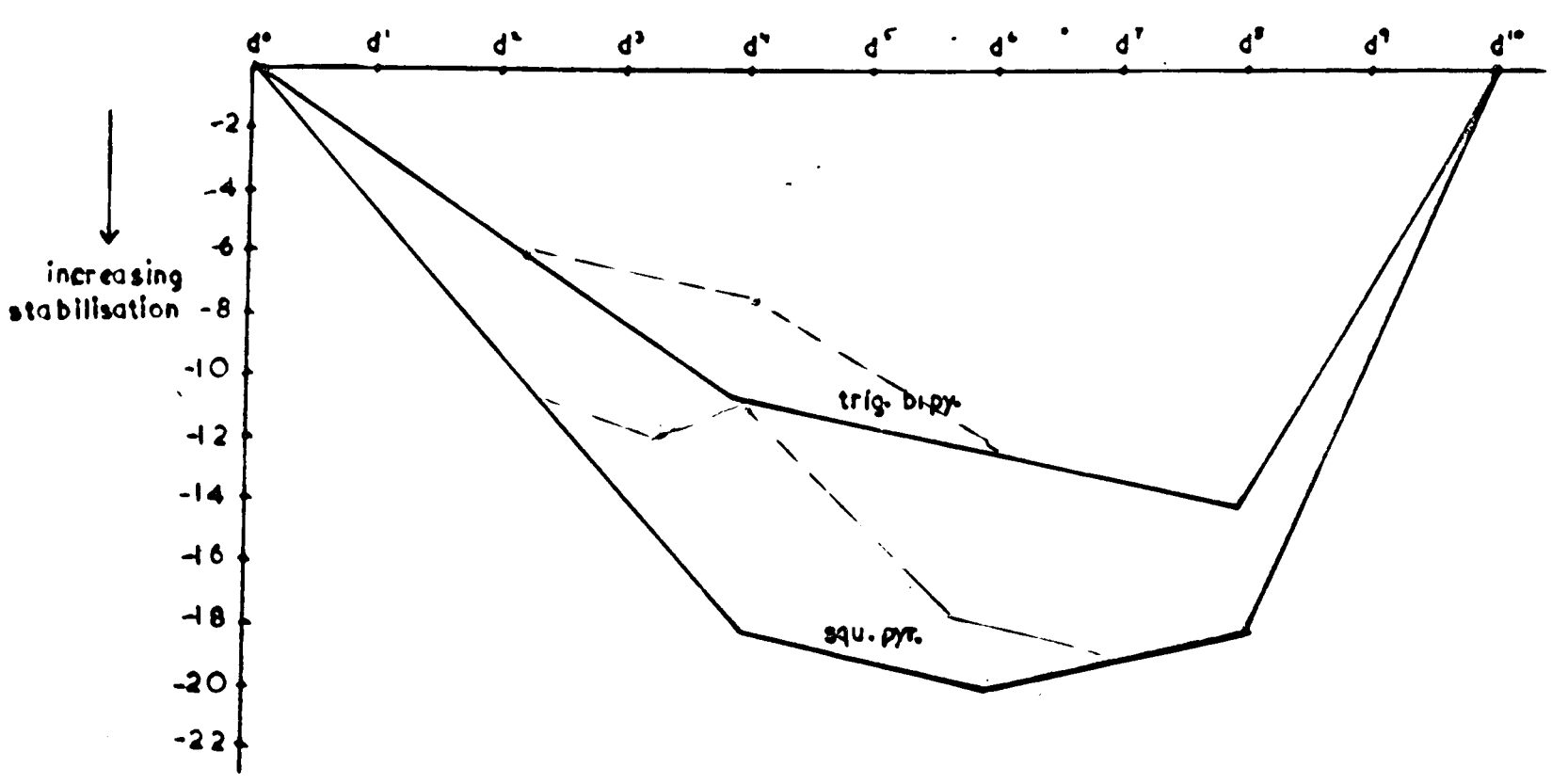

which is clearly much less favourable than the others. This is the $\underline{d}_{x^2-y^2}$ orbital for the square pyramid, and the $\underline{d}_{z^2}$ for the trigonal bipyramid.

Assuming that the energy levels are the same for any $\underline{d}^n$ configuration, the crystal field stabilisation for the trigonal bipyramidal and the square pyramidal geometries may be calculated for different $\underline{W}$ electron configurations. This is shown on the graph in Figure 1.3(b). There are two possible ways of filling the levels for reasonably strong fields. The continuous line on the graph assumes that the electrons are paired in each level before the next is filled, while the broken line assumes that electrons go into the lower group of orbitals before any pairing occurs. The last is the more realistic due to the consequent gain of exchange energy between electrons in different orbitals which are not very different in energy.

The graph demonstrates very clearly that the crystal field stabilisation energy is greater in $\underline{d}^1$ to $\underline{d}^9$ configurations for the square pyramidal geometry. In most cases, the difference is not great, but for $\underline{d}^5$ to $\underline{d}^8$ configurations the difference will probably be responsible for a square pyramidal geometry unless electron-pair repulsions, steric requirements of the ligand or crystal packing forces are very large.

For $\underline{d}^8$ configurations, the structural data appear to be consistent with these ideas. Trigonal bipyramidal complexes $Fe(CO)_5$,[10] $[Co(NCCH_3)_5]^+$ [11]

and $[Pt(SnCl_3)_5]^{3-}$ [12] have multiple-bonded ligands and thus high valency electron-pair repulsions, (see Section 1a, page 6) while $[Pt(QAS)I]^+$ (where QAS ≡ tris(o-diphenylarsinophenyline)arsine)[3] and $Pt(SnCl_3)_5^{3-}$ have ligands with a steric preference for a trigonal bipyramidal co-ordination (see Section 1c, page 17).

For $\underline{d}^8$ configurations, Ni(triars)Br_2 [17] and the triphosphino palladium dichloride (where the phosphine is 2-phenylisophosphindoline) [18] are almost square pyramidal. They both have a bromine atom in the apical position, and the bromine atom in the basal plane in both cases lies below the plane of the other three basal plane ligand atoms. Their geometries could be explained by assuming the square pyramid is preferred by the metal atom, but then a small distortion occurs to minimise the electrostatic repulsion between the bromine atoms. The crystal field stabilisation energy may be the dominant factor in these cases.

A further Pd(II) compound, trans-di-iodobis(dimethylphenylphosphine)palladium(II) has a square pyramidal geometry in the crystal state. As this is part of a polymeric array the stereochemistry does not give any useful evidence about the importance of crystal field stabilisation energy. Crystal packing forces (considered in Section 1d, page 21) are obviously important.

Although a considerable body of chemical and spectral information has accrued concerning pentaco-ordinate complexes of metals with $\underline{d}^8$ configurations, further crystallographic studies of these compounds are necessary to confirm tha structural speculation.

In order to gain more definitive structural evidence it was decided to determine the structure of a further $\underline{d}^8$ complex where crystal field stabilisation energy may be an important factor in determining the stereochemistry. The ligand should either be small and unidentate or alternatively polydentate but very flexible. Such a ligand appeared to be TPAS (TPAS ≡ o-phenylenebis-(o-dimethylarsinophenyl-methylarsine))[21], Figure 1.4(a), which could co-ordinate either in a square pyramidal or a trigonal bipyramidal geometry, provided it was not required to span two equatorial positions.

The ligand was synthesised by Dr. A. T. Phillip in Professor Nyholm's laboratory. It gives a series of pentaco-ordinate complexes with Pt(II) or Pd(II) of general formula $[M(TPAS)L']L''$ where M is either Pt(II) or Pd(II) and L' and L'' could be I^-, Br^-, Cl^-, NO_3^- and ClO_4^-.

Comparison of the IR data with that of $[M(diars)_2]^{2+}$ [diars ≡ (o-dimethylarsinophenylene)-dimethylarsine] indicated that the complexes were probably square pyramidal with L' in the apical position. Conductimetric titrations confirmed the existence of $[M(TPAS)L']^+$ in solution. The evidence is least conclusive when L' is Cl^- as the Pd-Cl and Pd-As stretching frequencies are very similar. The proposed structure is shown in Figure 1.4(b).

The author decided to determine the crystal structure of $[Pd(TPAS)Cl]ClO_4$. The chlorine (the smallest ligand, L') would cause least steric hindrance and the perchlorate would be the least likely to co-ordinate in the sixth position. The chemical analysis indicated

Fig. 1.4. $(Pd(TPAS)Cl)ClO_4 \cdot C_6H_6$

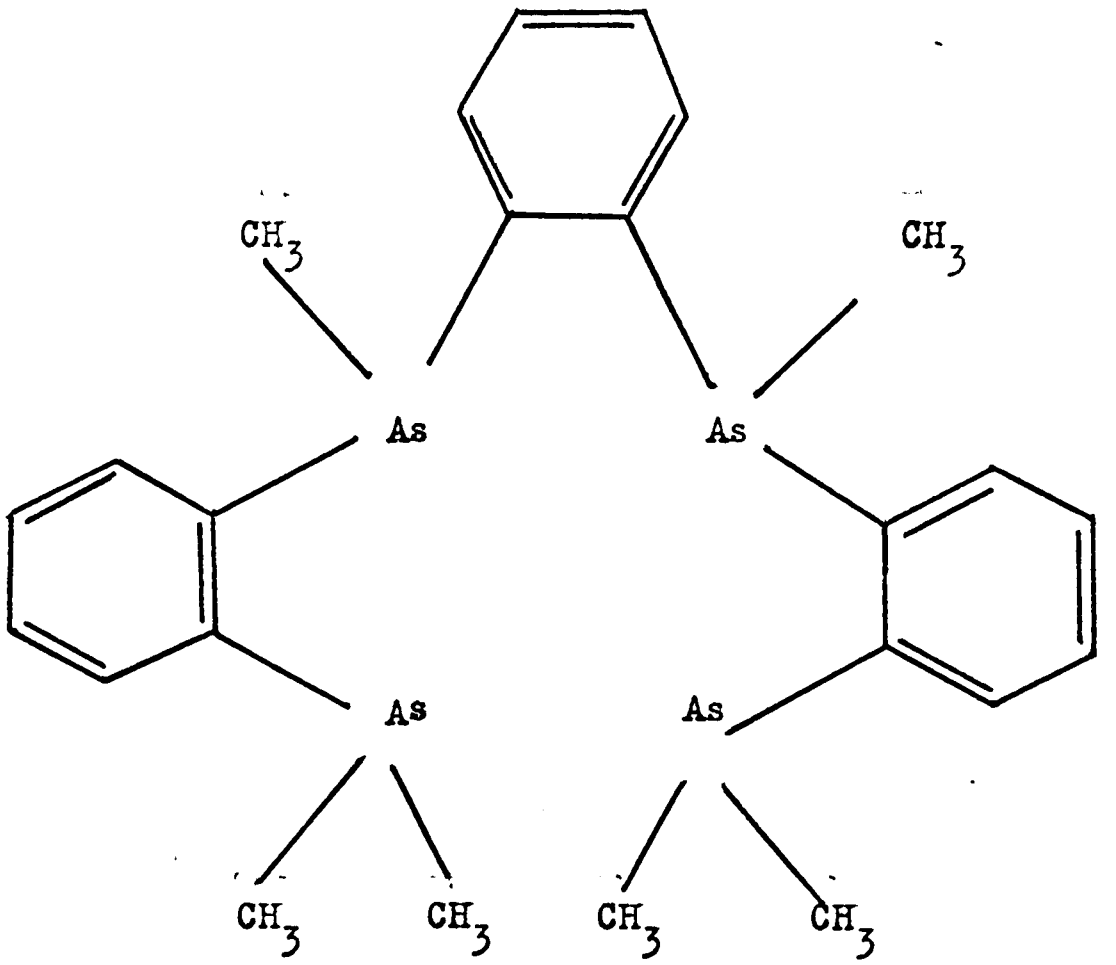

a) The ligand, TPAS.

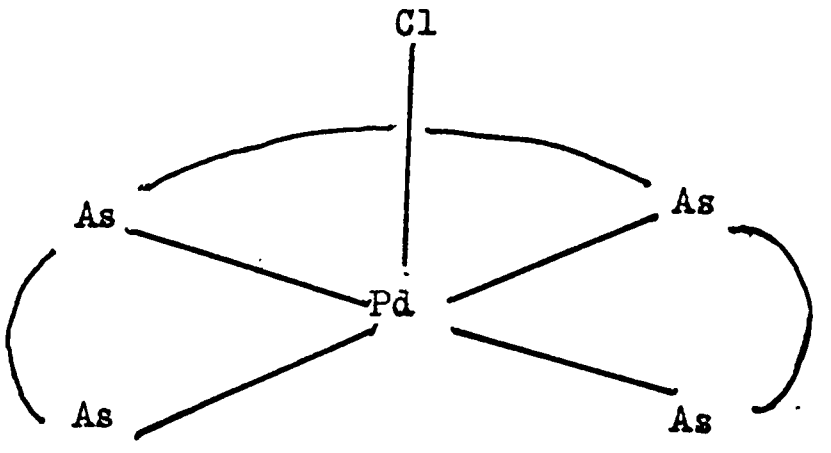

b) The proposed stereochemistry.

that the complex crystallises with one molecule of benzene of crystallisation.

A crystallographic analysis would determine which isomer of which geometry was assumed, and also indicate the nature of distortions such as extension of the apical bond and non-planarity of the basal plane atoms if it were a square pyramid.

The geometry of this complex should give information about the importance of crystal field stabilisation energy in determining the preferred stereochemistry. Only this factor prefers the square pyramidal geometry.

c) Steric requirements of the ligand:-

If the stabilisation energies resulting from valency electron-pair repulsions and crystal field stabilisation for the square pyramid and and the trigonal bipyramid are not very different, the geometry of the complex may be determined by the steric requirements of the ligand.

Two types of steric requirements are relevant. The first is that due to large ligand atoms, giving rise to large non-bonding-electron repulsions between ligands in the same co-ordination sphere. These intramolecular repulsions may strongly disfavour a particular geometry. The second is the steric preference of polydentate ligands for a particular geometry.

Intramolecular repulsions, of course, are present in all complexes. We can make an estimate of their relative importance by making calculations on simple electrostatic models. For instance, a trigonal

bipyramid with a central atom with a positive charge of +Z, ligands with charge -e and metal-ligand distances of r has an energy given by $E_{TBP} = 4.25 \frac{e^2}{r^2} - 5eZ$

For the equivalent square pyramid the energy is given by

$$E_{SP} = 4.5\frac{e^2}{r^2} - \frac{5eZ}{r^2}$$

if the basal plane atoms and the positively charged atom are all coplanar.

If the angle between the apical bond and the basal bonds (β) is not 90° the energy is given by:-

$$E_{SP} = \frac{e^2}{r^2}\left[\frac{2.5}{\sin^2\beta} + \frac{2}{1-\cos\beta}\right] - 5\frac{eZ}{r^2}$$

This is a minimum when $\beta = 103^\circ\ 34'$

Then $E_{SP} = 2.465 \frac{e^2}{r^2} - \frac{5eZ}{r^2}$

This shows that the trigonal bipyramid is the most stable. The square pyramid with the four basal plane ligand atoms coplanar with the central atom is much less stable, but a distortion giving a β angle of $103^\circ\ 34'$ gives a situation which is almost as favourable as the trigonal bipyramidal. These simple calculations give a guide to the relative stabilities of actual complexes although the charge on the ligands and central atom will vary and, of course, is very difficult to calculate. The bondlengths will also differ.

Complexes like $[Pt(SnCl_3)_5]^{3-}$ with very bulky ligands would be expected to be trigonal bipyramidal on this basis. The observed trigonal bipyramidal stereochemistry is also consistent with ideas

about valence electron-pair repulsions which, of course, must reinforce the non-bonding electron repulsions discussed here.

If the square pyramidal geometry is favoured by either ligand field stabilisation effects or crystal packing forces, a compromise geometry of a square pyramid with a basal angle of about 103° might be assumed. This is consistent with the fact that the metal atom lies above the plane of the four basal ligand atoms in most Cu(II), Ni(II) and Co(II) square pyramidal complexes.[4] Some examples are nitrosylbis[NN'-dimethyldithiocarbamato]cobalt(II)[22] where the β angle is 103° 30', bis(NN'-di-n-propyldithiocarbamato)copper(II)[23] where the angle is about 100°, and $M(DEAS)_2$ [where M = Co(II) or Ni(II) and DEAS is the Schiff base N-β-diethylamine-ethyl-5-chlorosalicylaldimine][24] which has a β angle of about 100°.

This factor might be of importance in the structure of $[Pd(TPAS)Cl]^+$, discussed in the previous section.

The second type of steric requirement of ligands is that of polydentate ligands which prefer to co-ordinate in a particular geometry.

Many of these ligands involve 1,2-substituted phenyl rings which span ligand atoms. A typical example is o-phenylene-bis(dimethylarsine). The distance between the arsenic atoms in the free ligand is about 3.4Å and with metal-arsenic bonds of about 2.4Å it will subtend a right angle at the metal atom. Therefore, this ligand could not co-ordinate at two equatorial positions of a trigonal bipyramidal

Fig. 1.5. $(Co(QP)Cl)BPh_4$

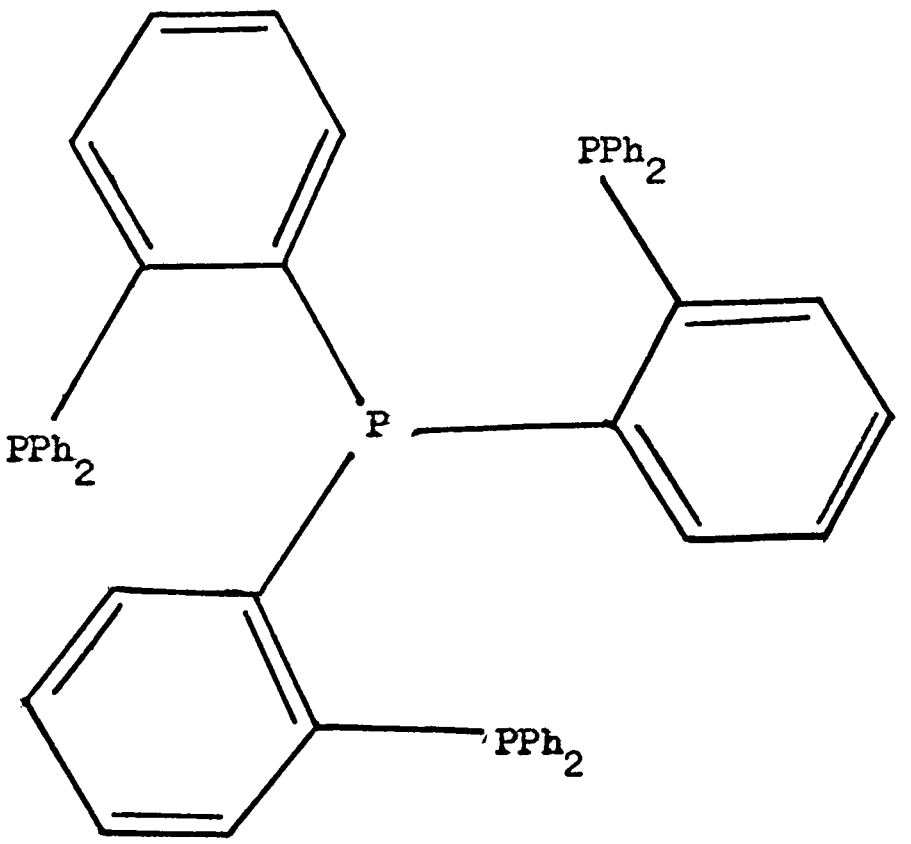

a) The ligand, QP.

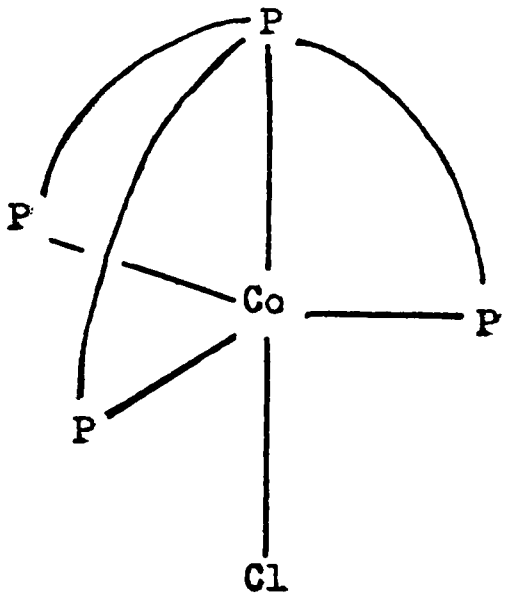

b) The proposed stereochemistry

complex with equatorial bonds of about 2.4Å.

The span of chelates is easier to estimate than the possible stereochemistry of the ligand atoms. It is easily shown that the ligand, QAS(tris-(o-diphenyl-arsinophenyl)arsine) prefers the trigonal bipyramidal geometry of $[Pt(QAS)I]^+$ but it would be difficult to preclude the formation of a square pyramid because the geometry of the arsenic co-ordination is very flexible.

To gain further information on the steric requirements of ligands, the structure of $[Co(QP)Cl]BPh_4$ (QP = tris(o-diphenylphosphinophenyl)phosphine)[25] has been determined. The ligand, QP, is shown in Figure 1.5(a). The complex was prepared by Venanzi et al.[25]

Chemical and spectroscopic data indicated that the complex has a trigonal bipyramidal co-ordination with the chlorine atom in the apical position. However, the $\underline{d}^7$ configuration should give rise to a Jahn Teller distortion of the equatorial plane of the trigonal bipyramid. Also the crystal field stabilisation energy for the trigonal bipyramid is less than that of a square pyramid for $\underline{d}^7$ configurations. How far from the trigonal bipyramid, the preferred geometry for the ligand, QP, would these factors distort the stereochemistry?

d) Crystal packing requirements:-

The geometry of many pentaco-ordinate complexes may be partially determined by their mode of packing in the crystal structure. This

may result in polymerisation or a distortion of the molecular geometry in the solid state.

An example of polymerisation to give pentaco-ordination is the formation of the red-form of trans-di-iodobis(dimethylphenylphosphine) palladium(II). The planar $(CH_3)_2(C_6H_5)P_2PdI_2$ group are joined through iodine bridges to give a polymeric array of distorted square pyramids about the palladium atoms.[19]

It is much more difficult to identify a distortion of geometry resulting from intermolecular interactions. An intermolecular distance of considerably less than the sum of the van der Waals radii of the atoms concerned may be indicative of strong intermolecular forces. However, it does not necessarily indicate a stereochemistry distorted by these forces. In fact, it most probably results from stereochemical rigidity. Also the fact that the undistorted molecule if packed in the same way as the observed one would have less van der Waals energy is not an argument that the molecule has been distorted to gain this energy. Changes in the geometry of most molecules in a crystal structure result in a loss of packing energy.

The most conclusive evidence for intermolecular forces is a comparative structural study in the gaseous and solid states using electron diffraction and X-ray diffraction methods respectively. Few molecules are volatile or simple enough to allow an electron diffraction study, however.

Crystal packing requirements may be postulated convincingly if no

other effects would give the observed distortion. Such an example is the crystal structure of antimonypentaphenyl.[26] The complexity of the molecule precludes an effective electron diffraction study. In the solid state, the molecule is almost square pyramidal although the analogous phosphorus and arsenic complexes are trigonal bipyramidal.[27] Valency-shell electron-pair and non-bonding electron repulsions would favour a trigonal bipyramidal geometry. Consider the following argument. The Sb-C bonds are 0.3Å longer than the average P-C bond. A trigonal bipyramidal $SbPh_5$ molecule would have intramolecular distances greater than the sum of the van der Waals radii between the phenyl carbons. A distortion of the square pyramidal geometry as a result of the intermolecular forces introduced on crystallisation might then lead to a gain in van der Waals attraction energy. This argument in the absence of others seems plausible. However, it is still difficult to reconcile with the trigonal bipyramidal stereochemistries of $Sb(Ph)_2Cl_3$[28] and $Sb(Ph)_3Cl_2$.[29]

Finally, if two identical molecules crystallise in the same asymmetric unit, or in two different crystal lattices and have different geometries in the two cases, this may be indicative of distortions due to crystal packing forces.

Packing requirements in the crystal might be the dominant factor if the bonds are weak, mainly ionic, and other factors such as electron-pair repulsions and crystal field stabilisation are unimportant.

Such a crystal structure is that of 1,10-phenanthrolinedimethyl thallium(III)perchlorate, prepared by Beattie et al..[30] It closely resembles N-pyridyl-dimethylthallium(III)perchlorate, which has a 'T'-shaped Me_2Tlpyr^+ cation.[30] Infrared and Raman data are indicative of a slightly bent dimethylthallium group in solution. Both complexes show a strong band at approximately 500 $cm.^{-1}$ (the Me-Tl-Me symmetric stretch) in the Raman, and a very weak band at 491 $cm.^{-1}$ in the infrared suggesting that Me-Tl-Me is weakly infrared active.[30]

The phenanthroline adduct in the solid might be pentaco-ordinate if the perchlorate is weakly unidentate. Strong perchlorate oxygen - thallium interaction giving a bond of considerable covalent character is precluded by the Raman and infrared spectroscopy of nujol mulls. These indicate only a very slight distortion of the ClO_4^- tetrahedron. They do not show the gross changes found for several co-ordinated perchlorate spectra.

The Tl-O interactions must therefore be weak, and the geometry of the complex in the crystal structure would probably be determined by packing requirements. The crystal structure determination of 1,10-phenanthroline-dimethyl-thallium-perchlorate is reported here.

The complexity of the Problem

Although each of the complexes studied by X-ray diffraction methods has been introduced in the discussion of one of the factors

thought to be important in determining the stereochemistry of pentaco-ordination, several factors might be important in each case. For (TTAs)Ag-$Co(CO)_4$ crystal packing factors might distort the geometry preferred by valency electron-pair repulsions. In $[Co(QP)Cl]^+$ the crystal field stabilisation energy might predominate despite the steric requirements of the ligand. In $[Pd(TPAS)Cl]^+$, crystal packing requirements or valency electron-pair repulsions may be more important than crystal field stabilisation. In each case the interplay of factors must be emphasised. In all cases, the results might enable a statement, "the structure is consistent with the dominance of this factor", to be made. The aim is to add to the body of structural information concerning pentaco-ordination which may give a better understanding of the stereochemical problem. A definitive answer to the problem is not yet feasible.

Part II of the thesis is concerned with X-ray diffraction studies of the four complexes while Part III comprises a discussion of the results of these studies in the light of the factors described above which may be important in the stereochemical problem of pentaco-ordination.

PART II

THE CRYSTAL STRUCTURE ANALYSIS

Introduction

The crystal structures of the four complexes $(TTAs)Ag\text{-}Co(CO)_4$, $[Pd(TPAS)Cl]ClO_4$, $[Co(QP)Cl]BPh_4$ and $[TlMe_2 1,10\text{-phen}]ClO_4$ described in the introduction to the stereochemical problem of pentaco-ordination have been determined by means of X-ray diffraction methods.

The structure analyses have involved indirect methods. In each case, chemical and structural features of the molecules were tentatively assumed, and information based on these assumptions was used in the structure analyses.

The structure analyses presented a variety of crystallographic problems. The problems varied in size from 83 atoms per asymmetric unit in the $[Co(QP)Cl]BP_4$ crystals to 20 in the $[TlMe_2 1,10\text{-phen}]ClO_4$ crystals. The determination of the space group of the $[Co(QP)Cl]BPh_4$ complex stimulated a full investigation into the use of intensity statistics of molecules containing heavy atoms. The Patterson functions of $[Pd(TPAS)Cl]ClO_4$, $[Co(QP)Cl]BPh_4$ and $[TTAs]Ag\text{-}Co(CO)_4$ involved interpretation by use of implication diagrams, analytical and superposition methods; there are seven, six and five heavy atoms respectively per asymmetric unit. The Fourier of the thallium complex was confused by diffraction ripples and over-determination of the phases by the thallium, whereas for $[Co(QP)Cl]BPh_4$ the Fourier was badly resolved due to the small number of phases determined correctly by the heavy atoms. The latter difficulty resulted in a study of anomalous dispersion techniques and the method of refinement by the

tangent formula in this type of problem.

As many parts of the structure analyses of the four complexes were very similar, the analysis of each will not be discussed separately. Parts of the analyses which have become routine are only briefly mentioned, so that more space can be devoted to describing the applications of more unusual techniques. Thus, there are full discussions of the use of recent developments in intensity statistics, of the interpretation of the Patterson functions, of the subsequent study of the badly resolved electron density maps, and of the use of anomalous dispersion techniques and the tangent formula. On the other hand, full details of the photography, determination of cell constants, the interpretation of clearly resolved electron density maps and the many cycles of least squares refinement are not included in the main discussion.

A complete summary of the crystal data, the determination and refinement of the structures and all the necessary structural data are given for each of the four complexes in the Appendices (pages 159 - 187)

It is hoped that this procedure will enable the reader to follow the discussion without being confronted with too much unnecessary detail.

Two sets of computer programmes have been written to make an analysis of intensity statistics and to calculate 'E' values and refine phases using the tangent formula. These are desciibed in the Appendices (pages 188-204). Details of the programmes are given, including flow diagrams, and information complementary to the

discussion of their use in this chapter.

CHAPTER 2

COLLECTION AND REDUCTION OF DATA

Initial Investigations

A preliminary X-ray diffraction study with Cu-K_α radiation was made with the crystals of the four complexes as a feasibility study. Oscillation, and zero and first layer Weissenberg photographs[31] were taken about two or three crystal axes. From these approximate cell dimensions, cell volume and space-group were determined. The densities of the crystals were measured by the method of flotation. Assuming the molecular formulae given by the chemists, the number of molecules per unit cell, n, was calculated for each crystal structure. A value close to four in each case confirmed the proposed molecular formulae. Figure 2.1 gives the molecular formulae, space-groups and cell dimensions derived from these preliminary investigations and also the pages of this thesis on which relevant chemical and further crystallographic information may be found.

None of the crystals was twinned, and there were no obvious signs of disorder such as streaking of spots.

Choice of crystals

The linear absorption coefficients (μ) of the crystals were

FIGURE 2.1

Molecular formula	$C_{30}H_{36}As_4Cl_2O_4Pd$	$C_{21}H_{23}AgAsCoO_4$	$C_{14}H_{14}ClN_2O_4Tl$	$C_{18}H_{62}BClCoP_4$
Structural formula	$[Pd(TPAS)Cl]ClO_4.C_6H_6$	$(TTAs)Ag\text{-}Co(CO)_4$	$[Me_2Tl1,10\text{-phen}]ClO_4$	$[Co(QP)Cl]BPh_4$
Page on which chemical information is summarised	15	8	24	21
Space group	$P2_1/c$	$P2_1/n$	$P2_1/c$	$P2_1nb$
Cell dimensions	11.1, 20.3, 18.2Å 90, 122, 90°	12.9, 16.9, 12.1Å 90, 100.3, 90°	7.5, 9.1, 23.5Å 90, 94, 90°	18.9, 18.2, 18.6Å 90, 90, 90°
Measured density	1.78	1.86	2.14	1.25
n = Number of molecules per unit cell	4	4	4	4
Page of Appendix giving crystallographic details	166	159	181	172

calculated for Cu-K_α radiation using the molecular formulae confirmed in the preliminary study. The values are given in the Appendices.

The choice of size of crystals is dependent upon the radiation used which is in turn dependent upon the values of the linear absorption coefficients.

The absorption coefficients of $[TlMe_2 1,10\text{-phen}]ClO_4$ and $[Pd(TPAS)Cl]ClO_4.C_6H_6$ increase with increasing wavelength of the incident radiation. The use of the shorter wavelength Mo-K_α radiation improved for $[Pd(TPAS)Cl]ClO_4.C_6H_6$ as only very small crystals were available. Further, the axis lengths of about 20Å in both of these complexes made indexing difficult with the equi-inclination Weissenberg method. In the case of $(TTAs)Ag\text{-}Co(CO)_4$, no apparatus with a changeable target was available.

Thus, in all these cases nickel-filtered Cu-K_α radiation was used with crystals less than optimum size, $2/\mu$. The crystals of $[Pd(TPAS)Cl]ClO_4C_6H_6$ were very small, irregular plates with a maximum thickness considerably less than $2/\mu$. Immersed in paraffin the crystals were cleaned mechanically of small adhering pieces of crystal. Approximately cube-shaped srystals of the other compounds were produced by cutting them under paraffin. This procedure minimised errors caused by absorption, which are greatly decreased as

the crystal approximates to a sphere.

The Cu-K_α radiation linear absorption coefficient of $[Co(QP)Cl]BPh_4$ is less than that of the other complexes, but there was considerable fluorescence. However, anomalous dispersion effects were observed. It was decided to collect both Bijvoet pairs, as it was not clear that the heavy atom method would be sufficient to determine the structure. Crystals of less than optimum size were used.

The crystal dimensions were measured accurately, and the orientations of the faces of the crystal relative to the crystallographic axes were recorded in order that absorption corrections to the intensities could later be calculated.

Accurate Cell Dimensions

Accurate cell dimensions were obtained from zero layer Weissenberg photographs about the three principal axes. These were calibrated by the superposition of aluminium powder lines. Measurements of the distances of reflections on one side of the film to the related reflections on the other side were made using a Cambridge travelling microscope. The known cell dimensions of the aluminium allowed corrections for film shrinkage, uncertain camera radius and eccentricity. This was carried out in two ways:-

1) A graph was drawn of the correction required against values of the Bragg angle, θ, and a correction for each reflection was then read directly. The cell dimensions were derived from reflections of high "sin θ" only.

2) The true Bragg angle, θ_t, is assumed to be related to the measured value, θ_m, by

$$\theta_t = \theta_m + k_1 \sin \theta_m \cos \theta_m + k_2 \theta_m$$

where '$k_1 \sin \theta_m \cos \theta_m$' is a correction for eccentricity and '$k_2 \theta_m$' allows for film shrinkage. k_1 and k_2 are derived by a least squares method from the aluminium powder lines, and corrections to the measured Bragg angles for the complex are calculated using these values. The calculations were computed by a programme written by Dr. B. T. Kilbourn.[33]

Accurate values of β for the monoclinic space groups were determined from values of $d_{(101)}$, $d_{(10\bar{1})}$, $d_{(100)}$ and $d_{(001)}$ by the method of triangulation.[31]

Collection and Measurement of data

Intensity data were collected by the equi-inclination Weissenberg technique[31] on a Nonius Weissenberg Camera, Type W.B., on a Hilger and Watts Microfocus X-ray Unit Y33.

Two-axis data (with the two shorter axes as rotation axes) were collected in all cases. Details of the number of layers collected on each axis are given in the Appendices (pages 159 - 187). The number of data that were collected for the crystal structure of the $[Pd(TPAS)Cl]^+$ complex was limited by the high temperature factors of this complex. Low-temperature apparatus was not available at this stage.

Measurements of the intensities of the reflections were made by visual comparison with a standard scale, prepared by isolating one of the reflections and recording it for a series of known time intervals. The scale was checked by measuring the intensity of each of the spots with a microdensitometer.

The multiple film technique with a five-film pack was used. The values of the film-factors used in bringing all these films onto the same scale invoked considerable discussion. The ratios of reflections on two film packs were consistently found to be less than 2.93, the experimentally determined transmission factor.[34] This seemed to be due to a systematic over-estimation of reflections measured at the low end of the usual scale. The result of using these calculated film factors would be to underestimate the intense reflections giving rise to data which may appear to suffer badly from extinction. The use of calculated film-factors had been general practice in the Oxford Laboratory, and these were used in the crystal structure analyses of compounds other than the $Co(QP)Cl^{+}$ complex. The inadequacies of this method were later realised, and experimental transmission factors were used for the data scaling of this complex.

Data reduction

Corrections for absorption, Lorentz factor, polarisation and spot shape were first applied to the measured intensities.

Absorption corrections for all crystals were calculated by the method of Busing and Levy,[35] using a programme written by R. H. B. Mais[36]

in Ferranti "Mercury" machine code and translated by the author into c-autocode for use on the NDF9 computer.

The absorption correction for a crystal of volume, V, and linear absorption coefficient, μ, is given by

$$A = \frac{1}{V} \exp\left[-\mu(r_p + r_d)\right] d\nu$$

where the primary and diffracted beam path-lengths are given by $\underline{r}_p$ and $\underline{r}_d$ for reflection by a volume element, $\underline{d}\nu$.

A set of orthogonal axes $\underline{x}$, $\underline{y}$, $\underline{z}$ are defined such that $\underline{z}'$ is parallel to the rotation axis and $\underline{y}$ is in the direction of one of the reciprocal axes. The crystal boundaries, which must not involve any re-entrant angles, are defined by equations of the form

$$\underline{a}_s \underline{x} + \underline{b}_s \underline{y} + \underline{c}_s \underline{z} - 1 = 0$$

where $\underline{a}_s$, $\underline{b}_s$ and $\underline{c}_s$ are the direction cosines of the perpendicular at the surface plane passing through the origin of the orthogonal axes, which must be inside the crystal.

With the aid of the direction cosines for reflections calculated from expressions given by Wells for the equi-inclination method the angle between the primary and diffracted beams is easily computed. Thus, for a given point in the crystal a knowledge of these angles combined with the perpendicular distance of the point from the surfaces through which the beam enters and leaves, the path-lengths of the primary and diffracted beams in the crystal are calculated.

The method reduces the integral by the Gauss quadrature method to a triple summation. The number of sampling points in each direction was made equal to the next integer greater than $4\mu t$, where t is the crystal thickness in that direction.

Two limitations of this method are apparent. The first of these is that the method leads to a ridiculous distribution of sampling points if the crystal has any of the orthogonal axes in the direction of a diagonal of a rectangular crystal. This leads to the choice of the same number of sampling points for different crystal widths. This difficulty was avoidable in all cases, except for the $[TlMe_2$1,10-phen$]ClO_4$ crystals. Here it would have been better to rewrite the computer programme to give a number of sampling points proportional to the thickness of the crystal in the direction of the orthogonal axes.

Secondly, if the absorption is considerable and the crystal large, most of the sampling points are chosen such that beams diffracted at these points would be effectively completely absorbed. It was hoped that the choice of crystals smaller than optimum size would avoid this source of error.

Corrections for absorption were made using the Busing-Levy method for the data of the four crystals. Lorentz factor and polarisation corrections were made using the standard formulae given by Buerger (Computer Programme:- Data Reduction 04, written by C. K. Prout.)

Spot shape corrections were made for the $[Co(QP)Cl]^+$ complex only. Here the a axis and b axis data were measured on the expanded and

contracted sides of the photograph respectively. Spot shape corrections were calculated empirically by plotting the reciprocal of the spot length against 'sin θ ' for each layer. The spot lengths were measured with a Cambridge travelling microscope. Values of the corrections could then be derived for reflections of any 'sin θ ' on any layer.

For the thallium complex, data collected on the expanded and contracted sides on the a and b axes respectively were merged. On both the other complexes data were measured on the contracted side for both axes.

Determination of layer scale-factors

The intensity data obtained by visual estimation from the Weissenberg photographs were on arbitrary scales. Layers of reciprocal space collected from two axes intersect, giving more equations than necessary to determine the scale-factors needed to put the data on a common scale.

38

In the Hamilton, Rollett and Spark method, the function minimised is

$$M = \sum_h \sum_i w_{hi}(F^2_{hi} - k_i^{-1} F^2_h)^2$$

where the reflection F^2_h is measured as F^2_{hi} on layer 'i' and is uncertain by $(w_{hi})^{-\frac{1}{2}}$. k_i is the scale-factor for layer 'i' and F^2_h is $(\sum w_{hi} k_i^{-1} F^2_{hi})/(\sum_i w_{hi} k_1)^{-2}$.

An advantage of this method is that the minimisation function is not altered by multiplying every k_i by the same factor. Therefore, k_i may be unity as no normalisation is required and consequently no latent vectors need be found.

Initially trial values of k_i derived from exposure times were used, which were improved by an iterative process. Weights were

estimated from the uncertainty of measurement of each reflection used in the scale-factor calculation. Factors such as the number of times the reflection was measured, the whereabouts on the visual comparison scale of the equivalent reflection and the effects of spot-shape errors were taken into account.

The data were placed on a common scale using the scale-factors calculated by this method by a programme written in autocode by Dr. Sparks. The scale-factor application programme was written in autocode and usercode for the KDF9 computer by Mr. O. J. R. Hodder.

Intensity statistics

A statistical analysis of the $\underline{F}^2$ values was required to provide two types of information:-

a) a knowledge of their absolute scale and an overall temperature factor for the crystal,

b) information about the space-group symmetry that cannot be obtained from systematic absences.

In the crystal structure analysis of $[TlMe_2^1,10\text{-phen}]ClO_4$, $(TTAs)Ag\text{-}Co(CO)_4$ and $[Pd(TPAS)Cl]ClO_4.C_6H_6$, the space groups are determined unambiguously by the symmetry of the reciprocal lattice and the systematic absences. Moreover, the calculation of absolute scale and of temperature factors was not required by this method. The temperature factors were estimated quite accurately by inspection of the Weissenberg photographs. More accurate values of these parameters

as well as the scale factor were then obtained by least squares refinement. The success of this method which is discussed in more detail on page 103, depends on the derivation of accurate atomic positions of heavy atoms (from the Patterson function) that are at least 90% of the scattering matter. Thus, no statistical analysis of $\underline{F}^2$ values was carried out for these complexes.

For the $[Co(QP)Cl]BPh_4$ crystals, both types of information were required from an analysis of the statistical properties of reciprocal space. First, the absolute scale and temperature factors could not be determined by least squares procedures. The values of these parameters were needed for the calculation of normalised $\underline{F}_o$ values, $\underline{E}$ values and for use in the Fourier syntheses. Secondly, in order to distinguish between $\underline{P2_1nb}$ and $\underline{Pmnb}$ a test for a centre of symmetry was required. This should confirm information from a piezo-electric test and the observation of anomalous dispersion effects both indicating the correct space group to be $\underline{P2_1nb}$.

As this type of problem involving several thousands of data has frequently re-occurred in the laboratory, the author decided to write a general computer programme to deal with intensity statistics, giving special emphasis to cases with heavy atoms. A discussion of the methods used as far as they are relevant to the structure of $[Co(QP)Cl]BPh_4$ is included in this section. A fuller description including flow diagrams and other details of the programme, which is written in C203 autocode for the KDF9 computer, are included in the

Appendix V , page 188.

a) The intensity may be expressed as

$$I_h = F_h F^*_h = \sum_{j=1}^{N} g_j^2 + 2 \sum_{j=1}^{N} \sum_{k>j}^{N} g_j g_k \cos\left[2\pi i \underline{h}.\underline{r}_{jk} \right]$$

where g_j is the scattering factor adjusted for thermal attenuation for atom $\underline{i}$. In calculating the mean, $\langle I_h \rangle$, Wilson assumed that the second term in the expression would cancel out, there being an equal chance of its being positive or negative. Thus

$$I_h \simeq \sum_{j=1}^{N} g_j^2$$

$$= \exp\left[-2B \sin^2\theta / \lambda^2 \right] \sum_{j=1}^{N} f_j^2$$

The measured intensities, $F_o^2(h)$ are on an arbitrary scale so that

$F_o^2(h) = \underline{K}\, I_h$

Thus, $$\ln\left[\langle F_o^2(h) \rangle / \sum_{j=1}^{N} f_j^2 \right] = \ln K - 2B \sin^2\theta / \lambda^2$$

and a plot of $\ln\left[\langle F_o^2(h) \rangle / \sum_{j=1}^{N} f_j^2 \right]$ versus $\sin^2\theta / \lambda^2$ should give a straight line, and thence $\underline{K}$ and $\underline{B}$.

The mean of the measured reflecioons was calculated allowing for multiplicity factors, and the following:-

1) Reflections in a sphere around the origin with $\sin\theta < \lambda / a_{min}$,

where a_{min} is the shortest axis length, must be excluded as the vectors for these in the phase-amplitude diagram cannot be treated as independent random variables.

2) Certain characteristic groups of reflections have abnormally high intensity averages. For instance, if a crystal has a mirror plane perpendicular to b, in projection on (010) atoms will overlap in pairs and the average intensity will then be given by

$$\sum_{j=1}^{N/2} (2f_j)^2 = 2\sum .$$

In this case the symmetry number is 2. Similar abnormally high local averages result from n-fold rotors or screw axes where the symmetry number is n and also glide planes. However, if reciprocal space were integrated to infinity, the off-diagonal terms must cancel out. Wilson's equation must be true even when these local averages must be compensated for in other parts of reciprocal space. In the case of glide planes or screw axes, this is achieved by systematic absences, but in cases of mirror planes and rotors there are parallel low intensity regions. In the latter regions, the mean does not appear to be affected by such a great percentage change as in the high local average regions; they cover greater regions of reciprocal space.[40]

In fact, if a mirror plane or rotor were known to occur, it would be best to modify the reflections in order to compensate for these abnormal local averages. However, as so little is known about these factors, it is probably unwise at the present time. The author has

divided only reflections in the abnormally high local average zones by symmetry numbers. This is probably the best procedure as ignoring these high local averages would tend to increase the local means at low $\sin\theta$, whereas the low local averages are more evenly distributed in reciprocal space. Of course, systematic absences in zones of reciprocal space must be ignored.

3) The Wilson plot may also be affected by a large off-diagonal term. This cannot be foreseen in most cases. However, it is wise to examine the Patterson function in conjunction with the intensity statistics, when an abnormally large peak due to superposition of several vector-peaks will give evidence of a perturbation of the Wilson plot or other intensity statistics. Of course, heavy atoms in the unit cell give rise to similar perturbations.

A Wilson plot was computed for the $[Co(QP)Cl]BPh_4$ crystals. The space group could be either Pmnb or $P2_1nb$. Due to this ambiguity, reflections 0,k,l were omitted from the calculations, but the reflections with high intensity averages due to glide planes were divided by the relevant symmetry numbers. Multiplicity numbers were allowed for and reflections of $\sin\theta <$ 1.52/18.25 were excluded. Values of K and B were calculated from the values of $\ln\left[\langle F_o^2(h)\rangle / \Sigma f_j^2\right]$ at different values of '$\sin^2\theta$' both graphically and by fitting a straight line by least squares in the computer (see Appendix V , page 188).

The values of K and B derived from the least squares fit to the Wilson plot are 15.7 and 1.7Å^2 respectively. The value of K compares

quite closely with 13.7, obtained by the final least squares refinement of all parameters.

b) The information about the space-group is obtained in two ways:-

1) The first is by examining doubtful zones of reciprocal space to see if they have abnormally high intensity averages. For this all the $\underline{F}^2$ values were corrected for known symmetry numbers, thermal vibrations and fall-off of intensity due to fall-off of the scattering factors with $\sin\theta$. The computer programme does this in the machine immediately after calculating B and K (see Appendix V , page 188).

The mean value of reflections (0,k,l) was compared to that of other reflections. This zone did not appear to have an abnormally high average - the first confirmation that the space-group is not Pmnb.

2) The second method was to analyse the intensity distribution of the whole of reciprocal space. The analysis of zones was not carried out as these are liable to lead to errors through non-randomness.

For a centrosymmetric crystal with a large number of random distributed, approximately equivalent atoms, the probability, $_1^-P(I)$, of finding an intensity between I and dI is given by:-

$$_1^-P(I)dI = (2\pi pI\Sigma)^{-\frac{1}{2}} \exp(-I/2p\Sigma)dI$$

while the corresponding expression for a non-centrosymmetric crystal is:-

$$_1P(I)dI = (p\Sigma)^{-1} \exp(-I/p\Sigma)dI$$ [41,42]

It is advisable to carry out as many tests as possible to determine whether the observed distribution is centric or acentric.

The following methods are all different ways of defining these distributions, and, of course, they should only hold when there are many randomly distributed, equivalent resolved atoms. All computations were made by the programme described in Appendix V, page 188.

Let z be defined as $\frac{I}{\langle I \rangle}$.

Initially plots of $\sqrt{p\Sigma}.P(F)$ against $z^{\frac{1}{2}}$ and $P(I)$ against z were computed for $(Co(QP)Cl)BPh_4$. The area under the curve between two values of z should give the probability of finding a value of F or z between these values.

These probability plots are very dependent on good and sufficient data. Although various authors have recommended their use with full three-dimensional data,[43] the plots for $[Co(QP)Cl]BPh_4$ were unlike the theoretical distributions probably due to sampling errors. No deductions were made from this work.

Next the equivalent cumulative plots were computed.[44] These are shown in Figure 2.2. The values of $N(z)$ and $N(F)$ at small values of z were ignored. This was because intensities less than the minimum on the visual comparison scale were ignored, and were interpolated as zero by the 'intensity-statistics' computer programme. The plots are close to the acentric distribution confirming the space group, $P2_1nb$. The centric and acentric distributions are not valid when the unit cell has non-crystallographic centres of symmetry, or when the atoms are few in number or differ in weight, or occupy both general and special

Figure 2.2

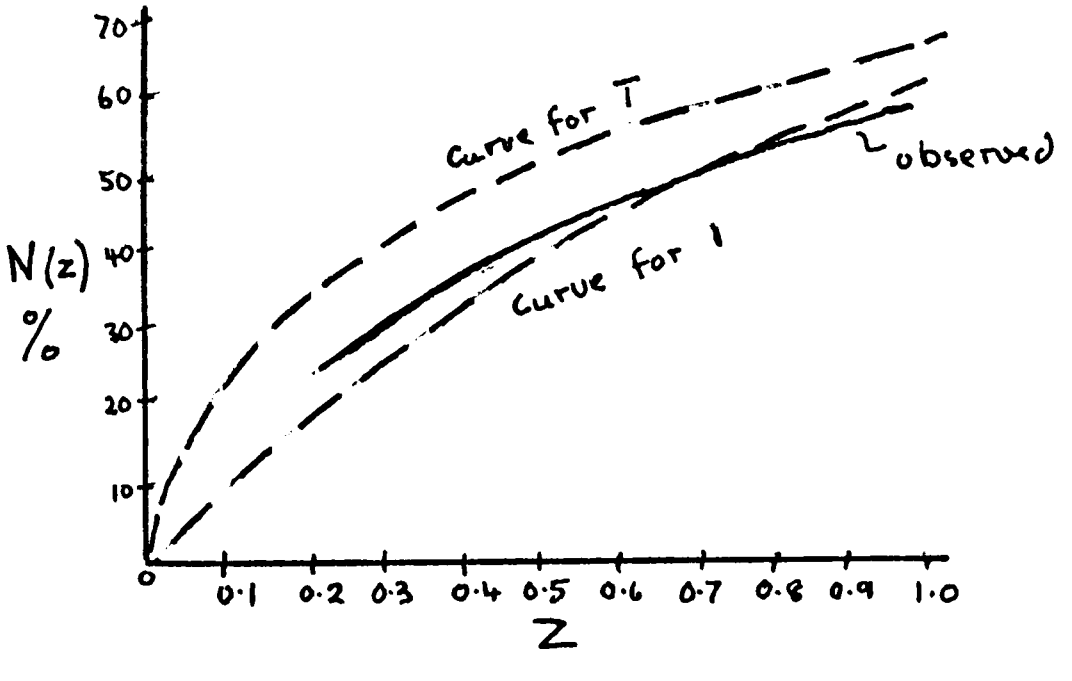

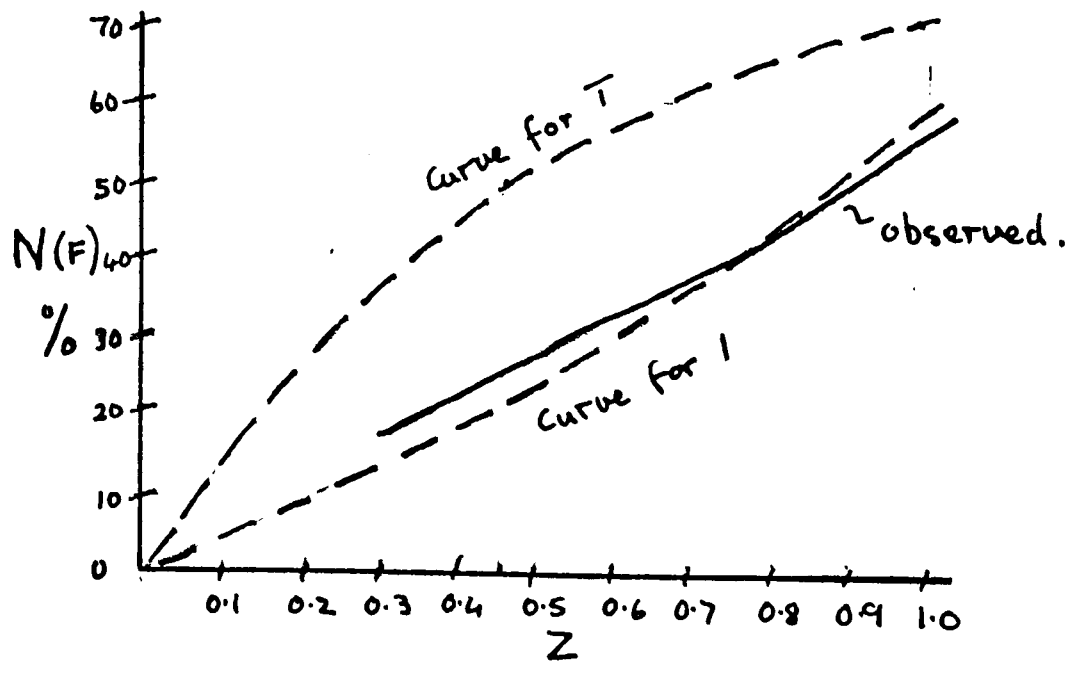

Cumulative probability graphs for $(Co(QP)Cl)^+$

positions. The success of the adaption of the methods described above to such cases has depended on the space group. They are most reliable when there is only one heavy atom in the asymmetric unit.

Hargreaves claims the use of general moment tests are more reliable.[45] The theoretical and experimental moments of $z(=I/\langle I\rangle)$ are compared, the rth moment of z being given by $\langle z^r\rangle = \langle I^r\rangle / \langle I\rangle^r$. The calculation of these theoretical moments for particular structures is not difficult. In fact only seven types of formulae are required to calculate the theoretical moments for atoms in general positions of all the triclinic, monoclinic and orthorhombic space groups except Fddd and Fdd2.

For $[Co(QP)Cl]BPh_4$ two possible space groups are $P2_1nb$ for which

$$\langle z^2\rangle = 2 - \tfrac{1}{2}S(4)/S(2)^2$$

$$\langle z^3\rangle = 6 - \frac{9}{2}\,S(4)/S(2)^2 + S(6)/S(2)^3$$

and Pmnb

where $$\langle z^2\rangle = 3 - \tfrac{3}{4}S(4)/S(2)^2$$

$$\langle z^3\rangle = 15 - \frac{45}{4}\,S(4)/S(2)^2 + \frac{5}{2}\,S(6)/S(2)^3$$

In these expressions $S(r) = \sum_{i=1}^{N} f^r$.

However, in $[Co(QP)Cl]BPh_4$, if the space group is Pmnb a cobalt, a chlorine and a phosphorus atom and some lighter atoms must lie on the

mirror plane. The positional parameters of the atoms lying on the mirror plane are only variable in two dimensions and give rise to a different expression for the geometrical structure-factor. The correct expressions are

$$\langle I_a \rangle = \langle I_g \rangle + \lambda^2 \langle I_s \rangle$$

$$\langle I_a^2 \rangle = \langle I_g \rangle + \lambda^4 \langle I_s^2 \rangle + 4\lambda^2 \langle I_g \rangle \langle I_s \rangle$$

$$\langle I_a^3 \rangle = \langle I_g \rangle + \lambda^6 \langle I_s^3 \rangle + 9\lambda^4 \langle I_g \rangle \langle I_s^2 \rangle + 9\lambda^2 \langle I_g^2 \rangle \langle I_s \rangle$$

where $\lambda = \frac{\text{No. of equivalent special positions in the unit cell}}{\text{No. of equivalent general positions in the unit cell}}$

where $\langle I_g^r \rangle$ and $\langle I_s^r \rangle$ are evaluated as above for the atoms in general and special positions.

The theoretical values of $\langle \underline{z}^2 \rangle$ and $\langle \underline{z}^3 \rangle$ for Co(QP)Cl BPh_4 were close to 2 and 6 for $\underline{P2_1nb}$ and 3 and 15 for $\underline{Pmnb}$, which are the values for the random model of equivalent resolved atoms. The observed values were 2.22 and 7.09 for $\langle \underline{z}^2 \rangle$ and $\langle \underline{z}^3 \rangle$, confirming the non-centrosymmetric space-group.

CHAPTER 3

SOLUTION OF THE PHASE PROBLEM

Patterson Functions[46]

Three-dimensional, sharpened Patterson functions were computed for the four crystal structures reported here. Two-dimensional functions were not computed; in all cases the required stereochemical information necessitated the use of more accurate three-dimensional studies. For the crystal structures of $[Pd(TPAS)Cl]ClO_4.C_6H_6$ and $(TTAS)Ag\text{-}Co(CO)_4$, two-dimensional analyses might have indicated the approximate stereochemistry and confirmed the existence of a metal-metal bond respectively. These were not proven chemically. However, the complexity of the Patterson functions resulting from these molecules with several 'heavy' atoms seemed to preclude any reliable conclusions from the two-dimensional functions.

The three-dimensional Patterson functions were computed using the general Fourier synthesis programme written by J. S. Rollett for the KDF9 computer.

The scales of the Patterson functions were adjusted to give an origin peak of 999 in order to simplify the map output routine. All peaks recorded in the following discussion are on this scale.

The expected peak-heights were calculated from the following approximation:-

$$\text{Height of Patterson peak (ij)} = \text{Height of origin peak} \times \frac{Z_i Z_j}{\sum_{j=1}^{N} Z_j^2}$$

where Z_i and Z_j are the atomic numbers of atoms i and j respectively.

Analytical procedures making full use of superposition methods and implication diagrams of Harker lines and sections were used in conjunction with the chemical information available in the interpretation of the Patterson functions. Usually it was difficult to decide the 'weight' to be given to the chemical information. $[Pd(TPAS)Cl]ClO_4.C_6H_6$, for instance, might have been trigonal bipyramidal, square pyramidal or some intermediate geometry, or even four co-ordinate. In fact, the chemists indicated the complex was square pyramidal with an apical chlorine atom. This proved to be incorrect. Thus, chemical information was always treated as suspect, and any hypothesis concerning the structure based on this was carefully checked as soon as possible.

The Patterson function of $[TlMe_2$1,10-phen$]ClO_4$ is not described. The solution was trivial. The crystal structures of the other three complexes contained between five and seven atoms per asymmetric unit, and the interpretations of their Patterson functions are described in detail.

The interpretation of the Patterson function of $[Pd(TPAS)Cl]ClO_4.C_6H_6$

This complex crystallises in space group $P2_1/c$ with one palladium, one chlorine and four arsenic atoms in the asymmetric unit (Appendix II, Page 166). Chemical information indicates that the complex has a square pyramidal stereochemistry with a chlorine in the apical position (Page 15).

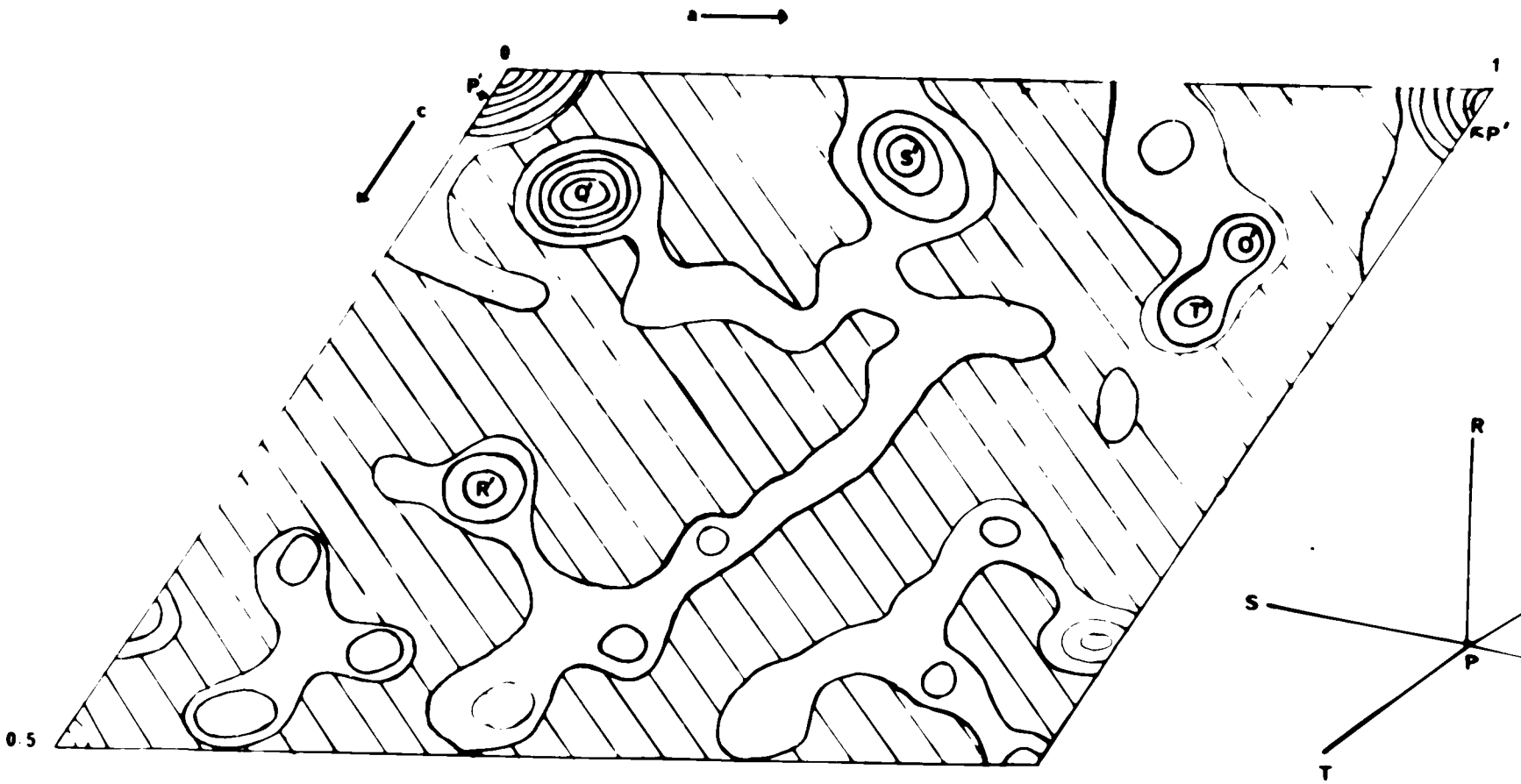

Fig 23 (a) $[Pd(TPAS)Cl]ClO_4$: PATTERSON SYNTHESIS

HARKER SECTION AT 'Y' = 0.5

Fig 23 (b)

The Harker section at $y = \frac{1}{2}$ was first investigated. (Figure 2.3(a), Page 51). An implication diagram of this Harker section was generated and sets of peaks corresponding to a projected square pyramid were investigated. Confusion was caused by the fact that the very large peak, Q', was not in fact a Harker peak, and also that peak heights were not consistent with the lighter ligand atom, chlorine, being at the apex of a square pyramid. A model given in Figure 2.3(b), Page 51 was chosen as the most reasonable arrangement of atoms.

To confirm this model intramolecular vectors were investigated. No arrangement could be found that was consistent with Q' being a Harker peak. Many of the intramolecular vectors were unresolved. Further it was discovered that peak Q' was clearly elongated compared with other peaks on the Harker section, confirming that this was not a Harker peak.

An investigation of the general vectors between the molecules related by the two-fold screw axis identified Q' as a superposition of three vectors between the ligand atoms, and indicated that U was probably the chlorine atom.

The interpretation of the Harker line, $(0, y, \frac{1}{2})$ given in Figure 2.4 was confused by the fact that palladium atoms related by the two-fold screw axis had almost the same x and y co-ordinates, so that the palladium inversion vector at y = 0.213 also fell on the Harker line. The palladium Harker peak at y = 0.288 was surrounded by unresolved ligand Harker peaks.

The general vectors between the molecules related by the glide plane, the inversion vector peaks and the corresponding general vector peaks were identified, giving final confirmation of the deductions already made.

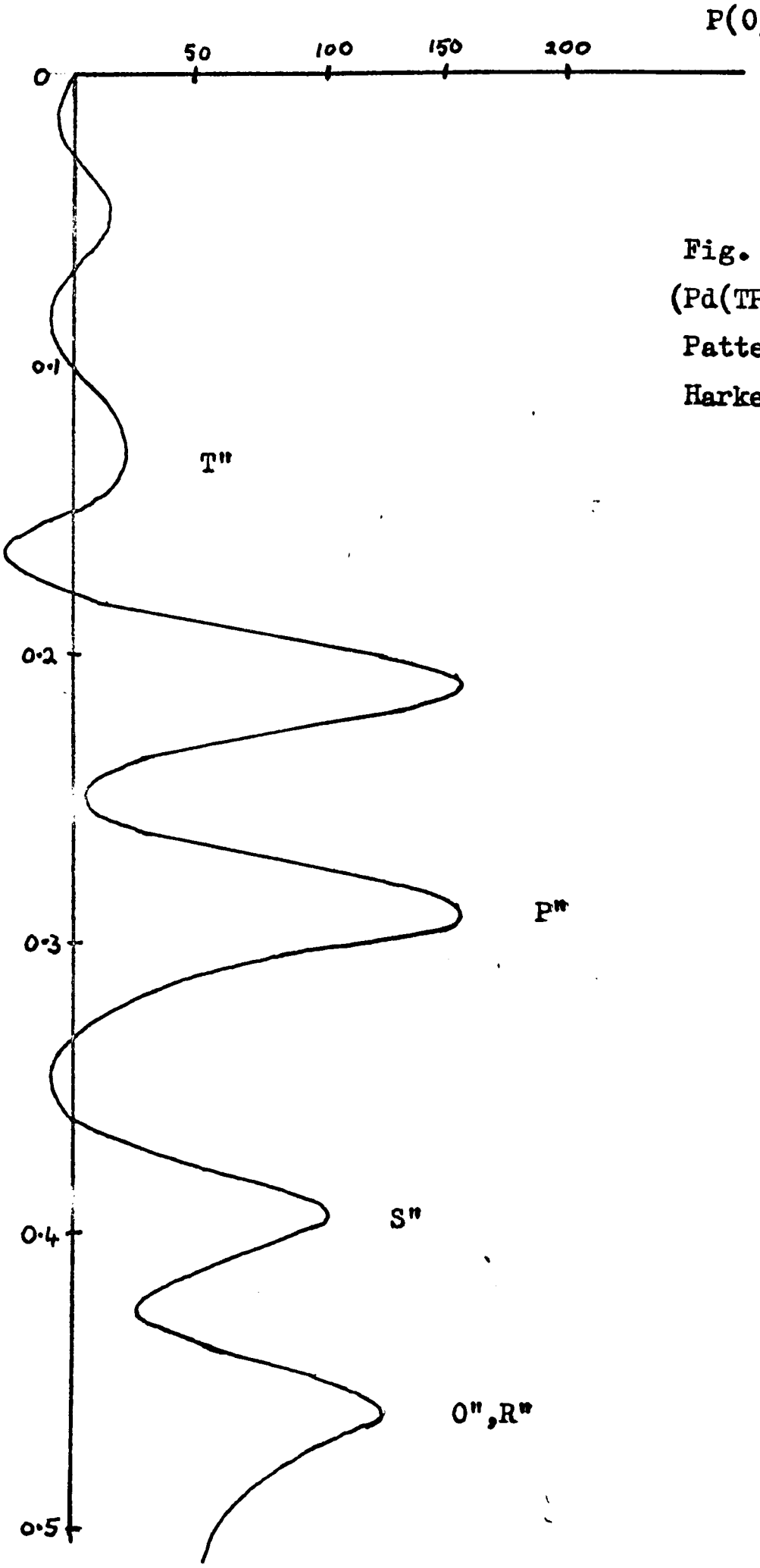

Fig. 2.4
$(Pd(TPAS)Cl)ClO_4$
Patterson Function
Harker Line $(0,y,\frac{1}{2})$

The co-ordinates and peak-heights of all the vector peaks identified were tabulated. They comprised 45 peaks apart from those related to vectors involving the atom U. The co-ordinates of the atoms of one molecule in real space were derived from these data, weighting the information from each peak according to its shape, and the degree of overlapping with other peaks. Thus, Harker line peaks were given little weight in the derivation of the atom co-ordinates, although they were very useful in the initial identification of vector peaks. The co-ordinates of the atoms derived from this Patterson function compared closely with the values derived from the least squares refinement after the placing of all the light atoms.

The fifth ligand atom, U, was correctly identified as the chlorine atom. It was not included in the subsequent Fourier synthesis, as most of the general vector-peaks between other ligand atoms and U (which are important in its correct positioning) were not identified with confidence.

The interpretation of the Patterson function of $(TTAS)AgCo(CO)_4$

This complex, which crystallises in $P2_1/n$, has five heavy atoms per asymmetric unit. Chemical evidence indicated that the three arsenic atoms and the cobalt atom form a distorted tetrahedron around the silver atom.

The solution of the Patterson function was a similar problem to the solution of the Patterson function of $[Pd(TPAS)Cl]ClO_4.C_6H_6$. However, as the Harker plane (Figure 2.5) contained several large non-Harker peaks, superposition and analytical procedures were first used to

Fig. 2.5. The Patterson Function of $(TTAS)Ag\text{-}Co(CO)_4$

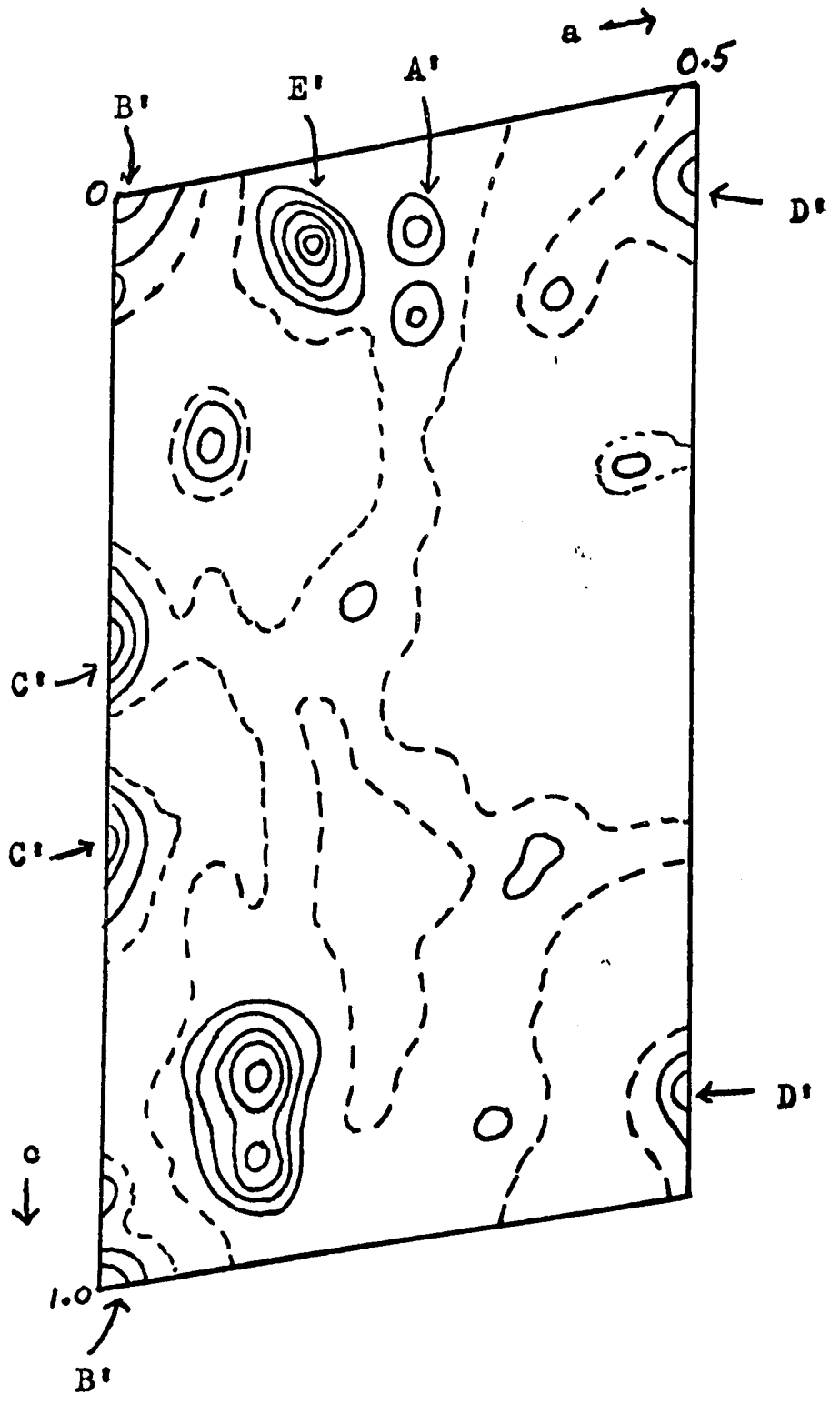

Harker Section $(\underline{x}, \frac{1}{2}, \underline{z})$

Scale : Origin peak ,P(0,0,0) = 999 .
Contours at intervals of 30.

identify intramolecular vector peaks to give the fundamental set. It was then possible to identify E' as the silver Harker peak and A', B', C' and D' as ligand Harker peaks on the Harker plane. The interpretation of the Patterson function was then completed by the systematic identification of all Harker-line vectors, inversion vectors and the corresponding general vectors.

This work confirmed the initially chosen fundamental set, indicating a distorted tetrahedral co-ordination of the silver with small $\langle$As-Co-As angles.

The interpretation of the Patterson function of $[Co(QP)Cl]BPh_4$

This compound crystallises in space-group $\underline{P2_1nb}$, with one cobalt complex cation and one tetraphenyl borate anion per asymmetric unit. Chemical and spectral evidence indicated that the cobalt complex had an approximately trigonal bipyramidal stereochemistry as required by the quadridentate phosphorus ligand, QP (page 21). The chlorine atom was assumed to occupy an axial site.

The fundamental space symmetry is $\underline{P2_1nb}$, for which an atom at $\underline{x}, \underline{y}, \underline{z}$ has equivalents at

$$(\tfrac{1}{2} + \underline{x}, \overline{\underline{y}}, \overline{\underline{z}}), (\underline{x}, \tfrac{1}{2} + \underline{y}, \tfrac{1}{2} - \underline{z}), (\tfrac{1}{2} + \underline{x}, \tfrac{1}{2} - \underline{y}, \tfrac{1}{2} + \underline{z})$$

due to the screw axis, $\underline{b}$ axis glide and diagonal glide respectively. The space group of the Patterson function is $\underline{Pmmm}$, one atom and its equivalents producing peaks in $P(\underline{x},\underline{y},\underline{z})$ at the points

$$(\tfrac{1}{2}, +2\underline{y}, +2\underline{z}), (0, \tfrac{1}{2}, +2\underline{z}), (\tfrac{1}{2}, \tfrac{1}{2} + 2\underline{y}, \tfrac{1}{2})$$

and symmetry related points.

A three-dimensional sharpened Patterson function was computed. The Harker lines resulting from the axial and diagonal glide planes (Figure 2.6) and the Harker section from the screw axis (Figure 2.7) are represented on a scale such that the origin peak is 999. Cobalt, phosphorus and chlorine Harker vectors should then occur with peak heights of 158, 52 and 72 respectively.

Usually, the Harker section is the best place to start the analysis of such a Patterson function, but in this case it clearly contains a considerable number of non-Harker peaks, and also the peaks on the

Fig. 2.6 The Crystal Structure of $(Co(QP)Cl)BPh_4$

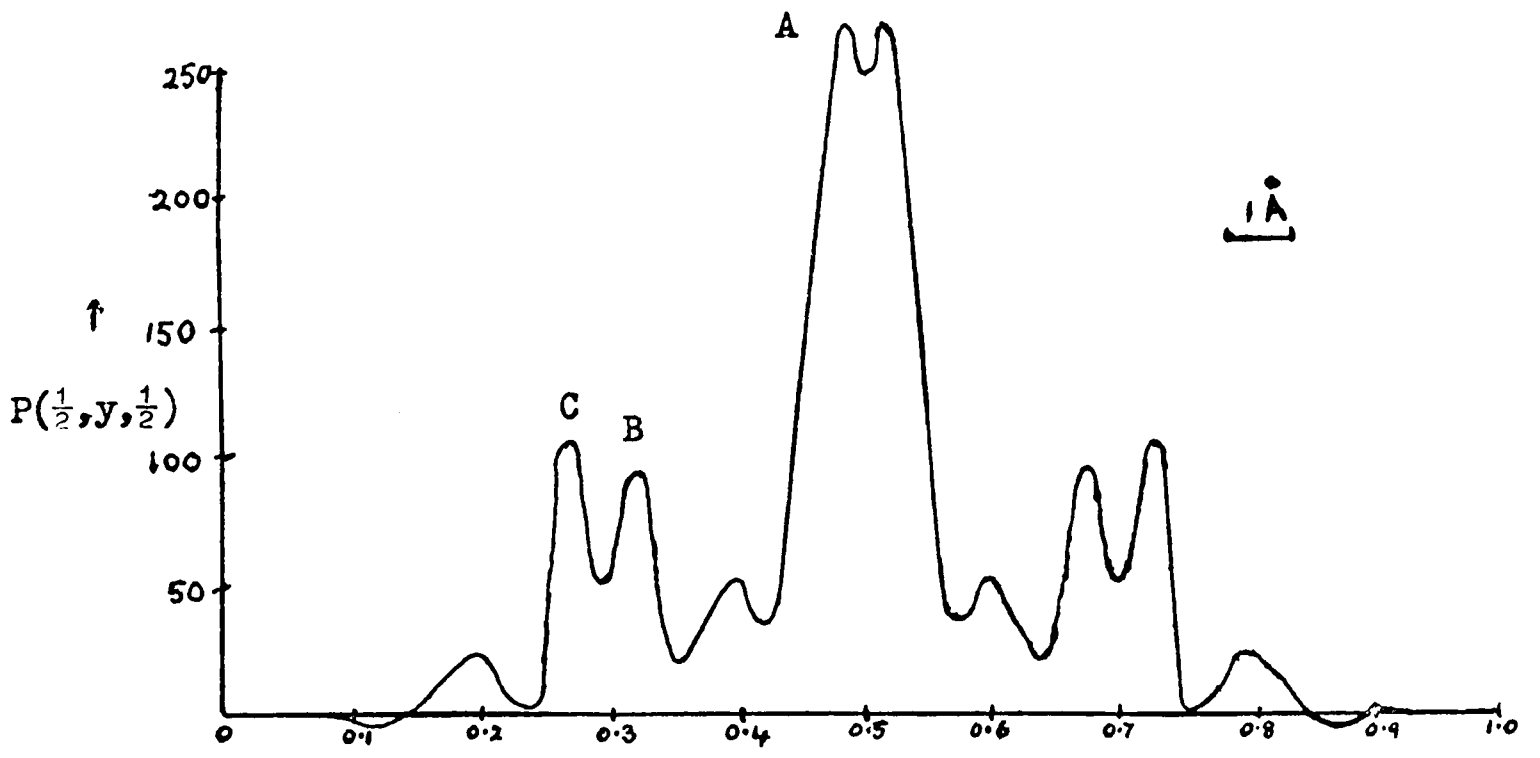

a) Harker Line ,$(\frac{1}{2},y,\frac{1}{2})$

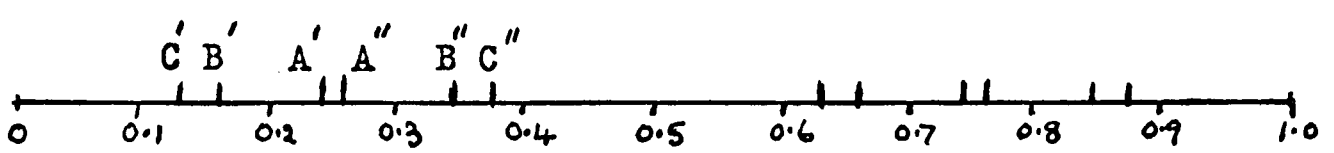

B) Implication diagram, $(\frac{1}{2},y,\frac{1}{2})$.

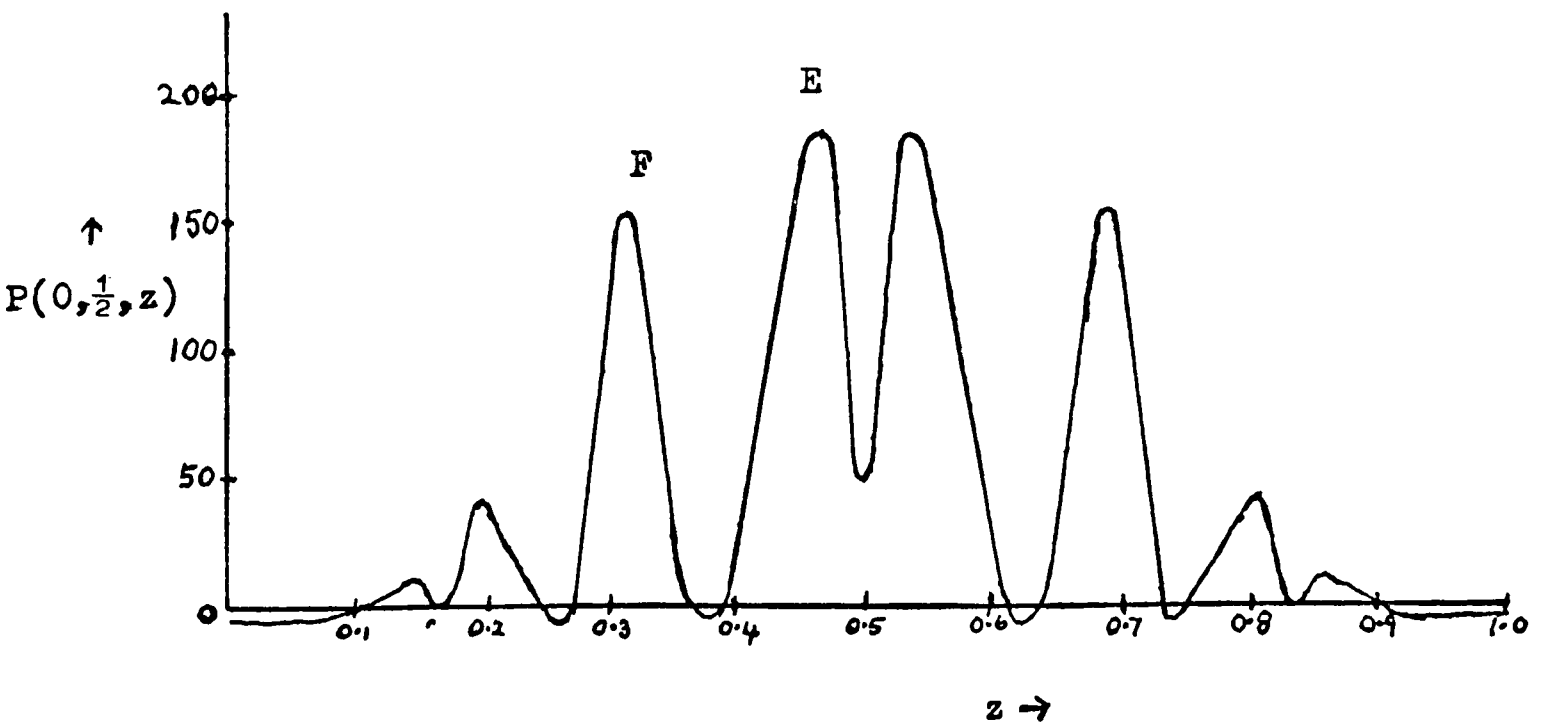

c) Harker Line ,$(o,\frac{1}{2},z)$

Figure 2.7

The Patterson Function for $[Co(QP)Cl]BPh_4$

Harker section

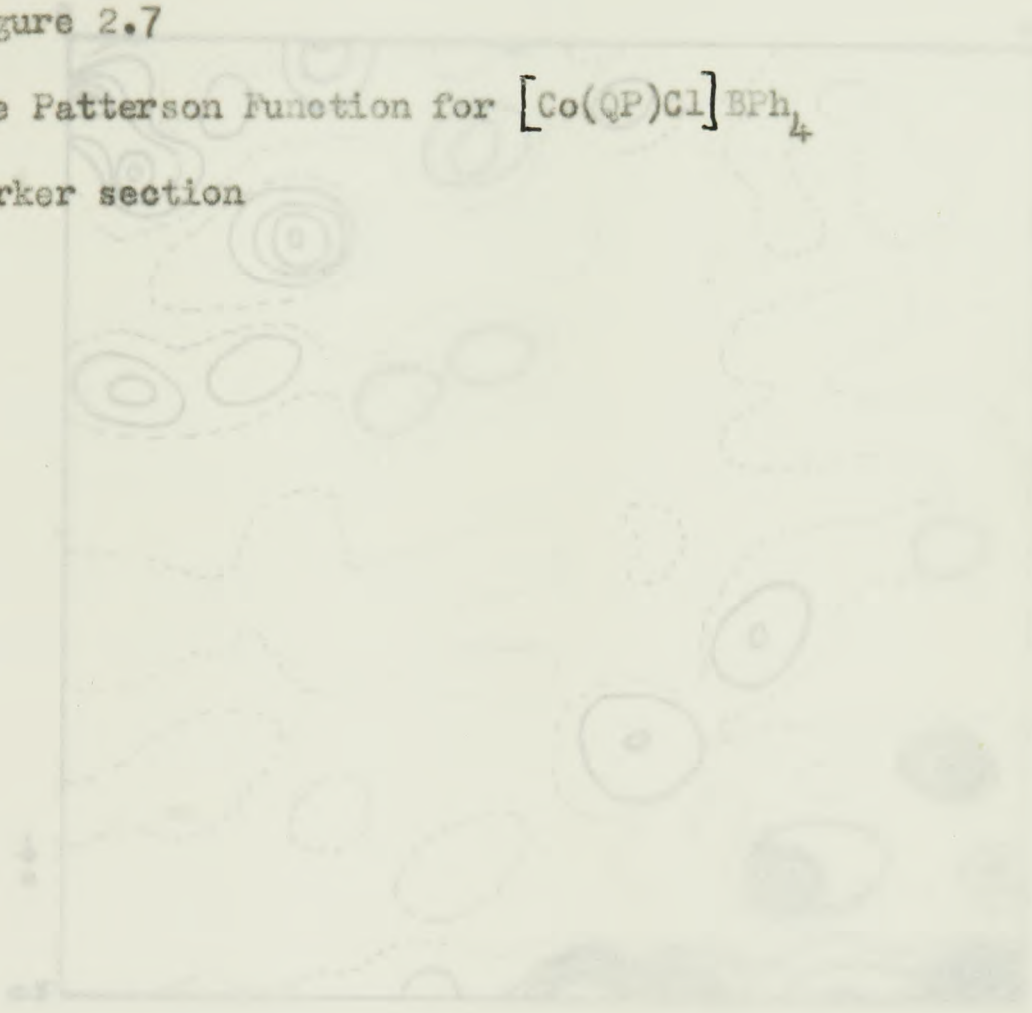

Figure 2.8

Implication Diagram

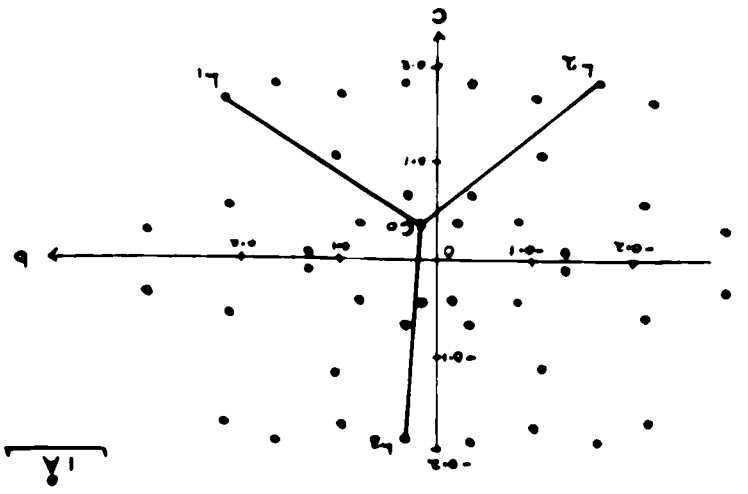
c
b
L1
L2
L3
1Å

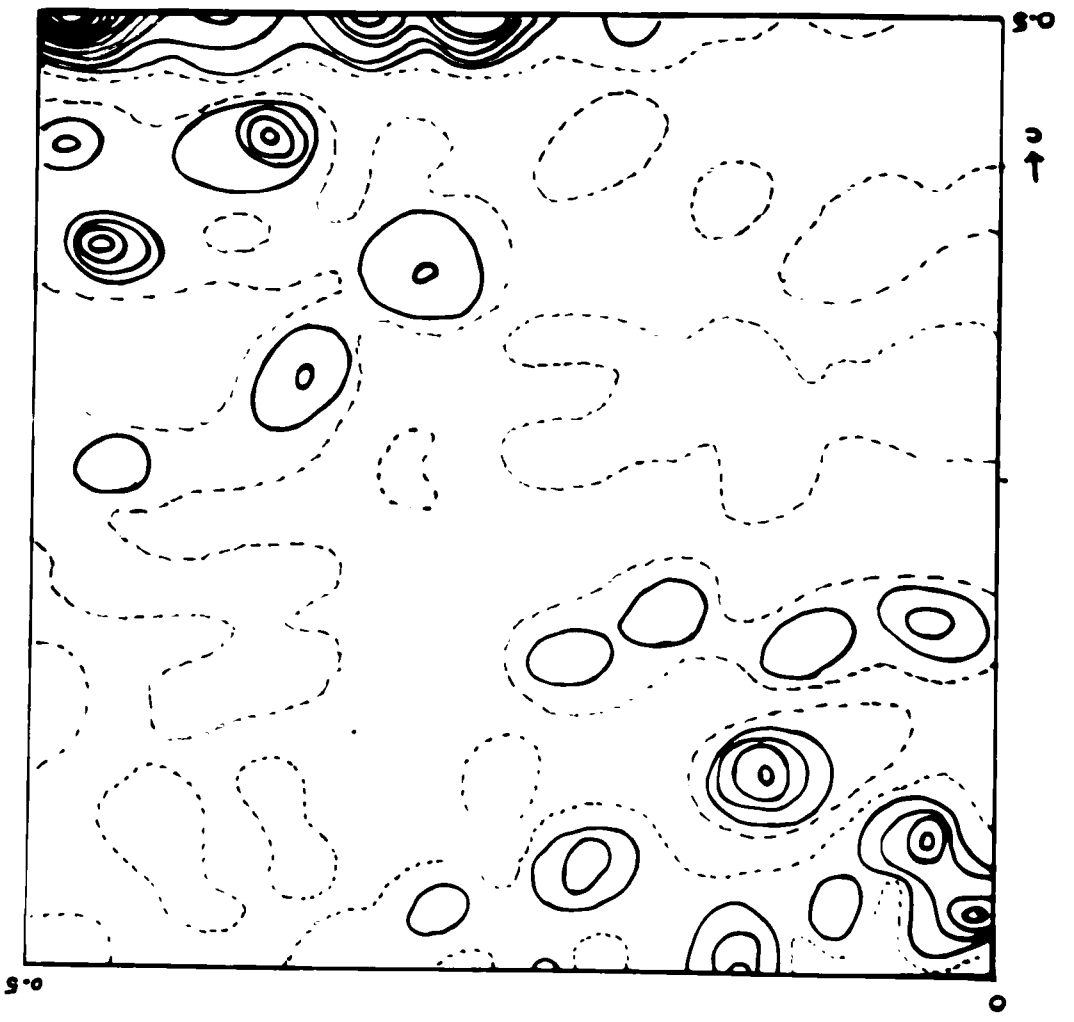
0.5
c
0.5
0
b

Harker line resulting from the diagonal glide. It seemed very likely that some of the peaks with y, and z co-ordinates less than 0.25 were the Harker peaks due to the screw axis, but the complexity of the implication diagram resulting from these peaks underlines the difficulty of starting the interpretation of the Patterson function at this point. Part of the implication diagram is shown in Figure 2.8. It has been generated by including all peaks of height 20 on the Harker section.

In fact the Harker line at $\frac{1}{2},y,\frac{1}{2}$ due to the diagonal glide was first interpreted. The reason for this was because the peak, A, was the only peak large enough to be a cobalt Harker peak, whereas two peaks were of the required height on the other Harker line.

The implication diagram corresponding to this Harker line is shown in Figure 2.6(b). The peak heights are not indicated, and the diagram has been generated using only peaks A, B and C on the Harker line.

Let A' be the position of the cobalt atom projected onto [010]. Now the covalent radii of Co(II) and P are given by Pauling as 1.30Å and 1.1Å, and therefore a Co-P bond length in the complex should be of the order of 2.40Å. Thus possible ligand atom positions projected onto [010] are C', B', B", C", A". The intramolecular bond lengths in projection would then be

A' A"	0.45Å
A' C'	1.83
A' B'	1.38
A' B"	1.84
A' C"	2.28

In the interpretation of the Patterson function, a trigonal

bipyramidal model is assumed (see Page 21). No distinction was made between the chlorine and the phosphorus ligand atoms, which were labelled as in Figure 2.9.

Using this model the Harker line could be interpreted in three different ways. These are as follows:-

1) The axis of the trigonal bipyramid is parallel to b (Figure 2.9(b1). The two axial bonds would then be about 1.8Å and 2.3Å if axial positions were at C' and C". This seemed unlikely at the time for two reasons. First, the peak at B would be difficult to explain, and certainly could not be a Harker peak. Secondly, the bond length of 1.8Å was much too short, even if it were slightly shortened by a non-coincidence of direction of the unit cell axis and the trigonal bipyramidal axis. This possibility was, therefore, excluded. In retrospect the evidence seems less conclusive as one of the axial bonds turned out to be very short at 2.06Å.

2) The axis of the trigonal bipyramid is perpendicular to b, but one equatorial bond, Co-L(1), of length 2.3Å, lay parallel to b with L(1) at C" (Figure 2.9(b2). The other two equatorial atoms, L(2) and L(3) would superpose in projection at B', This is possible as peak B is twice the height expected for a phosphorus Harker peak.

3) The axis of the trigonal bipyramid is perpendicular to b with one equatoial bond, Co-L(3), in the direction of c (Figure 2.9(b3). The Harker peaks of cobalt, L(3), L(4) and L(5) would then superpose. The two remaining equatorial ligand bonds would then make an angle of 30°

Fig. 2.9 .The Crystal Structure of $(Co(QP)Cl)BPh_4$

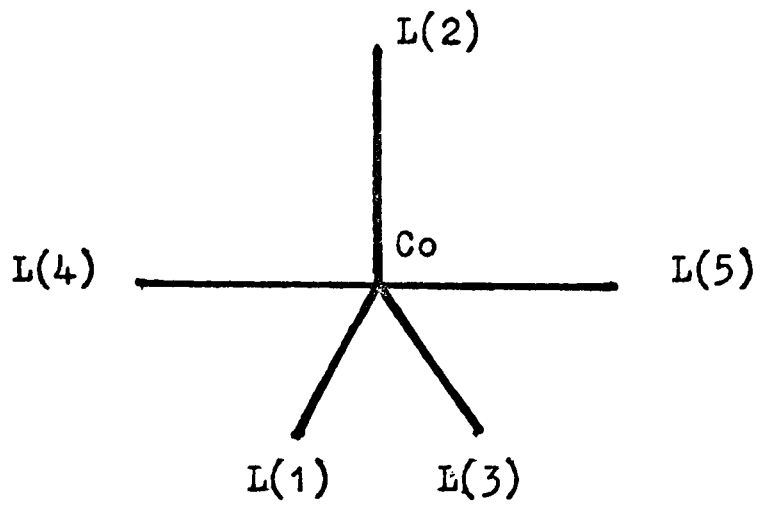

a) The labelling of the ligand atoms.

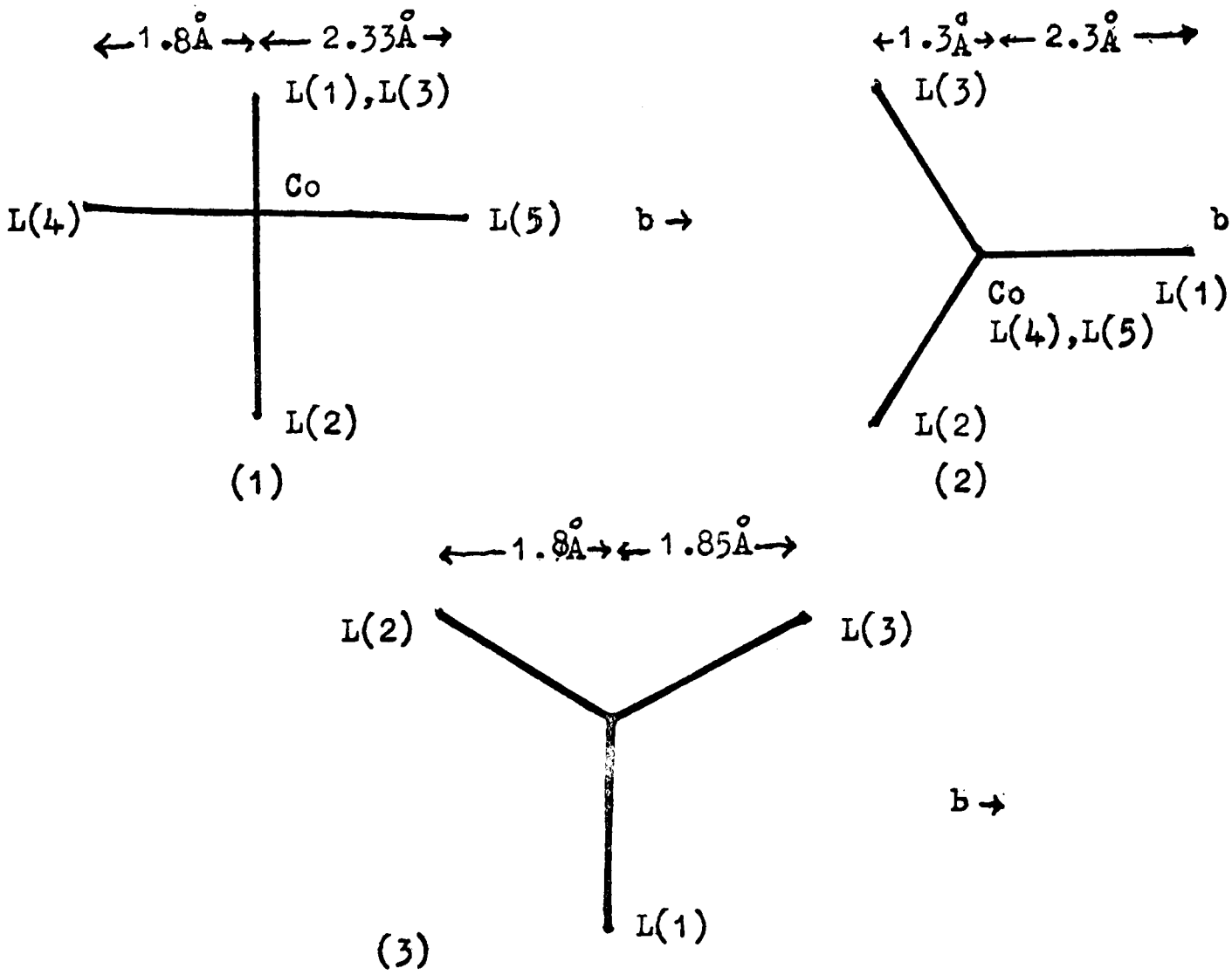

b) Interpretation of the Harker Line $(\frac{1}{2},y,\frac{1}{2})$
Three possible orientations for the trigonal bipyramid.

with b, and project onto b at C' and B".

With these two hypotheses in mind, possible general vectors between atoms of the diagonal glide plane related molecules were investigated. Also the superposition method was used. The co-ordinates of the vector peaks around the origin and the Harker peak, A, were listed. The vector set around the Harker peak was then put at the origin, and coincidences of points in the two superposed vector sets were used to delineate fundamental set. This set was in fact constant with the third hypothesis.

Vector peak positions for all intramolecular vectors and all general vectors between the six heavy atoms of the two molecules related by the diagonal glide were identified, and recorded.

These vectors showed that the axis of the trigonal bipyramid lay approximately parallel to a, with one equatorial bond parallel to c as shown in Figure 2.10 .

At this stage in the analysis, it was apparent that the approximate coincidence of the molecular axis with a crystal axis giving rise to the complete or partial superposition of many peaks would prohibit the exact locating of the molecular axis.

The second stage of the analysis of the Patterson function of the cobalt complex was the interpretation of the Harker line (0, $\frac{1}{2}$, z), due to the b axis glide plane. This Harker line is shown in Figure 2.6, and has two well resolved, very large peaks E and F.

Both these peaks have a greater peak height than required for a cobalt Harker peak.

The information derived previously indicated that the approximately trigonal bipyramidal model has its axis almost perpendicular to the c axis, which approximately bisects the angle between atoms L_1 and L_2 in the equatorial plane. The peak 'E' is consistent with this model if it represents the superposition of Harker vector peaks due to the cobalt and two ligand atoms $L_{(4)}$ and $L_{(5)}$. Peak 'F' results from the coincidence of Harker vectors from the ligand atoms $L_{(1)}$, $L_{(2)}$ and $L_{(3)}$. The general vector peaks resulting from two molecules related by the 'b' glide plane were then identified, and their co-ordinates recorded.

Finally, the Harker section at $\frac{1}{2}$, y, z was interpreted. This is shown with its implication diagram in Figure 2.7. There are a large number of non-Harker peaks on this section, which make its interpretation very confusing without some prior knowledge of the atomic positions. All the vectors between two molecules related by the two-fold screw axis were identified, and their position recorded.

Two disquieting facts were evident. The first was the very distorted nature of the trigonal plane of the trigonal bipyramid. Although most evidence of this was obscured by the overlapping of peaks in the Patterson function, it became very apparent in the Harker section analysis. The implication diagram (Figure 2.8) shows that one equatorial angle is about 135°. Although some distortion was expected (see Page 21), this seemed too large.

Secondly, although the elongated shapes of many vector peaks

indicated that the axis of the trigonal bipyramid was not parallel to a, it was impossible to locate it accurately. In fact, this confusion was added to by the fact that the angle, $L_{(4)}$ - Co - $L_{(5)}$, was about 170°, and the axial bonds differed considerably in length.

As a result of these difficulties, it was decided to use an undistorted geometry by Fourier and other refinement techniques. The axis of the trigonal bipyramid was moved away from the direction of a, as shown in Figure 2.10.

Although the positioning of the cobalt atom (X was put at 0.25) was fairly accurate, it can be seen by comparison with the overlay in Figure 2.10, that the ligand atom positions were considerably in error. The final co-ordinates derived in the structure analysis show the complex has an unexpectedly distorted stereochemistry.

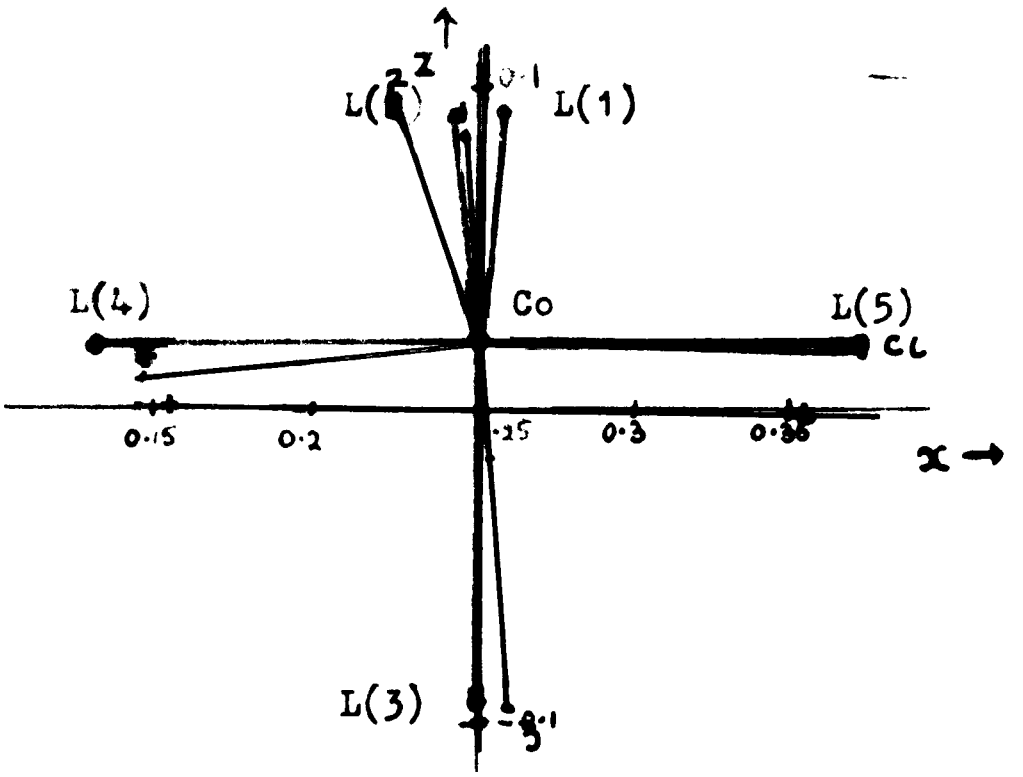

a) Projection on (010)

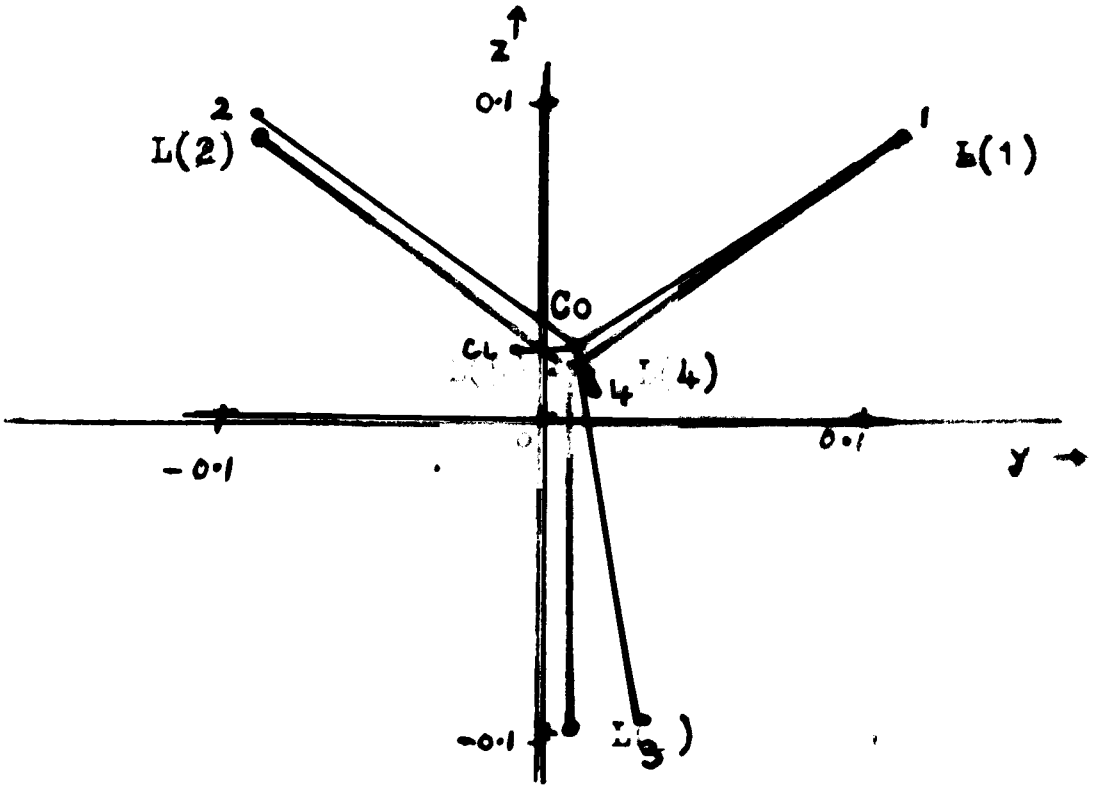

Fig.2.10 The Crystal Structure of $(Co(QP)Cl)BPh_4$

Heavy atom positions derived from the Patterson function. Final heavy atom positions are shown on the overlay.

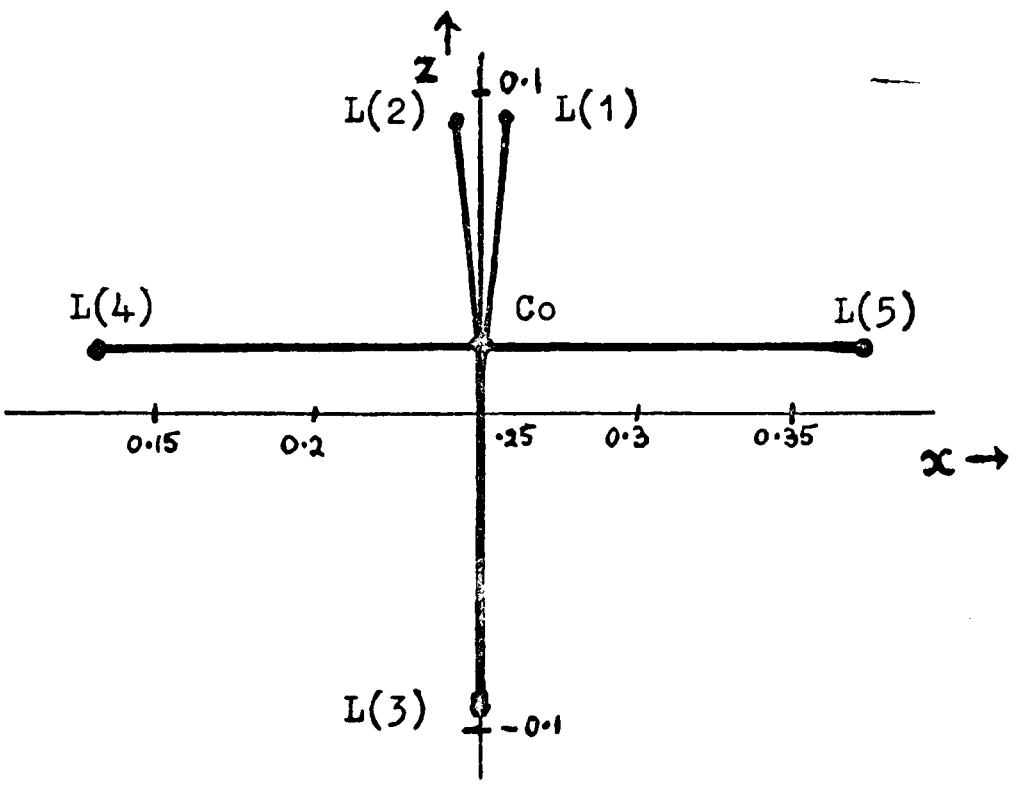

a) Projection on (010)

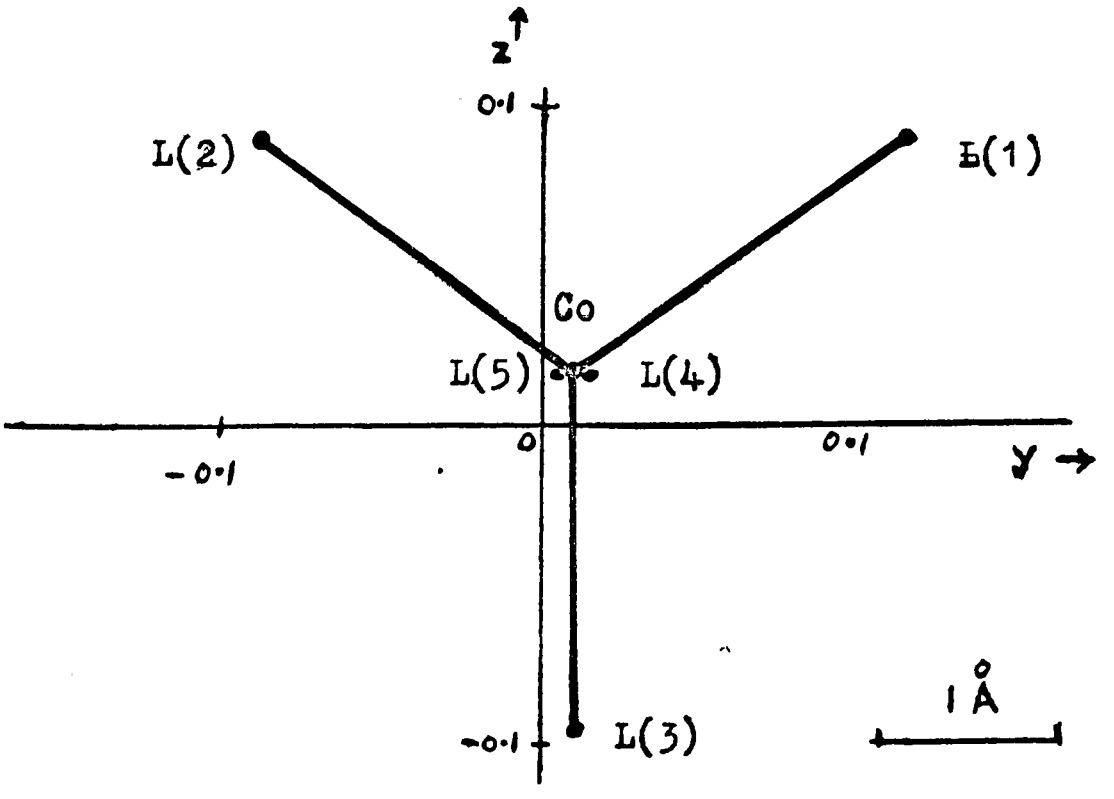

b) Projection on (100)

The location of light atoms in the crystal structures

The determination of the light atom positions and the refinement of positional isotropic vibrational parameters has involved Fourier syntheses, including the heavy atom method and anomalous dispersion techniques, and refinement by the least-squares method and the use of the tangent formula.

The heavy atom method

The graphs (Figure 2.11) calculated by Sim,[48,49] give the errors in phasing for centrosymmetric and non-centrosymmetric structures for different values of $\underline{r}$, where $\underline{r} = \sum f^2_H / \sum f^2_L$. The computations are strictly valid for cases of one heavy atom in triclinic space groups, but they give an approximate estimation of the usefulness of the heavy atom method for other cases.

The $\underline{r}$ values for the three centrosymmetric crystals are greater than 4, indicating that over 95% of the phases will be computed correctly. This is greater than the optimum condition of $\underline{r} \simeq 1$. The increased contribution of the heavy atoms to the scattering introduces errors due to diffraction ripples, and makes accurate data more necessary, without greatly increasing the number of phases which are correctly determined. This introduces serious errors into the analysis of the thallium complex where $\underline{r} \simeq 8$.

The non-centrosymmetric $\left[Co(QP)Cl\right]BPh_4$ crystals introduced errors due to a very small value of $\underline{r}$. If the phosphorus atoms had been located accurately, the problem would have been optimum for the heavy atom method.

However, as the cobalt only was positional correctly, a more realistic r value is 0.23. Then only 20% of the phases would be determined within 20° and 45% within 60°, which hardly seems sufficient to give information about the unknown parts of the structure. Besides this problem, the group of heavy atoms show pseudo-symmetry. The symmetry of the space group, Pmnb is simulated and the phases tend to be close to 0 and π .

Thus, the use of Fourier methods in the four crystal structure analysis presents difficulties due to both large and small r values.

The interpretation of the heavy-atom phased Fourier of the silver complex was similar to that of the palladium complex and will not be described.

The use of the heavy atom method in the structure analysis of $[Pd(TPAS)Cl]ClO_4 \cdot C_6H_6$

This pentaco-ordinate palladium complex has a quadridentate arsenic ligand, TPAS, (see Page 16), and a chlorine atom in the co-ordination sphere. The Patterson function (Page 50) indicated a square pyramidal co-ordination with a chlorine probably in the basal plane rather than at the apex as predicted by the chemists.

A Fourier synthesis was computed with phases calculated using the palladium and four arsenic positions, an overall isotropic vibration parameter estimated from visual inspection and an arbitrary scale, all of which had been refined by least squares.

The electron density map showed the palladium and four arsenic atoms

Fig. 2.11

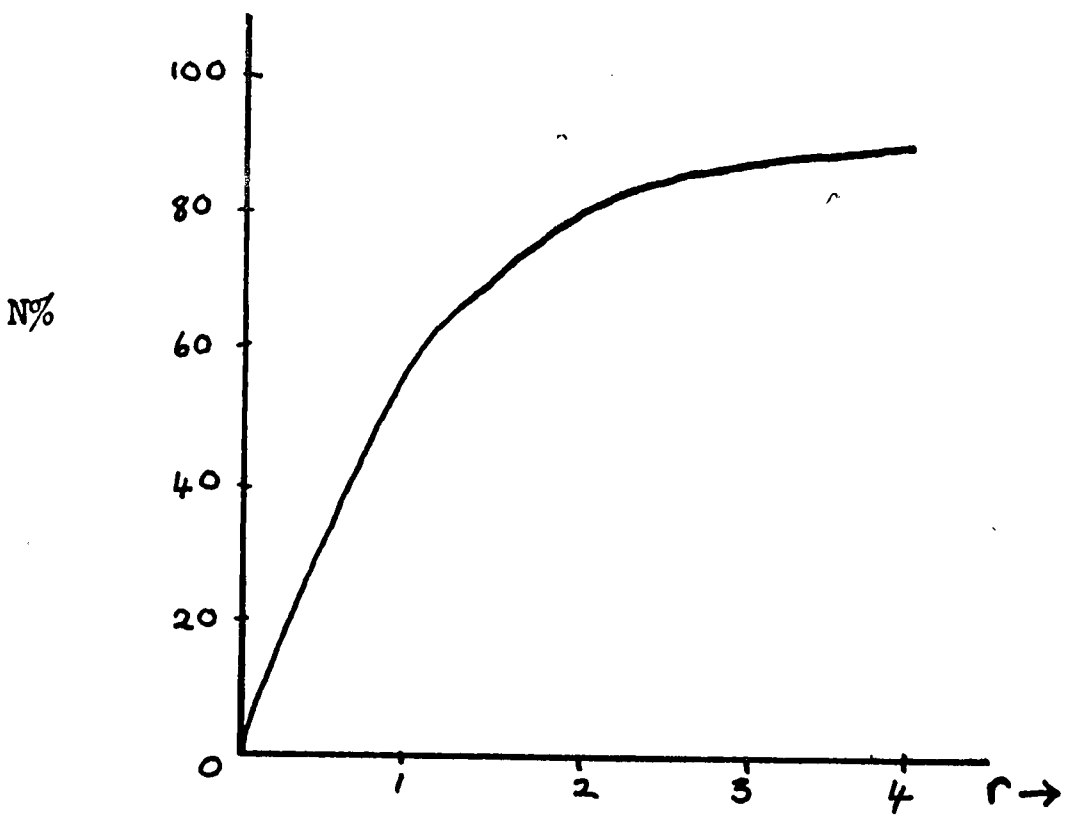

(a) Centrosymmetric structures:- The fraction,N , of structure factors whose signs are determined by a heavy atom

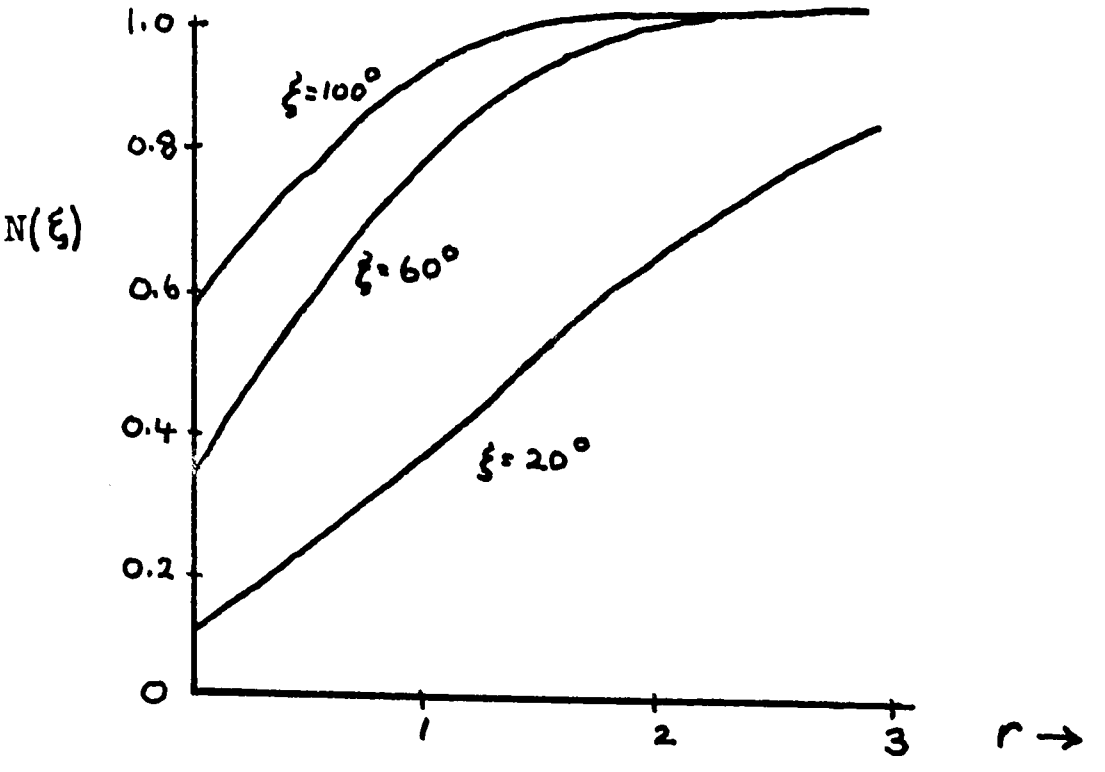

(b) Non-centrosymmetric structures:- errors if phase angle is assumed to be that of the heavy atom alone.

clearly, and, also, a further peak with height, 0.23 of the palladium peak due to the chlorine atom in the fourth basal-plane position.

Altogether, there are 28 ways of fitting the ligand on the square pyramid, but only 6 ways if the basal plane position, 4', (Figure 2.12b) is the chlorine atom. Of the six possible ways, four have bridging phenyl groups 1'-2', 3'-2', 1'-5', 3'-5', but only two have bridging groups in position 2'-5'. Thus, bridging phenyl groups in the first four positions were initially investigated. Arsenic-carbon bond lengths of $\pm$ 2Å in the plane of the phenyl ring were assumed.

The Fourier synthesis contained very many spurious electron density peaks, which confused the identification of the phenyl rings. Phenyl rings bridging arsenic atoms (1') and (5') and also arsenic atoms (2') and (3') were found, but the position of central phenyl rings with carbon atoms (231) to (236) could not be identified easily. The ring must bridge either arsenic atoms (1') and (2') or alternatively arsenic atoms (2') and (5'), but carbon atoms (231) and (236), (i.e., those bonded to the arsenic atoms) could not be found. In fact, peaks at carbon positions (232) to (235) were better resolved, and established the existence of a bridging ring between arsenic atoms (2) and (5). Thus, Figure 2.12(c2) gives the correct stereochemistry.

The next step was to attempt to identify the methyl carbons. This would be more difficult than identifying the phenyl carbons as the stereochemistry of four co-ordinate arsenic can be greatly distorted from tetrahedral and also they would probably be vibrating more than the phenyl carbons. Peaks corresponding methyl carbons, except C(11) and

Fig. 2.12. The location of the light atoms in the crystal structure of $(Pd(TPAS)Cl)ClO_4 \cdot C_6H_6$

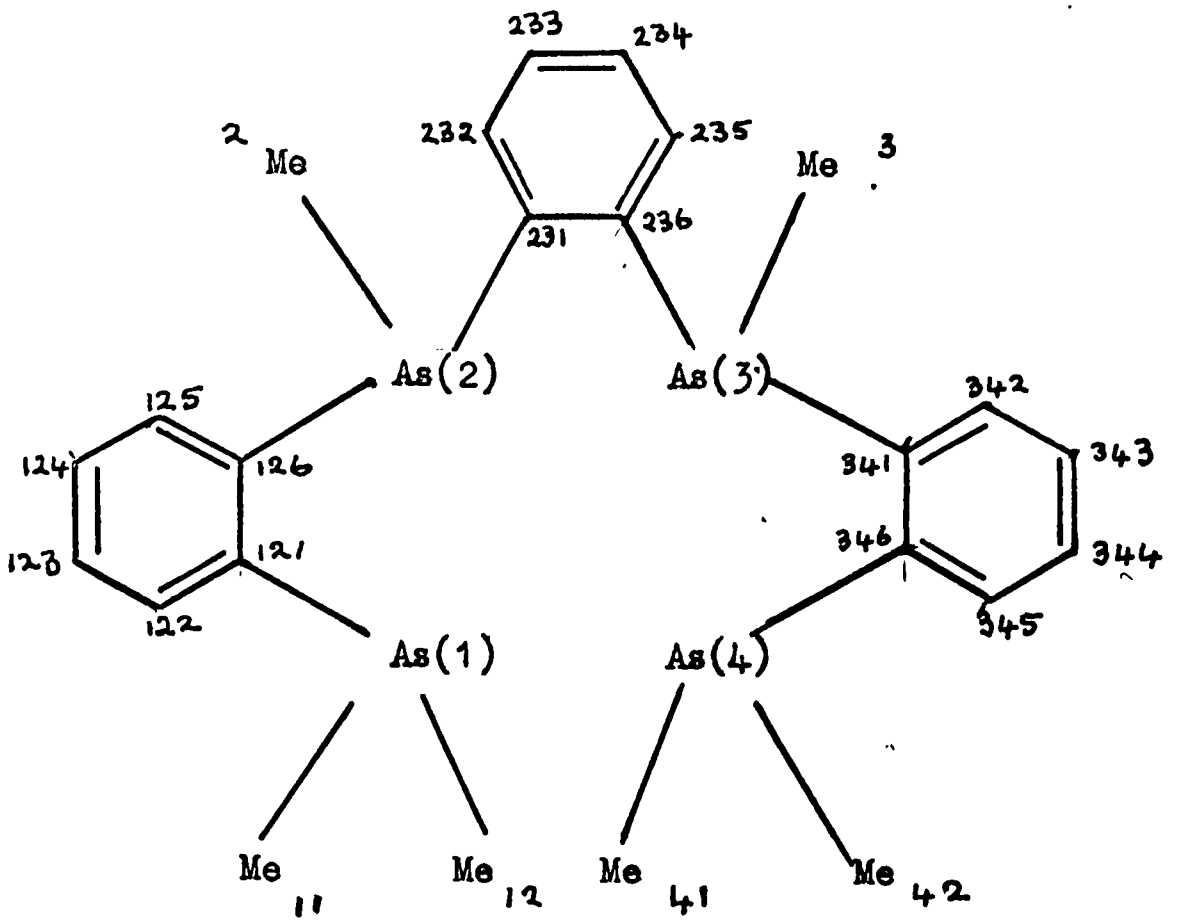

(a)

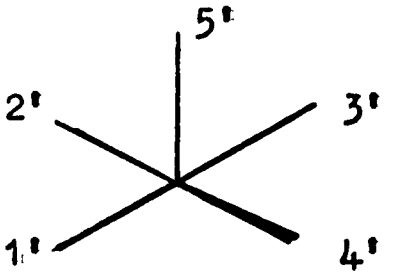

(b)

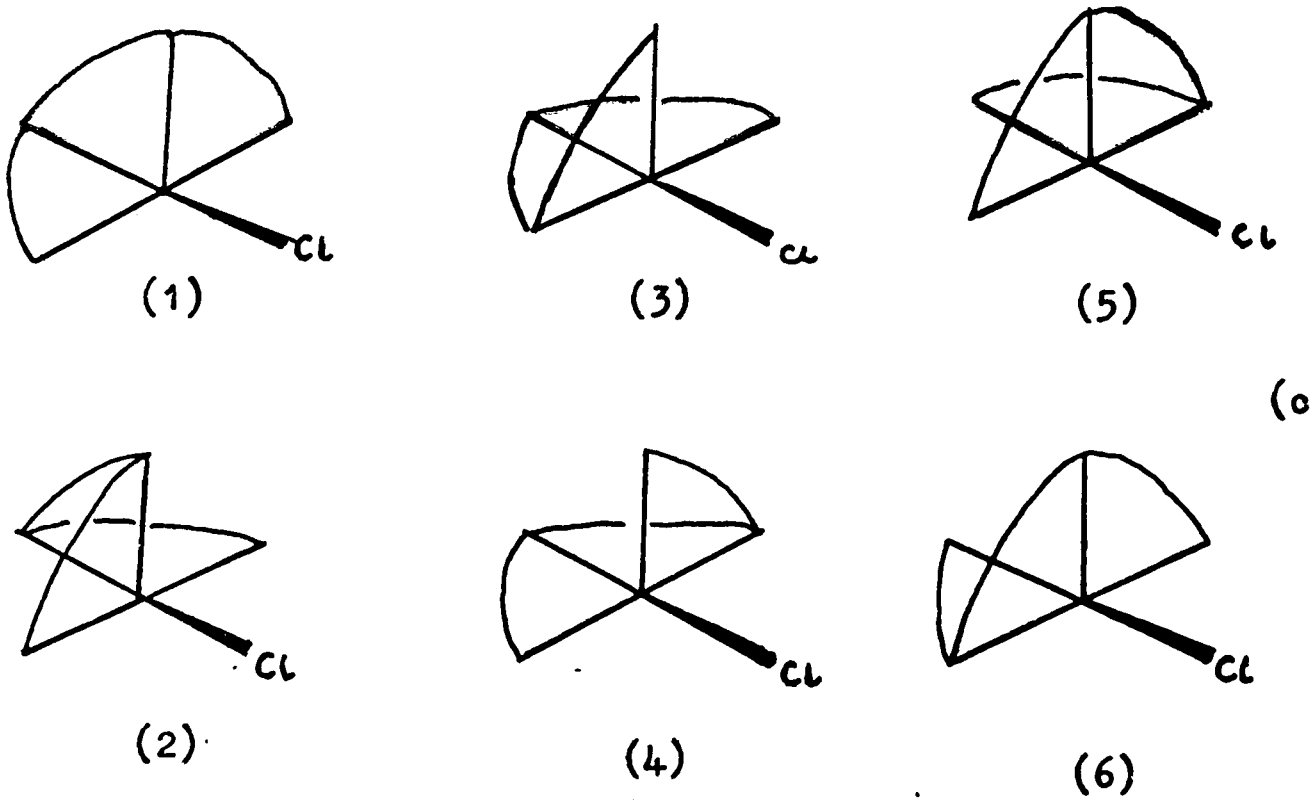

(c)

C(42) were identified.

A three-dimensional model of the crystal structure as it was at this stage was then built. The main feature of the crystal structure appeared to be a distorted hexagonal array of the palladium complex cations. The hexagonal hole enclosed by these cations was extended continuously through the crystal to give channels in the direction of the a axis. (See Figure 3.8)

The perchlorate molecules would most probably lie in this channel in the region of the palladium atoms which are positively charged. The closest of the larger peaks in the Fourier that had not been identified but could be the chlorine of the perchlorate molecules lay at about 5Å from the palladium atom. There were no peaks within covalant bonding distance i.e., about 3Å of the palladium atom.

The peak at 5Å from the palladium atom was chosen tentatively as the chlorine atom. The chlorine to oxygen distance in the perchlorate group should be about 1.4Å. The many badly resolved peaks at about this distance from the chlorine peak appeared, at first, to indicate disorder or possibly rotation of the perchlorate group. However, if a tetrahedral model for the perchlorate group was assumed one particular orientation appeared to be considerably more plausible than the others. The positions of atoms for the perchlorate in the orientation were recorded.

Finally, possible carbon atom positions for the included benzene molecule were found. These peaks were the most badly resolved of all the phenyl carbons. The benzene ring is included in the channel as shown in

Figure 3.8 , page 125 .

A further Fourier synthesis was computed after refinement of the positional and assumed isotropic vibrational parameters by the method of least squares. The purpose of this Fourier synthesis was both to confirm and improve the positions derived from the initial heavy atoms synthesis, and secondly to locate the three remaining carbon atoms. This was achieved by using J. S. Rollett's programme 'Fourier Analyser for Testing Atomic Locations', (F.A.T.A.L.), in which local maxima of electron density are found by interpolation, using a least squares fit of a function of the form,

$$\rho(xyz) = \exp(a + bx + cy + lz + ex^2 + fy^2 + yz^2 + hyz + kyz + lxy).$$

The ten parameters are first determined using nineteen points in the electron density, and the maximum is found for the (x,y,z)for which

$$(\partial \ln \rho_{xyz})/\partial_x = (\partial \ln \rho_{xyz})/\partial_x = (\partial \ln \rho_{xyz})/\partial_x = 0.$$

The programme identifies maxima above a value determined by the user, indicates non-elliptical peaks and records the electron density at points at which an atom was placed for the calculation of structure factors.

A 'FATAL' demonstrated that all the atomic positions chosen from the heavy atom Fourier were close to the correct positions except for one of the carbon atoms in the included benzene ring. At this position there was a region of negative electron density, although all the other carbon atom positions seemed to be correct. A new position for this atom was derived from the geometry of the benzene ring and the known positions. In five other cases, atomic positions were shifted by about

0.25Å. This included two of the perchlorate oxygens and a methyl carbon. Peaks resulting from the remaining carbon atoms were also identified.

The use of the heavy atom method in the crystal structure analysis of $[Me_2Tl1\text{-}10phen]ClO_4$

The location of the light atoms from the heavy atom Fourier synthesis for this complex was similar to the analysis described above for the palladium complex. However, the electron density map was confused by large diffraction ripples. A section of this map through the thallium atom is given in Figure 2.14. These diffraction ripples were not caused by serious series termination effects but are merely emphasised by the very high proportion of the scattering power due to the thallium atom. The positions of the ripples corresponded to those calculated by the Fourier transform method[47] for data within the Cu-K_α reciprocal sphere.

The computation of an electron density map was in fact a mistake. A difference Fourier would have been more suitable. However, even this would not have eliminated all the spurious electron density. Although most of the phases were determined correctly, the large contribution of the thallium atom to the structure factors necessitated very accurate intensity measurements in order to estimate the part contributed by the light atoms. In fact, the identification of the phenanthroline ring proved difficult, although a retrospective slant Fourier (shown in Figure 2.13) demonstrates that once the phenanthroline plane is determined the spurious electron density does not greatly interfere with its interpretation.

Fig. 2.13 'Slant Fourier' in plane of thallium and 1,10-phenanthroline in the crystal structure determination of $(TlMe_2 1,10\text{-phen})ClO_4$

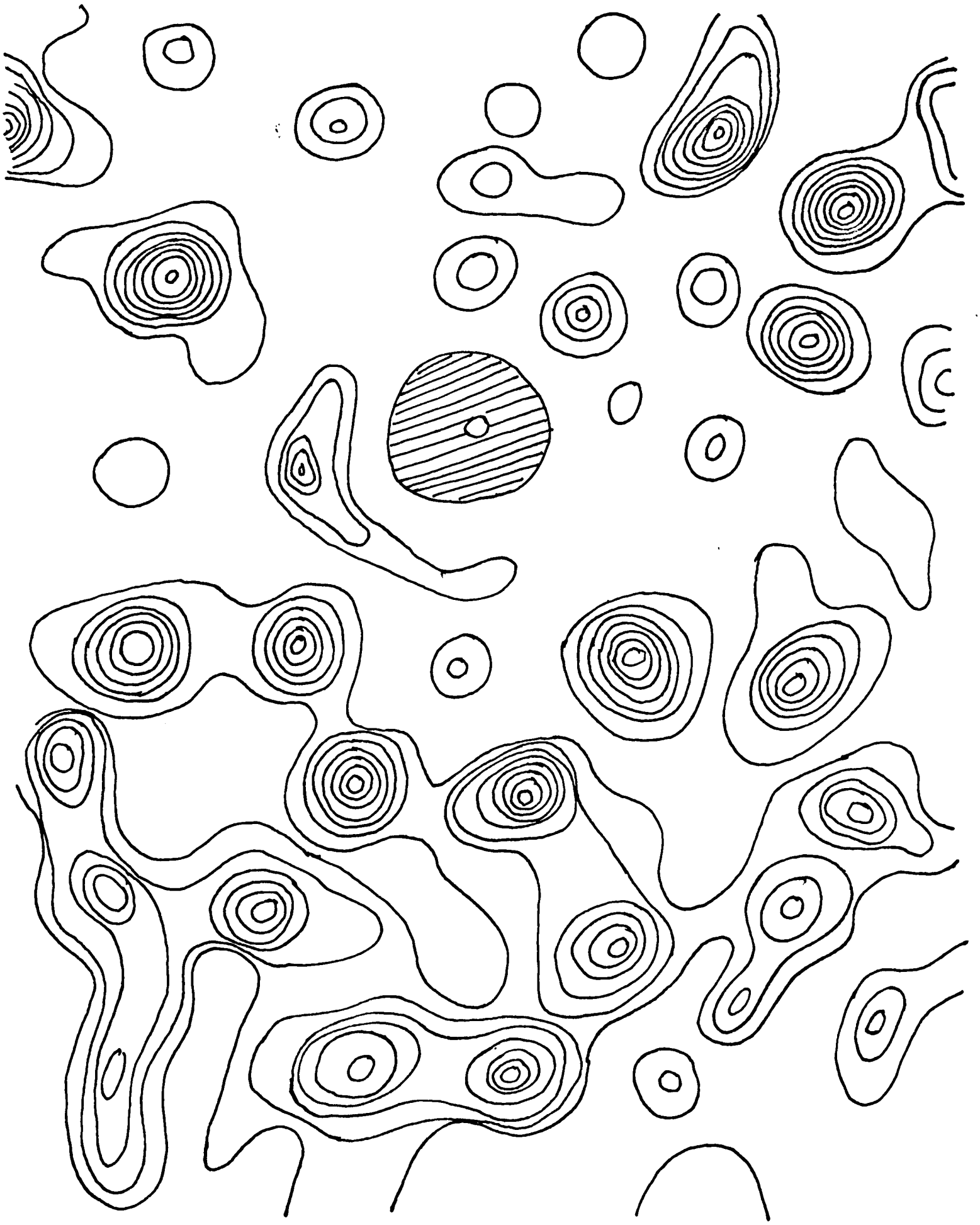

FIG. 2.14 DIMETHYL-1,10-PHENANTHROLINE-THALLIUM PERCHLORATE

FOURIER SYNTHSIS: SECTION THROUGH THALLIUM

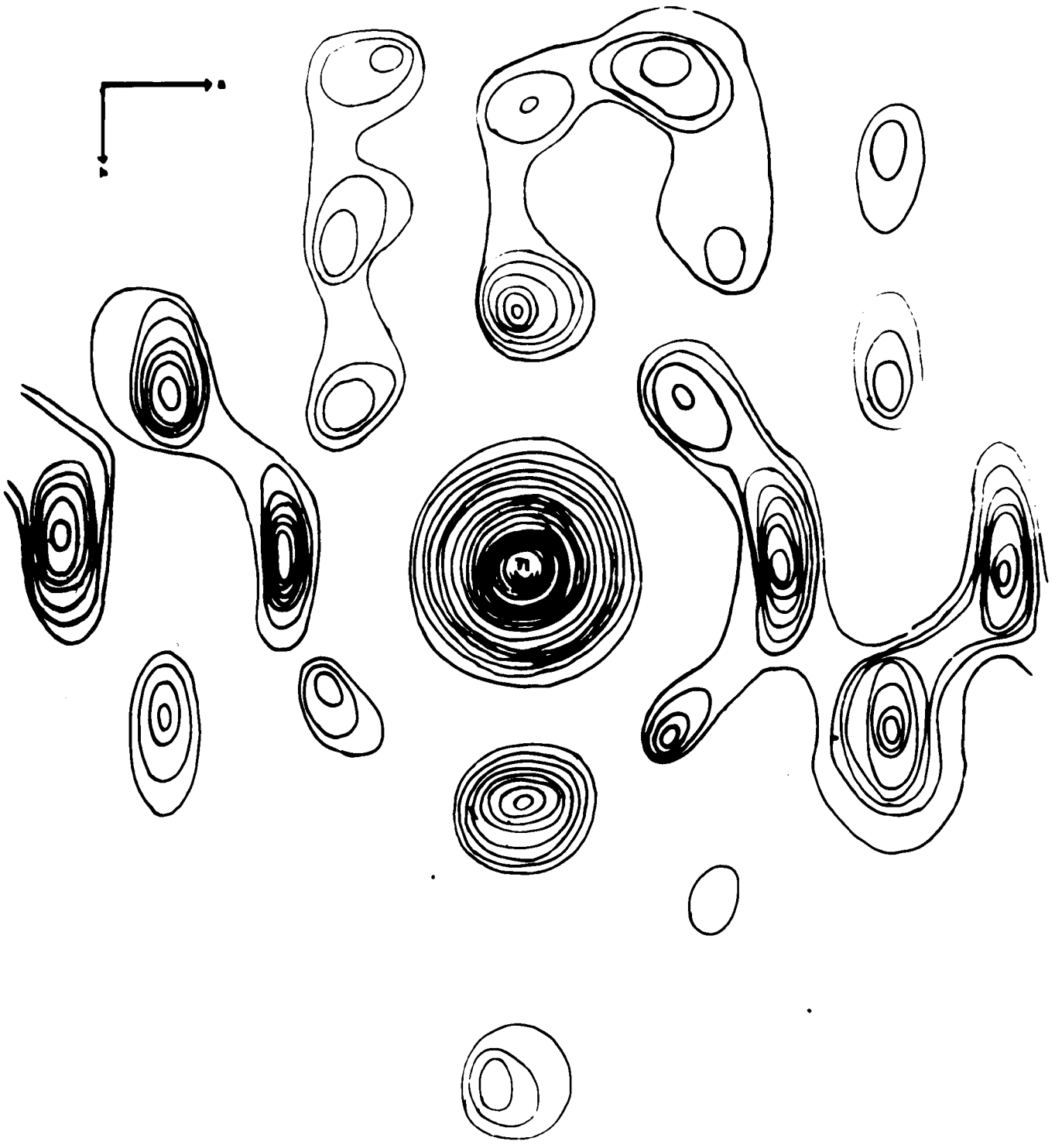

Although the R value for the structure factors computed from the thallium and chlorine positions was 0.145, the methyl carbons could not be identified from this Fourier synthesis.

The location of the light atoms in the crystal structure of $[Co(QP)Cl]BPh_4$

The interpretation of the Patterson function (Page 57), gave the position of the cobalt atom, but only very approximate positions for the ligand atoms due to the overlapping of vector peaks.

The co-ordination appeared to be approximately trigonal bipyramidal, with the axis of the trigonal bipyramid parallel to the a axis, giving rise to pseudosymmetry. The heavy atom positions almost simulated the symmetry of Pmnb. Thus the atoms are almost related by a centre of symmetry, and the phase angles of their contributions to the structure factors are close to either 0 or π . If these phase angles were then used to calculate the electron density, the map would almost be centrosymmetric.

The combination of the problem of pseudosymmetry with the fact that the Sim r value is considerably less than the optimum value for the heavy atom method indicated that normal Fourier methods may not be successful. The use of anomalous scattering and direct refinement of the phases by the tangent formula were also investigated at the same time as the Fourier syntheses were used. They are described on pages 86 - 96.

Structure factors were computed using the cobalt and five inaccurate ligand positions. Phosphorus scattering factors were used for all the ligand atoms. The temperature factor and the scale factor derived by

the Wilson method and were used. Figure 2.15 gives the distribution of phase angles of these structure factors. The large number of phase angles close to 0 and π illustrates the problem of pseudosymmetry. The R-value was 50%.

A three-dimensional Fourier synthesis using these phase angles was computed.

The difficulty of interpreting the Fourier consisting of two superposed structures (related to each other by a mirror plane through the cobalt atom) underlined the importance of making use of any chemical information available. The ligand, QP, has three phenyl rings bridging phosphorus atoms and the positions of these phenyl rings are better defined by the phosphorus atoms than are the terminal phenyl rings. Therefore it was decided to compute the Fourier synthesis for the volume in which these bridging phenyl groups might be. Unfortunately, part of the electron density map around $P_{(3)}$ was lost due to a computer operating error.

A section of the Fourier synthesis is shown in Figure 2.16, illustrating its false mirror plane symmetry. The electron density map contained no resolved peaks of electron density that could unambiguously be interpreted as carbon atoms.

The cobalt and ligand atom peak positions in the electron density map were carefully deduced, and twice the difference of these positions and the calculated positions used as the shift to improved positions. This resulted in an arrangement of heavy atoms which was less pseudosymmetrical. In particular, the position of ligand atom, $L_{(5)}$, (see page) was

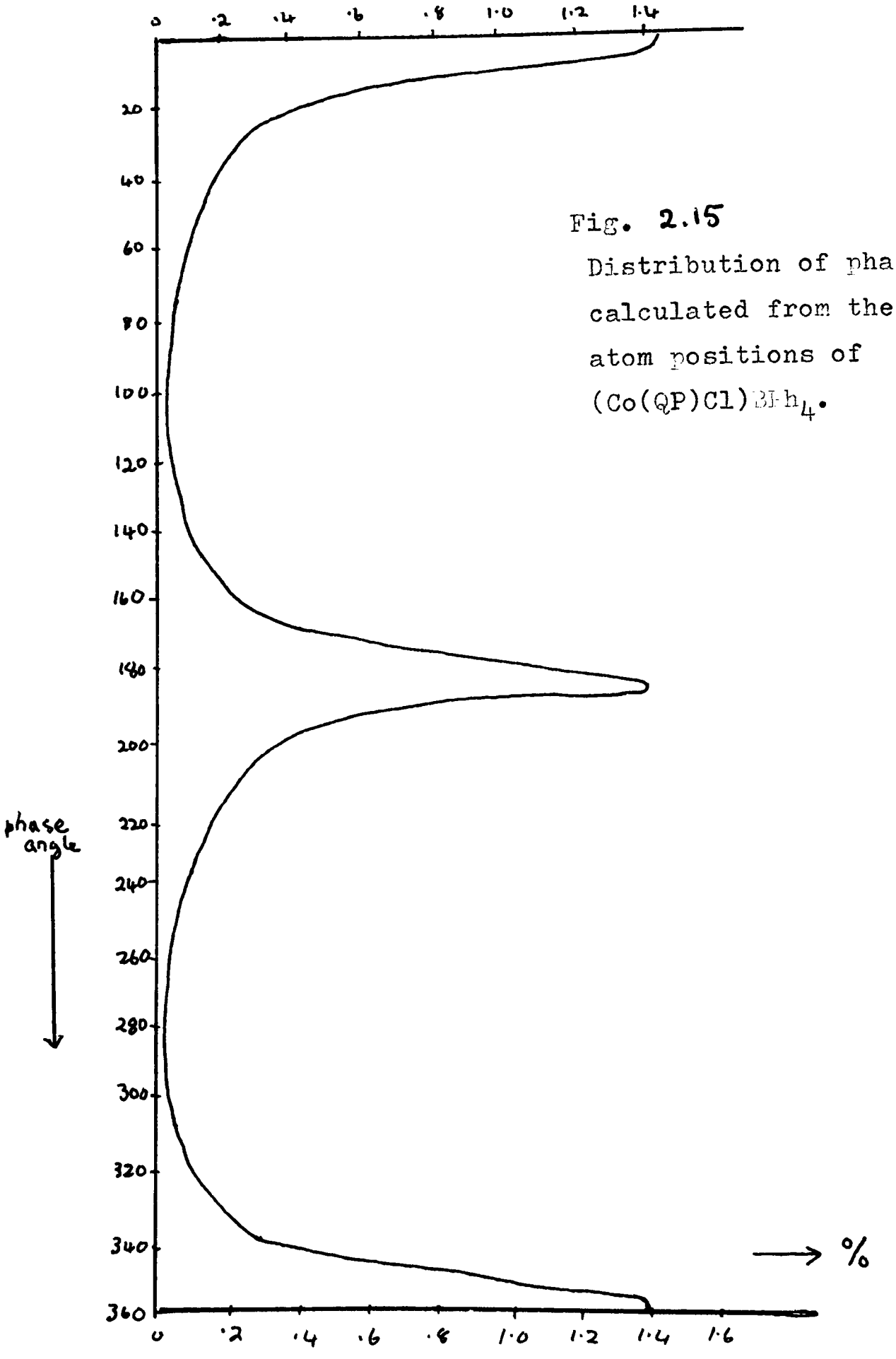

Fig. 2.15

Distribution of phases calculated from the heavy atom positions of $(Co(QP)Cl)BPh_4$.

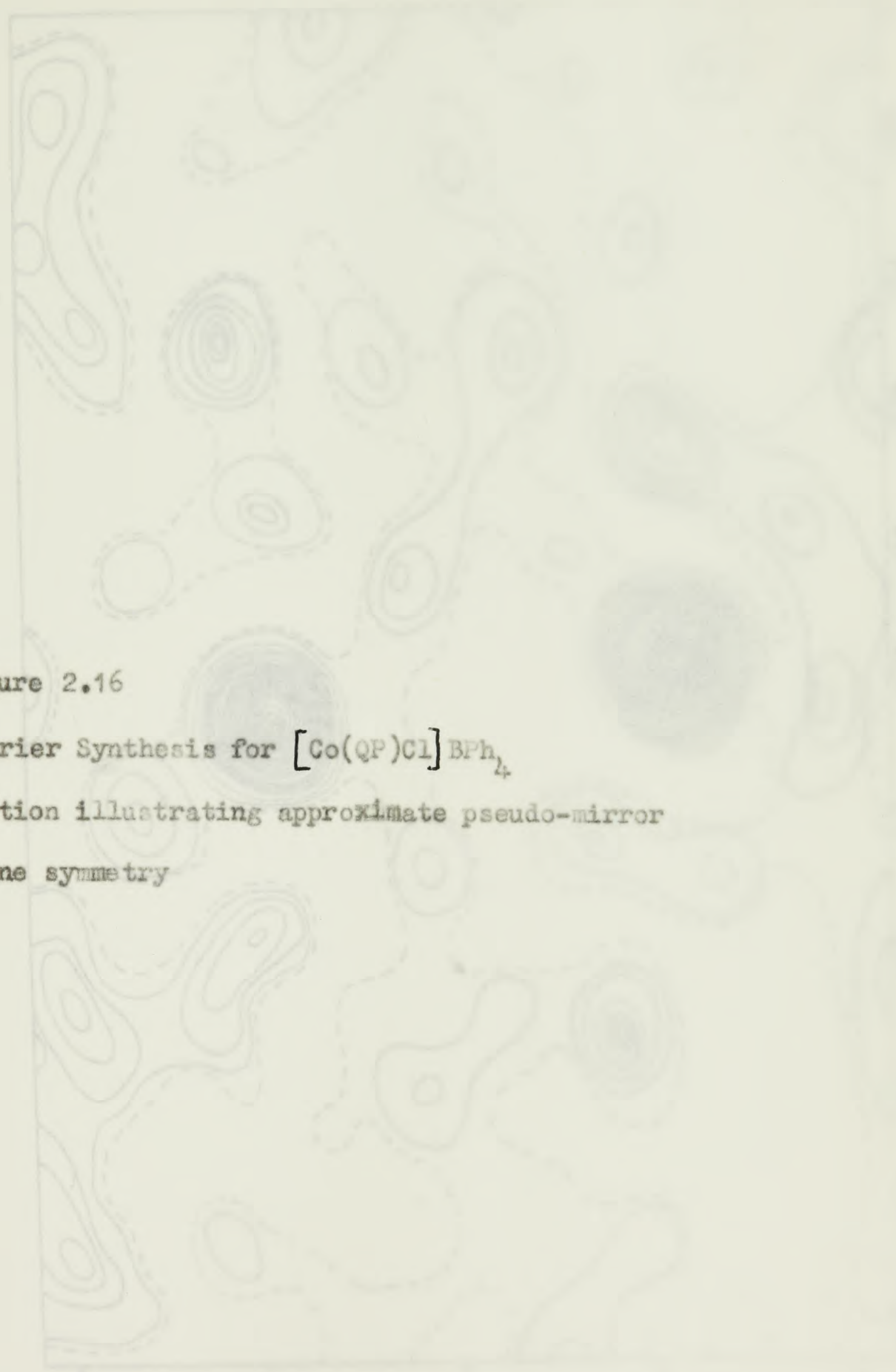

Figure 2.16

Fourier Synthesis for $[Co(QP)Cl]BPh_4$

Section illustrating approximate pseudo-mirror plane symmetry

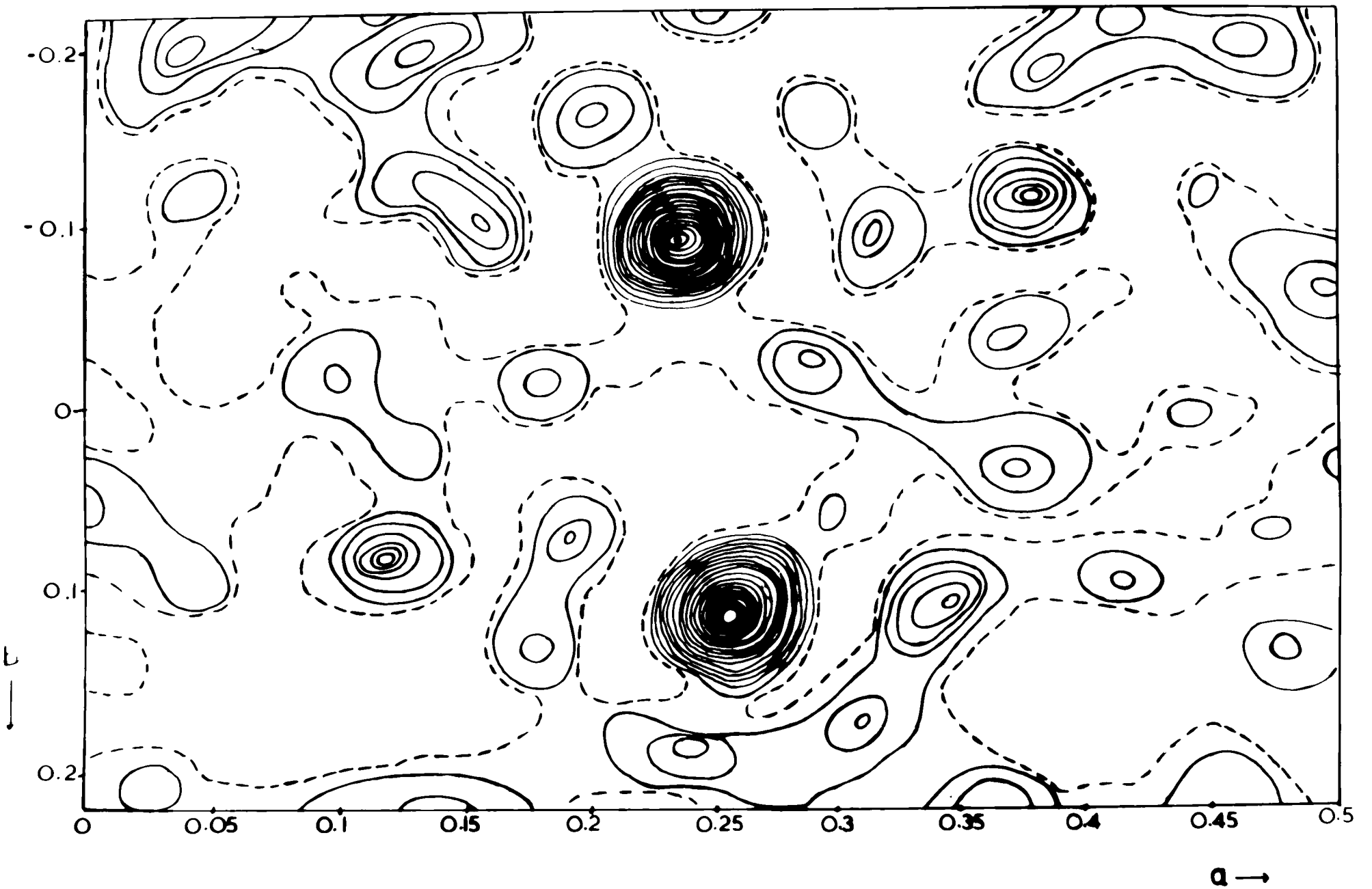
-0.2
-0.1
0
0.1
0.2
b
0
0.05
0.1
0.15
0.2
0.25
0.3
0.35
0.4
0.45
0.5
a

moved considerably closer to the cobalt atom. The position derived from the Patterson was

x	y	z
0.1300	0.0175	0.0208

The position from the electron density map was

0.1450	0.0235	0.0050

compared with the final position of

0.1453	0.0184	0.0048

This new position was accepted only after some hesitation as the Co-P bond would be about 2.0Å long, which seemed very short.

Next attempts to place the phenyl bridging rings were made. The fact that the peak in the electron density map corresponding to $L_{(5)}$ was much smaller and also the Co-L(5) bond length was shorter indicated that L(5) was a phosphorus atom. It seemed impossible for Co-Cl to be as short as 2.0Å although a Co-P bond might be as a result of π bonding or steric requirements of the ligand. Thus atom L(5) was tentatively put as the fourth phosphorus atom, P(4), and phenyl rings bridging P(1) and P(4) and also P(2) and P(4) were next investigated.

The electron density in both these regions would represent badly resolved phenyl bridging rings superposed as a result of the pseudo-symmetry on the terminal phenyl rings bonded to P(1) and P(2). Assuming P-C bond lengths of 1.8Å and the normal geometry of the phenyl rings, trial models were tested until the best fit with the electron density was obtained. The lack of resolution in the electron density necessitated a bold approach. The electron density map in Figure 2.17 is a projection

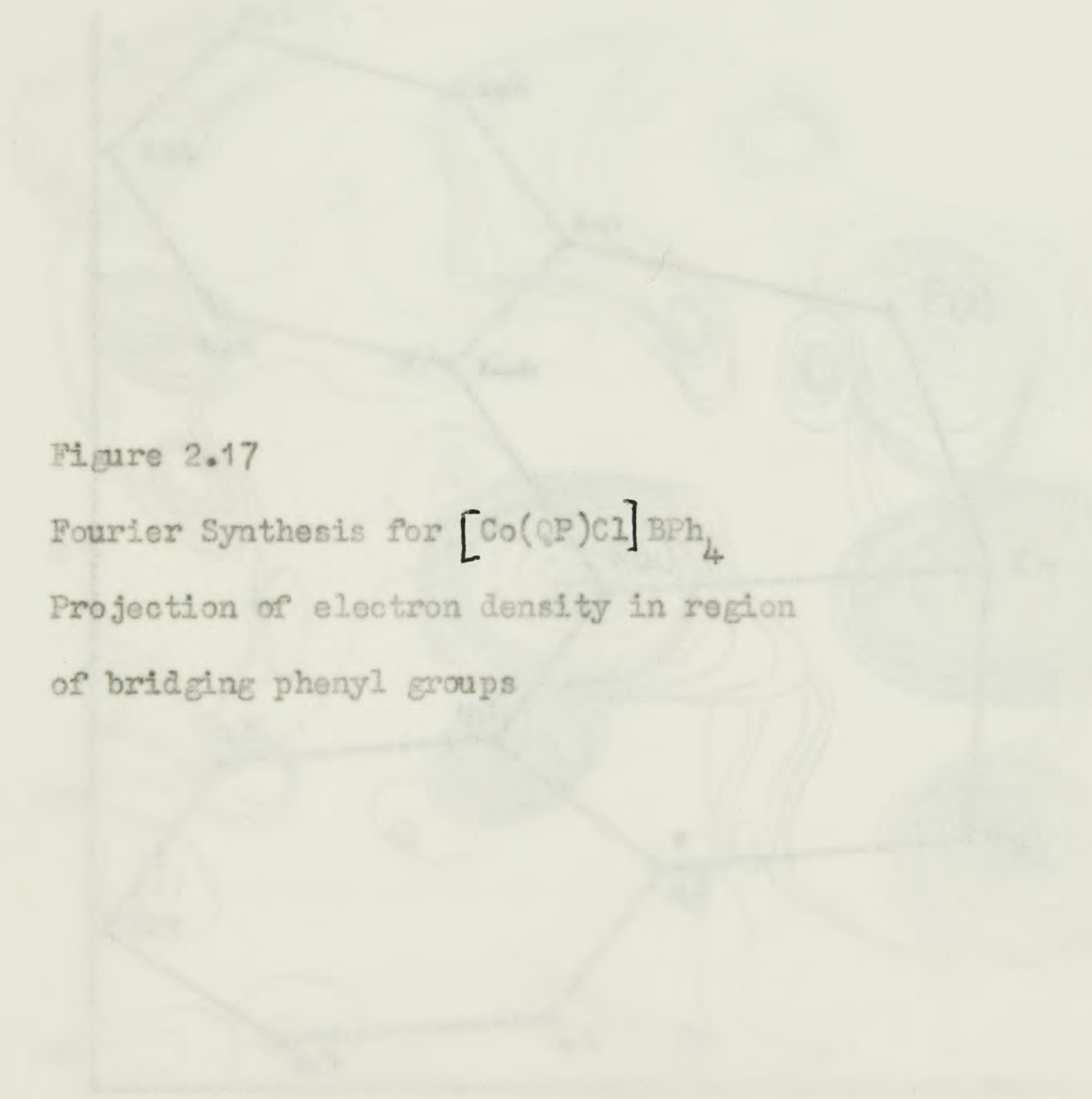

Figure 2.17

Fourier Synthesis for $[Co(QP)Cl]BPh_4$

Projection of electron density in region

of bridging phenyl groups

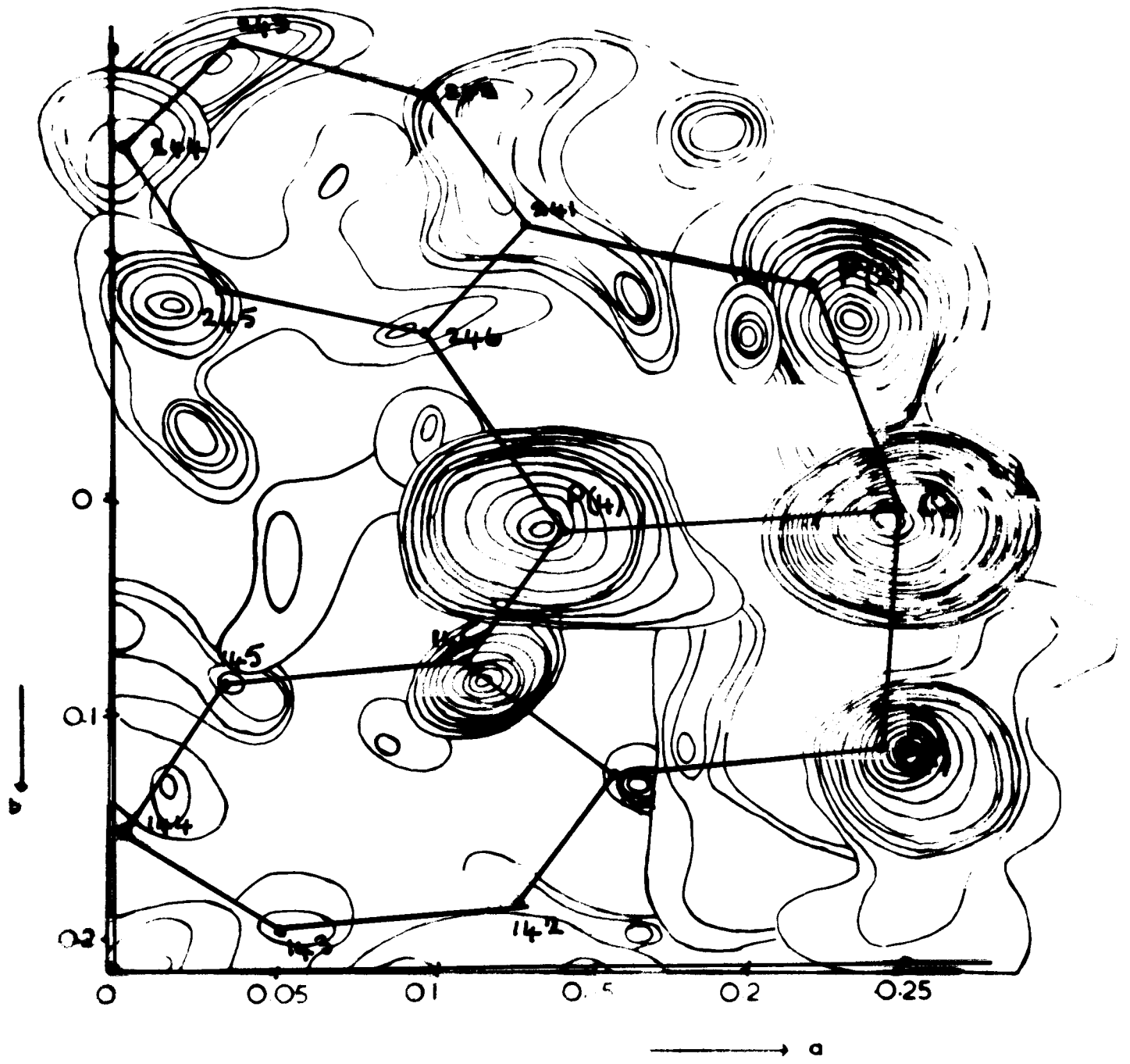
0
0.1
0.2
0
0.05
0.1
0.5
0.2
0.25
b
a

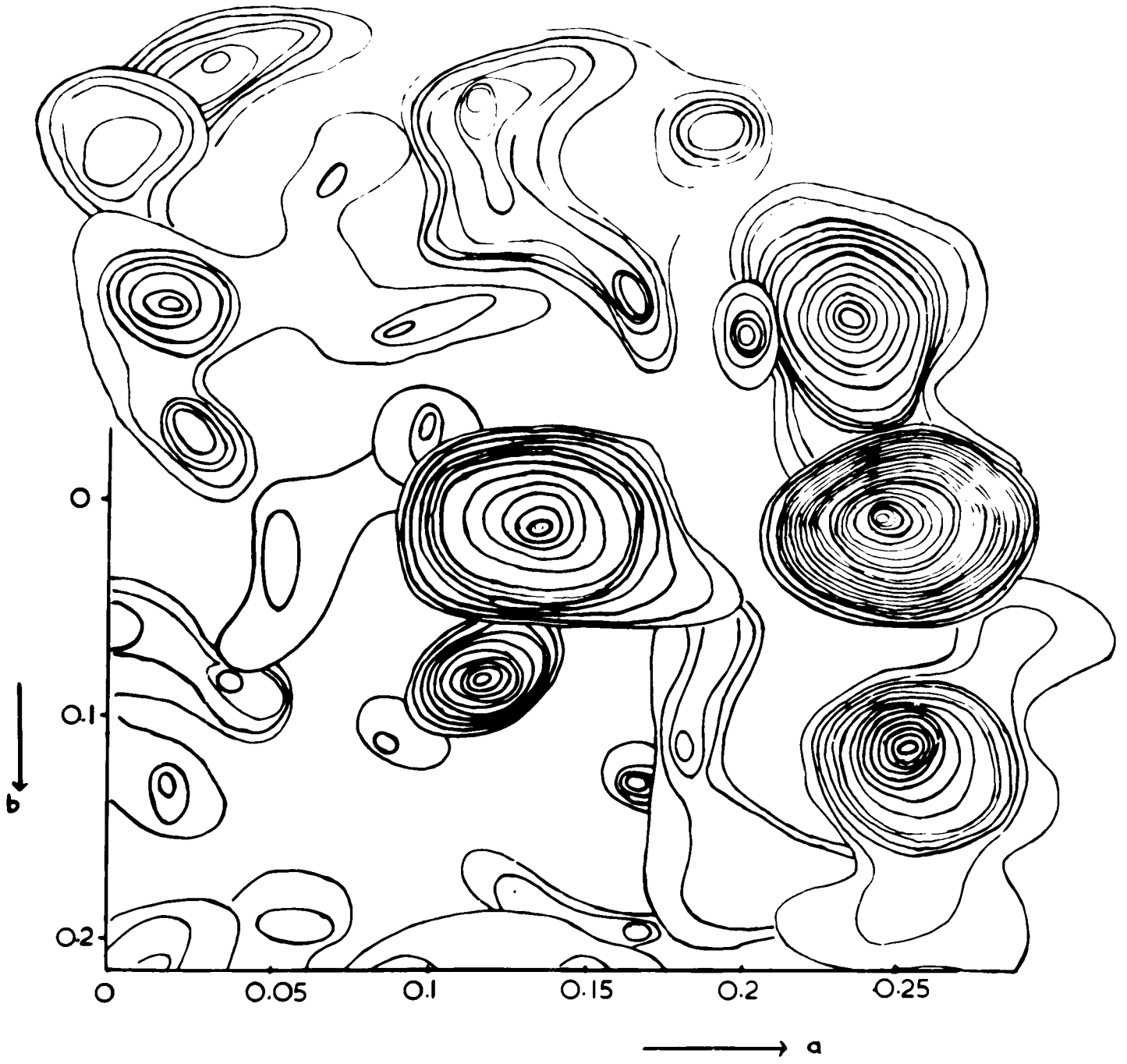
0
0.1
0.2
b
0
0.05
0.1
0.15
0.2
0.25
a

of the electron density within 1.5Å of the planes through the phenyl ring positions chosen. This, of course, considerably clarifies the interpretation of the electron density map.

The overlay shows the positions of the carbon atoms derived from this electron density map, and the final positions for these atoms.

The positional parameters of the heavy atoms and the two phenyl rings were then used to calculate structure factors. The residual was 0.42.

At this stage least squares refinement was used to improve the positions of the heavy atoms. Full matrix least squares was used. As the proportion of scattering matter located was small and the positional parameters were both inaccurate and possibly leading to 'inverse overlap' the results were treated with caution.

A Fourier synthesis was computed using the phase angles calculated from the improved positional parameters. The electron density map was interpreted in a similar way to the first. The positional parameters input were improved, and further phenyl rings were identified. This process was accomplished with the help of model building. Trial structures were postulated, and phenyl ring positions identified after some unsuccessful attempts.

The trial bridging phenyl ring and the four terminal rings attached to P(1) and P(2) and part of one attached to P(3) were identified, and their positional parameters calculated accurately.

Structure factors were then calculated using the heavy atom positional parameters, and positional parameters of thirty nine carbon atoms. The

positional parameters of one of the phenyl rings, attached to P(1) were omitted from this as they were not well determined. The temperature factors of the carbon atoms were fixed at $\underline{U} = 0.06\text{Å}^2$. The residual was 0.282.

The cobalt and five ligand atom positions were then improved by three cycles of full-matrix least squares refinement. The residual decreased to 25.5%.

Distances and angles between the heavy atom positions derived from the least squares refinement and light atom positions derived from the electron density map were calculated.

A difference synthesis was also calculated using these positional parameters.

The distance and angles calculations and the difference map were used together to improve the positional parameters for the thirty nine carbon atoms. For instance, the phenyl ring bridging P(2) and P(4) had carbon to carbon bond lengths between 1.1Å and 1.65Å. These were improved to between 1.3Å and 1.5Å by shifting the carbon atoms giving rise to unreasonable carbon to carbon bond lengths in the direction of residual electron density on the difference electron density map.

The difference electron density map also allowed the determination of the remaining fifteen QP carbon atoms and also the twenty-five atoms of the tetraphenyl borate anion. The location of all atoms was considerably aided by the constant use of model building for all hypotheses concerning the structure.

Distance and angle calculations showed that the postulated structure

was probably correct. The structure factors calculated using these positional parameters and isotropic vibrational parameters (u) varying between 0.04 and 0.06 gave a residual of 0.236. The refinement of these parameters was then accomplished by the method of least squares.

The use of anomalous dispersion techniques

The crystals of $\left[Co(QP)Cl\right]BPh_4$ exhibited anomalous dispersion effects.

Anomalous scattering results from the form, $f = f' + if''$ for the atomic scattering factor, which gives rise to the failure of Friedel's law, $F^2 \neq \bar{F}^2$. When anomalous scattering occurs

$$F = F_L + F'_H + iF''_H = F' + iF''_H$$

where the structure factors include the geometrical factor as well as the components of the atomic scattering factors. For $\left[Co(QP)Cl\right]BPh_4$ in $\underline{P2_1nb}$, the cobalt atoms are in a centrosymmetric array, whereas the lighter atoms (L) are not. The imaginary part of the scattering factor, f''_P, for the phosphorus atoms is 0.5 electrons while f''_{Co} is about 4 electrons. As the scattering power is proportional to the square of the scattering factors, the contribution of phosphorus and chlorine imaginary anomalous scattering factors to the Bijvoet difference will be small. Moreover, as the phosphorus and chlorine atoms are not well placed from the Patterson function, the contributions of f''_P and f''_{Cl} to F''_H will be inaccurately computed and are best ignored in the calculation of phases by anomalous dispersion techniques.

An Argand diagram assuming only f''_{Co} contributes to F''_H is given in Figure 2.19. Thus, F" has a phase of either 90° or 270°.

Several methods have been suggested for use of measured Bijvoet difference to improve or calculate the phases. Okaya and Pepinsky [50,51] recommend the computation of the 'odd' Patterson function given by

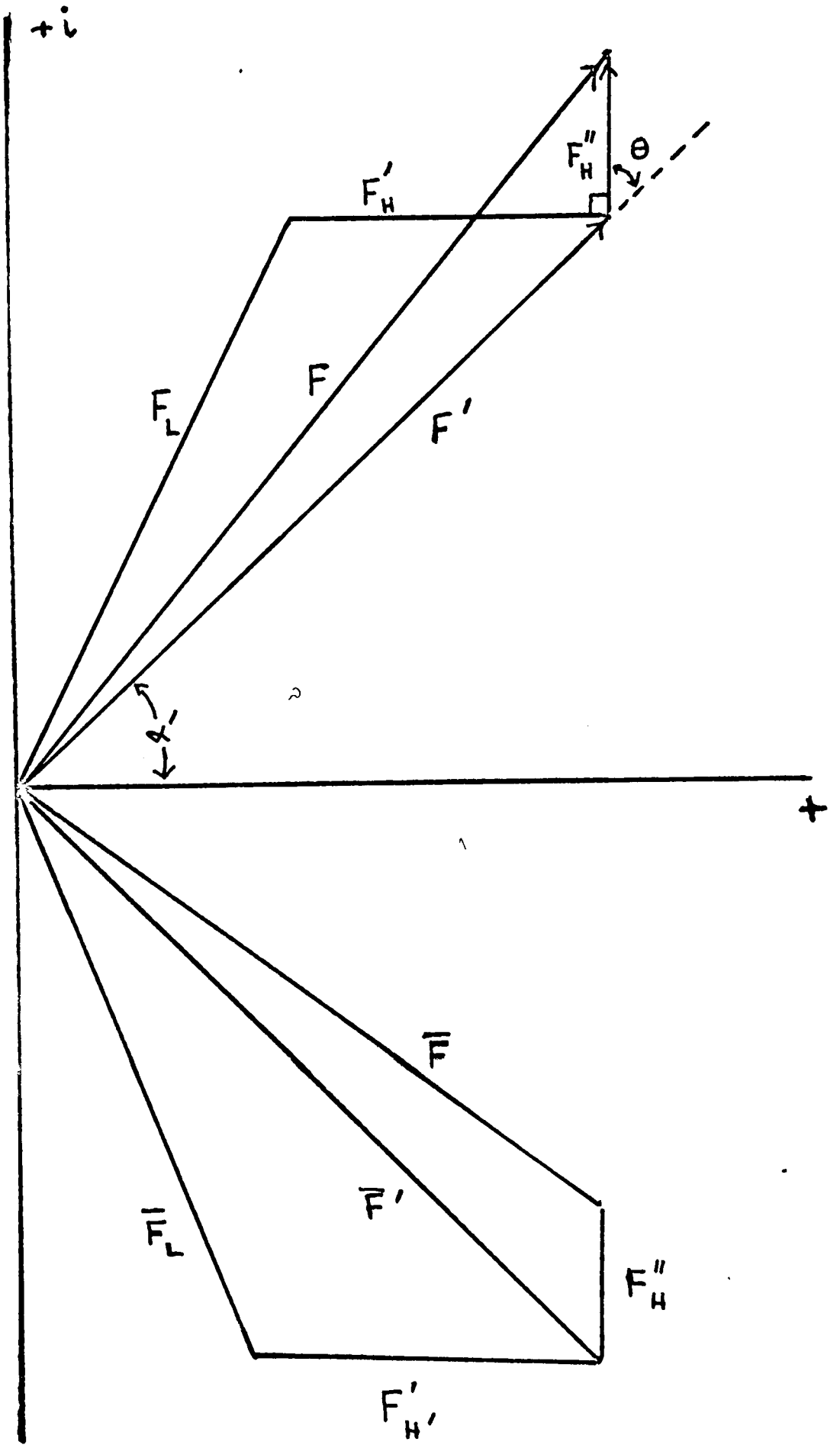

Fig. 2.19 Argand diagram for anomalous scattering.

$$^{pe}(r) = \frac{1}{V} \sum_{\underline{H}}' \left\{ |F_{\underline{H}}|^2 - |F_{\overline{\underline{H}}}|^2 \right\} \sin 2\pi \underline{H}.\underline{r}$$

where the sum is taken over half the reciprocal-lattice points. The $^{po}(r)$ function has peaks of height $f'_j f''_k - f''_j f'_k$ at $\underline{r} = \underline{r}_i - \underline{r}_j$. There is thus no origin peak, but there is a centre of antisymmetry. However, coincidence of some of the p(n-p) positive peaks with the equal number of negative peaks due to the p equivalent anomalous scatterers of the n atoms limits the usefulness of this method.

The even function given by

$$^{pe}(r) = \frac{1}{V} \sum_{\underline{H}}' \left\{ |F_{\underline{H}}|^2 + |F_{\overline{\underline{H}}}|^2 \right\} \cos 2\pi \underline{H}.\underline{r}$$

has positive peaks at $\underline{r} = \underline{r}_i - \underline{r}_j$ and $\underline{r} = \underline{r}_j - \underline{r}_i$. A weighted sum of the two functions could be used to compensate for the negative peaks of $^{pe}(r)$ [52].

Ramachandran and Raman's β-anomalous synthesis[53] suffers from the same limitations as $^{po}(r)$ synthesis. It is antisymmetrical. However, the absolute configuration of the molecule is retained by both syntheses.

An alternative method suggested by Raman and Ramachandran[54] is based on the work of Peerdeman and Bijvoet.[55] In the Argand diagram in Figure 2.19 let the angle between the vectors F' and F" be θ. Then

$$\Delta = F^2 - \overline{F}^2 = 4F'F_H'' \cos \theta$$

and

$$F^2 + \overline{F}^2 = 2F'^2 + 2F_H''^2$$

Whence $\cos \theta = \Delta / 4F'F_H'' = \Delta / 4F_H'' \left(\frac{F^2 + \overline{F}^2}{2} - F_H''^2 \right)^{\frac{1}{2}}$

Of this expression, F" can be calculated from the known position of the heavy atom, cobalt in this case, and $|F|^2$ and $|\bar{F}|^2$ are measured from the data collected. If the phase of the anomalous scattering atom is α_p, then

$$\alpha' = \alpha_p + \pi/2 - \theta$$

This expression is applicable even when the anomalous scatterers are not in a centrosymmetric array. However, due to the ambiguity of determining θ from $\cos\theta$, there is still an ambiguity in determining the phase α'.

This ambiguity can be resolved in several ways other than by using isomorphous replacement which with $[Co(QP)Cl]BPh_4$ is not possible. The most commonly used of these methods is to take the phase closest to the heavy atom phase.

The author decided to try two methods for using the measured Bijvoet differences. They were the weighted sum of the $P^o(r)$ and $P^e(r)$ functions, and the Bijvoet-Ramachandran-Raman method. Unfortunately, time limitations have made it impossible to write the necessary computer programmes to investigate the first method.

Although Bijvoet differences always occur between reflections F^2_{hkl} and $\bar{F}^2_{hkl}$, Bijvoet differences cannot always be observed between reflections in adjacent quadrants. It can be seen from the Argand diagram that the sign of the phase of the two reflections must be different. In $\underline{P2_1nb}$, this means that to observe a Bijvoet difference, reflections with a change of sign of the $\underline{h}$ index must be compared.

Thus, if the Weissenberg technique is used in collecting data, the b or c axes must be rotation axes so that the reflections with a Bijvoet difference can fall in adjacent quadrants. A total of about 5000 independent reflections were collected of which 2100 were Bijvoet pairs measured from adjacent quadrants from the b axis.

These reflections were put on an absolute scale, and the overall isotropic vibrational parameter determined from the Wilson plot was used in the subsequent analysis.

For the Bijvoet-Ramachandran-Raman method the values of F" were calculated by the structure factor calculation programme written by J. S. Rollett, which had been modified by P. J. R. Hodder. These values were then used to calculate 'cos ' as described above. Where $|\cos\theta|$ was greater than one, θ was taken as 0° or 180°. The phase, α' was then deduced taking the phase closest to the cobalt atom phase. A three-dimensional Fourier synthesis was then computed using these phases.

The electron density map showed the phosphorus and chlorine atoms clearly, allowing their location with considerable accuracy compared with the positions derived from the Patterson function or other Fourier syntheses. Also all the light atoms of the cation were easily identified, peaks of over two electrons and often of the expected height occurring within all of the carbon atom positions finally determined.

The success of the Bijvoet-Ramachandran-Raman method can be best analysed in the light of knowledge of the final structure deduced.

Although this is best analysed statistically, a small randomly chosen group of reflections will be used to exemplify the points made. A table is included in Figure 2.20 giving the information relevant to the discussion for these reflections.

The first column gives the cobalt atom phase, which of course is always 0 or 180°. The final column gives the phase given by the final structure. The average phase difference was about 45°. The phases derived from anomalous dispersion are given in the third column. The average difference between these phases and the final calculated ones was 23°. These values are close to those for complete set of data.

In the sample set, taking the phase closest to the heavy atom phase resolved the ambiguity correctly in every case. Most probably a weighting scheme would not have significantly improved the electron density map. A weighting scheme that has been suggested by Lipscomb is to weight each reflection by $\cos(\alpha' - \alpha_H)$, where α' is the phase derived from the anomalous dispersion method and α_H is the heavy atom phase. When the heavy atoms form a centrosymmetric array, this means that those reflections where α' is close to 90° or where $\underline{A}$ is close to zero will be weighted down in the Fourier synthesis. This will serve to reduce the contribution of just those reflections which are important in breaking the pseudo-symmetry. The weighting function will give zero weight to a structure factor which has a phase of 90° given correctly by anomalous dispersion. It appears that the Lipscomb weighting scheme is

Fig.2.20 Phases (in degrees) at different stages in the structure analysis of $(Co(QP)Cl)BPh_4$ for a random sample of reflections

Indices of reflection b	c	a	Phase based on position of Cobalt	Cobalt and 5 ligandatom	Phase from anomalous dispersion	Phase at R=0.111.
1	1	4	0	0	-63	-70
1	8	19	0	6	36	40
2	2	7	0	28	-69	-3
2	15	9	-180	179	165	-167
3	3	5	-180	-120	-133	-110
3	10	4	-180	123	-180	-179
4	4	6	-180	179	138	69
4	13	9	-180	175	-148	-127
5	6	10	0	-10	-52	-79
6	0	10	-180	-169	-157	-146
6	9	5	180	175	162	132
7	1	4	0	19	-47	-64
8	5	7	0	-5	-45	-23
9	6	6	0	45	-7	19
10	3	1	-180	-176	172	180
13	1	13	180	-46	174	180
13	1	3	0	-60	-20	-41

certainly unsuitable in the present case, and could be improved by choosing a scheme which weighted up the reflections where θ is close to zero.

The formula for anomalous scattering relating the Bijvoet difference, Δ, to F" can be re-expressed when the anomalous scatterers are centrosymmetric. Thus:-

$$\Delta = 4F''F' \cos\theta = 4F''B'$$

The Bijvoet difference unambiguously determines B' but there is an ambiguity in the sign of A.

Thus $A = \pm \sqrt{F^2 - B^2}$

This emphasises the real problem - to determine the sign of A.

Lipscomb has suggested some methods of determining this which will

now be examined critically.

The first of these is to calculate an approximation to A from other parts of the structure. In the analysis above the information about the positions of the phosphorus and chlorine atoms is not used. The sign of A derived from these positions or possibly the actual value of A could be used to combine with B derived from the Bijvoet difference. Because of the incorrectly determined ligand atom positions, this method was not used. A retrospective analysis (Figure 2.20) shows that the values of A determined by this method would have significantly decreased the usefulness of the synthesis in this case.

A more useful suggestion would seem to be to transform the pseudo-

symmetrical electron density map phased on the heavy atom, or, better, to assume atoms are at the positions of resolved peaks on this centrosymmetrical map, and transform this. A good approximation to $\underline{A}$ should be given. Unfortunately the Sim $\underline{r}$ value for $[Co(QP)Cl]BPh_4$ is so small that the map does not have clearly resolved peaks. The difficulty of transforming the electron density map is prohibitive in this case.

Despite the lack of use of these methods in the present case for improving the structure factor calculation, the discussion of them has lead to certain suggestions concerning their use. It seems inconsistent of Lipscomb to recommend the use of $|\underline{A}|$ calculated by one method and $|\underline{B}|$ by another. The anomalous scattering method determines $\underline{B}$ uniquely but $\underline{A}$ ambiguously, while the reverse is true for the method of transforming the pseudo-symmetric Fourier function. Lipscomb shows it worthwhile to include A from the transform method in the structure determination of Leurocristine. This means simply that the sign of $\underline{A}$ is more accurately determined from the transform than from the heavy atom phase or that $|\underline{A}|$ is closer to the correct value than the $|\underline{A}|$ determined from anomalous dispersion. If the first is the case, one should surely use $\underline{B}$ and $|\underline{A}|$ from anomalous dispersion with the sign of $\underline{A}$ from the Fourier transform. If the second instance is true, one should use $|\underline{B}|$ and $\underline{A}$ from the Fourier transform, and the sign of $\underline{B}$ from anomalous dispersion study. If one is unsure of the relevant course a mean $|\underline{A}|$ and $|\underline{B}|$ could be used along with signs determined by the relevant method. In the crystal structure determination of Leurocristine it would probably have been better to

determine the phase from |B| and |A| calculated from the Fourier transform of the heavy atom phased pseudo-symmetrical electron density map.

The power of the Raman-Ramachandran technique has been clearly demonstrated. The fact that it produced results after the difficult analysis of the non-anomalous Fourier syntheses are the fault of the author. An enthusiasm to see chemical results combined with a scepticism of his ability to measure Bijvoet differences accurately enough to make the anomalous dispersion technique successful resulted in insufficient emphasis in preparing the anomalous data and requisite computer programmes at the initial stages of the analysis.

The use of the tangent formula for the refinement of phases

Let the quasi-normalised structure factor be defined

$$\mathcal{E}_{\vec{h}} = \sum 2^{-\frac{1}{2}} \sum_{j=1}^{N} f_j \exp(2\pi i \vec{h}.\vec{r}_j)$$

Then $$\mathcal{E}_{\vec{k}} \cdot \mathcal{E}_{\vec{h}-\vec{k}} = \sum 2^{-1} \sum_{j=1}^{N} f_j^{\,2} \exp(2\pi i \vec{h}.\vec{r}_j)$$

$$+\sum 2^{-1} \sum_{\substack{j \neq j' \\ 1}}^{N} \sum f_j f_{j'} \exp\left\{2\pi i \vec{k}.\vec{r}_j + (\vec{h}-\vec{k}).\vec{r}_{j'}\right\}$$

If the average is taken over all values of k, then the second term, the double average becomes zero and

$$\left\langle \mathcal{E}_{\vec{k}} . \mathcal{E}_{(\vec{h}-\vec{k})} \right\rangle_{\vec{k}} = \sum 2^{-1} \sum_{j=1}^{N} f_j^{\,2} \exp(2\pi i \vec{h}.\vec{r}_j)$$

If the structure contains equal atoms

$$\left\langle \mathcal{E}_{\vec{k}} \mathcal{E}_{(\vec{h}-\vec{k})} \right\rangle_{\vec{k}} = N^{-\frac{1}{2}} . \mathcal{E}_{\vec{h}}$$

The normalised structure factor is given by

$$E_{\vec{h}}^{\,2} = F_{\vec{h}}^{\,2} / p\Sigma_2, \text{ where } \underline{p} \text{ is the symmetry number.}$$

The normalised structure factors are, of course, equal to the '$\underline{z}$' used in intensity statistics (see Chapter 2, page 45).

Then $$\left\langle E_{\vec{k}} . E_{(\vec{h}-\vec{k})} \right\rangle_{\vec{k}} = N^{-\frac{1}{2}} . E_{\vec{h}} \qquad (1)$$

This expression may be written in an alternative form which is useful

in application.

$$E_{\vec{h}} = |E_{\vec{h}}| \cos \alpha_{\vec{h}} + i\, |E_{\vec{h}}| \sin \alpha_{\vec{h}}$$

Also from (1)

$$E_h = N^{\frac{1}{2}} \left\langle |E_{\vec{k}}| \cdot |E_{\vec{h}-\vec{k}}| \left[\cos(\alpha_{\vec{k}} + \alpha_{(\vec{h}-\vec{k})}) + i \sin(\alpha_{\vec{k}} + \alpha_{(\vec{h}-\vec{k})}) \right] \right\rangle$$

Thus

$$\tan \alpha_{\vec{h}} = \frac{\left\langle |E_{\vec{k}}||E_{(\vec{h}-\vec{k})}| \sin(\alpha_{\vec{k}} + \alpha_{(\vec{h}-\vec{k})}) \right\rangle}{\left\langle |E_{\vec{k}}||E_{(\vec{h}-\vec{k})}| \cos(\alpha_{\vec{k}} + \alpha_{(\vec{h}-\vec{k})}) \right\rangle}$$

This formula may be used to refine phases which are inaccurately determined.[57,58]

The tangent formula has been little used until recently. Its main application has been to the refinement of phases derived by the symbolic addition method of Karle and Karle. As the symbolic addition method depends on probability relationships, or more fundamentally on inequalities which impose no restriction on the phase of $F_{\vec{h}}$ when the crystal is very complex, the tangent formula has been used with structures with only a small number of atoms per unit cell. However, G. A. Mair has investigated the use of the tangent formula in protein crystallography, with the intention of using it to remove the ambiguity in the phase determination by isomorphous substitution.

The use of the tangent formula in protein crystallography lead the author to investigate its use with $\left[Co(QP)Cl\right]BPh_4$ at the stage when the cobalt and ligand atoms had been determined from the Patterson function. Although the pseudo-symmetry had been partially destroyed, the phases were still close to 0° and 180° and the electron density map computed

using these phases was very difficult to interpret. As an anslysis of a non-centrosymmetric light atom structure studied in Professor Hodgkin's group also required the use of tangent formula refinement, the author decided to write a general programme in C203 autocode with KDF9 usercode, in the time consuming parts. A programme to calculate normalised structure factors was also written in C203 autocode. The general strategy of these programmes along with a detailed flow diagram is included in Appendix VI, page 195

Phases were calculated from the cobalt and inaccurate phosphorus positions, and $\underline{E}$ values computed from the observed intensities. The tangent formula was then used to refine these phases. Two cycles of refinement were carried out for E values above 1.5 and 1.3 respectively. The criteria for accepting a calculated phase are discussed fully in the Appendix.

Unfortunately, this work was not useful in improving the phases, at this stage of the analysis. However, the method could be considerably improved. All the phases are determined inaccurately in this case, Nevertheless, structure factors can be calculated from the inaccurate heavy atom positions. Where the calculated structure factor is small compared with the observed structure factor magnitude, the phase is less likely to be correctly determined, and these phases could be weighted down in a similar way to that used in normal weighted Fourier syntheses. A retrospective analysis shows that of about 25% of the reflections which had $F_o \rangle 2F_c$, 30% had phase errors of over 100° and 60% had phase errors over 50°. This means that of the 12% of reflections with phases with

errors greater than 100°, about 70% would be removed by eliminating the reflections where $F_o \rangle 2F_c$. This would lead to a considerable improvement in effectiveness of the tangent formula (and, of course, Fourier methods).

Furthermore, it would be interesting to examine the effectiveness of this method at other stages in the X-ray analysis. This work could profitably be carried out now that the requisite computer programmes are available.

Least squares refinement of positional and isotropic vibrational parameters

The method of least squares was used to refine positional and isotropic vibrational parameters in all the crystal structure determinations reported here. The computations were made using J. S. Rollett's structure factor and least squares programme.

The weighted observational equations written as linear equations for the correction of parameters are of the form:-

$$\sum_{j=1}^{m} \sqrt{w}\, \frac{\partial [|F_c(h)|/k]}{\partial p_j} \delta p_j = \sqrt{w} \left[|F_o(h)| - \frac{1}{k} |F_c(h)| \right] = \sqrt{w}\, \Delta$$

Unit weights were used initially, and only when all the scattering matter had been included in the structure factor calculation were weights dependent on the size of $|F_o(h)|$ used. The relative weights were then calculated from the equation

$$\frac{1}{w} = 1 + \left[\frac{|F_o| - p_1}{p_2} \right]^2$$

where p_1 and p_2 are parameters chosen to remove the dependence of $w\Delta^2$ on $|F_o|$. No facilities were available for the application of individual weights inversely proportional to the variance. Reflections measured at less than the minimum on the scale used for measuring the intensities were omitted from these calculations.

If the observational equations are written in matrix notation:-

$$A \delta p = b$$

The normal equations are then:-

$$\underline{A}^T\underline{A}\,\delta p = \underline{A}^T\underline{b}$$

The standard deviations were obtained in the usual way from the diagonal elements of the matrix $\underline{N}$, which is the inverse of $\underline{A}^T\underline{A}$.

Due to the large number of positional and isotropic vibrational parameters of the four structures, full matrix least squares was not often possible. In all cases, the four parameters refined for each of the heavy atoms in the initial stages of the structure determination were refined using a full matrix. In the initial stages of the structure determination, the full matrix refinement has the best chance of succeeding. In the intermediate stages of refinement when more parameters are introduced, some of the off-diagonal elements of $\underline{A}^T\underline{A}$ were omitted, but in the final stages as many as possible were included in order that the standard deviations should be meaningful.

Very little has been written about the relative efficacy of full matrix and block-diagonal methods of refinement and the effects of ignoring various off-diagonal elements. However, three points are clear.

1) The vibrational parameters and the overall scale factor are strongly correlated. They were always included in the same matrix.

2) Positional parameters $\underline{x}_i$, $\underline{y}_i$ and $\underline{z}_i$ of the $\underline{i}$th atom must be included in the same matrix if the axes $\underline{x}$, $\underline{y}$ and $\underline{z}$ are not orthogonal.

3) If the structure is non-centrosymmetric but contains a centrosymmetric group of atoms, there may be "inverse overlap" between the atoms related by the pseudo-centre of symmetry. Off-diagonal elements of the matrix $\underline{A}^T\underline{A}$ such as

$$\sum_{i=1}^{s} w_i \frac{\partial |Fc(h)|_i}{\partial x_1} \cdot \frac{\partial |Fc(h)|_i}{\partial x_2}$$

may be large if atoms 1 and 2 are related in this way. Srinivasen[60] has shown that the block-diagonal approximation breaks down in this situation, but Maslen has shown that the full matrix procedure is not satisfactory either.[61] He points out the only advantage of using the full matrix is that it gives an indication of the presence of inverse overlap by showing a large standard deviation for the parameters concerned.

This problem seemed relevant in the refinement of $[Co(QP)Cl]BPh_4$ parameters. The positions initially chosen for the apical phosphorus and the chlorine atom were within 0.3Å of being related by the pseudo-symmetry of Pmnb. As a result the parameters of these atoms were always included in the same matrix. However, no large standard deviations resulting from "inverse overlap" were observed.

The intermediate stages of the structure refinement of $(TAS)Ag\text{-}Co(CO)_4$ and $[Pd(TPAS)Cl]ClO_4.C_6H_6$, only off-diagonal elements between heavy atoms and between carbon atoms in the same phenyl ring were included. The crystal structure of $[TlMe_2$1,10-phen$]ClO_4$ involved fewer parameters so that all positional parameters were included in one matrix for the refinement at all stages.

However, the crystal structure of $[Co(QP)Cl]BPh_4$ presented a more difficult problem. Three positional parameters and one vibrational parameter for each of the eighty five atoms plus one overall parameter gives a total of 341 parameters to be refined. Actually one of the x

parameters in $P2_1nb$ must be fixed because the choice of origin in this direction is arbitrary. Therefore the x co-ordinate of cobalt was fixed at 0.25 to avoid a singularity. The 340 parameters were then refined in two consecutive cycles of least squares. The programme was limited to 181 parameters in one cycle. In each cycle the cobalt was included. Eight submatrices were used in each case. In the first cycle, the positional parameters for the heavy atoms and each of six phenyl rings were refined in separate submatrices. In the second cycle, the positional parameters for the remaining seven phenyl rings were refined in separate matrices one of which contained the cobalt and boron positional parameters. The overall parameter and the isotropic vibrational parameters were included in a further submatrix in both cycles.

The refinement of the heavy atoms without including the light atoms in the three centrosymmetric structures greatly improved their accuracy. Trial least squares refinement of the heavy atom parameters in the cobalt complex when only a small amount of the scattering matter had been included can also be seen retrospectively to have been useful.

Also the use of least-squares to refine an arbitrarily chosen scale initially for the centrosymmetric structures was in every case very successful owing to the large proportion of the scattering power due to the heavy atoms.

The heavy atom parameters were refined between each Fourier synthesis used in the location of further light atoms.

When all the light atoms had been located, their positional and

isotropic vibrational parameters were refined in the way described above using unit weights for two or three cycles and then further cycles of refinement with the weighting scheme above were made. Convergence occurred at residuals of between 0.08 and 0.10.

A final difference map was computed. No peaks greater than one electron were apparent in any case. The anisotropic vibration did not seem to be great in any of the crystal structures. Also the presence of heavy atoms made the identification of hydrogen atoms from the difference map impossible for a sceptic. As the geometry of the phenyl rings was not important in the chemical discussion of the complexes, no attempt was made to compute the hydrogen atom positions from the known geometry of the phenyl rings.

Details of the refinements are included in the Appendices.

Calculation of bond lengths, angles and their standard deviations

Bond lengths and angles were calculated using the programme written by Dr. J. S. Rollett.

Calculations were made after positional parameters had been derived from Fourier syntheses, and also after every two or three cycles of least squares. These bond lengths and angles were then used in conjunction with information from the electron density map and the least squares shifts and standard deviations to improve the positional parameters.

The standard deviations of bond lengths and angles were calculated using the formulae due to Cruickshank[62] and Darlow[63] respectively.

All values of bond lengths, angles and their standard deviations are given in the Apendices on Pages

The bond lengths of the perchlorate group of $[Pd(TPAS)Cl]ClO_4.C_6H_6$ were exceptionally short. They were 1.42(5), 1.42(5), 1.36(6) and 1.38(5)Å. The values are consistently shorter than 1.45Å, the 'correct' length, although taken individually their standard deviations in parentheses indicate that they are only different from the correct value to about a 5% level of significance.

This error is probably due to thermal vibration. It is impossible to make a rigorously appropriate corrections without a knowledge of their joint distribution, but in this case, we can make a useful estimate from a simplified model of the vibrating system. The mean

separation can be calculated by the method of Busing-Levy assuming a riding model, i.e., the vector separation of the chlorine and the oxygen atoms is independent of the position of the chlorine atom.[64]

As anisotropic refinement programmes were not available, only isotropic vibrational parameters were used:-

$\bar{u}_{Cl}^2 = 0.147$ Å^2 for the chlorine atom

$\bar{u}_{O}^2 = 0.187$ Å^2 for the mean value for the oxygen atoms.

The bond length, S_o, calculated from an electron density map is an underestimation of the mean interatomic separation of the atoms, $\bar{S}$, given by:-

$$\bar{S} - S_o = \left[\bar{u}_o^2 - \bar{u}_{Cl}^2\right] / S_o$$

$$= 0.04 / 1.395 \text{ Å}$$

$$= 0.028\text{Å}$$

if the mean observed bond length is used.

This correction must be an underestimate as an anisotropic vibrational study would show that vibration in directions perpendicular to the chlorine to oxygen bond is greater than the averaged isotropic vibration calculated by the least squares refinement method.

Thus the short chlorine to oxygen bond lengths have no chemical significance.

PART III

DISCUSSION OF

RESULTS OF THE CRYSTAL

STRUCTURE ANALYSES

AND

THEIR RELEVANCE TO

THE STEREOCHEMICAL PROBLEM

OF

PENTACO-ORDINATION

CHAPTER

VALENCY-SHELL ELECTRON-PAIR REPULSIONS

The Crystal and Molecular Structure of (TTAS)Ag-Co(CO)$_4$

The crystal and molecular structure of (TTAS)Ag-Co(CO)$_4$ was determined in order to give information on the importance of valency-shell electron-pair repulsions in determining the stereochemistry of pentaco-ordination (Section 1(a), page 6).

The crystal data, the atomic positional and isotropic vibrational parameters, and the bond lengths with their estimated standard deviations are given in Appendix I (page 159). The R value is 0.102.

The molecular geometry is shown in Figure 3.1 and 3.2, projected onto (1 0 0) and (0 0 1) respectively.

The most interesting features of the molecular structure are the following. The cobalt is pentaco-ordinated in the form of a distorted trigonal bipyramid with a cobalt-silver bond of 2.66( )Å in the axial position, and the equatorial cobalt-carbon bonds are bent towards the silver atom. The silver atom has a distorted tetrahedral stereochemistry, co-ordinated to the ligand, TTAS, as well as the cobalt atom.

The stereochemistry of the cobalt atom is very similar to that in triphenylphosphorous gold-cobalt tetracarbonyl, Figure 3.3, the crystal and molecular structure of which has been determined by the author previously.[14] This also has a distorted trigonal bipyramidal stereo-

Figures 3.1 and 3.2

The Molecular Structure of $(TTAS)AgCo(CO)_4$

Figure 3.3

The Molecular Structure of $Ph_3PAu\text{-}Co(CO)_4$

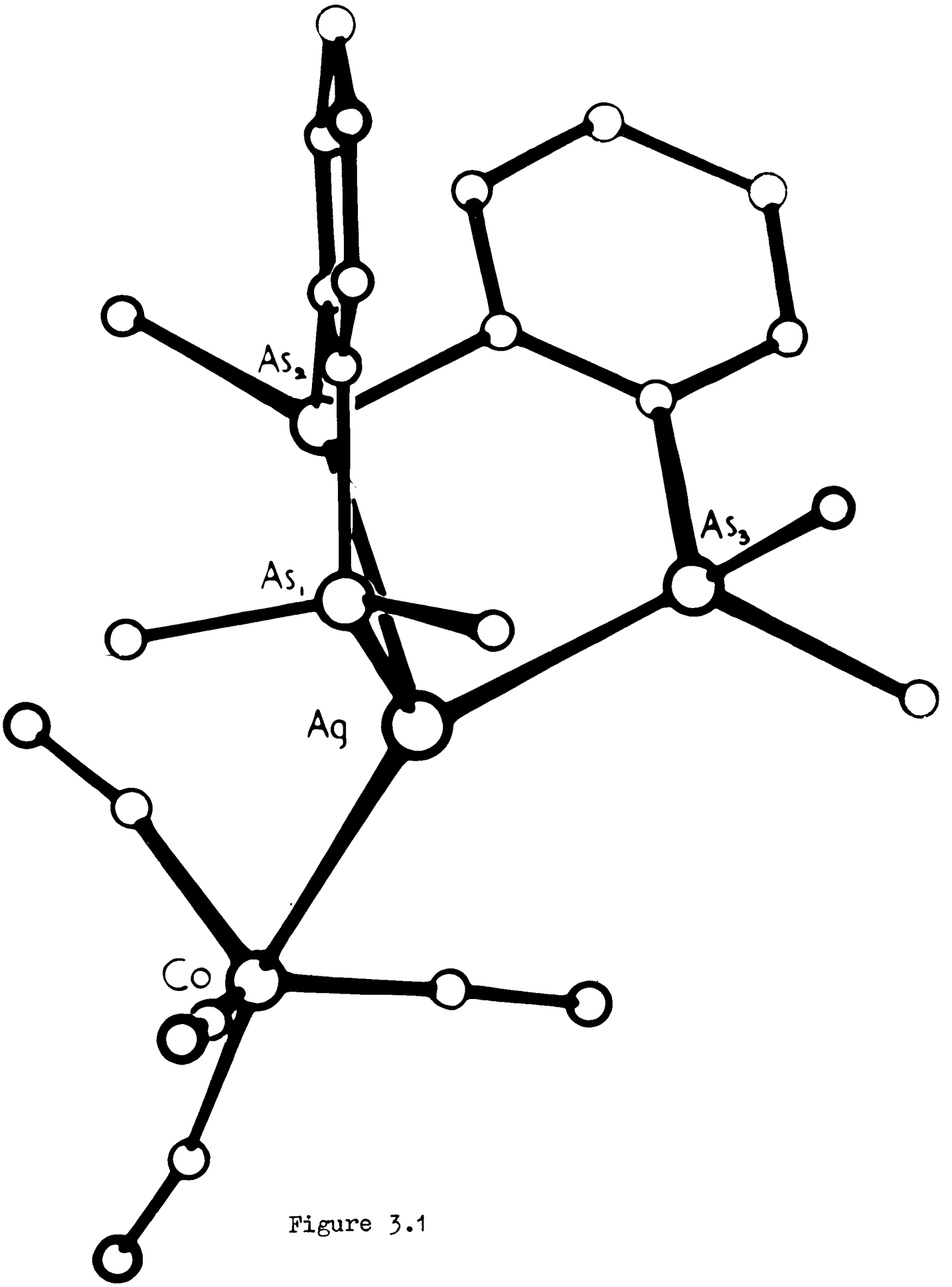

Figure 3.1

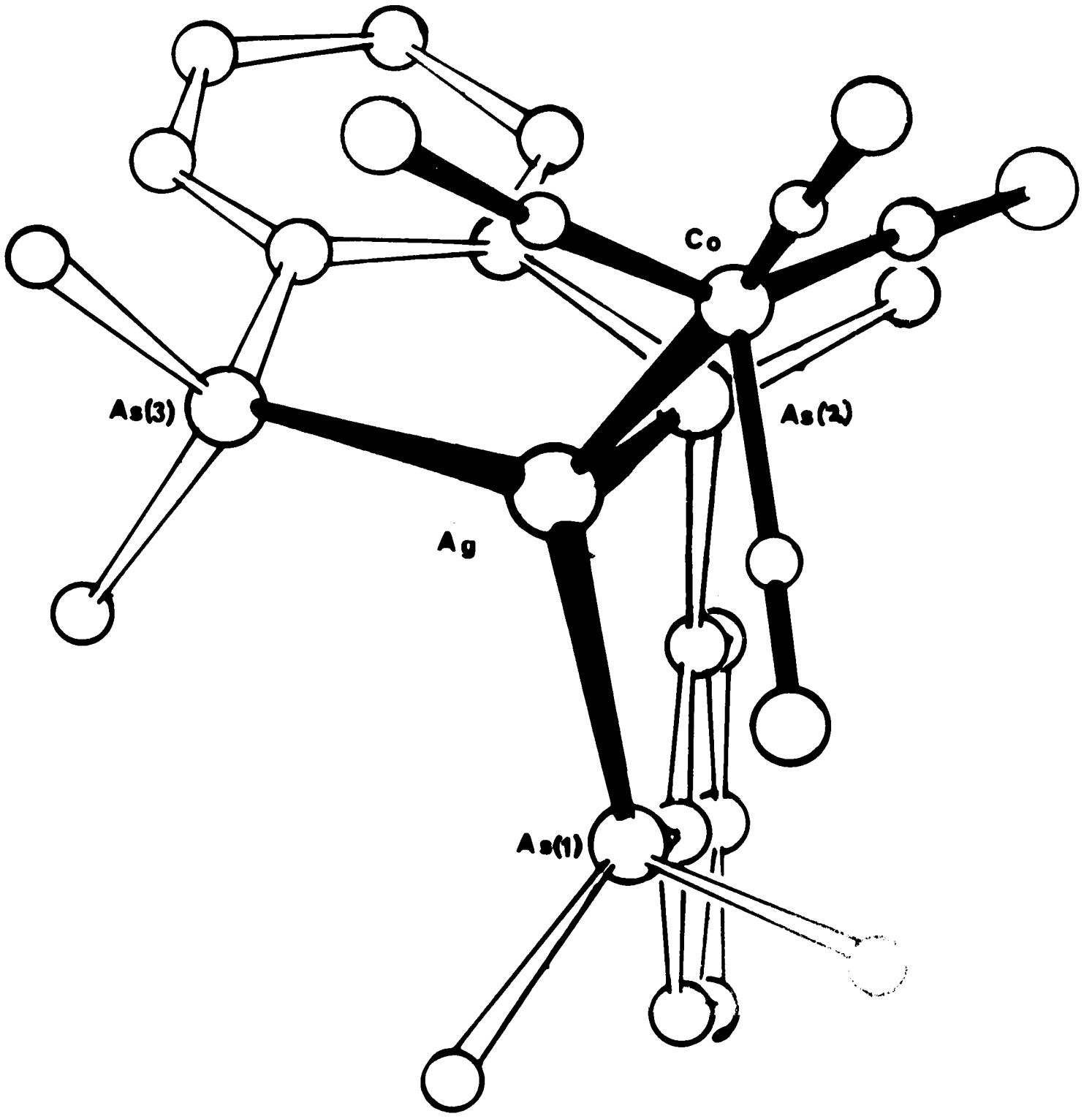

Figure 3.2

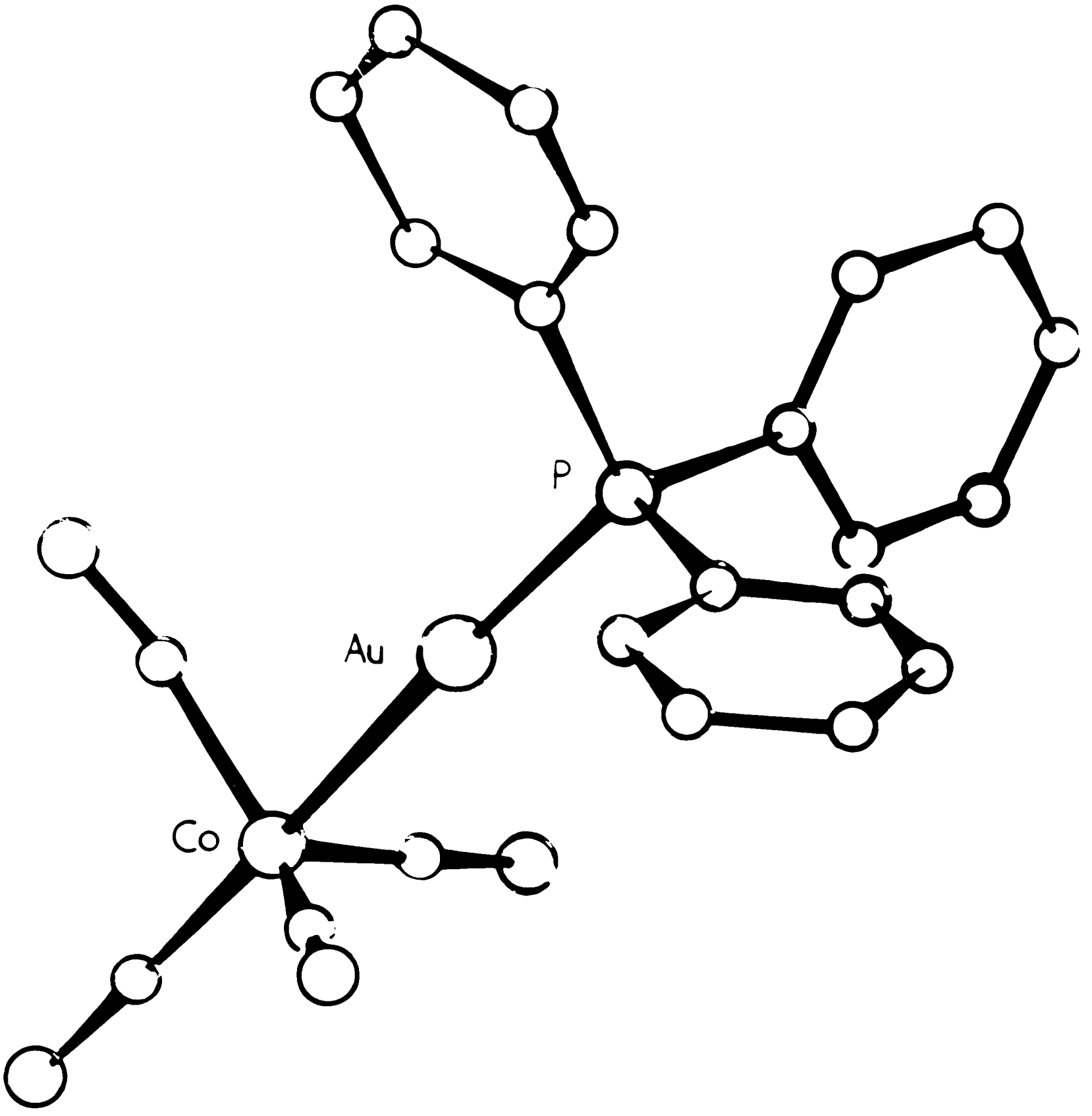

Figure 3.3

chemistry of the cobalt atom with a cobalt-gold bond of length 2.50Å in the axial position and the equatorial carbonyl groups bent towards the gold atom.

The stereochemical features of these molecules are shown diagramatically in Figure 3.5.

Before the discussion of the stereochemistry of the cobalt atom in these molecules, it is convenient to consider the co-ordination at the silver and gold atoms.

The stereochemistry of the silver and gold atoms

The bond lengths and angles of the stereochemistry of the silver atom are shown in Figure 3.4.

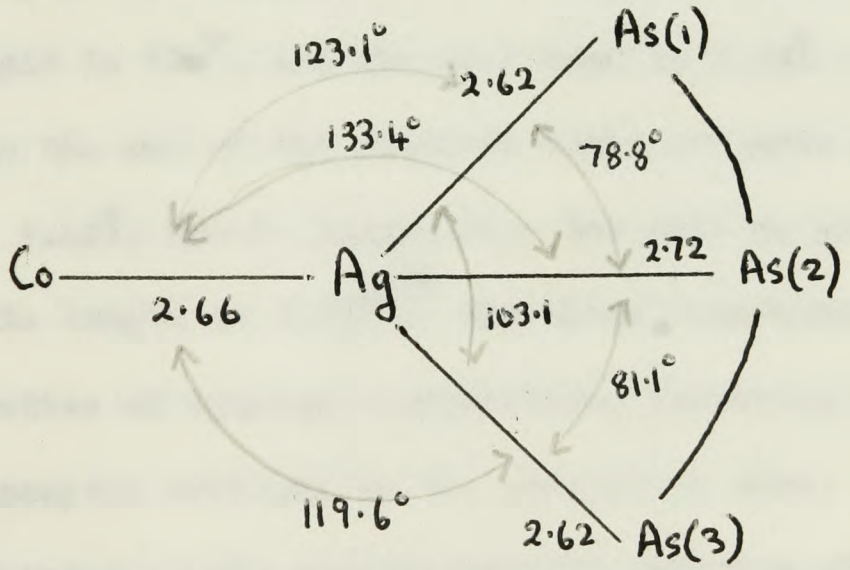

The ligand, TTAS, spans As(1) and As(2), and A(2) and A(3). The angles As(1)-Ag-As(2) and As(2)-Ag-As(3) are about 80°, and these angles are determined by the bridging span of the ligand, TTAS. The

angles, of course, are considerably less than those of an ideal tetrahedron.

The stereochemistry of the silver atom can then be further explained by assuming that these steric requirements of the TTAS ligand cause a strain - . The resultant forces attempt to bring the angles ⟨Co-Ag-As(1), ⟨Co-Ag-As(2) and ⟨Co-Ag-As(3) closer to 108°. As(2) is joined to As(3) and A(1) by briding phenyl groups while As(1) and As(3) are only joined to one other arsenic atom by a bridging phenyl group. The resultant equilibrium attained leads to a large Co-Ag-As(2) angle, and an Ag-As(2) bong length which is greater than both Ag-As(1) and Ag-As(3). A similar geometry is found in the stereochemistry of the copper atom in (TTAS)Cu-$Mn(CO)_5$.[33]

In triphenylphosphine gold-cobalt the gold is two co-ordinate. The Co-Au-P angle is 178°, and the Au-P bond is 2.23Å in length. This is shorter than the sum of the covalent radii off gold and phosphorus, which is about 1.42Å, but is longer than the gold to phosphorus bond in Cl_3P-Au-Cl (P-Au length is 2.19Å).[65] The short P-Au bond lengths are probably indicative of synergic interaction, involving a π-donor bond to empty d_{xy} acceptor orbitals on the phosphorus atom. This back-bonding is increased by the electronegative chlorine atoms in Cl_3P-Au-Cl and so the P-Au bond in this complex would be expected to be shorter than that in Ph_3P-Au-$Co(CO)_4$.

<u>The stereochemistry of the cobalt atom</u>

Before considering the repulsions between bonding electrons in the different orbitals in these complexes it is first necessary to consider

the type of bond, and thus the electron density in the cobalt to carbon and metal to metal bonds. For this it is necessary to consider the covalent radii of these atoms.

The use of covalent radii is always open to criticism; this instance is certainly no exception. The oxidation states of gold, silver and cobalt may be considered to be 0 or alternatively -I and I for the noble metals and cobalt respectively. In these low oxidation states most metal-ligand bonds involve some multiple bonding, and so covalent radii are often derived by extrapolation of a series of covalent radii found in higher oxidation states. Alternatively the covalent radii may be derived from metal to the same metal bond distances if these are available. Here again the bond lengths are affected by factors such as double bonding or a lengthening of the bond by non-bonding electron repulsions. Finally the covalent radius varies with the co-ordination number. Thus covalent radii must be derived by as many methods as possible, their individual accuracy assessed and the results of the different methods compared. From these an estimate of the covalent radius may be derived along with the accuracy expected for this value.

Few complexes are available from which a two co-ordinate covalent gold radius for $Ph_3PAu\text{-}Co(CO)_4$ can be derived. The gold to gold distance in the metal is 2.88Å. The co-ordination for the gold is twelve, and thus the covalent radius for the two co-ordinate Au(0) should be smaller than 1.44Å. The Au(1)-P distances vary from 2.19Å

in Cl_3PAuCl[65] to 2.34Å in a gold-manganese bonded complex. This is indicative of some double bonding in these complexes which varies with the acceptor properties of the phosphorus d orbitals. Gold chlorine distances in the $AuCl_2^-$ ion[66] and Cl_3PAuCl are in close agreement, however, at 2.31 and 2.33Å respectively. Allowing a covalent radius for chlorine of 1.0Å, this gives a covalent radius for Au(1) as 1.32±0.02Å.

Cobalt is five co-ordinate in the complex studied. In the metal it is twelve co-ordinate and gives a covalent radius of 1.25Å which will be too large. Accurate three-dimensional crystal structure determinations have been made for several complexes containing Co-Co bonds[67-70], which vary in length from 2.45Å to 2.52Å, and therefore the covalent radius may be taken as 1.24± 0.02Å for Co(0).

Thus a simple covalent bond between Au(I) and Co(0) would be 2.56Å± 0.04Å. The observed bond length is 2.50± 0.02Å between, say Au(0) and Co(0) which may have been expected to be longer than 2.56Å. The bond is thus a predominantly single covalent bond, with some shortening maybe due to electronegativity differences, or possible to a very small amount of double bonding.

The covalent radius for silver should, as a result of the lanthanide contraction be the same as that of gold. However, in $(TTAS)AgCo(CO)_4$ the silver is four co-ordinate; the radius should be larger. This adequately accounts for the greater length of the silver to cobalt bond of 2.67Å, which is therefore also a single covalent bond.

Cobalt-carbon bond lengths in the two molecules are as follows:-

	$(TTAS)Ag\text{-}Co(CO)_4$	$Ph_3P\text{-}Au\text{-}Co(CO)_4$
Co-C(4)	1.71 Å	1.71 Å
Co-C(5)	1.77	1.76
Co-C(6)	1.64	1.62
Co-C(7)	1.78	1.83

The standard deviations of the bond lengths indicate that these bonds are not different at 0.1% level of significance. The mean value is 1.73(6). However, the sum of the covalent radii for cobalt and carbon single bonds is 2.01Å (1.24Å + 0.77Å). Therefore, these bonds must involve considerable multiple bonding.

To summarise, the valency-shell of the cobalt atoms in the complexes, $(TTAS)Ag\text{-}Co(CO)_4$ and $Ph_3P\text{-}Au\text{-}Co(CO)_4$, contain four multiple bonds to the carbonyl carbon atoms, and a single bond to the silver and gold atoms respectively.

The stereochemistry observed in the two complexes is shown in fig. 3.5.

Consider the following argument concerning valency-shell electron-pair repulsions.

The discussion above has indicated that the Co-C bonds are multiple bonded. If this is so the bonds will be very bulky compared with single covalent bonds, and repulsion terms between the electrons in the bonds of the cobalt valency-shell will become important in determining the stereochemistry. As a result the trigonal bipyramid will

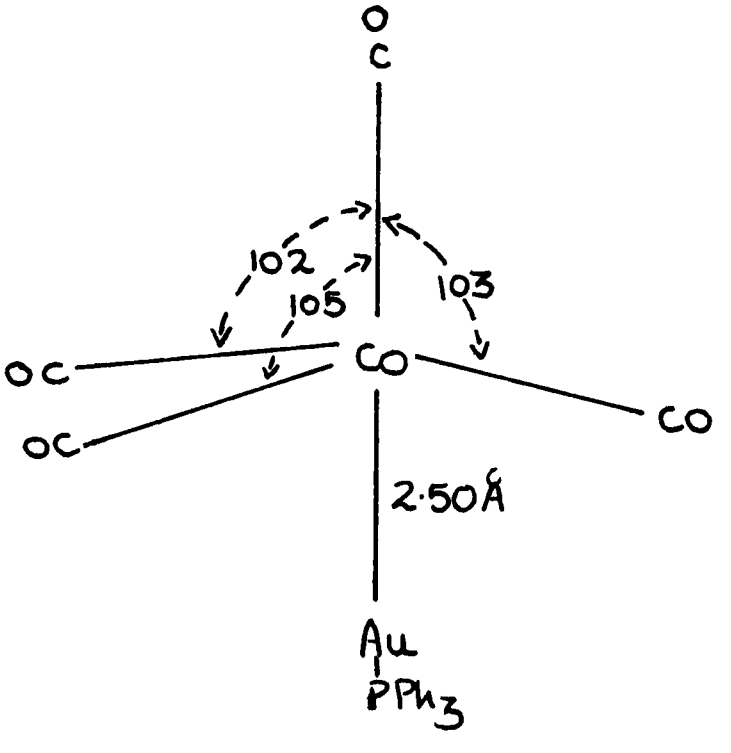
O
C
102°
105°
103°
OC
CO
OC
CO
2·50Å
Au
PPh3

Figure 3.5

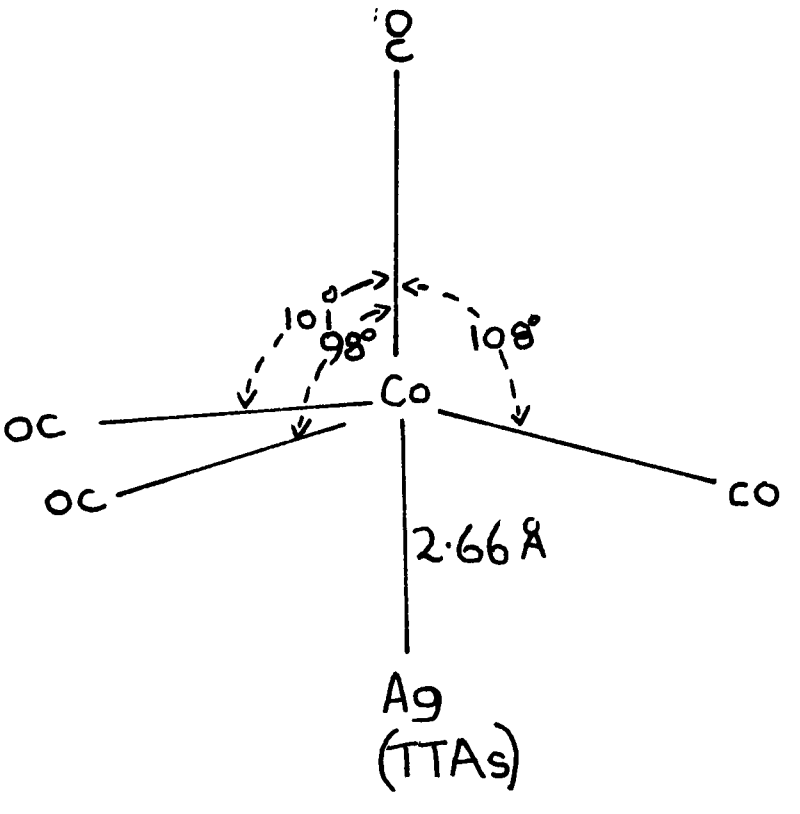
O
C
101°
98°
108°
OC
Co
OC
CO
2·66 Å
Ag
(TTAs)

be the strongly favoured geometry. The observed geometry is distorted trigonal bipyramidal.

Secondly, it was indicated in Section 1(a) that repulsion experienced by an electron-pair in an axial bond of a trigonal bipyimidal stereochemistry is greater than that experienced by an equatorial electron pair. It is thus likely that the most bulky bonds will occupy equatorial positions in the trigonal bipyramidal geometry. Thus, carbonyl groups should occupy the equatorial positions. In both $(TTAS)Ag\text{-}Co(CO)_4$ and $Ph_3P\text{-}AuCo(CO)_4$, the metal-metal bond occupies an axial position. This argument parallels Gillespie's arguments explaining the occurrence of the inert pair and double bond of SF_4 and SF_4O[8] respectively in the equatorial positions of the trigonal bipyramidal geometries.

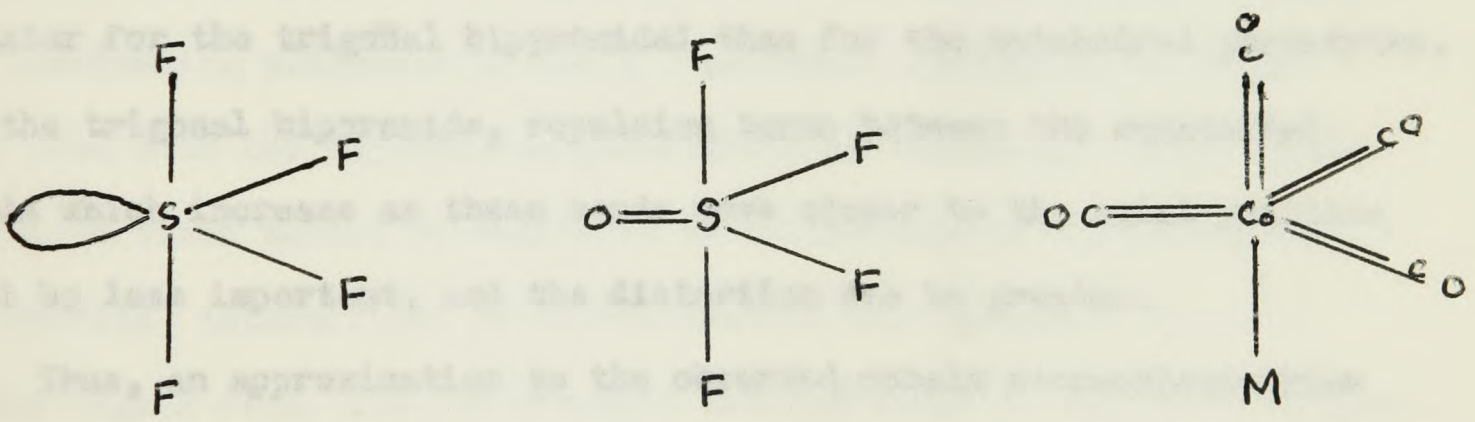

However, the trigonal bipyramidal model has a bulky Co-C bond in one axial position. In order to decrease the destabilizing influence of the consequent repulsions, a better model would be a distorted trigonal bipyramid with the angle between the axial metal-metal bond and equatorial bonds less than 90°, so that the repulsions between

axial and equatorial bonds are equilibrated. The observed geometry of the distorted trigonal bipyramidal stereochemistries is such that the angles between the axial and equatorial Co-C bonds are 96°, 102° and 108° in (TTAS)Ag-$Co(CO)_4$ and 100°, 102° and 103° in Ph_3PAu-$Co(CO)_4$.

A similar banding of carbonyl groups towards a metal-metal bond is observed in $Mn_2(CO)_{10}$[71], (TTAS)Cu-$Mn(CO)_4$[33], Ph_3P-Au-$Mn(CO)_5$[72] and Me_2Sn $Mn(CO)_5$[33] and all other metal-metal bonded carbonyls. These distortions could all be explained by valency-shell electron-pair repulsions, although previously packing requirements and non-bonding electron repulsions have been used to explain their stereo-chemistries.

The explanation of these distortions from idealised trigonal bipyramidal and octahedral geometries in terms of valency-shell electron-pair repulsions is consistent with the fact that the distortions are greater for the trigonal bipyramidal than for the octahedral geometries. In the trigonal bipyramids, repulsion terms between the equatorial bonds which increase as these bonds move closer to the axial position will be less important, and the distortion can be greater.

Thus, an approximation to the observed cobalt stereochemistries in (TTAS)Ag-$Co(CO)_4$ and Ph_3P-Au-$Co(CO)_4$ can be explained in terms of valency-shell electron-pair repulsions.

Consider now the effect of the other three factors discussed in the introduction to this thesis:-

b) Crystal field stabilization energy effects

c) Steric requirements of the ligand

d) Packing requirements in the crystal.

b) The d-electron configuration of the cobalt in (TTAS)Ag-$Co(CO)_4$ and Ph_3PAu-$Co(CO)_4$ can be described as d^8 or d^9 depending on whether the cobalt is considered to be Co(0) or Co(I). The crystal field stabilization energy for these electron configurations would favour the square pyramidal geometry. The valency-shell electron-pair repulsion terms must dominate in this instance.

c) The ligands are all unidentate so that steric requirements of the ligand must be restricted to repulsions between non-bonding electrons.

Repulsions between the non-bonding electrons of the ligand atoms would favour the trigonal bipyramidal geometry. These arguments do not, however, offer an explanation for the distortion of the carbonyl groups towards the large gold atom in Ph_3PAu-$Co(CO)_4$.

Alternatively, consider the effect of the large repulsion between the non-bonding electrons of the d^{10} electron configuration of the gold atom with the non-bonding d-electrons of the cobalt atom. These repulsion terms cannot be decreased as in the case of cobalt-carbon non-bonding interactions by delocalisation into acceptor orbitals on the ligand atom, i.e. by synergic interaction. A distorted trigonal bipyramid may, however, minimise the non-bonding d-electron repulsions.

Let the metal-metal bond be in the z direction. The largest repulsion terms would then be between the spherical d^{10} electron shell on the gold or silver atom and the d_{xz} and d_{yz} orbitals on the cobalt atom. If these orbitals are mixed with a little p_x and p_y orbitals, two new

orbitals for each pair hybridised will be given. For instance, the mixing of the p_x and d_{xz} orbitals can be diagramatically shown as:-

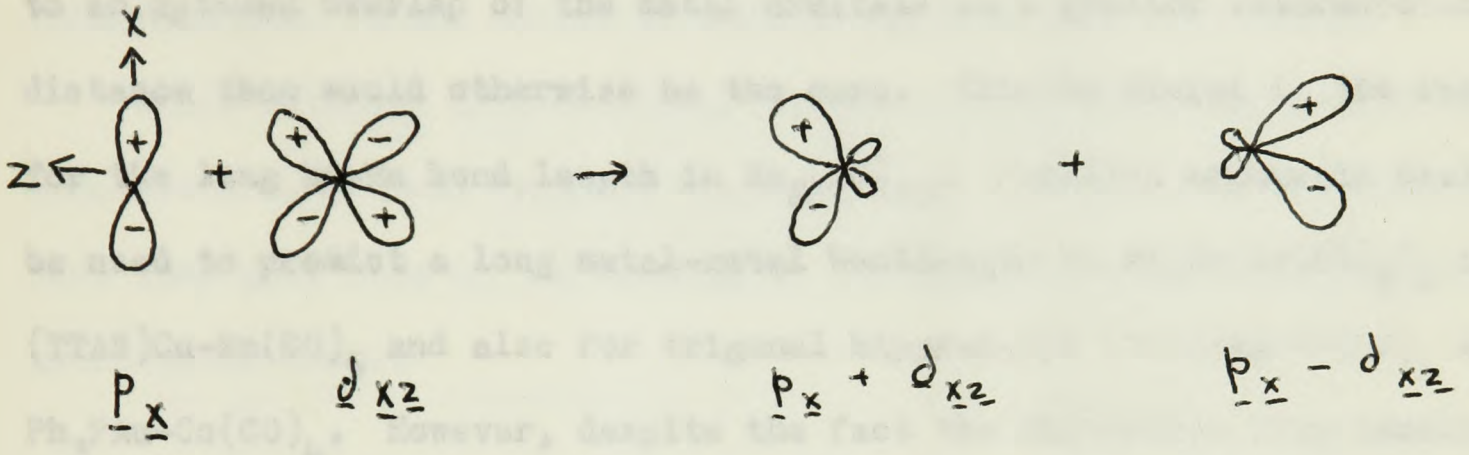

p_x d_{xz} $p_x + d_{xz}$ $p_x - d_{xz}$

If a hybrid is formed with a little d_{xz} mixed with p_x orbital, this would give good overlap for a σ -bond in the direction of an equatorial position bent towards the apex of a distorted trigonal bipyramidal arrangement of ligand orbitals. The hybrid orbital d_{xz} with a little p_x could then be occupied by non-bonding electrons, which would have the correct symmetry to overlap with any equatorial ligand acceptor orbitals to stabilize the stereochemistry by a synergic interaction. Finally the new hybrid orbital occupied by the non-bonding electrons would then be mainly pointing away from one apical position of the trigonal bipyramid.

Stated in another way, we conclude that a bending of the equatorial carbonyl groups towards the apical silver or gold atoms may be indicative of a rehybridisation of the non-bonding orbitals of the cobalt to decrease the destabilizing influence of non-bonding electron repulsions between the cobalt and gold or silver atoms.

A similar argument has been put forward by R. Mason to explain the

distortion in $Mn_2(CO)_{10}$.[73] By an extension of the argument using non-orthogonalised orbitals he concludes that the rehybridisation leads to an optimum overlap of the metal orbitals at a greater intermetallic distance than would otherwise be the case. This he claims is the reason for the long Mn-Mn bond length in $Mn_2(CO)_{10}$. Parallel arguments could be used to predict a long metal-metal bondlength in $Me_2Sn(Mn(CO)_5)_2$ and (TTAS)Cu-$Mn(CO)_5$ and also for trigonal bipyramidal (TTAS)Ag-$Co(CO)_4$ and Ph_3PAu-$Co(CO)_4$. However, despite the fact the distortion from idealised geometry is often greater in these complexes, in no case is the metal-metal bond longer than the sum of the estimated covalent radii.[33,72]

Nevertheless, the less dubious derivation of the interrelation of the non-bonding d-electron repulsions and the distorted trigonal bipyramidal geometries of (TTAS)Ag-$Co(CO)_4$ and Ph_3PAu-$Co(CO)_4$ may still be considered an alternative explanation for the observed stereochemistries.

d) Intermolecular forces must also be considered. Packing requirements in the crystal structure may be responsible for the distortion of the trigonal bipyramidal geometry.

In (TTAS)Ag-$Co(CO)_4$, the shortest intermolecular distance is 3.2Å between the axial carbonyl oxygen of one molecule and a methyl group of the ligand, TTAS, or a molecule related by a centre of symmetry. The apical carbonyl group is bent away from this methyl group towards C(6) giving a $\angle$ C(4)-Co-Ag angle of 168°.

There are no very short intermolecular distances between the equatorial carbonyl oxygen atoms in the crystal structure of (TTAS)Ag-$Co(CO)_4$. However, the intramolecular distance between methyl carbon C(31) and oxygen

O(7) is 3.7Å. This is less than any intermolecular distance between O(7) and any other atoms. The angle $\angle$ Ag-Co-C(7) is less than 90°. Intermolecular forces cannot be used to explain this distortion.

Thus, although intermolecular forces are probably responsible for some distortions from trigonal bipyramidal geometry, it seems unlikely that they give rise to the bending of the carbonyl groups towards the metal-metal bonds.

To conclude, valency-shell electron-pair repulsions are probably responsible for the trigonal bipyramidal stereochemistry of (TTAS)Ag-Co$(CO)_4$ and Ph_3PAu-Co$(CO)_4$. The importance of valency-shell electron-pair repulsions is consistent with the axial metal-metal bonds and the distortion of the carbonyl groups towards this bond. Rehybridisation of the electron orbitals of cobalt to decrease the non-bonding electron repulsions between the cobalt and gold or silver atoms must be considered an alternative explanation for the bonding of the equatorial bonds. Intermolecular forces do not appear to be the main factor in causing this distortion although they may be responsible for minor distortions of the carbonyl groups. Crystal field stabilization energy effects are unimportant compared with valency-shell electron-pair repulsions.

CHAPTER 5

CRYSTAL FIELD STABILISATION ENERGY EFFECTS

The Crystal and Molecular Structure of $[Pd(TPAS)Cl]ClO_4.C_6H_6$

The molecular structure of $[Pd(TPAS)Cl]ClO_4.C_6H_6$ has been analysed in order to gain further information on the importance of crystal field stabilisation energy in determining the stereochemistry of pentaco-ordination.[76]

The chemical information available about this complex has been discussed in Section 1.b., page 15 and crystallographic data are summarised in Appendix II , page 166 . The R value is 0.085.

The complex unipositive ion is shown in Figure 3.6. The palladium has a square pyramidal co-ordination with the chlorine atom in the basal plane. Consider first the packing of this pentaco-ordinate complex ion with the perchlorate ion and the clathrated benzene.

Figure 3.7 shows the structural relationship of the pentaco-ordinate ion with the perchlorate ion, which is not disordered. The closest oxygen of the perchlorate ion is at 3.8Å from the palladium atom, and the palladium to oxygen vector makes an angle of about 80° with the basal plane of the square pyramid. The van der Waals radii

Figure 3.6

The Structure of the cation, $\left[Pd(TPAS)Cl\right]^{+}$

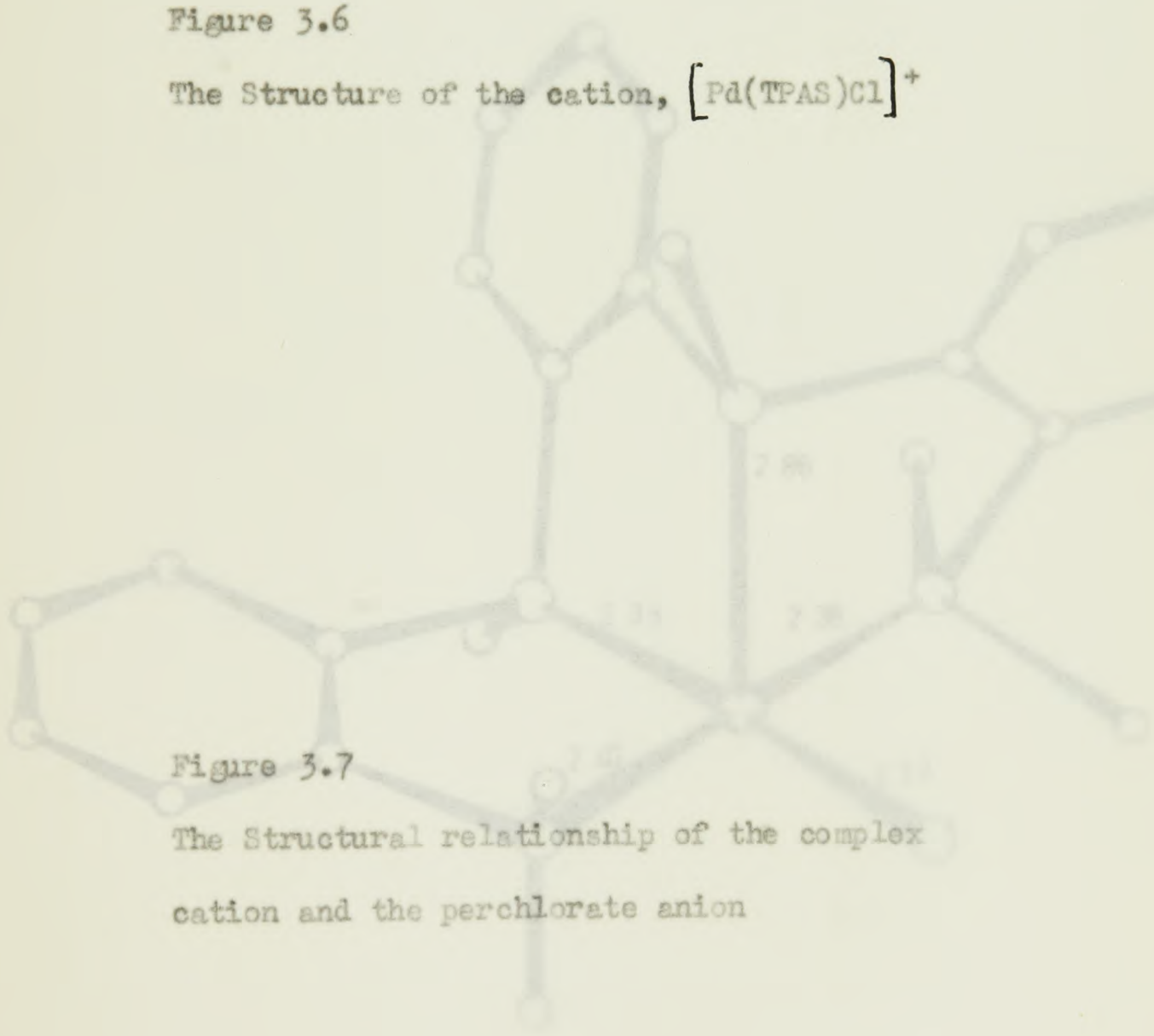

Figure 3.7

The Structural relationship of the complex cation and the perchlorate anion

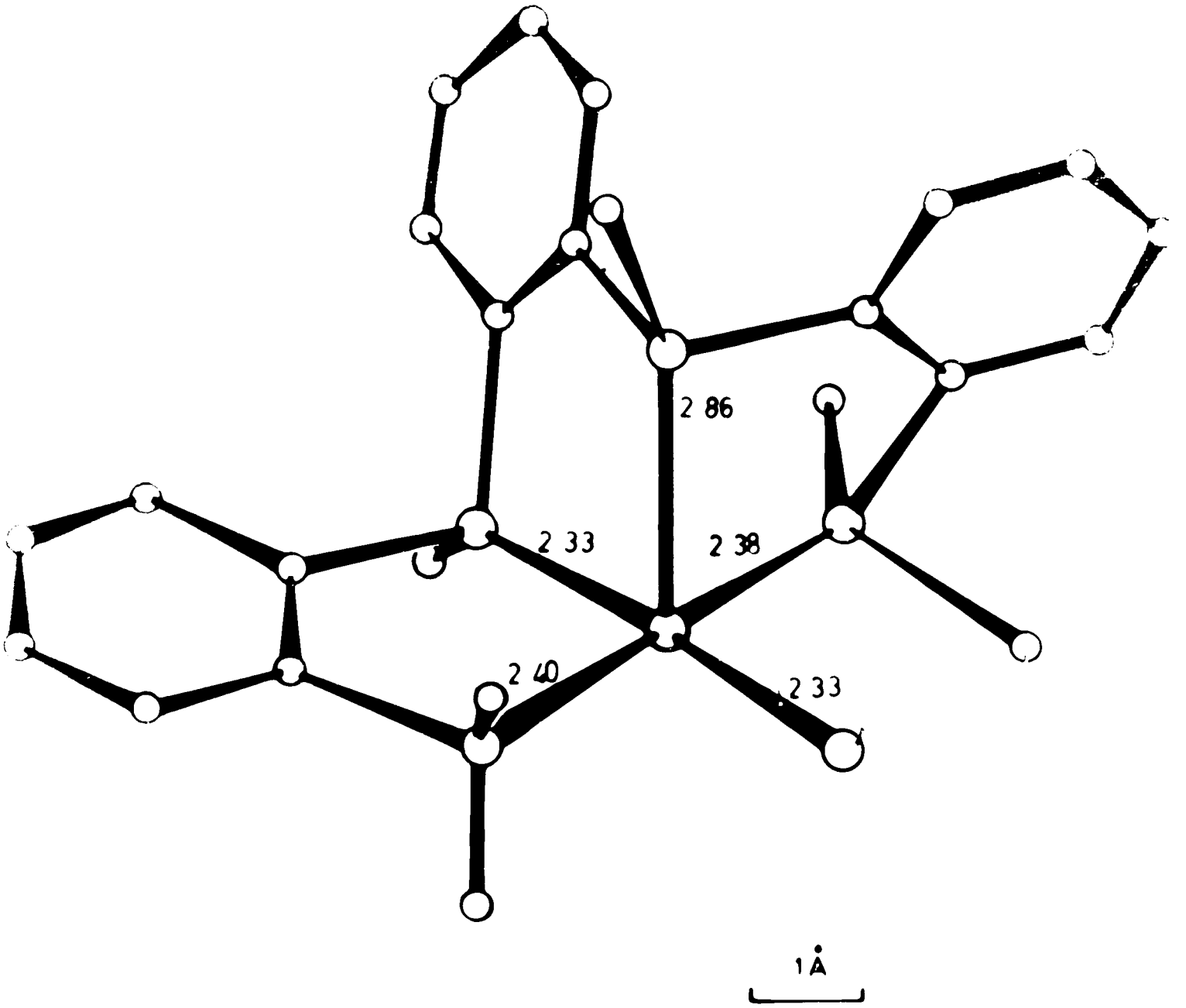

Figure 3.6

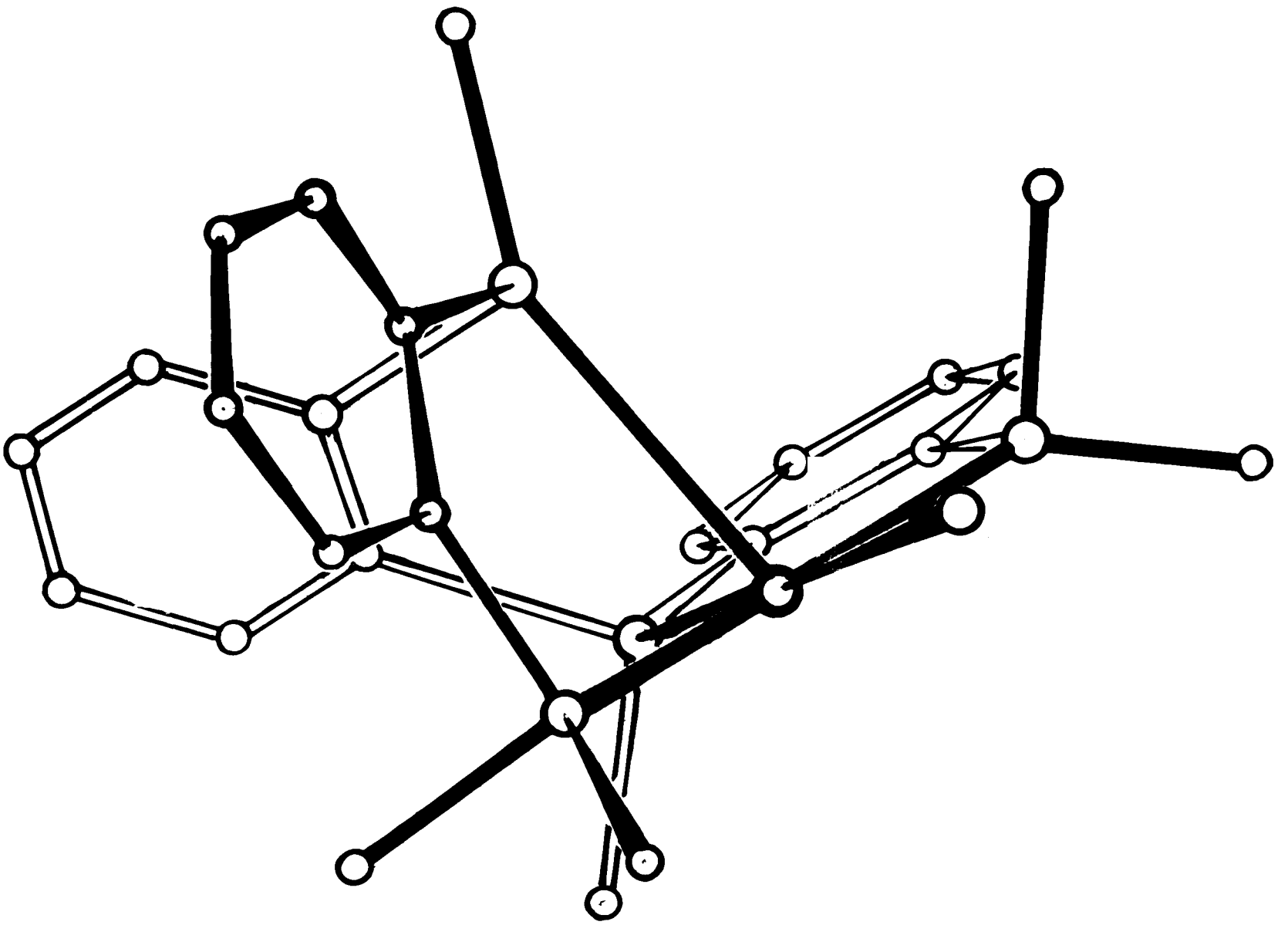

Figure 3.7

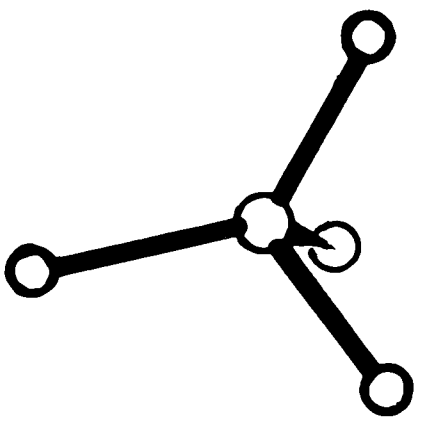

of the oxygen and palladium are 1.40Å and 1.28Å respectively[5]. The sum of these, 2.68Å, is considerably less than the observed interatomic distance and, therefore, no delocalisation of charge between the complex ion and the perchlorate ion is possible. The juxtaposition of the palladium and perchlorate oxygen in the crystal structure arises from an electrostatic attraction which at the observed distance must be weak.

Figure 3.8 shows the packing of the molecules in the unit cell projected down the a axis. Six large positive ions are arranged in an approximately hexagonal array, leaving a large hole in the centre. The hexagonal hole is in fact a channel which runs through the crystal, in the direction of the a axis, and a set of channels form a honeycomb-like structure. As the perchlorate ions, which are held in these channels in a zig-zag pattern, are small compared with the channel width, cavities still remain. The structure is stabilised by inclusion of benzene to form a clathrate complex. Each benzene is completely surrounded by an array of positive and negative ions, and there are no abnormally short intermolecular distances.

In two five co-ordinate complexes of second and third row transition metals[19,74] the pyramidal co-ordination is made octahedral by the close approach of an hydrogen in the sixth position. In the structure of a polymeric square pyramidal palladium diphosphine diodide determined recently[19], a phenyl hydrogen is 2.8Å from the palladium atom. Although the positions of the hydrogens in the present structure have

Figure 3.8

The Crystal Structure of $[Pd(TPAS)Cl]ClO_4.C_6H_6$

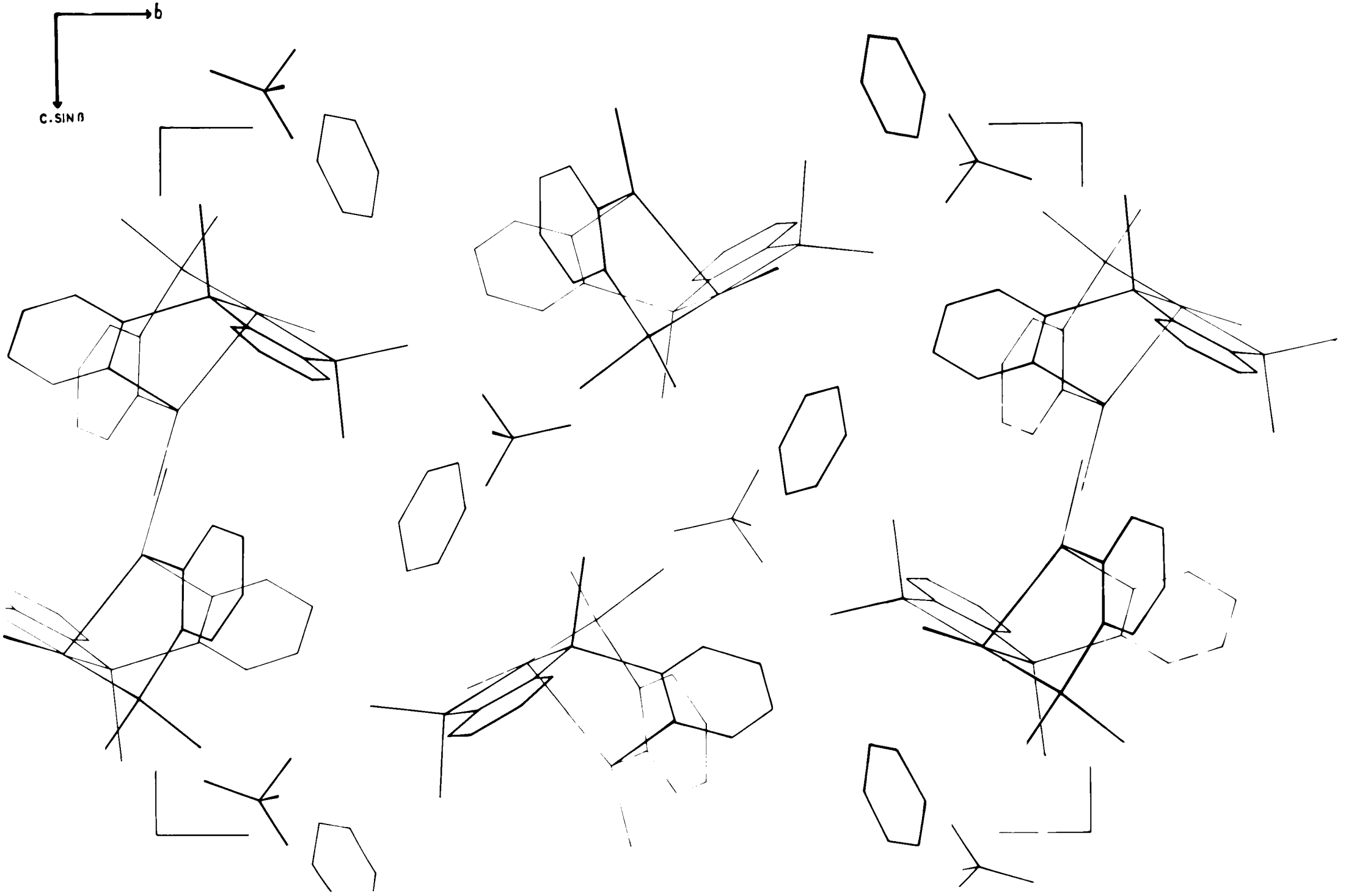
b
C.SIN β

not been determined, the closest approach possible of an hydrogen atom to the palladium atom would be 3.5Å, and then the angle between the Pd - H vector and the square basal plane would be about 45°. The hydrogens, therefore, must be well away from the sixth position and the ion can be considered as pentaco-ordinate.

Thus it is clear that there is no delocalisation of charge between the cation and either the perchlorate ion or the clathrated benzene. Consider now the co-ordination of the palladium in the cation which is not that of a regular square pyramid (Figure 3.6, page 123). The palladium-arsenic bonds in the basal plane are significantly different in length, and the apical bond is almost 0.5Å longer than any of those in this plane, although the atoms in the basal plane are almost coplanar with the palladium atom. The apical bond makes an angle of about 81° with this plane.

The steric requirements of the ligand must be considered in relation to the preferred geometry. The ligand, TPAS, is quite flexible. Previous work[36] on the crystal structures of complexes with polydentate arsenic ligands with phenyl bridging groups has shown that although the bridging span (the distance between two arsenics attached to the same phenyl group) must be close to 3.3Å, the co-ordination round the arsenic atoms is very flexible. For instance, in $Ru(QAS)Br_2$[36], the angles at the arsenic atoms were significantly different from the regular tetrahedral angle; values were observed to vary from 94° to 150°. If similar distortions are

allowable, the ligand, TPAS, could co-ordinate in either a square pyramidal geometry or a trigonal bipyramidal geometry provided that in the latter it is not required to span two equatorial positions.

In fact the extreme length of the palladium to apical arsenic bond in the observed structure causes this arsenic to have a very distorted co-ordination similar to that in $Ru(QAS)Br_2$[36]. The apical atom is pulled to one side by the rest of the ligand so that the As(1) - As(2) and As(2) - As(3) bridging distances are both 3.3Å as required. The Pd - As(2) vector then makes an angle of 81° with the basal plane. The mean distortion from the regular tetrahedral angle is 15° at this apical arsenic atom.

The basal plane of the square pyramid, however, is not greatly distorted. The palladium, chlorine and three arsenic atoms lie within 0.06Å of the best least squares plane through them. This is unlike the co-ordination of many square pyramidal complexes where the metal atom lies above the basal plane[4]. A distortion of the geometry so that the palladium atom was above the plane of the four ligand atoms would decrease electron-pair repulsions at the expense of the crystal field stabilisation energy. It appears that in this case electron-pair repulsions are less important, and crystal field stabilisation energy more important in determining the stereochemistry. Moreover, crystal field stabilisation energy is greater for the square pyramidal geometry observed here than for the trigonal bipyramidal geometry ...

(Section 1.b, page 8). It is most probably this factor which predominates in this case, and is responsible for the square pyramidal geometry.

In contrast, the square pyramidal complex, triphosphine palladium dibromide[19], where the phosphine is 2-phenyl iso-phosphindoline, has the bromine in the basal plane distorted by 10° from the best least squares plane through the phosphorus and palladium atoms. This may result from steric repulsions due to the larger size of the bromine atom compared with the chlorine atom in $[Pd(TPAS)Cl]^+$. Also spectral work on $[Pd(TPAS)I]^+$ indicates that the iodine is in the axial position[20]. An iodine atom in the apical position where the bond should certainly be longer would be less subject to steric repulsions than an iodine atom in the basal plane.

The great length (2.86Å) of the apical arsenic to palladium bond is similar to those observed in other square pyramidal complexes of transition metals in this part of the periodic table[18,17]. The $\underline{d}^8$ electron configuration in a strong field will have two electrons in the $\underline{d}_{z^2}$ orbital which is directed towards the apical bond, but the $\underline{d}_{x^2-y^2}$ orbital in the basal plane will be unoccupied. An extension of the apical bond results in a stabilisation due to the consequent decrease of repulsion between the valence electron pair in this bond with the prolate core of $\underline{d}^8$ electrons.[8]

Alternatively, the long bond may be considered in terms of stabilisation in a square pyramidal crystal field. The energy levels

of the d orbitals have been given in Section 1.b, page 9 . They are

$$E(d_{x^2-y^2}) = K\mu(4B_0+4/7B_2+19/21B_4)+K\mu_z(B_0-2/7B_2+1/21B_4)$$

$$E(d_{z^2}) = K\mu(4B_0-4/7B_2+3/7B_4)+K\mu_z(B_0+2/7B_2+2/7B_4)$$

$$E(d_{xy}) = K\mu(4B_0+4/7B_2-16/21B_4)+K\mu_z(B_0-2/7+1/21B_4)$$

$$E(d_{xz},d_{yz}) = K\mu(4B_0-2/7B_2-2/7B_4)+K\mu_z(B_0+1/7B_2-4/21B_4)$$

Let K be considered a constant in this analysis. The basal plane dipoles are considered equal (with value μ) while the axial dipole may have a different dipole μ_z. The fact that B_2/B_4 varies only slightly for moderate variations of the palladium-dipole distance allows the treatment of small variations of the palladium ligand distance by varying the μ value.[75] An increase in the axial bond length will be equivalent to a decrease in the effective dipole μ_z. The expressions for the energy levels of the d orbitals show that this results in a relative stabilisation of the d_{z^2}, d_{xz} and d_{yz} orbitals and a relative destabilisation of the d_{xy} and $d_{x^2-y^2}$ orbitals. For a strong field d^8 electron configuration, this gives an increase in crystal field stabilisation energy.

The Pd - As bond lengths in the basal plane also differ to a small extent among themselves. The bonds are all different to a 0.1% level of significance, and this may be due to the steric

requirements of the ligand. However, the Pd - As bond trans to the chlorine atom is 2.331Å which is considerably shorter than the two Pd - As bonds trans to each other of lengths 2.375Å and 2.408Å. This is consistent with a smaller trans-effect for the chlorine atom than for the arsenic ligand.

In conclusion, it can be said that the crystal structure determination underlines the importance of crystal field stabilisation energy for the d^8 electron configuration where it is greater for the square pyramidal geometry. Steric requirements of the ligand, TPAS, do not preclude the formation of a trigonal bipyramidal stereochemistry although they do appear to result in distortions from the idealised square pyramidal geometry in the observed structure. Valency-shell electron-pair repulsions seem to be less important than crystal field stabilisation energy in determining the stereochemistry of the pentaco-ordinate $[Pd(TPAS)Cl]^+$ complex ion.

Chapter 6

Steric Requirements of the Ligand
The Crystal and Molecular Structure of $[Co(QP)Cl]BPh_4$.

The structure of $[Co(QP)Cl]BPh_4$ is relevant to the stereochemical problem of penta co-ordination. It represents a situation where the steric requirements of the ligand prefer a different stereochemistry from that giving the greatest crystal field stabilization. Further, a perfect trigonal bipyramidal geometry would not be allowed by the Jahn Teller effect for this low-spin d^7 complex.

A diagram of the ligand, QP, and the structure proposed as a result of chemical spectroscopic work has been given in the introduction, (p. 21). The crystal data, the atomic positional and isotropic vibrational parameters, and the bond-lengths and bond-angles with their estimated standard deviations are given in Appendix III (p. 172). The R value is 0.111.

The geometry of the cation shown in figures 3.9, 3.11 and 3.12 is in fact intermediate between a square pyramid and a trigonal bipyramid, but is closest to a trigonal bipyramid with one equatorial angle of 137.2°, a short axial Co-P bond and P-Co-P angles between the axial and equatorial Co-P bonds of less than 90°.[77] A full discussion of the nature of this distorted stereochemistry must follow a consideration of the molecular structure of the crystal.

The molecular structure projected onto (010) is shown in figure 3.10.

Figure 3.9

The geometry of the $[Co(QP)Cl]^+$ cation

Figure 3.10

The Crystal Structure of $[Co(QP)Cl]BPh_4$

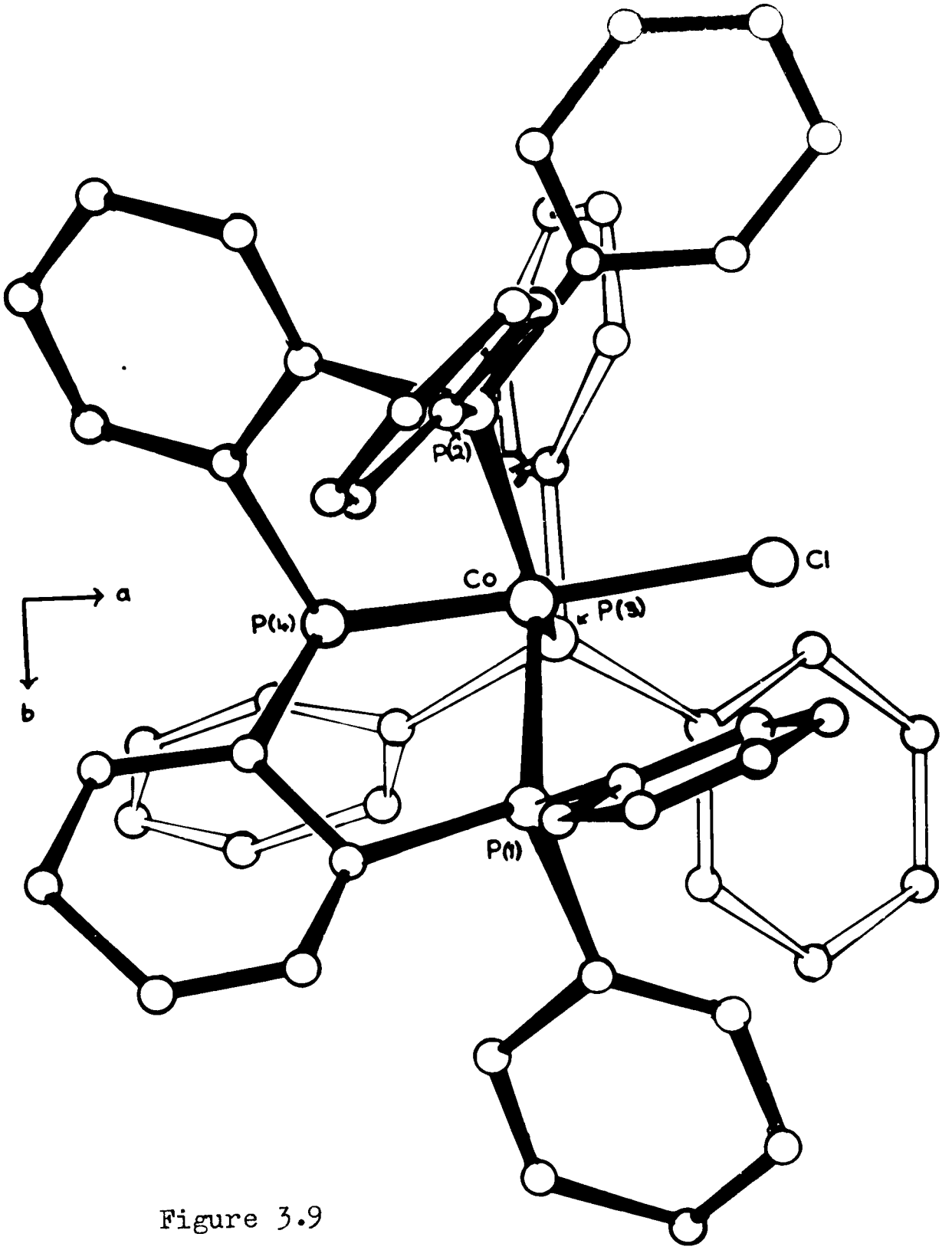

Figure 3.9

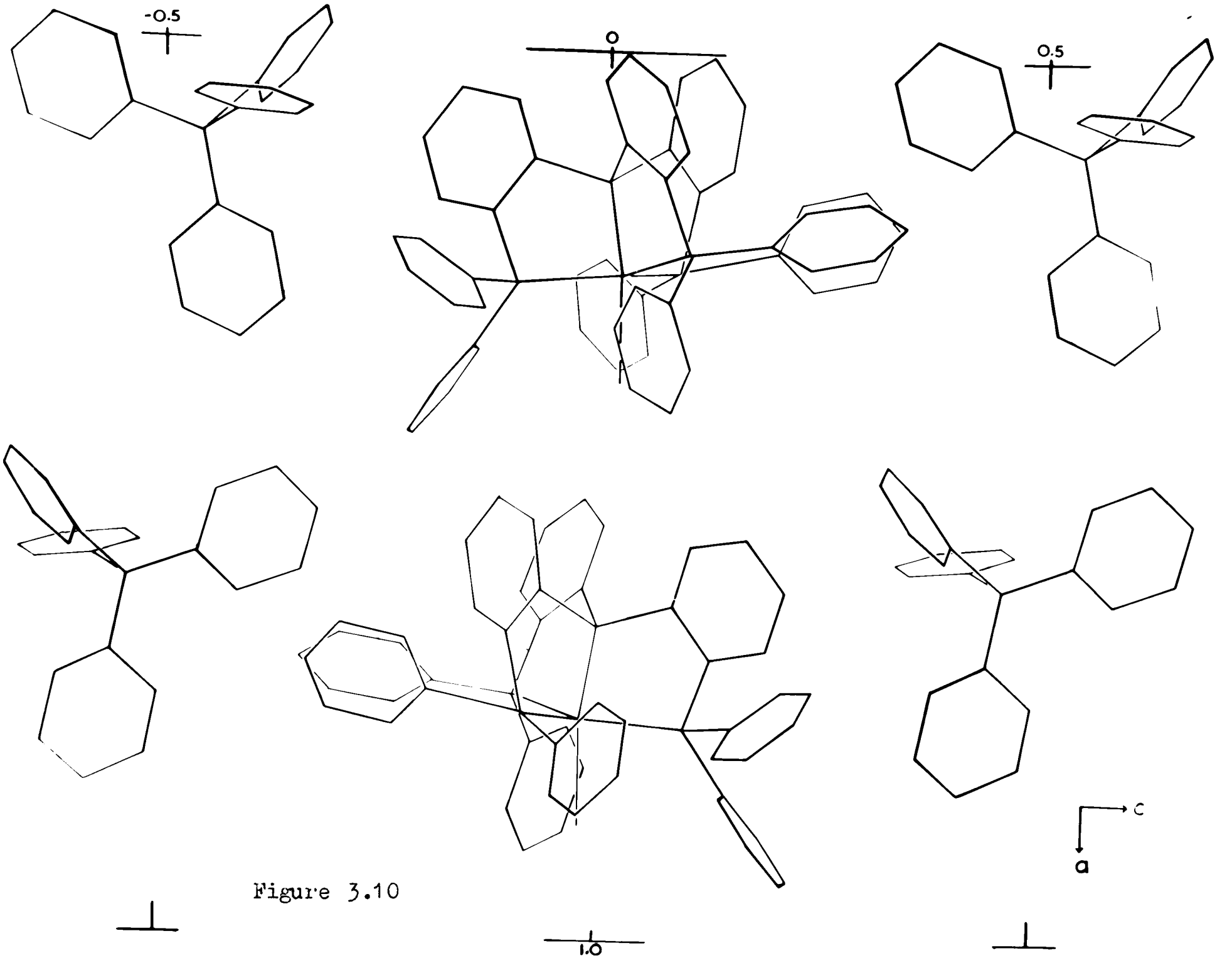

Figure 3.10

The main feature is the linear chain of screw-axis related molecules running continuously through the crystal in the direction of the a axis. Molecules related by the two-fold screw axis fit snugly into each other giving maximum separation of the negatively charged chlorine atoms. Projected onto (100), these chains of screw-axis related molecules form a face-centred array with tetraphenyl borate ions filling the channels between these molecules.

The stability of the molecular structure with a tetraphenyl borate ion is probably due both to its large size and its irregular shape which allow many Van der Waals contacts with the very large and irregular shaped complex cations. The use of smaller anions almost always resulted in solvent of crystallisation. As the solvents were different for the iron and nickel analogues, crystals with the tetraphenyl borate ion were studied in each case in an attempt to provide an isomorphous series. In fact, neither $[Fe(QP)Cl]BPh_4$ nor $[Ni(QP)Cl]BPh_4$ proved to be isomorphous with either $[Co(QP)Cl]BPh_4$ or each other.

Consider now the geometry of the complex cation, $[Co(QP)Cl]^+$. The stereochemistry of the pentaco-ordinate unipositive complex ion is shown in figures 3.9 and 3.12, and the bondlengths (of average standard devaition, 0.01Å) are shown in figure 3.11. The angles defining the stereochemistry are:-

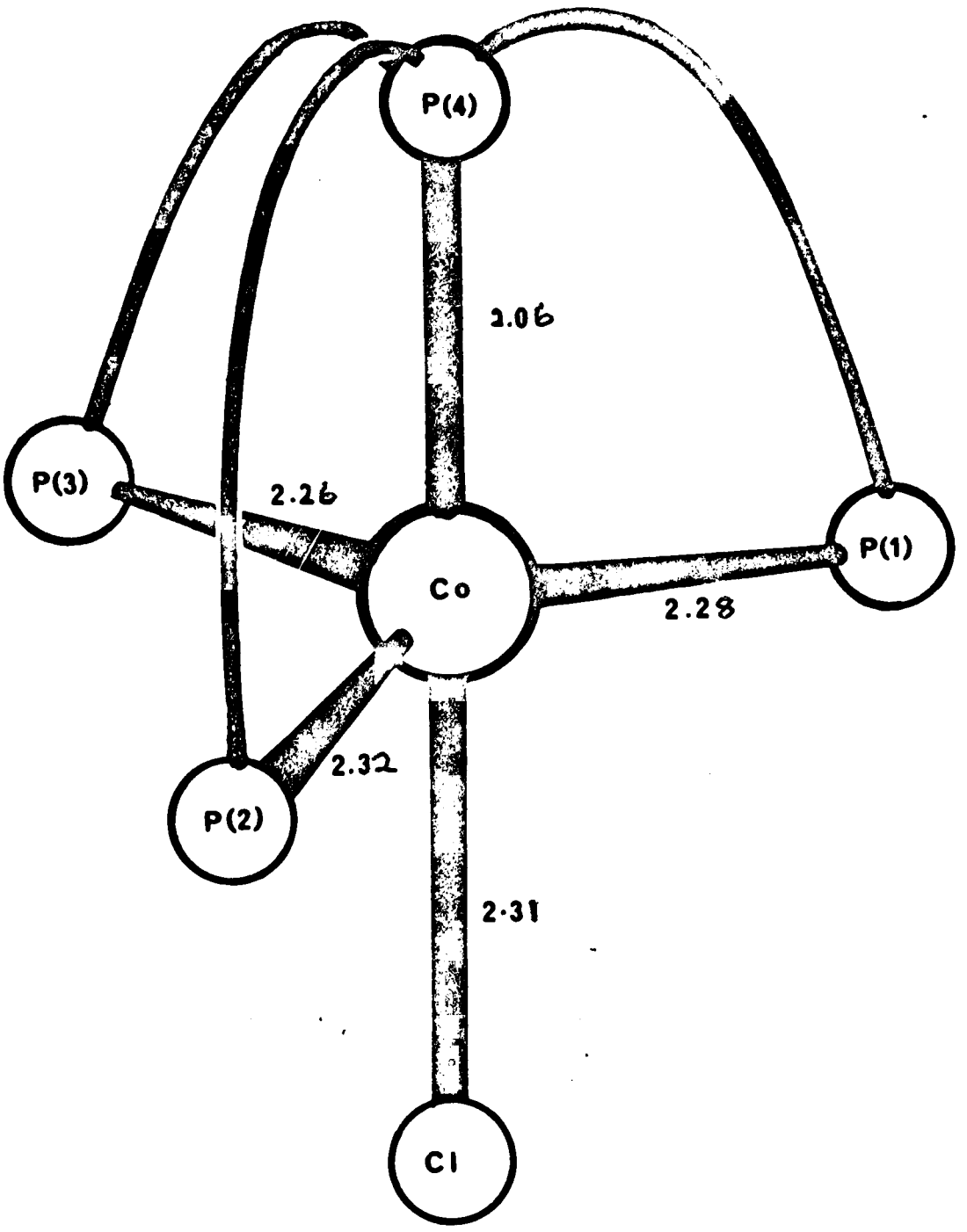

FIGURE 3.11

P(1)-Co-P(2) = 108.5°; P(1)-Co-P(3) = 112.9°; P(2)-Co-P(3)== 137.2°

P(1)-Co-P(4) = 87.1°; P(2)-Co-P(4) = 85.9°; P(3)-Co-P(4) = 85.9°

P(1)-Co-Cl = 99.4°; P(2)-Co-Cl = 97.4°; P(3)-Co-Cl = 86.3°

P(4)-Co-Cl = 171.4°

with standard deviation of 0.2°.

These values differ slightly from those communicated to the Chemical Society previously[77] as a result of correcting the observed structure factor magnitudes for the imaginary part of the scattering factor (see Appendix III).

The most significant features of the distorted trigonal bipyramidal co-ordination of the cobalt are:-

(a) the large distortion from three-fold axial symmetry

(b) the bending of the equatorial Co-P bonds towards the apical phosphorus atom

(c) the very short apical Co-P bond length.

None of these distortions from trigonal bipyramidal geometry can be attributed to the steric requirements of the ligand, QP. These points will now be considered.

<u>(a) The distortion from three-fold axial symmetry.</u>

One of the equatorial P-Co-P angles is 137.2° compared with the other two of 108.5° and 112.9° in the $[Co(QP)Cl]^+$ ion. This surprisingly large distortion from trigonal symmetry is not found in the related complexes $[Ni(TAP)CN]^+$ (TAP = tris (o-diphenylarsinophenyl)phosphine)[78]

Figure 3.12

Complex Ion	Stereochemistry	Ligand
$(Co(QP)Cl)^+$	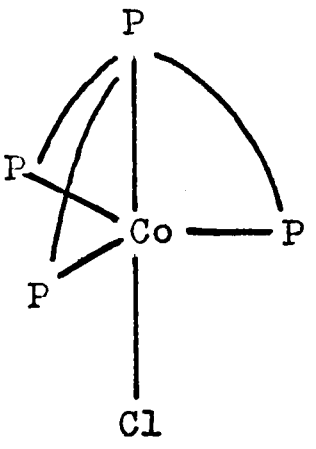	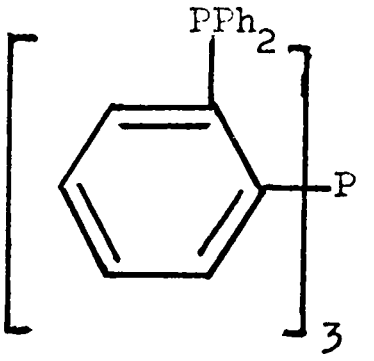
$(Pt(QAS)I)^+$	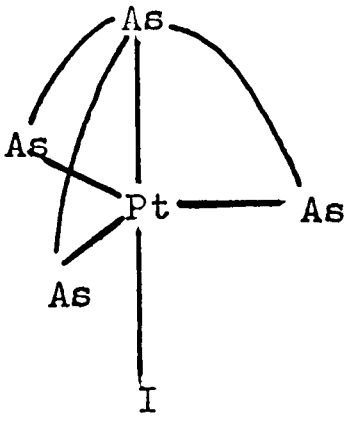	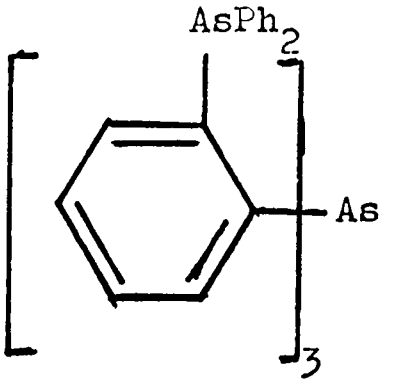
$(Ni(TAP)CN)^+$	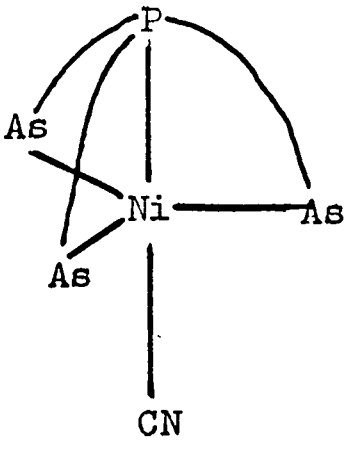	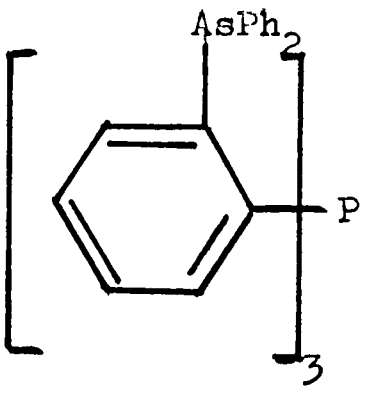

where the equatorial angles are close to 120°, or in $[Pt(QAS)I]^+$ (QAS = tris (o-diphenylarsinophenyl)arsine) where the largest angle is 122°.[3] However, a similar stereochemistry is found in $CoBr_2(PPh_2)_3$,[78] a low spin, distorted trigonal bipyramidal complex with one equatorial angle of 136°. In this complex, two bromine atoms occupy equatorial positions, and so the complex cannot have trigonal symmetry in any case.

Venanzi has attributed the small distortion from trigonal symmetry in $[Pt(QAS)I]^+$, i.e. the angle of 122°, to a gain in crystal field stabilization energy.[79] Crystal field stabilization energy is greater for a square pyramidal than for a trigonal bipyramidal co-ordination for $\underline{d}^8$ and also $\underline{d}^7$ electron configurations; the distortion of 122° was described as a distortion towards a square pyramidal geometry. However, crystal field stabilization energy is a more important factor for platinum(II) complexes than for cobalt (II) complexes. It appears unlikely that it would give rise to a distortion of 17.2° in the cobalt (II) case but only 2° in the platinum (II) case. Furthermore, crystal field stabilisation energy should be greater for a square pyramidal $(Ni(TAP)CN)^+$ complex,[80] but this shows no distortion from trigonal symmetry. It is unlikely, therefore, that the distortion in $[Co(QP)Cl]^+$ results from a gain in crystal field stabilization in moving towards a square pyramidal geometry.

It appears possible, therefore, that the distortion arises from

large spin orbit coupling effects, but probable that it is a Jahn-Teller effect. The degeneracy of the $\underline{d}_{x^2-y^2}$ and $\underline{d}_{xy}$ orbitals must be removed in a low-spin $\underline{d}^7$ electron configuration.

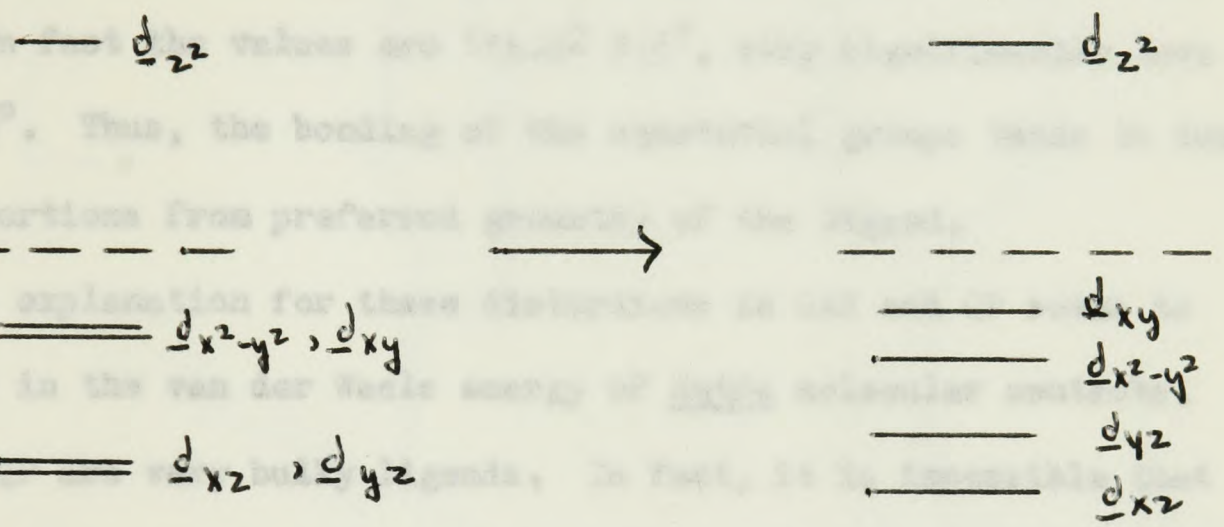

This may give rise to a Jahn-Teller distortion of the equatorial trigonal symmetry as observed in $[Co(QP)Cl]^+$.

b) The bending of the equatorial Co-P bonds towards the apical phosphorus atom and the non-linear P-Co-Cl system.

The angles between the three equatorial and the axial Co-P bonds are $86.5 \pm 0.6^\circ$. The stereochemistry of the $[Pt(QAS)I]^+$ ion is similar, the angles between the axial and the equatorial Pt-As bonds being 86°. However, in the $[Ni(TAP)CN]^+$ ion the bonds are bent towards the cyanide group with P-Ni-As angles of $94.7 \pm 0.3^\circ$.[30]

At first sight these facts appear to be related to the more rigid requirements of the bridging phenyl rings in QP and QAS than in TAP, where the bridging is by an aliphatic chain. However, this is disproven by the geometry of the bridging system in QP. If in fact the bridging span (the distance between two phosphorus atoms bonded to the same

benzene ring) was strained so that the equatorial groups are pulled towards the axial phosphorus, then it would be expected that the P-C-C angles of the bridging system would be slightly greater than 120°. In fact the values are 114.9± 2.5°, very significantly less than 120°. Thus, the bonding of the equatorial groups tends to increase the distortions from preferred geometry of the ligand.

The explanation for these distortions in QAS and QP seems to be found in the van der Waals energy of <u>intra</u> molecular contacts. QAS and QP are very bulky ligands. In fact, it is impossible that they should co-ordinate to give a molecule with C_{3v} symmetry, because steric repulsions between the terminal phenyl groups would cause too large repulsion terms. Figure 3.13 shows clearly that of the phenyl rings attached to a phosphorus atom, one is pushed up and the other is pushed down towards the apical chlorine atom, so that their positions alternate around the equatorial plane.

Although this distortion reduces phenyl-phenyl repulsions, it brings phenyl groups very close to the chlorine atom. The resultant repulsion terms would, however, be reduced if the equatorial phosphorus atoms are moved towards the apical phosphorus atom, and it is the author's contention that this is the cause of the lack of planarity of the phosphorus atoms with the cobalt atom. The non-linear P-Co-Cl system may also result from repulsions between the chlorine atom and the phenyl groups which are distorted from trigonal symmetry.

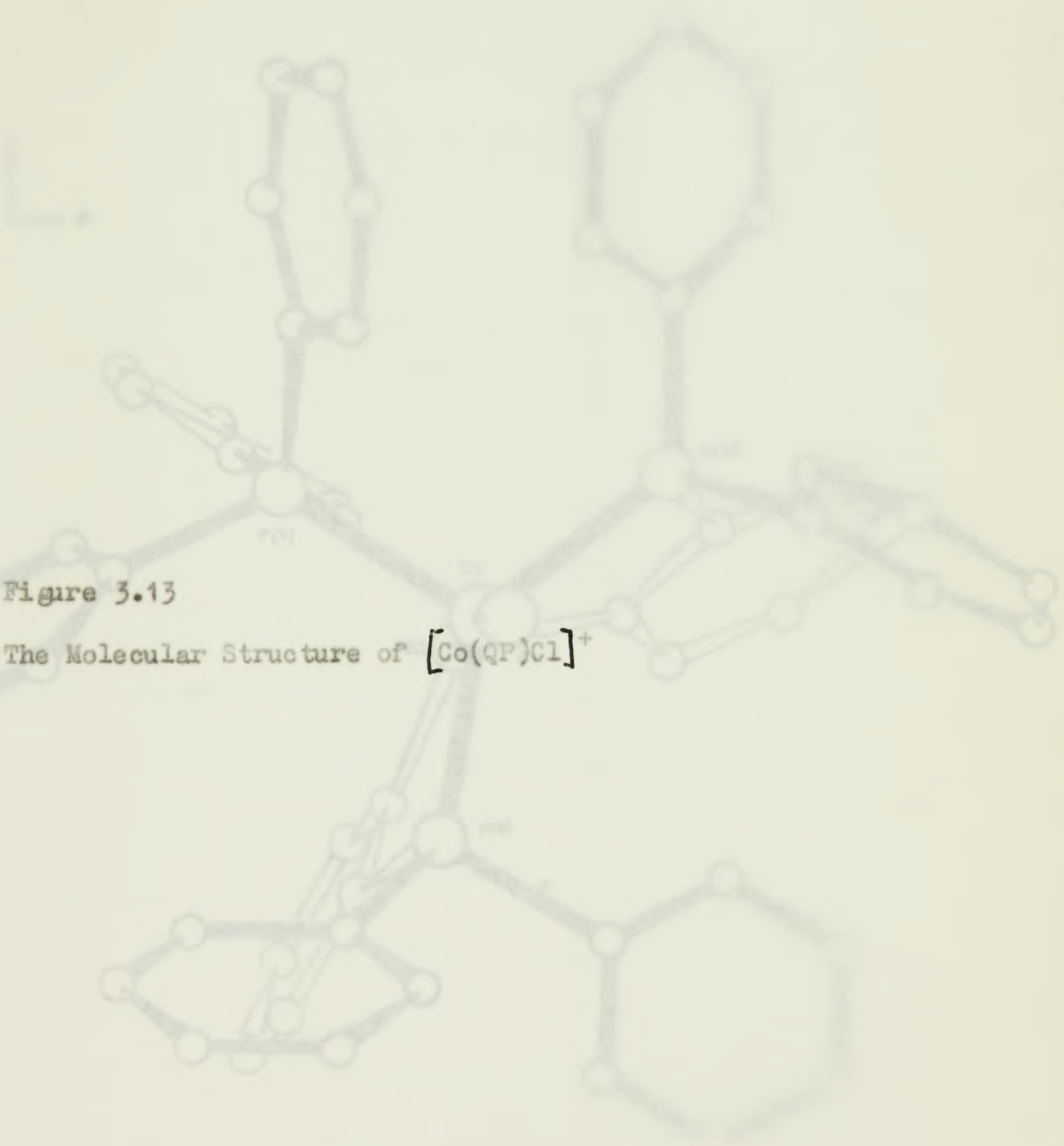

Figure 3.13

The Molecular Structure of $[Co(QP)Cl]^{+}$

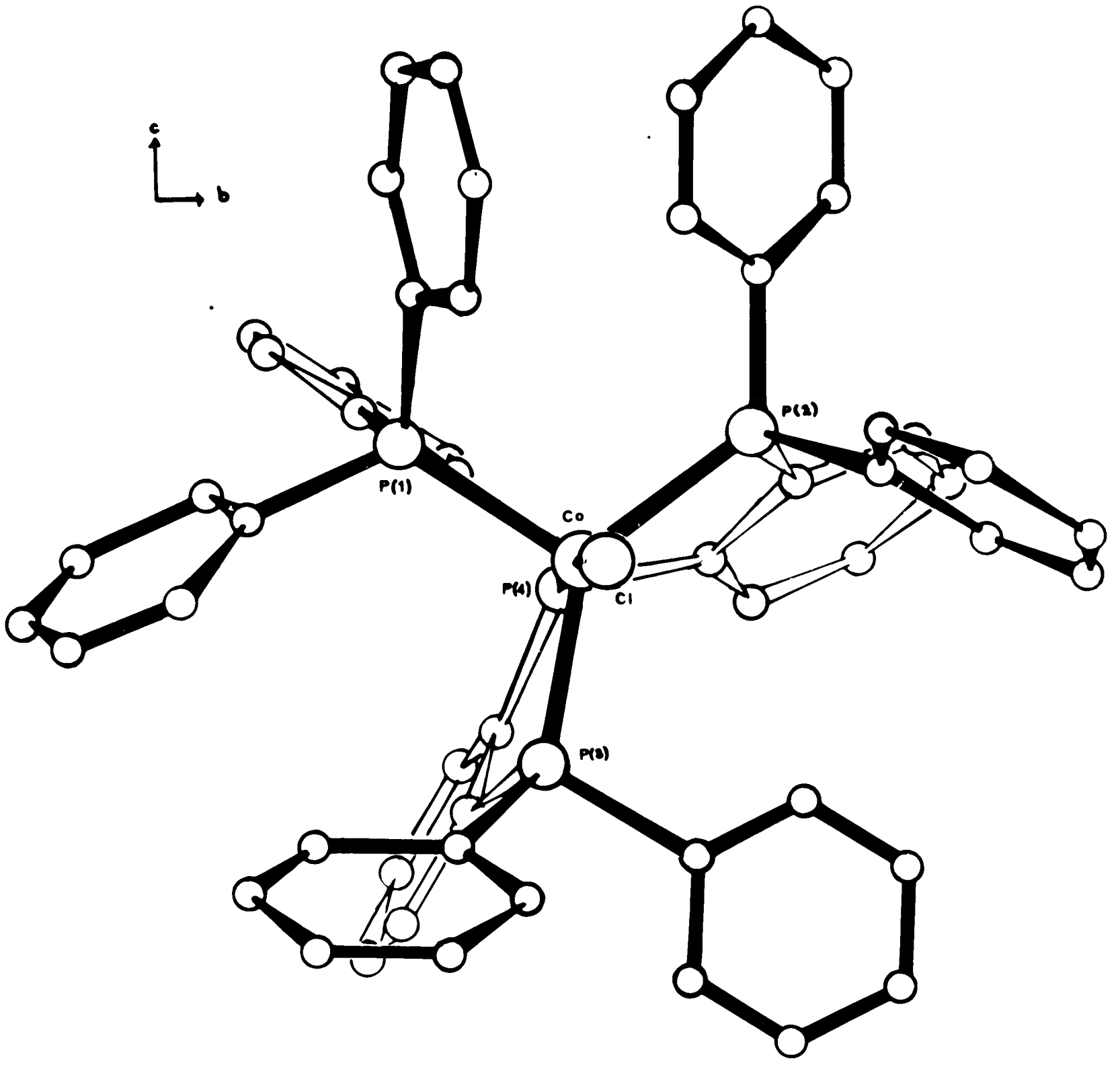
c
b
P(1)
Co
P(4)
Cl
P(2)
P(3)

The arguments are consistent with the almost linear As-Pt-I system, and the lack of coplanarity of the arsenic atoms and the platinum atom in $[Pt(QAS)I]^+$,[3] and with lack of similar distortions in $[Ni(TAP)CN]^+$, where the large phenyl groups are replaced by methyl groups.[80]

c) The short axial Co-P bond.

In both $[Co(QP)Cl]^+$ and $[Pt(QAS)I]^+$ the axial metal ligand bond is much shorter than the equatorial bonds. In the complex cobalt cation, the axial bond is 2.057Å while the equatorial bond lengths are 2.261, 2.280 and 2.318Å all of standard deviation 0.004Å. Similarly, in the platinum complex cation the axial bond is 2.31Å compared with 2.43, 2.45 and 2.49Å for the equatorial bonds.

By the same argument used in the previous section it is easily established that these differences are not due to steric requirements of the ligand bridging groups.

They may, however, be explained by simple crystal field theory. In a trigonal bipyramidal crystal field with three-fold axis in the z direction, the energies of the d-orbitals are given on page 12. The d_{z^2} orbital is considerably destabilized compared with other orbitals and thus for the d^7 and d^8 electron configurations of the cobalt (II) and platinum (II) complexes this orbital will be unoccupied. In this situation an increase in the effective dipole in the axial position relative to that in the equatorial position or in other words a decrease in the metal-axial atom distance will increase the energy of the d_{z^2}

orbital, but stabilise the occupied orbitals. Thus a shorter axial bond will give a greater crystal field stabilisation in both complexes, and the author attributes these short bonds to this effect.

Gillespie[8] has predicted a shorter axial bond in trigonal bipyramidal complexes with a $\underline{d}^7$ or $\underline{d}^8$ electron configuration. He attributes the distortion to repulsions between the valency-shell electron-pairs and the oblate core of $\underline{d}^7$ or $\underline{d}^8$ electrons. This argument is equivalent to that given above in terms of crystal field stabilization energy.

In conclusion, it appears that the loss of trigonal symmetry preferred by the ligand, QP, in the complex cation $[Co(QP)Cl]^+$ results from a Jahn Teller effect. This may be the explanation for the lack of isomorphism of the series $[M(QP)Cl]BPh_4$ where 'M' is Fe(II), Co(II) and Ni(II). The short apical Co-P bond has been attributed to a gain of crystal field stabilization energy.

Thus, it appears that the steric requirements of the ligand, QP, are not as important as may have been deduced by analogy with QAS in $[Pt(QAS)I]^+$.

CHAPTER 7

PACKING REQUIREMENTS IN THE CRYSTAL STRUCTURE:-

The Crystal and Molecular Structure of $[TlMe_2 1,10\text{-phen}]ClO_4$

This chapter concerns the crystal and molecular structure of $[TlMe_2 1,10\text{-phen}]ClO_4$. Little could be deduced from chemical and spectroscopic work about the stereochemistry of this complex in its crystal structure except that $[TlMe_2 1,10\text{-phen}]^+$ group resembles the T-shaped $[TlMe_2 pyr]^+$ cation which has a slightly bent thallium dimethyl group, (Section 1.d, page 21). The perchlorate oxygen interaction with the thallium must be weak, but nothing was known of its nature. A reasonable hypothesis appeared to be that the perchlorate ion was weakly unidentate giving rise to a five co-ordinate thallium atom. As the thallium-oxygen and thallium-nitrogen bonds must be predominantly ionic in character, the stereochemistry of this pentaco-ordination would probably be determined by the packing requirements in the crystal structure.

Before considering the co-ordination of the thallium in $[TlMe_2 1,10\text{-phen}]ClO_4$, it will be convenient to summarise the chemistry of this type of σ-bonded organometallic cations.

The dimethyl thallium ion is one of a group of σ-bonded organometallic cations, stable in aqueous solutions of formula, $\underline{R}_{\underline{n}}M^{z+}$, where $\underline{n}$

is less than the maximum co-ordination of the metal, M. The stability of these cations depends on the fact that the metal is not so electropositive that hydrolysis of the M-C bond occurs, or so electronegative that the cations are strong acids and give hydroxide salts. Thus stable ions are formed with Au(III), Hg(II), Tl(III), Pb(IV) and Sn(IV).

This group of organometallic cations in fact resemble metal cations, and they can be considered in the context of general inorganic chemistry. The dimethyl thallium ion resembles the univalent thallium cation, Tl^{+}.

There are two types of cations. First, the methyl mercury and dimethyl gold cations tend to be soft acids and these tend to have low co-ordination numbers. Secondly, most other organometallic cations formed from metal cations with a d^{10} electron configuration tend to be hard acids. The thallium dimethyl ion has been described as a hard but weakly polarising acid which forms complexes of low stability and with hard bases. It is less polarising than the dimethyl tin(IV) cation.

The adducts of these cations are unusual in that they may involve highly covalent, kinetically inert metal-carbon bonds together with highly polar, labile bonds from the metal to other ligands. Their co-ordination numbers tend to be higher than those for soft acids.

Few adducts of the dimethyl thallium ion have been structurally investigated, however.

In 1938, an incomplete structure analysis of dimethyl acetylacetanato thallium(III) appeared to indicate that the dimethyl thallium group was

not linear but that the thallium was tetrahedrally co-ordinated. The compound's appreciable vapour pressure and solubility in organic solvents was claimed to support this conclusion.[81]

The geometry of the dimethyl thallium ion itself was established in the early crystal structure determination of dimethyl thallium iodide by Powell and Crowfoot in 1932. The ion was found to be linear.[82]

Since the crystal structure analysis of $[TlMe_2]1,10\text{-phen}]ClO_4$, was begun, the crystal structure of diethyl-salicylaldehydato-thallium(III) has been determined.[83] This has a six co-ordinate thallium atom with a slightly bent thallium dimethyl group, and its structure will be considered in detail later.

The crystal and molecular structure of $[TlMe_2]1,10\text{-phen}]ClO_4$ have now been determined. The crystal data, positional and isotropic vibrational parameters, bond lengths and bond angles are given in Appendix IV, page 181 . The reliability factor is 0.088.

The crystal and molecular structure of $[TlMe_2]1,10\text{-phen}]ClO_4$ are in fact very unusual. The hypothesis that the thallium is five co-ordinate has been disproved, but packing requirements in the crystal structure do appear to be important in determining the stereochemistry.

The molecular structure is shown in Figure 3.14, which is a projection on (010).

The plane of the phenanthroline bisects the angle of 168.3° (of standard deviation 1.5°) made at the thallium by the methyl carbons, which are bent away from the phenanthroline group. The thallium atom is

Figure 3.14

The Crystal Structure of $[TlMe_2 1,10\text{-phen}]ClO_4$

Projection onto (010)

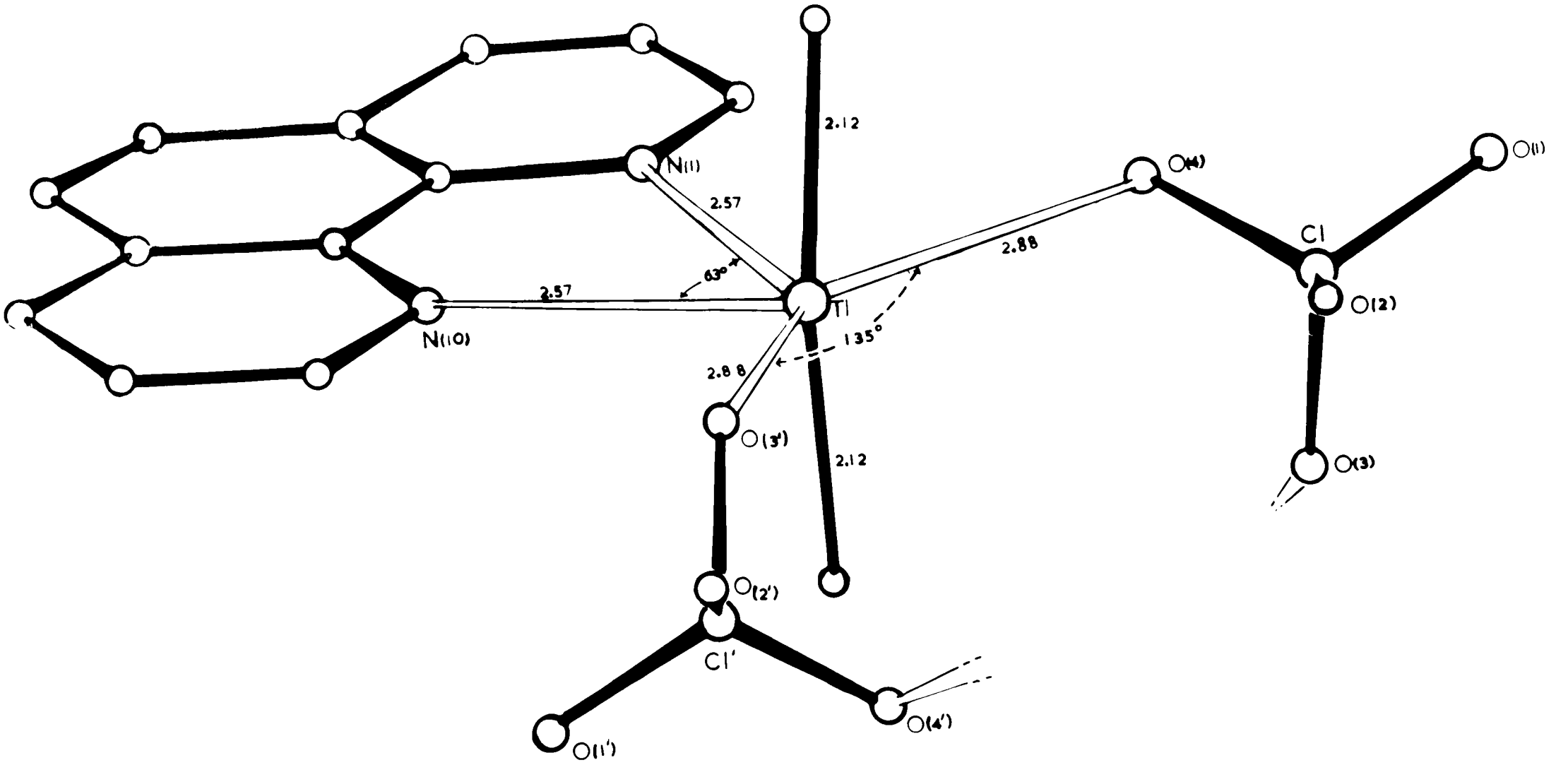
2.12
N(1)
2.57
O(4)
O(1)
Cl
2.57
63°
2.88
N(10)
Tl
O(2)
135°
2.88
O(3)
O(3')
2.12
O(2')
Cl'
O(4')
O(1')

0.06Å from the plane of the phenanthroline group. Two oxygen atoms from the perchlorate groups occupy positions approximately in the plane of the thallium and phenanthroline so that the O-Tl-O angle is 135.8°. The thallium, two oxygens and two nitrogens are all within 0.12Å of the best least squares plane through them. There is almost a non-crystallographic mirror plane perpendicular to and bisecting the phenanthroline, and containing the thallium atom and carbon atoms of the methyl groups.

Figure 3.15 shows the (001) projection of the structure. The screw axis is vertical in the plane of the projection. The weakly co-ordinating bidentate perchlorate groups bridge to give a helical structure with its units related by a two-fold screw axis. In describing complexes of organometallic cations, it is convenient to use the terminology of Grdenic, which was developed to describe the co-ordination of mercury complexes[84]. The shorter, covalent bonds comprise the characteristic co-ordination. In the case, there are two covalent thallium-carbon bonds of length 2.13 (5) and 2.12 (5)Å. Thus, the characteristic co-ordination number is two.

The effective co-ordination is defined to include all those atoms surrounding the thallium at a distance less than the sum of the van der Waals radii. The co-ordinating atoms in the plane of the phenanthroline are shown in Figure 3.16b. The effective co-ordination of sic is completed by two nitrogens at 2.57 (3)Å and two oxygens at 2.86 (4) and 2.89 (4)Å from the thallium atom.

Figure 3.15

The Crystal Structure of $TlMe_2$ 1,10-phen ClO_4

Projection on (001)

Figure 3.16

The co-ordination of thallium compared with

that in dimethyl-salicylaldehydato-thallium(III)

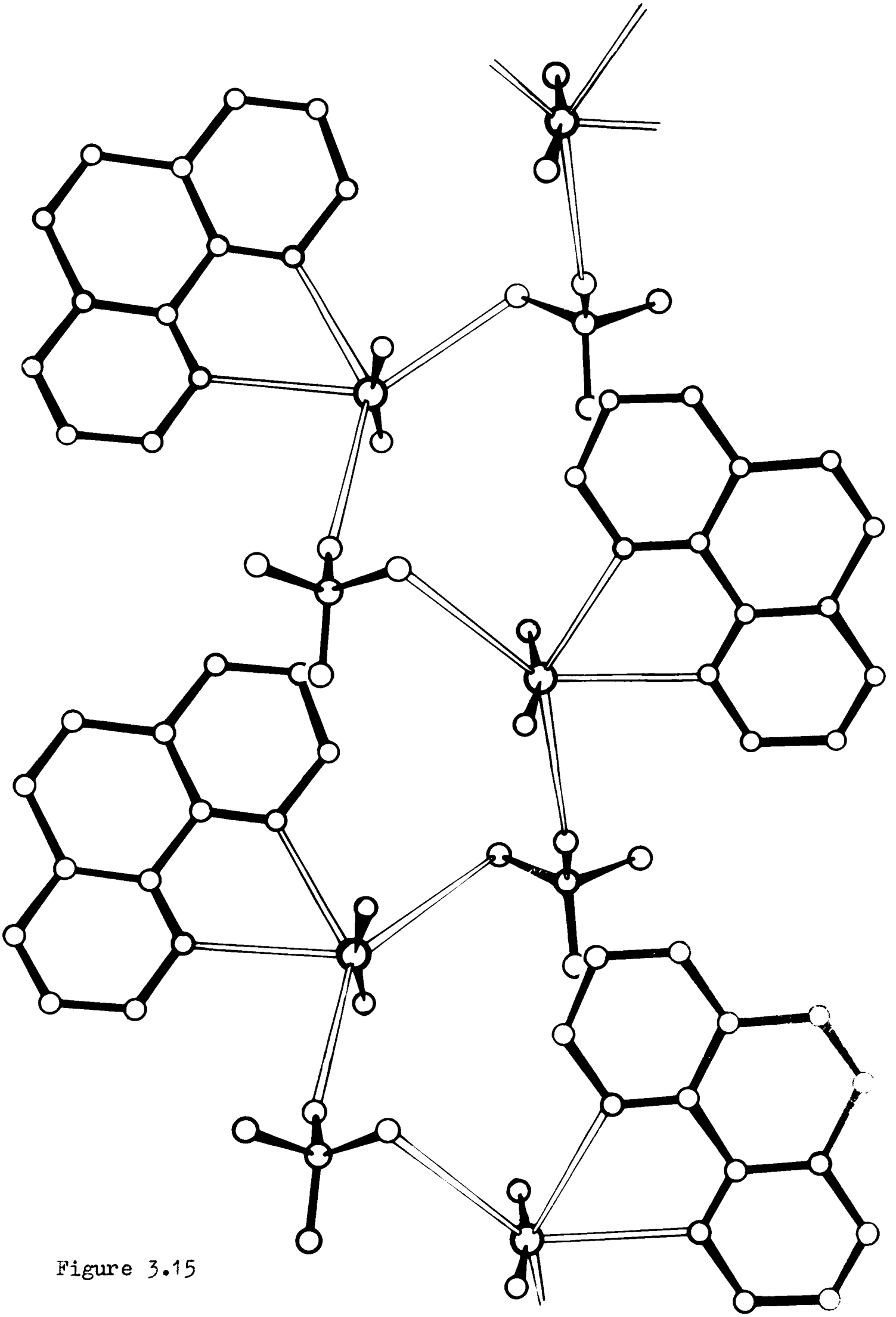

Figure 3.15

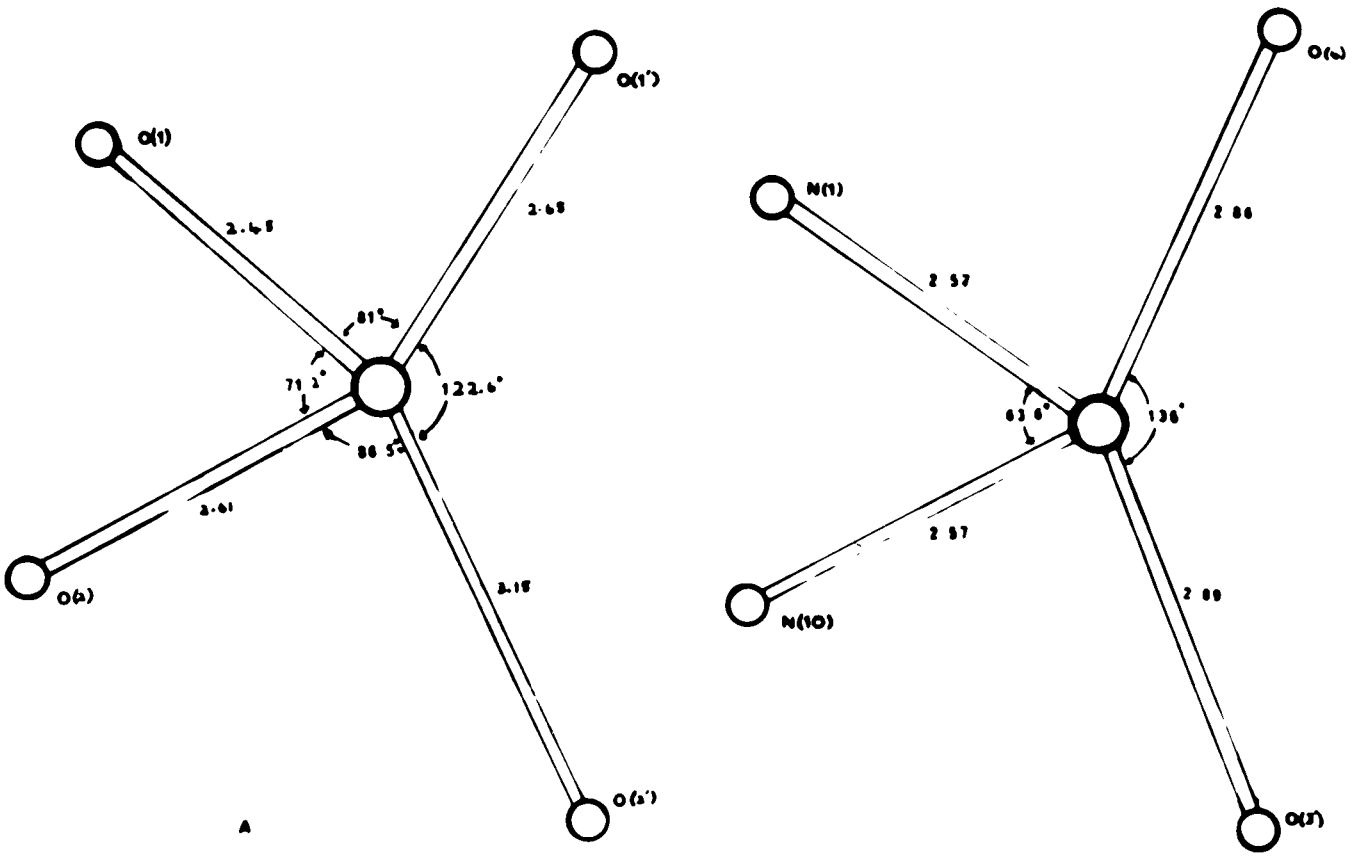
O(1)
O(1')
2.68
81°
71.2°
122.6°
88.5°
2.61
O(4)
3.15
O(4')
A
N(1)
O(3)
2.86
2.57
63.6°
136°
2.57
N(10)
2.89
O(3')
B

Figure 3.16

What type of bonding does this imply?

The radius of the thallium dimethyl ion is 1.22Å, as derived from the structure of dimethyl thallium chloride.[82] The two thallium-oxygen bonds are longer than the ion-dipole contact distance between the dimethyl thallium ion and a lone pair of the perchlorate oxygen atom. This could be about 2.62Å. The bonds of length 2.86 and 2.89Å are thus purely electrostatic in nature.

However, the observed thallium to nitrogen distances of 2.57Å (of standard deviation 0.03Å) are significantly shorter than 2.72Å, the sum of the dimethyl thallium ion radius and the van der Waals radius of nitrogens. This may be due to a partial covalent character of these bonds.

The stereochemistry of the complex compares closely with the dimethyl salicylaldehydato thallium(III).[83] This polymerises to give a similar six co-ordination. The bonds in the equatorial plane are shown in Figure 7.16a. They consist of predominantly electrostatic bonds. The shorter 2.46Å bond may have some partial covalent character. The similarities between the two stereochemistries are apparent.

In each case one angle is restricted by the geometry of the ligand to a value which is considerably less than 90°. In the phenanthroline adduct it is 63.6°. As a result the O-Tl-O angle can be 135.8° in this case. This large angle helps to minimise distances between the dimethyl thallium cation and the perchlorate anion, and

to minimise repulsions between the two dimethyl thallium cations and repulsions between the perchlorate ions. The geometry of the salicylaldehydato adduct may be explained in a similar way.

Thus, the electrostatic thallium-oxygen bonds probably have no directional properties.

The co-ordination of these complexes may be described in terms of a distorted pentagonal bipyramid with one equatorial position vacant. This can be easily seen in Figure 3.14. In fact, in the phenanthroline adduct a further oxygen O(2) is just outside this vacant position in the pentagonal bipyramid. It is, however, outside the effective co-ordination sphere (as defined by Grdenic) at 3.6Å from the thallium atom.

The distortions from linearity of the dimethyl thallium group in the salicylaldehydato and the phenanthroline adducts may be explained in two ways.

First, the dimethyl thallium group has an asymmetric environment of charges. The methyl groups of the phenanthroline adduct are bent away from the phenanthroline towards the large angle of 135.8°. In fact, they occupy a position so that the distances of the methyl carbon atoms to both the phenanthroline nitrogen atoms and the closest perchlorate oxygens are not significantly different. The departure from linearity of the dimethyl thallium group is then nearly 12°. The charge repulsion terms between the methyl carbon atoms and the four atoms (two nitrogens and two oxygens) are then effectively minimised

(assuming the oxygen and nitrogen atoms have the same effective electrostatic charge). Also in the salicylaldehydato adduct the methyl carbons occupy positions such that the charge repulsion terms are decreased relative to a situation with a linear dimethyl thallium group. In this case they move in the direction of the long Tl-O bond so that the C-Tl-C angle is 172° (see Figure 3.16).

Both these distortions may equally well be described in terms of repulsion between the bonding electrons of the thallium valency shell. In the phenanthroline complex, the Tl-N may have a partial covalent character, while the Tl-O bonds are certainly electrostatic in nature (see above). Repulsions between the valency electron-pairs of the Tl-C bonds and the small amount of delocalised electron density in the Tl-N bonds may then account for the bonding of the dimethyl thallium group away from these bonds.

In both cases, the distortions are greater than any departure from linearity in organomercury complexes. Here the largest departure is 4°, which occurs in mercuric diethylene oxide.

Both structures emphasise the difficulty of forming more than two covalent bonds with thallium(III). This may be considered a result of the relativity large s-p separation in this part of the periodic table. The other mainly electrostatic bonds confirm the idea that the dimethyl thallium cation is a weakly polarisable, hard acid, but tends to have a higher co-ordination number than a soft acid organometallic cation.

These results contradict any predictions based on the crystal structure of dimethyl-acetylacetonato-thallium(III).[81] Here, the thallium

is said to be tetrahedrally co-ordinated. A re-examination of the crystals (which were prepared by Professor Beattie at the author's request) showed that they were very thin and easily bent. A study of the crystals by X-ray techniques confirmed the cell dimensions given by Cox, Wardlaw and Shorter in 1938. The space group given, $C222_1$, was difficult to confirm. The crystals gave poor photographs, had large absorption for Cu-K_α radiation and underwent a solid state reaction after a two or three day period. Photography with Mo-K_α radiation was unsuccessful due to the poor quality of the crystals. The photographs had reflections with non-randomly distributed intensities, corresponding presumably to the Fourier transform of the thallium atoms. As the percentage of scattering matter resulting from the carbon and oxygen atoms is very small, parts of the transform where there is no resultant contribution from the thallium atoms may easily be confused for systematic absences. The author feels that there is insufficient evidence for the space group $C222_1$. Space groups $\underline{C2/c}$ or $\underline{Cc}$ seem possible.

The tetrahedral co-ordination deduced by Cox, Wardlaw and Shorter is depended on the space group symmetry and is therefore suspect. However, given their own assumptions about symmetry, they do not consider all the possibilities. A polymeric chain structure similar to that in the salicylaldehydato complex with an almost linear dimethyl thallium group and a six co-ordinate thallium atom is quite consistent with their assumptions, and indeed packs into the crystal unit cell with reasonable intermolecular distances. Professor Beattie has confirmed our suspicions

of a nearly linear dimethyl thallium group with some infrared and Raman data. However, before any conclusions can be made with certainty better crystals must be obtained and a full three-dimensional X-ray analysis must be carried out.

If the complex does involve a tetrahedral thallium atom, the ideas that the dimethyl thallium cation is a weakly polarising, hard acid, and that the large s-p separation is important in favouring the commonly found linear two co-ordination of covalent bonded atoms must be revised.

The crystal structure of dimethyl 1,10-phenanthroline thallium perchlorate has provided further information on the co-ordination and stereochemistry of dimethyl thallium complexes. The hypothesis that the complex is pentaco-ordinate in the crystal structure is disproven. Nevertheless, the observed structure does underline the importance of packing requirements in determining the stereochemistry of complexes in their crystal structures.

CHAPTER 8

Conclusion

The X-ray analyses of these four co-ordination complexes indicate two generalisations concerning the study of the stereochemistry of pentaco-ordination.

In the first place, X-ray analyses are an essential prerequisite to the discussion of pentaco-ordinate stereochemistries; in every case the analyses reported here added information that was not proven by the chemical or spectroscopic investigations, and in most cases was unsuspected before these studies. For instance, in $[TlMe_2$1,10-phen$]ClO_4$ the effective co-ordination number was not known before the study, and even the geometry of the thallium dimethyl group was only tentatively suggested to be non-linear. In $[Pd(TPAS)Cl]ClO_4.C_6H_6$, the evidence for the square pyramidal structure was inconclusive. Indeed the suggestion that the chlorine occupied the apical positions has been proved incorrect. This indicates that the evidence also did not preclude a trigonal bipyramidal geometry, and certainly gave little information about a weakly co-ordinating ligand in the sixth position. In all cases the X-ray analyses have indicated interesting distortions from ideal geometries. The equatorial ligand atoms of the two ligand bipyramidal complexes are not coplanar with the metal atoms; the apical bond of $[Pd(TPAS)Cl]^+$ is very long while the axial Co-P bond of $[Co(QP)Cl]^+$ is exceptionally short; and finally the large distortion from

trigonal symmetry was totally unexpected and has necessitated the re-examination of a detailed theoretical paper concerning its visible and ultraviolet spectra.[86] The X-ray analyses have done more than merely confirm suggested structures; they have provided new and vital information concerning the stereochemical problem of pentaco-ordination.

Secondly, the X-ray anlyses have emphasised the complexity of the problem. The structures determined are certainly consistent with arguments concerning valency-shell electron-pair repulsions, crystal field stabilisation energies, steric requirements of the ligands and packing requirements in the crystal, but they in no way prove the correctness of these assumptions. In many cases all four factors are probably important, and the crudeness of the methods available for estimating their relative importances may effectively prohibit the prediction of the stereochemistry of many pentaco-ordinate complexes.

Nevertheless, the comments of Muetterties and Schunn in their recent Quarterly Review[4] seem unduly pessimistic - "Clearly an attempt to rationalise geometry for a particular pentaco-ordinate species on the basis of crude, qualitative considerations such as π-bonding and the like is quite unrealistic in view of the subtle energy differentiation between the two idealised geometries." Their statement is based on the assumption that all energy differences due to the factors important in determining the stereochemistry will be of the order of 6 K-cal, derived from work on PCl_5.[75] They ignore the calculations of Ciampolini which indicate differences due to crystal

field stabilisation energy of about 20 K-cal and also the fact that valency-shell electron-pair repulsions which may predominate in PCl_5 are not likely to give such large energy differences between the idealised geometries as when multiple bonds are involved.

The review article seems to be unsatisfactory on other counts. The review indicates that no further work need be carried out for d^8 complexes. It is unclear why no further work is required but it appears Muetterties and Schunn consider the structural data and thoery to be consistent. No reference to Gillespie's valency-shell electron-pair repulsions theory[8] is contained in the review, but the following statement is made, "The Pauling hybrid approach, electrostatics or the Gillespie-Nyholm non-bonding repulsion considerations, and simple molecular orbital treatments yield similar conclusions about geometry at least for $\underline{d}^0$, $\underline{d}^8$ and $\underline{d}^{10}$ configurations." This surely is not true for $\underline{d}^8$ configurations.

Moreover, the analyses of structural data is alsoopen to criticism. The statements are based on "cumulative structural information". For instance, they gave thirty five examples of trigonal bipyramidal complexes with unidentate ligands, six of which are transition metal complexes and <u>five</u> of these have d^8 electron configurations. These are:- $[Co(NCCH_3)_5]^+$, $RhH(CO)(P(Ph)_3)_3$, $Fe(CO)_5$, $Pt(SnCl_3)_5^{3-}$ and $Ir(CO)Cl(SO_2)[Ph_3P]_2$, trisphosphino-palladium dibromide where the phosphine is 2-phenylisophosphindoline and $Ni(Ph_2MeAsO)_4ClO_4$. These comprise all the structural information available for pentaco-ordinate complexes of metals of $\underline{d}^8$ configuration with unidentate ligands. There

are five trigonal bipyramids and three square pyramids. They then conclude:-

"These structural data though somewhat sparse clearly indicate that the trigonal bipyramidal geometry will be the more common ground state geometry at least for d^8 configurations."

The large number of square pyramidal d^8 complexes with chelate ligands are ignored, without any attempt being made to access the steric requirements of the ligands concerned. This is a pity because most unidentate chelates found in pentaco-ordinate complexes like $(NCCCH_3)$, (CO) and $(SnCl_3)^-$ involve strongly multiple bonding ligands which may consistently favour a trigonal bipyramidal geometry.

The author feels that this analysis of "cumulative structural information" is not useful unless the four factors discussed in this thesis are considered. The complexity of a scientific hypothesis and the difficulty of applying the arguments in practice offer no comment on the validity of that hypothesis. The work reported here has underlined the importance of considering the many factors which may be important in determining the stereochemistry. The structural results enable certain predictions to be made concerning the structure of other pentaco-ordinate complexes where one of the factors discussed here would clearly predominate, but the proof of these hypotheses concerning the stereochemistry of pentaco-ordination awaits the many X-ray and other structural analyses designed to test these predictions.

PART IV

APPENDICES

DATA

AND

DESCRIPTION OF

COMPUTER PROGRAMMES

APPENDIX I

THE X-RAY ANALYSIS OF (TTAs)Ag-Co(CO)$_4$

Data

Table 4.1a

Crystal data: $C_{21}H_{23}AgAs_3CoO_4$, M = 730.9; monoclinic; a = 12.91, b = 16.91, c = 12.07Å, β = 100° 17'; U = 2601.7Å^3; Dm = 1.862 (by flotation); Z = 4; Dc = 1.866; space group $P2_1/n$; F(000) = 1416; Cu-Kα radiation, μ = 160. The structure analysis was based on 1451 non-zero independent reflections, visually estimated from five layers on the 'a' axis and seven layers on the 'c' axis.

B) Determination and Refinement of the Crystal Structure of (TTAS)Ag-Co$(CO)_4$

	Structure Factor Calculation assuming isotropic vibrations			Least-Squares Method of refinement			Dist. Angles	Fourier Methods	
	Atoms Included	R	Agree. Anal.	Cycle	Parameters Refined	Wtg. Scheme		Type	Atoms Located
								Patterson	Ag,3As,Co
A	Ag,3As,Co from Patterson			1	Scalefactor	Unit Weights			
		0.390		2	K,X,Y,Z,B, for Ag,3As,Co	"			
	Ag,3As,Co from previous cycle of least squares	0.322		3		"			
		0.250		4		"		Electron Density Map	All carbon and oxygen atoms
		0.226	✓	5		"	✓		
B	All atoms from map	0.173		6	K+ ,X,Y,Z,B for all atoms	"			
	all atoms from previous cycle of least squares	0.149		7		"		Difference Synthesis	Repositioned 3 carbon atoms
C	All atoms from map	0.133		8	"	"			
	All atoms from least squares	0.123	✓	9	"	"	✓		
D	"	0.123		10	"	p_1=90			
	"	0.117	✓	11	"	p_2=40	✓		
E	"	0.111		12	"	p_1=100			
	"	0.102	✓	13	"	p_2=40	✓	Difference Synthesis	

Table 4.1c

The Crystal Structure of triarsinesilver-cobalt-tetra-carbonyl

	X/a	Y/b	Z/c	U(Å²)
Ag	0.3293(2)	0.4710(1)	0.2867(2)	0.071(1)
As(1)	0.2515(3)	0.4365(2)	0.4578(3)	0.068(1)
As(2)	0.1134(3)	0.4306(2)	0.2055(3)	0.059(1)
As(3)	0.2482(3)	0.6115(2)	0.2391(3)	0.070(1)
Co	0.5049(4)	0.4208(3)	0.2069(4)	0.069(2)
C(11)	0.1985(35)	0.5196(24)	0.5474(35)	0.098(13)
C(12)	0.3348(35)	0.3723(24)	0.5711(35)	0.104(13)
C(121)	0.1146(27)	0.3744(19)	0.4221(28)	0.064(10)
C(122)	0.0767(29)	0.3350(21)	0.5012(30)	0.082(12)
C(123)	0.9767(33)	0.2897(23)	0.4790(33)	0.094(11)
C(124)	0.9186(32)	0.2829(21)	0.3718(33)	0.085(10)
C(125)	0.9582(30)	0.3250(21)	0.2880(30)	0.072(9)
C(126)	0.0583(27)	0.3695(18)	0.3218(27)	0.058(9)
C(2)	0.0319(33)	0.3842(23)	0.0714(33)	0.089(12)
C(236)	0.0827(26)	0.6023(18)	0.2184(26)	0.059(9)
C(235)	0.0170(34)	0.6764(24)	0.2188(33)	0.082(12)
C(234)	0.8993(37)	0.6715(25)	0.2025(35)	0.099(13)
C(233)	0.8472(33)	0.5990(24)	0.1958(32)	0.088(12)
C(232)	0.9146(29)	0.5253(20)	0.1933(29)	0.067(10)
C(231)	0.0267(26)	0.5289(18)	0.2108(26)	0.062(8)
C(31)	0.2651(39)	0.6552(28)	0.1011(38)	0.114(15)
C(32)	0.2738(37)	0.7053(25)	0.3397(36)	0.108(14)
C(4)	0.6215(35)	0.3783(24)	0.1767(33)	0.101(12)
O(4)	0.6982(27)	0.3429(19)	0.1431(26)	0.127(10)
C(5)	0.3872(35)	0.3879(23)	0.1131(35)	0.088(12)
O(5)	0.3200(26)	0.3697(17)	0.0426(26)	0.119(9)
C(6)	0.5202(40)	0.3909(28)	0.3272(43)	0.112(15)
O(6)	0.5410(27)	0.3617(19)	0.4164(29)	0.124(11)
C(7)	0.5325(33)	0.5226(25)	0.1871(33)	0.096(12)
O(7)	0.5431(26)	0.5888(19)	0.1726(25)	0.126(10)

Positional and isotropic vibrational parameters with standard deviations.

Table 4.1d

Bond lengths and angles in (TTAs)Ag-Co(CO)$_4$

	Å		Å
Ag - Co	2.66	C(131) - C(122)	1.33
Ag - As(1)	2.62	C(122) - C(123)	1.40
Ag - As(2)	2.72	C(123) - C(124)	1.42
Ag - As(3)	2.62	C(124) - C(125)	1.44
		C(125) - C(126)	1.44
As(1) - C(11)	1.99	C(126) - C(121)	1.44
As(1) - C(12)	1.95		
As(1) - C(121)	1.97	C(231) - C(232)	1.48
As(2) - C(126)	2.03	C(232) - C(233)	1.37
As(2) - C(21)	1.99	C(233) - C(234)	1.39
As(2) - C(231)	1.97	C(234) - C(235)	1.52
As(3) - C(236)	1.98	C(235) - C(236)	1.33
As(3) - C(31)	1.98	C(236) - C(231)	1.44
As(3) - C(32)	2.02		
Co - C(4)	1.71	Co - C(6)	1.64
Co - O(4)	2.95	Co - O(6)	2.86
Co - C(5)	1.77	Co - C(7)	1.78
Co - O(5)	2.91	Co - O(7)	2.93

Table 4.1e

The crystal structure of triarsinesilver-cobalt-tetra-carbonyl.

Bond angles with standard deviations in degrees.

Co	-	Ag	-	As(1)	133.4	(0.2)
Co	-	Ag	-	As(2)	123.1	(0.2)
Co	-	Ag	-	As(3)	119.6	(0.2)
As(1)	-	Ag	-	As(2)	78.8	(0.2)
As(1)	-	Ag	-	As(3)	103.1	(0.2)
As(2)	-	Ag	-	As(3)	81.1	(0.2)
Ag	-	As(1)	-	C(11)	122.0	(1.3)
Ag	-	As(1)	-	C(12)	122.9	(1.3)
Ag	-	As(1)	-	C(121)	109.8	(1.1)
C(11)	-	As(1)	-	C(12)	97.8	(1.9)
C(11)	-	As(1)	-	C(121)	99.9	(1.7)
C(12)	-	As(1)	-	C(121)	100.2	(1.7)
Ag	-	As(2)	-	C(126)	105.1	(1.0)
Ag	-	As(2)	-	C(2)	136.5	(1.3)
Ag	-	As(2)	-	C(231)	104.5	(1.0)
C(126)	-	As(2)	-	C(2)	105.3	(1.6)
C(126)	-	As(2)	-	C(231)	99.2	(1.4)
C(2)	-	As(2)	-	C(231)	100.4	(1.5)
Ag	-	As(3)	-	C(236)	106.7	(1.0)
Ag	-	As(3)	-	C(31)	117.4	(1.5)
Ag	-	As(3)	-	C(32)	123.7	(1.3)
C(236)	-	As(3)	-	C(31)	99.9	(1.8)
C(236)	-	As(3)	-	C(32)	100.5	(1.7)
C(31)	-	As(3)	-	C(32)	104.7	(1.9)
C(121)	-	C(122)	-	C(123)	117	(3)
C(122)	-	C(123)	-	C(124)	121	(3)
C(123)	-	C(124)	-	C(125)	120	(3)
C(124)	-	C(125)	-	C(126)	121	(3)
C(125)	-	C(126)	-	C(121)	123	(3)
C(126)	-	C(121)	-	C(122)	120	(3)

Table 4.1e (cont.)

C(231)	-	C(232)	-	C(233)	119	(3)
C(232)	-	C(233)	-	C(234)	120	(3)
C(233)	-	C(234)	-	C(235)	121	(3)
C(234)	-	C(235)	-	C(236)	121	(3)
C(235)	-	C(236)	-	C(231)	118	(3)
C(236)	-	C(231)	-	C(232)	121	(3)
Ag	-	Co	-	C(4)	169.2	(1.5)
Ag	-	Co	-	C(5)	76.7	(1.5)
Ag	-	Co	-	C(6)	71.9	(1.9)
Ag	-	Co	-	C(7)	85.8	(1.4)
C(4)	-	Co	-	C(5)	107.8	(2.1)
C(4)	-	Co	-	C(6)	97.6	(2.5)
C(4)	-	Co	-	C(7)	101.3	(2.1)
C(5)	-	Co	-	C(6)	119.7	(2.5)
C(5)	-	Co	-	C(7)	110.6	(2.1)
C(6)	-	Co	-	C(7)	116.7	(2.4)
Co	-	C(4)	-	O(4)	172	(4)
Co	-	C(5)	-	O(5)	171	(4)
Co	-	C(6)	-	O(6)	172	(4)
Co	-	C(7)	-	O(7)	176	(4)

Table 4.1f

Structure factors for observed reflections

for $(TTAs)Ag\text{-}Co(CO)_4$

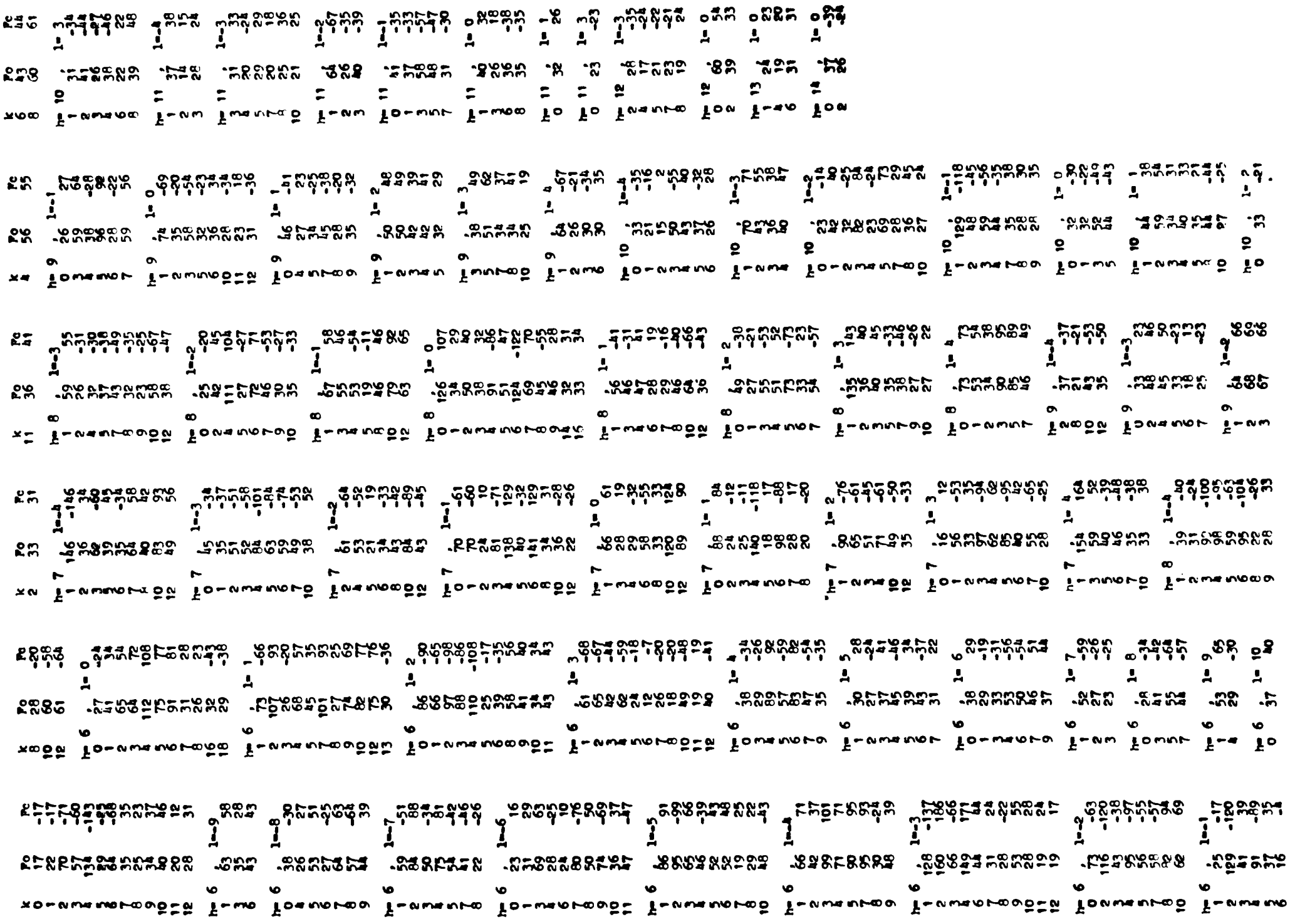

APPENDEX II

THE X-RAY ANALYSIS OF $[Pd(TPAS)Cl]ClO_4.C_6H_6$

Data

Table 4.2a

Crystal data:- $C_{30}H_{36}As_4Cl_2O_4Pd$; M = 937.6; red irregular plates parallel to (010); Space group, $P2_1/c$; a = 11.07 ± 0.015, b = 20.34 ± 0.02, c = 18.24 ± 0.02Å, β = 122.1 ± 0.1°; U = 3478Å^3; D_m = 1.785 (by flotation); Z = 4; D_c = 1.791; Cu - K_α radiation, μ = 111. The structural analysis has been based upon 1175 non-zero independent F_{hkl} values, visually estimated from layers 0kl to 6kl and hk0 to hk2, collected by the equi-inclination Weissenberg technique.

B) Determination and refinement of the Crystal Structure of $(Pd(TPAS)Cl)\ ClO_4 \cdot C_6H_6$

	Structure factor calculation assuming isotropic vibrations: Atoms Included	R	Agree. Anal.	Least-squares method of refinement: Cycle	Parameters Refined	Wtg. Scheme	Dist. Angles	Fourier Methods: Type	Atoms Located
								Patterson	Pd, 4As, Cl
A	Pd,4As from Patterson	0.85		1	Scalefactor	Unit			
A		0.423		2	K+ X,Y,Z,B, for Pd,4As	Weights			
A	Pd,4As from previous cycle of least squares	0.363		3	"	"		Difference Fourier	All other atoms
A		0.301							
B	All atoms from Fourier	0.241		4	K+ X,Y,Z,B, for all atoms	"			
B	All atoms from previous cycle of least squares	0.189		5		"			
B		0.182	✓				✓	Electron Density Map (FATAL)	Corrected positions for Cl(1),C(43) C(53),C(31) C(126),C(236) O(2), O(4) Shifted other atom positions by small amounts
C	"	0.148		6	K+ X,Y,Z,B, for 11 atoms	"			
C	"	0.133		7		"			
C	"	0.131		8	K+ X,Y,Z,B, for all atoms	"			
C	"	0.112	✓				✓		
D	"	0.106		9	"	p_1=120			
D	"	0.102	✓	10	"	p_2= 20	✓		
E	"	0.089		11	"	p_1=90			
E	"	0.085	✓	12	"	p_2=20	✓	Difference Fourier	

Table 4.2c Positional and isotropic vibrational parameters with standard deviations in parentheses.

	x/a	y/b	z/c	U_{iso} / Å^2
Pd	0.0099(3)	0.1067(1)	0.2384(2)	0.086(1)
As(1)	-0.0672(5)	0.0253(2)	0.3008(3)	0.092(2)
As(2)	-0.1115(5)	0.0118(2)	0.1018(3)	0.092(2)
As(3)	0.2198(5)	0.0530(2)	0.2730(3)	0.081(2)
As(4)	0.0781(5)	0.1877(2)	0.1734(3)	0.102(2)
Cl(1)	-0.188 (1)	0.171 (2)	0.2036(7)	0.13 (1)
C(11)	-0.136 (4)	0.060 (2)	0.370 (2)	0.10 (1)
C(12)	0.055 (5)	-0.048 (2)	0.374 (3)	0.13 (2)
C(121)	0.232 (5)	-0.018 (2)	0.213 (3)	0.11 (1)
C(122)	-0.323 (5)	-0.054 (2)	0.225 (3)	0.12 (1)
C(123)	-0.448 (4)	-0.085 (2)	0.160 (3)	0.10 (1)
C(124)	-0.467 (5)	-0.089 (2)	0.076 (3)	0.11 (1)
C(125)	-0.365 (5)	-0.063 (2)	0.060 (3)	0.11 (1)
C(126)	-0.243 (4)	-0.027 (2)	0.130 (3)	0.09 (1)
C(21)	-0.193 (4)	-0.019 (2)	-0.024 (3)	0.12 (1)
C(231)	-0.044 (5)	0.447 (2)	0.341 (3)	0.11 (1)
C(232)	0.018 (5)	-0.119 (2)	0.137 (3)	0.11 (2)
C(233)	0.124 (5)	-0.166 (2)	0.173 (3)	0.11 (1)
C(234)	0.256 (5)	-0.146 (2)	0.239 (3)	0.12 (1)
C(235)	0.292 (4)	-0.082 (2)	0.268 (3)	0.12 (1)
C(236)	0.179 (4)	-0.039 (2)	0.226 (2)	0.08 (1)
C(31)	0.382 (4)	0.041 (2)	0.393 (2)	0.10 (1)
C(341)	0.311 (4)	0.095 (2)	0.223 (2)	0.10 (1)
C(342)	0.431 (4)	0.070 (2)	0.218 (2)	0.10 (1)
C(343)	0.485 (4)	0.110 (2)	0.182 (3)	0.10 (1)
C(344)	0.427 (5)	0.170 (2)	0.139 (3)	0.11 (1)
C(345)	0.312 (4)	0.195 (2)	0.138 (2)	0.10 (1)
C(346)	0.245 (4)	0.158 (2)	0.177 (3)	0.10 (1)
C(41)	-0.067 (5)	0.201 (2)	0.052 (3)	0.12 (2)
C(42)	0.132 (5)	0.275 (2)	0.230 (3)	0.12 (2)
Cl(2)	-0.2656(6)	-0.1197(8)	0.444 (1)	0.147(5)
O(1)	-0.392 (2)	-0.151 (2)	0.381 (2)	0.18 (1)
O(2)	0.317 (4)	0.446 (2)	0.070 (3)	0.19 (2)
O(3)	-0.230 (4)	-0.146 (2)	0.521 (4)	0.20 (2)
O(4)	0.155 (5)	0.367 (2)	0.067 (3)	0.18 (2)
C(51)	0.330 (5)	-0.167 (3)	0.476 (3)	0.15 (2)
C(52)	0.289 (6)	-0.167 (2)	0.540 (3)	0.13 (2)
C(53)	-0.366 (5)	0.200 (2)	0.382 (3)	0.13 (2)
C(54)	0.473 (5)	-0.239 (3)	0.621 (3)	0.14 (2)
C(55)	0.515 (6)	-0.240 (3)	0.562 (3)	0.14 (2)
C(56)	0.438 (5)	-0.204 (3)	0.489 (3)	0.15 (2)

Table 4.2d Bond lengths with their standard deviations in parentheses.

Pd - As(1)	2.408(7) Å	C(121)-C(122)	1.35(7)
Pd - As(2)	2.860(7)	C(122)-C(123)	1.40(7)
Pd - As(3)	2.331(7)	C(123)-C(124)	1.43(6)
Pd - As(4)	2.375(7)	C(124)-C(125)	1.41(6)
Pd - Cl(1)	2.33(4)	C(125)-C(126)	1.41(6)
		C(126)-C(121)	1.47(6)
As(1)-C(11)	1.92(5)		
As(1)-C(12)	1.97(5)		
As(1)-C(121)	1.90(5)		
As(2)-C(126)	1.94(5)	C(231)-C(232)	1.39(6)
As(2)-C(21)	2.06(5)	C(232)-C(233)	1.38(7)
As(2)-C(231)	1.97(5)	C(233)-C(234)	1.37(7)
		C(234)-C(235)	1.38(6)
As(3)-C(236)	2.01(4)	C(235)-C(236)	1.38(6)
As(3)-C(31)	1.98(4)	C(236)-C(231)	1.36(6)
As(3)-C(341)	1.90(5)		
As(4)-C(346)	1.92(5)		
As(4)-C(41)	1.95(5)		
As(4)-C(42)	1.99(5)		
		C(341)-C(342)	1.45(6)
		C(342)-C(343)	1.35(6)
		C(343)-C(344)	1.40(6)
Cl(2)-O(1)	1.42(5)	C(344)-C(345)	1.36(6)
Cl(2)-O(2)	1.42(5)	C(345)-C(346)	1.48(6)
Cl(2)-O(3)	1.36(7)	C(346)-C(341)	1.46(6)
Cl(2)-O(4)	1.38(5)		
C(51)-C(52)	1.46(8)		
C(52)-C(53)	1.38(8)		
C(53)-C(54)	1.42(8)		
C(54)-C(55)	1.35(9)		
C(55)-C(56)	1.35(9)		
C(56)-C(51)	1.33(8)		

Table 4.2e
Bond angles and their standard deviations (in parentheses) in degrees

As(1)- Pd - As(2)	= 80.1(0.2)	Pd -As(4) -C(346)	= 109(1.4)
As(1)- Pd - As(3)	= 95.9(0.2)	Pd -As(4) -C(41)	= 112(1.5)
As(1)- Pd - As(4)	= 178.2(0.2)	Pd -As(4) -C(42)	= 117(1.5)
As(1)- Pd - Cl(1)	= 89.8(0.7)	C(346)-As(4)-C(41)	= 106(2.0)
As(2)- Pd - As(3)	= 81.9(0.2)	C(346)-As(4)-C(42)	=104(2.0)
As(2)- Pd - As(4)	= 99.3(0.2)	C(41)- As(4)-C(42)	= 108(2.1)
As(2)- Pd - Cl(1)	= 101.8(0.7)		
As(3)- Pd - As(4)	= 85.7(0.2)	As(1)-C(121)-C(126)	= 116(3.5)
As(3)- Pd - Cl(1)	= 173.7(0.7)	As(1)-C(121)-C(122)	= 125(3.6)
As(4)- Pd - Cl(1)	= 88.60(0.7)	As(2)-C(126)-C(121)	= 124(2.8)
	=	As(2)-C(126)-C(125)	= 117(2.8)
Pd -As(1)-C(11)	115(1.3)	As(2)-C(231)-C(232)	= 120(2.9)
Pd -As(1)-C(12)	= 124(1.5)	As(2)-C(231)-C(236)	= 124(3.0)
Pd -As(1)-C(121)	= 110(1.5)	As(3)-C(236)-C(231)	= 118(2.9)
C(11)-As(1)-C(12)	= 101(2.0)	As(3)-C(236)-C(235)	= 115(2.7)
C(11)-As(1)-C(121)	= 101(2.0)	As(3)-C(341)-C(342)	= 127(2.8)
C(12)-As(1)-C(121)	= 103(1.7)	As(3)-C(341)-C(346)	= 116(2.7)
		As(4)-C(346)-C(341)	= 118(1.6(
Pd -As(2)-C(126)	= 97(1.3)	As(4)-C(346)-C(345)	= 123(2.7)
Pd -As(2)-C(21)	= 154(1.3)		
Pd -As(2)-C(231)	= 97(1.3)	O(1)-Cl(2)-)O(2)	= 99(3.5)
C(126)-As(2)-C(21)	= 103(1.9)	O(1)-Cl(2)- O(3)	= 106(3.1)
C(126)-As(2)-C(231)	= 99(2.0)	O(1)-Cl(2)- O(4)	= 111(3.7)
C(21)-As(2)-C(231)	= 97(1.9)	O(2)-Cl(2)- O(3)	= 115(3.8)
		O(2)-Cl(2)- O(4)	= 117(3.7)
Pd -As(3)-C(236)	= 110(1.3)	O(3)-Cl(2)- O(4)	= 107(3.6)
Pd -As(3)-C(31)	= 123(1.3)		
Pd -As(3)-C(341)	= 112(1.0)		
C(236)-As(3)-C(31)	= 103(1.7)		
C(236)-As(3)-C(341)	= 105(1.8)		
C(31)-As(3)-C(341)	= 101(1.9)		

Table 4.2f

Structure factors for $[Pd(TPAS)Cl]ClO_4.C_6H_6$

k	Fo	Fc
h= 1	l= 3	
1	238	230
2	192	181
3	170	175
4	24	21
5	79	-77
6	66	-63
7	19	-21
8	71	-71
10	48	52
11	68	-73
12	95	93
h= 1	l= 4	
0	100	100
1	37	40
2	44	-36
3	163	-152
4	45	-46
5	246	-226
6	36	-36
7	49	-42
8	56	51
9	110	-123
10	72	72
14	47	-53
15	26	-27
16	34	-34
h= 1	l= 5	
1	141	-123
2	121	-117
3	284	-275
4	98	-97
5	41	-43
6	72	74
7	43	-36
8	87	38
10	82	-81
11	51	57
12	71	-82
13	25	-29
h= 1	l= 6	
0	48	-50
1	39	-40
2	104	-103
3	92	81
4	31	34
5	134	140
6	49	57
7	172	-177
9	74	-74
10	84	-94
h= 1	l= 7	
1	37	33
2	30	-29
3	42	46
4	61	73
5	23	-21
6	130	-134
7	30	-37
8	55	-65
9	51	-53
10	39	39
11	57	-56
h= 1	l= 8	
0	67	-85
1	20	20
3	20	23
4	102	-92
5	39	-41
6	88	-104
7	68	-73
8	80	81
10	32	37
11	26	19
h= 1	l= 9	
1	25	-20
2	54	-58
4	114	117
5	79	88
6	43	50
h= 1	l= 10	
0	69	64
1	27	27
2	78	63
4	53	77
5	54	68

k	Fo	Fc
h= 2	l=-12	
1	56	-58
3	73	-67
4	54	-51
5	39	-35
6	28	-18
7	41	-41
h= 2	l=-11	
1	167	-154
2	91	-91
3	43	-35
4	31	37
h= 2	l=-10	
0	82	-82
1	66	55
2	58	59
3	161	147
4	69	69
5	79	79
7	41	39
8	38	39
9	76	69
11	42	35
h= 2	l=-9	
1	118	107
2	77	77
3	129	116
5	28	-37
6	29	-28
8	53	-50
h= 2	l=-8	
0	132	124
3	150	-148
4	100	-96
5	106	-99
6	36	45
7	58	54
9	47	-37
10	64	-63
h= 2	l=-7	
2	109	-98
4	45	-34
5	175	180
6	102	86
7	78	78
8	64	53
11	81	75
h= 2	l=-6	
0	197	180
2	93	91
3	63	67
4	196	177
6	135	128
7	108	-104
8	56	-51
10	54	-51
11	48	-45
13	68	-62
17	43	-43
h= 2	l=-5	
1	30	28
2	185	177
3	65	57
4	81	73
6	220	-211
7	94	-88
8	126	-134
9	31	-27
11	86	-46
12	45	-49
16	56	-57
h= 2	l=-4	
0	269	-291
1	141	-138
2	86	-91
3	184	-169
4	204	-191
5	78	-66
6	174	-160
7	41	42
8	105	98
10	70	80
13	30	26
h= 2	l=-3	
2	78	-72
3	81	-78
4	104	-98
6	157	159
7	64	56
8	132	106

k	Fo	Fc
h= 3	l=-4	
1	112	-75
2	213	-71
3	167	-34
4	48	-43
5	39	-74
6	93	
7	23	
8	48	
9	43	
10	58	
11	56	
h= 3	l=-3	
0	96	
1	103	
2	54	
3	47	
4	58	
5	14	
6	22	
7	41	
8	71	
9	43	
h= 3	l=-2	
1	107	
2	94	
3	68	
4	134	
5	19	
6	58	
7	35	
8	112	
9	54	
10	47	
11	68	
12	35	
13	24	
h= 3	l=-1	
0	124	
1	110	
2	56	
3	53	
4	88	
5	23	
6	62	
7	95	
8	136	
9	35	
10	26	
11	10	
12	28	
h= 3	l= 0	
0	175	
1	42	
2	72	
3	140	
4	25	
5	65	
6	25	
7	124	
8	33	
9	76	
10	78	
11	63	
h= 3	l= 1	
0	48	
1	23	
2	215	
3	97	
4	144	
5	15	
6	126	
7	69	
8	149	
h= 3	l= 2	
1	85	
2	113	
3	55	
4	163	
5	89	
6	14	
7	35	
8	15	
9	61	
10	46	
11	54	
12	58	
13	97	
14	22	

k	Fo	Fc
h= 3	l=-12	
0	74	
1	72	
2	34	
3	40	
4	63	
5		
6		
7		
8		
9		
10		
11		
12		
13		
14		
15		
h= 3	l=-11	
1	117	
2	244	
3	177	
4	57	
5	40	
6	101	
7	23	
8	49	
9	49	
10	54	
11	55	
h= 3	l=-10	
1	108	
2	119	
3	75	
4	62	
5	77	
6	23	
7	32	
8	49	
9	62	
10	40	
h= 3	l=-9	
1	121	
2	122	
3	77	
4	160	
5	28	
6	64	
7	37	
8	111	
9	60	
10	74	
11	42	
12	22	
h= 3	l=-8	
1	171	
2	132	
3	78	
4	64	
5	80	
6	24	
7	66	
8	96	
9	150	
10	36	
11	39	
12	19	
13	36	
h= 3	l=-7	
1	174	
2	51	
3	100	
4	165	
5	32	
6	86	
7	28	
8	129	
9	34	
10	82	
11	89	
12	69	
h= 3	l=-6	
1	36	
2	30	
3	243	
4	96	
5	161	
6	20	
7	124	
8	66	
9	174	
h= 3	l=-5	
1	49	
2	120	
3	55	
4	174	
5	43	
6	18	
7	37	
8	21	
9	79	
10	45	
11	56	
12	63	
13	101	
14	31	

k	Fo	Fc
h= 4	l= 0	
4	44	-48
6	115	120
8	65	-52
10	70	58
12	33	-30
14	102	-96
16	36	27
h= 4	l= 1	
3	99	90
4	24	-18
5	122	109
6	135	-135
7	38	40
8	106	107
9	153	-149
10	43	40
h= 4	l= 2	
0	152	-145
1	220	-180
2	64	49
3	71	61
4	225	211
5	81	-26
6	45	85
7	90	61
8	72	-19
9	26	-44
10	37	38
11	38	-40
12	40	89
13	101	-24
14	18	-23
17	23	
18		
h= 4	l= 3	
0	132	-129
1	341	313
2	374	324
3	221	190
4	29	-30
5	125	-105
6	48	-35
7	107	-106
11	42	33
12	47	-46
14	63	-69
h= 4	l= 4	
0	151	132
1	114	101
2	60	59
3	139	-148
4	177	-159
5	185	-169
6	147	-147
7	83	-75
8	168	-169
9	47	-51
11	47	-46
12	48	-51
14	37	-35
h= 4	l= 5	
0	56	-58
1	57	-46
2	258	-264
3	169	-155
4	110	-100
5	49	54
6	54	-58
7	48	38
8	29	-32
9	34	-28
10	36	32
11	31	-28
h= 4	l= 6	
0	143	-140
1	83	-83
2	179	-173
4	27	36
5	129	129
6	122	125
7	143	142
8	97	-96
9	102	-96
10	23	-16
h= 4	l= 7	
0	46	41
1	40	43
2	55	66
3	125	139
4	47	49
5	47	-62
6	53	-58

k	Fo	Fc
18	45	-40
20	26	-21
h= 4 , l=-1		
1	102	-113
2	87	75
3	228	-233
4	107	106
5	83	-75
6	100	-92
7	51	-53
8	100	-93
10	21	18
11	67	57
12	20	-17
16	58	-46
18	33	-21
h= 4 , l= 0		
0	107	96
1	40	-39
2	18	20
3	110	103
4	167	-167
5	133	123
6	147	-144
7	55	53
8	41	32
9	100	96
12	42	-40
14	42	-45
15	45	33
h= 4 , l= 1		
1	20	21
2	123	-113
3	148	146
4	29	-21
5	13	-20
6	52	39
8	31	33
9	38	-38
10	16	13
11	82	-82
16	58	53
h= 4 , l= 2		
0	196	-214
1	60	57
2	88	-79
3	60	-63
4	58	50
5	69	-68
6	29	28
7	25	17
8	29	25
9	30	-27
10	28	-30
12	25	24
13	35	37
14	51	43
h= 4 , l= 3		
1	42	-37
2	174	169
3	46	-43
4	78	68
5	43	39
6	77	70
10	40	44
11	55	50
12	80	76
h= 4 , l= 5		
1	68	63
2	133	-123
4	68	-57
5	49	40
6	72	-62
h= 4 , l= 6		
0	118	-115
h= 4 , l= 7		
2	60	60
3	45	37
4	41	44
h= 4 , l= 9		
2	31	-33
3	58	-51
4	44	-41
h= 5 , l=-13		
1	45	36
4	65	50
h= 5 , l=-12		
0	68	57
1	41	-38
k	Fo	Fc
2	86	63
4	43	32
5	39	33
h= 5 , l=-11		
1	102	-87
2	103	-78
4	83	-63
7	45	-38
9	64	-60
10	66	-39
11	52	-41
h= 5 , l=-10		
0	162	-142
1	62	55
2	123	-109
3	44	27
4	67	-52
5	47	-41
7	37	-36
h= 5 , l=-9		
2	94	78
3	67	-68
4	29	28
5	44	-40
h= 5 , l=-8		
0	157	148
1	33	-24
3	46	-36
4	87	-82
6	62	-45
7	38	26
8	45	-44
h= 5 , l=-7		
1	96	-112
2	94	-100
4	25	-18
7	48	-41
8	79	74
9	72	-64
10	44	40
14	69	60
h= 5 , l=-6		
2	42	43
3	64	69
4	76	72
5	49	47
6	72	70
8	61	50
9	64	60
11	76	78
13	43	53
h= 5 , l=-5		
2	101	126
3	95	111
4	92	97
6	39	-34
7	72	71
8	62	-48
9	70	65
h= 5 , l=-4		
2	85	105
3	83	-93
6	70	-61
7	42	37
8	42	38
9	53	-49
h= 5 , l=-3		
2	44	-47
3	44	48
4	90	-86
5	111	114
6	43	42
8	73	63
h= 5 , l=-2		
0	52	-52
1	30	18
2	51	-45
4	91	84
5	33	-28
6	105	108
7	32	-32
9	41	-38
11	54	-50
15	28	-25
17	30	-28
18	42	-35
h= 5 , l=-1		
1	27	21
2	80	73
k	Fo	Fc
3	104	-91
4	81	77
5	73	-72
6	96	-89
7	53	-52
8	79	-72
9	46	-44
10	30	-25
12	49	-48
14	35	-39
16	56	-51
17	32	23
18	21	-21
h= 5 , l= 0		
1	68	-67
3	39	-41
4	122	-109
5	36	30
6	93	-93
9	43	41
10	39	-35
h= 5 , l= 1		
1	73	-61
2	91	-82
3	48	42
4	67	-59
5	24	-24
6	29	27
7	21	28
8	24	24
9	16	16
h= 5 , l= 2		
0	134	-135
1	54	49
2	51	-47
3	23	24
4	35	37
5	24	19
7	34	34
8	23	-24
9	42	-37
10	22	-18
14	35	26
15	26	-24
h= 5 , l= 3		
2	127	115
3	51	-50
4	37	26
h= 5 , l= 4		
0	138	128
2	44	36
h= 5 , l= 5		
2	85	-80
5	49	38
7	63	43
h= 5 , l= 6		
0	61	-61
4	51	36
h= 6 , l=-13		
1	77	61
4	109	92
h= 6 , l=-12		
1	64	-51
4	60	47
h= 6 , l=-11		
1	109	-82
2	77	-55
3	82	59
4	105	-89
5	44	35
6	56	-39
8	43	-36
h= 6 , l=-10		
0	156	-117
1	100	80
2	118	-92
3	53	43
4	67	-48
h= 6 , l=-9		
1	117	104
2	122	98
3	58	-51
4	71	59
6	35	34
7	43	-43
h= 6 , l=-8		
3	122	-104
k	Fo	Fc
4	54	-48
6	47	-50
8	59	-51
11	51	-42
h= 6 , l=-7		
2	83	-91
3	77	-76
4	31	22
h= 6 , l=-6		
3	108	134
4	61	63
5	68	70
7	34	33
9	59	56
10	41	-35
11	43	40
h= 6 , l=-5		
2	85	102
3	63	72
6	44	-41
7	34	29
h= 6 , l=-4		
3	108	-116
4	33	-27
5	60	-53
7	34	38
h= 6 , l=-3		
2	70	-70
5	77	85
6	84	93
7	50	51
8	62	62
11	57	56
h= 6 , l=-2		
0	20	16
1	19	-16
2	58	54
3	72	73
4	126	125
5	39	35
6	88	87
7	44	-37
8	24	-15
14	27	23
15	25	-20
17	24	-23
18	29	-23
h= 6 , l=-1		
1	58	62
2	28	24
3	44	36
5	65	-61
6	123	-116
7	24	-26
8	92	-86
11	33	-31
h= 6 , l= 0		
0	51	-46
2	29	-30
3	41	-38
4	86	-86
5	31	-28
6	77	-80
8	33	34
h= 6 , l= 1		
1	54	-50
3	21	-20
6	80	81
8	47	44
10	29	-26
12	32	-24
h= 6 , l= 2		
1	32	31
2	14	-19
4	32	29
8	64	-61
9	24	-28
10	62	-54
h= 7 , l=-2		
0	63	61
2	85	85
3	50	47
4	106	109
6	66	61
7	50	-46
9	26	19
10	30	-27
11	23	17
h= 7 , l=-1		
k	Fo	Fc
1	36	32
2	25	-24
3	53	47
6	80	-82
7	28	19
8	66	-57
9	43	43
h= 7 , l= 0		
0	35	-33
2	16	-20
4	70	-67
6	48	-39
7	30	29
8	53	50
10	44	34
h= 7 , l= 1		
6	70	60
8	38	35
9	27	-28
h= 7 , l= 2		
5	40	-34
6	25	18
7	27	-29
8	47	-44
9	20	-26
10	35	-34
h= 8 , l=-2		
0	43	29
1	26	-23
2	45	44
4	46	45
6	37	27
7	48	-41
9	28	22
10	21	-16
11	28	27
13	20	24
15	21	18
h= 8 , l=-1		
1	26	19
3	41	34
4	27	21
7	42	35
8	48	-32
9	48	41
h= 8 , l= 0		
4	18	-23
5	22	18
6	18	-19
7	22	26
8	39	34
h= 9 , l=-2		
0	44	-36
6	25	19
9	24	21
11	20	22
h= 9 , l=-1		
1	30	25
2	37	27
4	24	19
7	26	23
h= 9 , l= 0		
0	35	29
2	27	20
h= 10 , l=-2		
0	41	-31
3	38	32
5	27	22
h= 10 , l=-1		
1	29	24
2	23	19
h= 11 , l=-2		
0	22	-14

APPENDIX III

THE X-RAY ANALYSIS OF $[Co(QP)Cl]BPh_4$

Data

Table 4.3a

Crystal data: $C_{78}H_{62}BClCoP_4$, M = 1224.5 orthorhombic; space group $P2_1nb$; cell dimensions - a = 18.85 ± 0.02, b = 18.25 ± 0.02, c = 18.60 ± 0.02Å; U = 6398.6Å^3, D_m = 1.25 (by flotation), Z = 4, D_c = 1.27; F(000) = 2556; Cu-K_α radiation, μ = 36.8.

Two axis data: 4416 reflections on b axis giving 2316 non-zero independent reflections on averaging hkl and $\bar{h}kl$; 2300 non-zero independent reflections on a axis. In final stages of the analysis, the reflections were corrected for the imaginary part, F", calculated from atomic positions.

Table 4.3b

X-ray Analysis of $(Co(QP)Cl)BPh_4$

Patterson Function

Cobalt and innacurate ligand positions

Calc. structure factors . Refined phases by tangent formula.

Calculated Structure Factors and Fourier

Improved Co,5L positions
Found 12 carbons of phenyl bridging rings

Calc. Structure factors

Refined Co,5L positions by least-squares

R=0.42

Calc. structure factors, difference Fourier and distance angles.

Improved input positions
Found five further phenyl rings

Refined Co and 5L positions

R=0.255

Calc. Difference synthesis and distance angles

Found remaining carbon atoms

Calc. structure factors and refined all positional and isotropic vibrational parameters

R= 0.111

Calc. Structure Factors
Calc. phases using anomalous dispersion
Calc. Fourier

Found most of QP ligand atoms

Fig. 4.1 The ligand, QP.

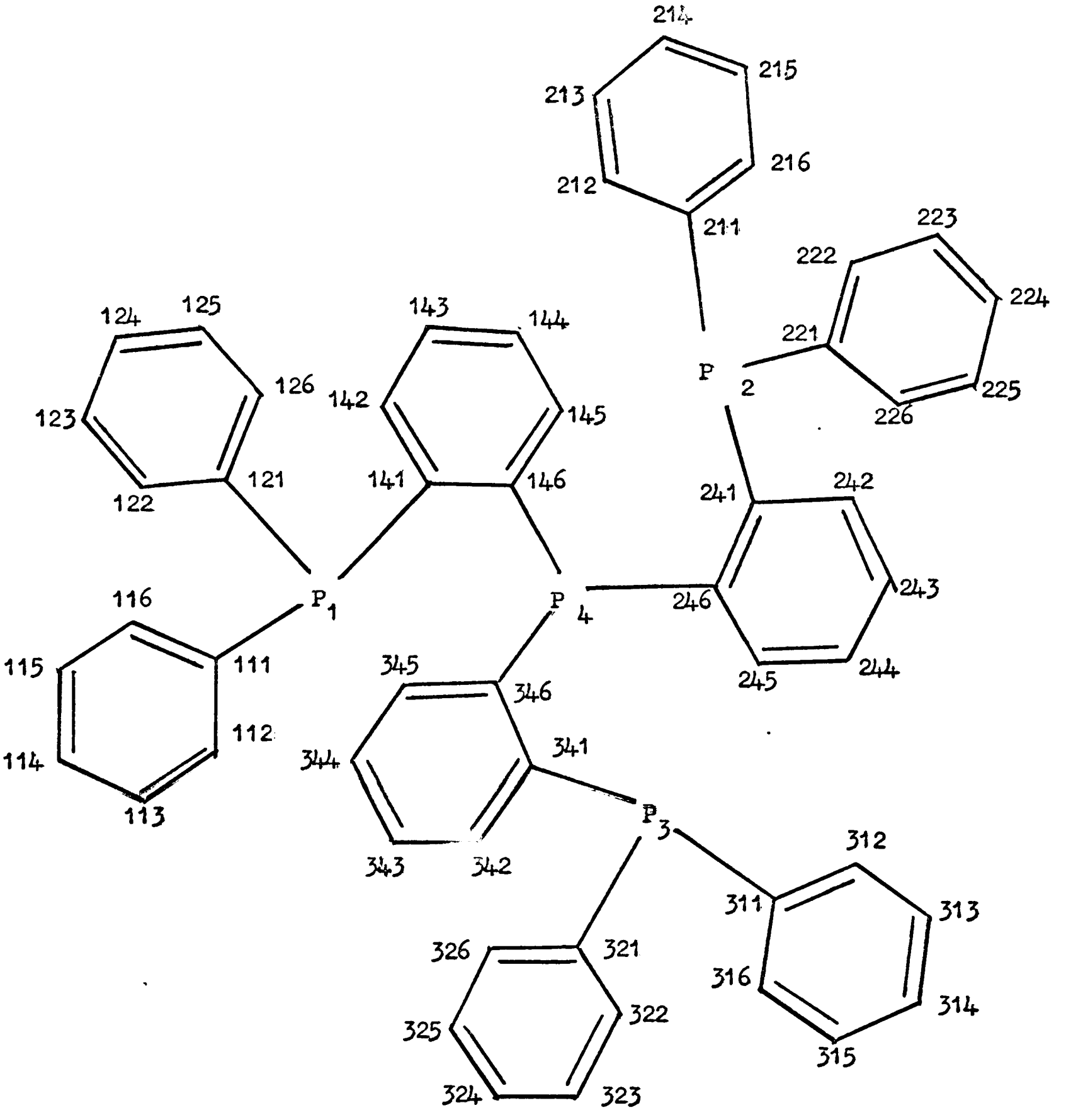

Table 4.3c The Crystal Structure of $[Co(QP)Cl]BPh_4$

Positional and isotropic vibrational parameters with standard deviations

		Y	Z	X	U
27	1	0.00727	0.02077	0.25000	0.020
15	1	0.11301	0.08566	0.24365	0.027
15	2	-0.09004	0.09579	0.22262	0.024
15	3	0.02720	-0.09861	0.25933	0.030
15	4	0.01683	0.00561	0.14259	0.023
17	1	-0.00870	0.01992	0.37119	0.048
6	141	0.12787	0.10671	0.15148	0.050
6	142	0.18913	0.14149	0.12376	0.061
6	143	0.19591	0.14993	0.05082	0.051
6	144	0.14771	0.11964	0.00388	0.035
6	145	0.08911	0.07746	0.03197	0.044
6	146	0.07794	0.06820	0.10363	0.012
6	241	-0.11765	0.06926	0.13664	0.033
6	242	-0.18257	0.09267	0.10217	0.035
6	243	-0.20359	0.06546	0.03784	0.045
6	244	-0.15514	0.02144	0.00028	0.047
6	245	-0.08934	-0.00455	0.03149	0.027
6	246	-0.06949	0.02171	0.09881	0.033
6	341	0.07068	-0.12488	0.17896	0.032
6	342	0.11042	-0.19359	0.16861	0.060
6	343	0.12947	-0.21268	0.09461	0.046
6	344	0.11081	-0.16645	0.04250	0.050
6	345	0.07468	-0.10206	0.05076	0.038
6	346	0.05461	-0.08043	0.11808	0.022
6	111	0.10993	0.17296	0.28657	0.036
6	112	0.07107	0.18281	0.34929	0.096
6	113	0.07317	0.24089	0.39255	0.110
6	114	0.09729	0.30569	0.34858	0.120
6	115	0.15166	0.29936	0.30575	0.117
6	116	0.14803	0.22982	0.27028	0.121
6	121	0.19953	0.04553	0.27140	0.029
6	122	0.22507	0.05538	0.33786	0.032
6	123	0.29110	0.02025	0.35997	0.040
6	124	0.32530	-0.02563	0.30748	0.046
6	125	0.30252	-0.03045	0.24102	0.061
6	126	0.23645	-0.00127	0.21816	0.039
6	211	-0.09130	0.19345	0.21474	0.032
6	212	-0.13463	0.23904	0.26050	0.060
6	213	-0.13154	0.31087	0.24269	0.080
6	214	-0.09523	0.33923	0.18936	0.072
6	215	-0.05318	0.29744	0.14683	0.072
6	216	-0.04738	0.22383	0.16554	0.068

6	221	-0.16587	0.07542	0.27789	0.038
6	222	-0.23012	0.03527	0.25970	0.033
6	223	-0.28571	0.01306	0.30225	0.048
6	224	-0.28327	0.03563	0.37326	0.049
6	225	-0.22059	0.07833	0.39998	0.062
6	226	-0.16403	0.09683	0.35133	0.044
6	311	0.07394	-0.14410	0.33270	0.048
6	312	0.15905	-0.13951	0.32883	0.068
6	313	0.19836	-0.17185	0.38525	0.079
6	314	0.15581	-0.20566	0.43792	0.066
6	315	0.08769	-0.21216	0.43601	0.070
6	316	0.03820	-0.17743	0.38236	0.047
6	321	-0.06055	-0.14714	0.25955	0.038
6	322	-0.12000	-0.11590	0.28609	0.058
6	323	-0.18452	-0.15553	0.28683	0.110
6	324	-0.18844	-0.22665	0.25601	0.102
6	325	-0.12597	-0.26386	0.24136	0.114
6	326	-0.04929	-0.22387	0.24144	0.094
6	11.	0.06676	0.55672	0.18345	0.048
6	12	0.09373	0.62096	0.21119	0.049
6	13	0.08801	0.63426	0.28616	0.089
6	14	0.05430	0.58745	0.33047	0.072
6	15	0.02727	0.52576	0.30255	0.076
6	16	0.03120	0.50367	0.23104	0.067
6	21	-0.02536	0.56511	0.07691	0.058
6	22	-0.07556	0.51834	0.06216	0.064
6	23	-0.15952	0.53159	0.05250	0.104
6	24	-0.17365	0.60632	0.06254	0.111
6	25	-0.12345	0.66450	0.06419	0.094
6	26	-0.05067	0.63700	0.08124	0.077
6	31	0.12208	0.59716	0.05158	0.043
6	32	0.19547	0.60356	0.08085	0.091
6	33	0.23846	0.64272	0.03554	0.083
6	34	0.20746	0.67264	-0.02546	0.081
6	35	0.15149	0.67463	-0.05138	0.109
6	36	0.10481	0.63412	-0.00576	0.076
6	41	0.08161	0.46308	-0.07052	0.035
6	42	0.11453	0.41271	0.11498	0.048
6	43	0.13377	0.34318	0.08616	0.058
6	44	0.12123	0.32461	0.01926	0.046
6	45	0.08620	0.37580	-0.02759	0.066
6	46	0.06463	0.43960	-0.00111	0.053
5	1	0.06373	0.54342	-0.09726	0.042

***

Table 4.3d The Crystal Structure of $[Co(QP)Cl]BPh_4$

Selected bond lengths with their standard deviations in parentheses

		Å
Co	- P(1)	2.280 (4)
Co	- P(2)	2.318 (4)
Co	- P(3)	2.261 (4)
Co	- P(4)	2.057 (4)
Co	- Cl	2.309 (6)
P(1)	- C(141)	1.81 (3)
P(1)	- C(111)	1.82 (2)
P(1)	- C(121)	1.82 (2)
P(2)	- C(241)	1.77 (2)
P(2)	- C(211)	1.83 (2)
P(2)	- C(221)	1.78 (2)
P(3)	- C(341)	1.78 (2)
P(3)	- C(311)	1.83 (2)
P(3)	- C(321)	1.84 (2)
P(4)	- C(146)	1.77 (2)
P(4)	- C(246)	1.80 (2)
P(4)	- C(346)	1.80 (2)

Mean Values

C	- C of phenyl ring	1.40 (4)
C	- B of anion	1.67 (4)
P	- C of cation	1.80 (2)

Table 4.3e The Crystal Structure of $[Co(QP)Cl]BPh_4$

Selected bond angles and their standard deviations (in parentheses) in degrees

P(1)	- Co	- P(2)	108.5	(0.2)
P(1)	- Co	- P(3)	112.9	(0.2)
P(2)	- Co	- P(3)	137.2	(0.2)
P(1)	- Co	- P(4)	87.1	(0.2)
P(2)	- Co	- P(4)	85.9	(0.2)
P(3)	- Co	- P(4)	85.9	(0.2)
P(1)	- Co	- Cl	99.4	(0.2)
P(2)	- Co	- Cl	97.4	(0.2)
P(3)	- Co	- Cl	86.3	(0.2)
P(4)	- Co	- Cl	171.4	(0.2)
Co	- P(1)	- C(141)	107.0	(0.8)
Co	- P(1)	- C(111)	115.1	(0.6)
Co	- P(1)	- C(121)	120.0	(0.6)
C(141)	- P(1)	- C(111)	103.9	(1.0)
C(141)	- P(1)	- C(121)	103.7	(1.0)
C(111)	- P(1)	- C(121)	105.4	(0.8)
Co	- P(2)	- C(241)	104.7	(0.6)
Co	- P(2)	- C(211)	128.9	(0.7)
Co	- P(2)	- C(221)	109.7	(0.6)
C(241)	- P(2)	- C(211)	101.5	(0.9)
C(241)	- P(2)	- C(221)	104.9	(0.9)
C(211)	- P(2)	- C(221)	104.6	(0.9)

			o	
Co	- P(3)	- C(341)	106.0	(0.6)
Co	- P(3)	- C(311)	125.3	(0.8)
Co	- P(3)	- C(321)	110.1	(0.7)
C(341)	- P(3)	- C(311)	105.3	(1.0)
C(341)	- P(3)	- C(321)	104.8	(1.0)
C(311)	- P(3)	- C(321)	103.7	(1.0)
Co	- P(4)	- C(146)	111.9	(0.5)
Co	- P(4)	- C(246)	110.8	(0.6)
Co	- P(4)	- C(346)	114.0	(0.5)
C(146)	- P(4)	- C(246)	104.4	(0.8)
C(146)	- P(4)	- C(346)	103.7	(0.7)
C(246)	- P(4)	- C(346)	111.3	(0.8)
P(1)	- C(141)	- C(146)	113.2	(1.5)
P(4)	- C(146)	- C(141)	117.1	(1.3)
P(2)	- C(241)	- C(246)	117.0	(1.4)
P(4)	- C(246)	- C(241)	114.1	(1.4)
P(3)	- C(341)	- C(346)	115.4	(1.3)
P(4)	- C(346)	- C(341)	112.4	(1.2)
C(11)	- B	- C(21)	102.6	(2.1)
C(11)	- B	- C(31)	113.1	(2.1)
C(11)	- B	- C(41)	116.3	(2.1)
C(21)	- B	- C(31)	109.9	(2.1)
C(21)	- B	- C(41)	109.8	(2.1)
C(31)	- B	- C(41)	105.1	(2.1)

Mean value for C - C - C of phenyl rings 120.1 (2.5)

Table 4.3f

Structure factors for $[Co(QP)Cl]BPh_4$

Data: h,k,l,F_o',F_c,$\emptyset$

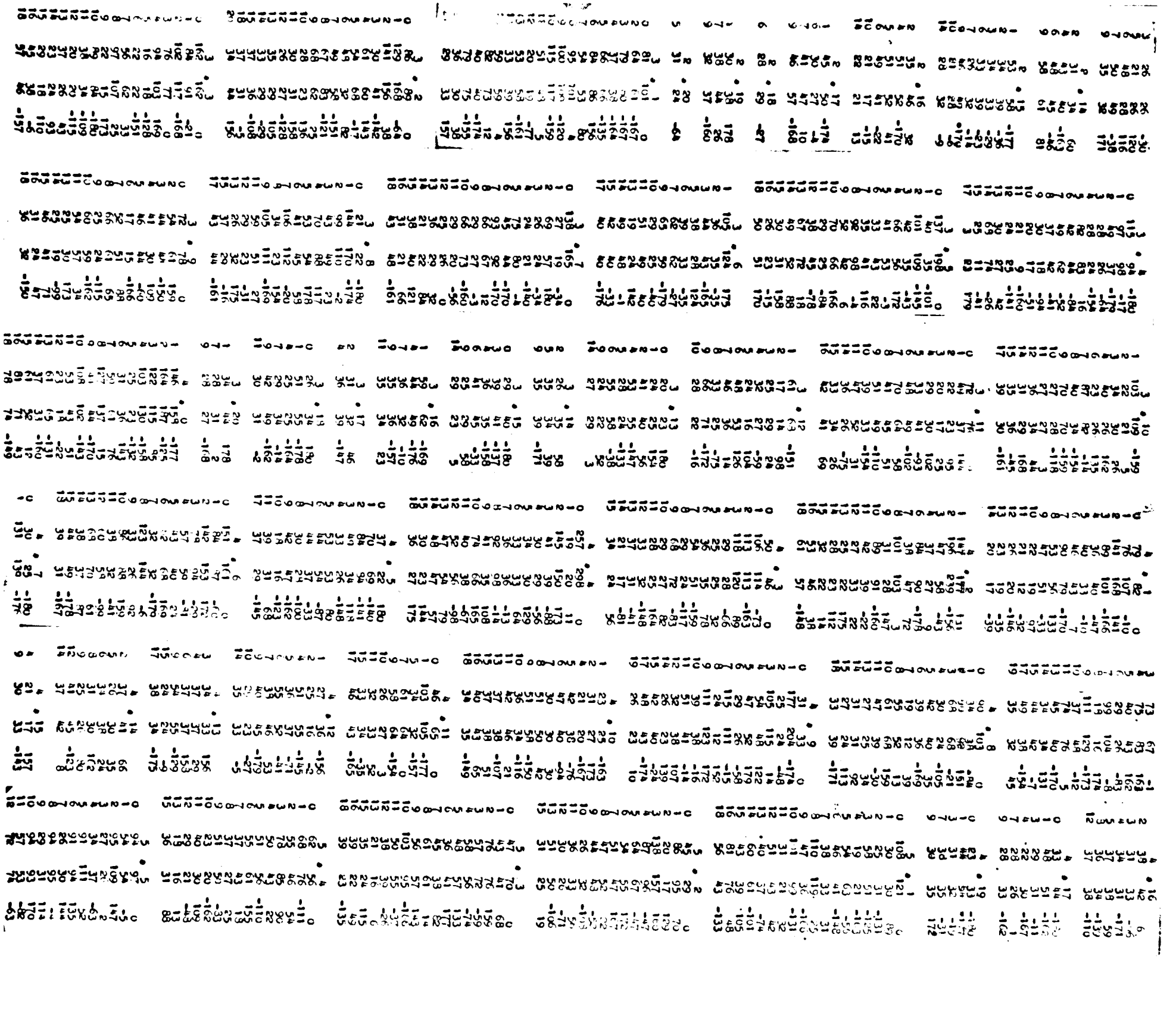

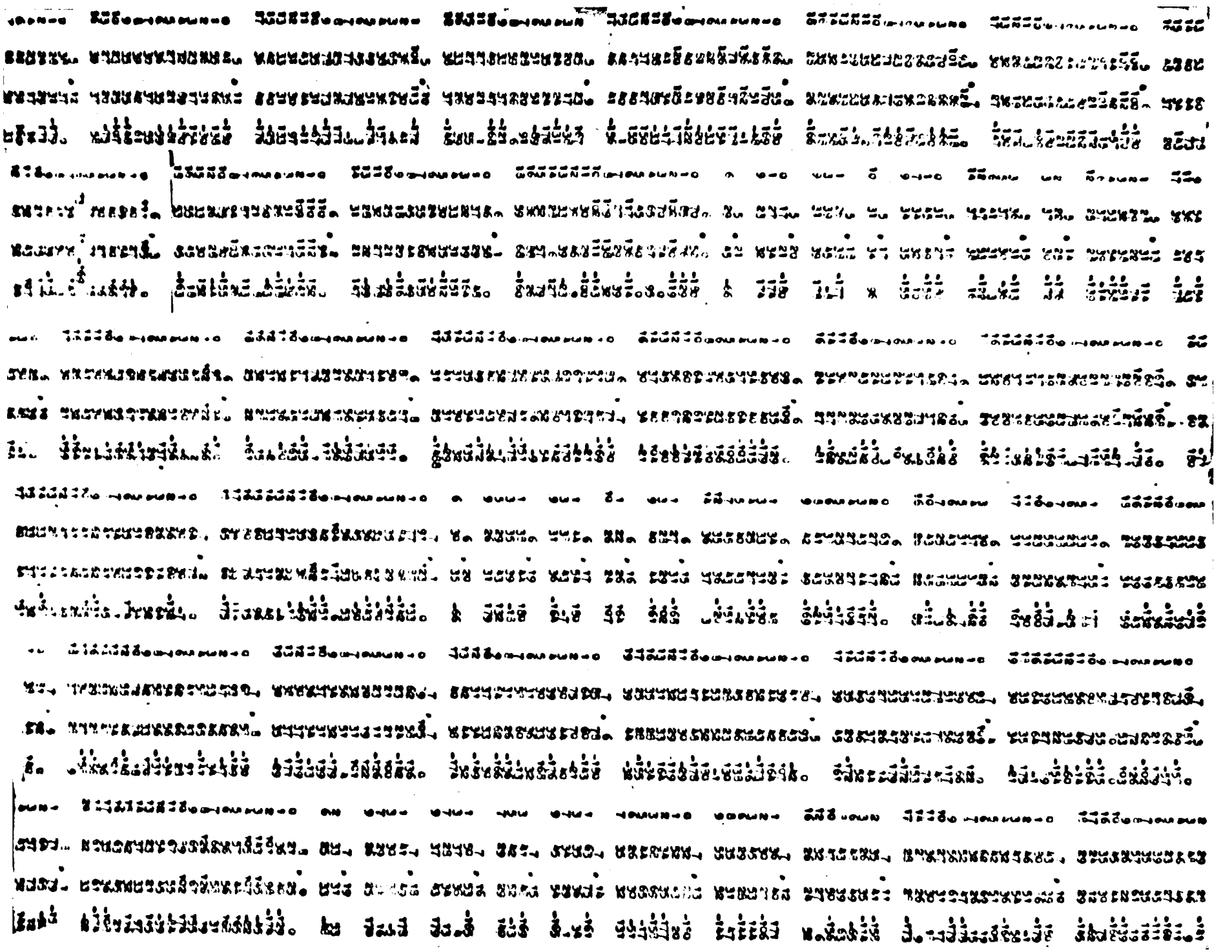

	14 , 5		
0	47	49	-170
2	46	46	-97
3	29	29	64
4	33	37	-61
	14 , 6		
0	4[illegible]	55	0
1	51	53	171
2	52	51	-176
3	55	57	-55
4	27	2[illegible]	14
6	4[illegible]	47	-168
7	31	29	-14
8	54	57	-21
9	40	34	115
10	43	4[illegible]	-171
11	47	[illegible]9	-56
12	37	35	4
13	34	33	6[illegible]
	14 , 7		
0	48	45	-180
1	51	46	-175
2	53	58	-16
6	37	32	-14
7	39	32	-61
10	36	3[illegible]	-34
12	29	25	125
	14 , 8		
1	44	52	164
3	42	42	-26
7	34.	39	36
	14 , 9		
1	45	49	190
2	44	40	-4
4	52	54	146
5	35	27	172
6	37	33	-12
7	52	43	-12
9	29	34	161
	14 , 10		
7	45	50	92
9	29	31	-113
	14 , 11		
1	44	54	-167
3	39	49	16
7	38	32	18
9	33	33	-174
	15 , 1		
3	37	27	-124
5	35	40	-74
7	30	46	94
9	[illegible]3	30	-168
11	[illegible]	36	13
13	[illegible]	32	-131
	15 , 2		
0	[illegible]2	43	0
2	52	60	-156
4	4[illegible]	46	-6
6	40	39	147
7	2[illegible]	18	56
10	26	29	-176
12	27	27	-76
	15 , 3		
2	33	35	-156
3	60	50	-75
6	40	39	-171
7	32	25	1[illegible]
11	44	44	-52
	15 , 4		
4	2[illegible]	29	-9
6	47	55	119
7	35	28	14
12	30	20	-64
	15 , 5		
0	55	40	0
2	40	62	-156
3	64	69	-56
4	31	33	24
5	29	27	127
6	45	47	176
7	40	32	4
[illegible]	[illegible]	4[illegible]	-17
9	43	44	14[illegible]
11	62	55	-47
	15 , 6		
2	43	41	-21
10	31	30	-27
	15 , 7		
0	50	56	0
2	57	4[illegible]	-164
3	4[illegible]	50	-37
4	31	37	-25
9	35	31	169
11	42	37	-43
	15 , 8		
4	63	63	163
5	[illegible]	23	134
6	40	41	-26
7	42	42	-56
10	46	52	-30
12	37	34	133
	15 , 9		
9	28	3[illegible]	-124
	15 , 10		
2	31	50	2
4	39	47	167
5	31	2[illegible]	-1[illegible]0
7	42	39	-4
10	2[illegible]	24	-19
	15 , 11		
3	33	37	-167
4	30	35	-177
7	32	25	102
	15 , 12		
5	32	15	-149
7	35	33	15
	16 , 0		
2	41	41	87
3	22	16	-91
4	28	35	141
5	36	43	-79
6	39	32	-143
7	54	54	90
9	34	29	-[illegible]4
14	35	3[illegible]	179
	16 , 1		
2	32	26	-158
	16 , 2		
2	26	16	-172
3	31	32	-43
7	49	49	82
9	31	26	-133
	16 , 3		
2	22	29	-158
6	29	30	96
7	41	39	29
	16 , 4		
2	39	50	-162
3	51	45	-49
4	43	42	-26
6	32	39	157
7	43	37	60
9	30	29	16[illegible]
11	43	40	-62
	16 , 6		
3	44	42	-41
4	32	35	4
6	43	42	151
9	35	32	143
11	52	51	-4
	16 , 7		
2	45	52	-38
4	42	45	178
6	47	49	-4
	16 , 9		
2	38	33	-27
4	55	65	172
5	24	15	146
6	40	45	-10
7	38	26	-79
	16 , 10		
4	35	34	160
7	31	31	114
	16 , 11		
4	29	35	163
5	29	17	169
	17 , 1		
2	41	44	-15[illegible]
3	38	35	-41
6	39	30	-162
7	38	34	62
9	39	29	-167
10	2[illegible]	3[illegible]	-[illegible]
	17 , 2		
11	42	41	21
	17 , 3		
2	25	30	-152
3	34	29	-35
6	44	45	141
7	3[illegible]	41	67
10	27	21	174
	17 , 5		
2	29	36	-165
3	24	29	-43
6	41	36	136
	17 , 7		
3	24	27	-4[illegible]
	18 , 0		
1	60	59	136
2	41	34	-12[illegible]
3	49	42	-71
5	40	24	129
9	40	33	1[illegible]0
11	44	3[illegible]	-52
	[illegible] , 2		
2	25	37	-129
9	34	31	16[illegible]
	1[illegible] , 3		
3	42	39	21
9	37	40	-151
11	32	36	17
	19 , 1		
3	43	4[illegible]	-35
4	24	23	14
9	32	2[illegible]	139
11	49	54	-56
	19 , 2		
2	34	38	4
3	30	3[illegible]	30
4	34	29	14[illegible]
5	24	26	167
	19 , 3		
5	28	11	-159
9	31	2[illegible]	-176
	19 , 4		
3	30	29	17
	20 , 0		
3	59	56	-32
5	36	31	164
9	35	31	144
11	33	38	-57
	20 , 1		
6	23	25	-16
	20 , 2		
3	29	27	-4[illegible]
9	31	23	164
11	23	27	-45
	20 , 3		
4	37	43	159
6	34	30	-15
	20 , 4		
9	2[illegible]	29	-137
	21 , 1		
3	38	39	-33
5	28	29	175
9	24	25	177
	21 , 2		
6	32	28	-9
	21 , 3		
9	25	27	-165

APPENDIX IV

THE X-RAY ANALYSIS OF $[TlMe_2 1,10\text{-phen}]ClO_4$

Data

Table 4.4a

Crystal data: $C_{14}H_{14}ClN_2O_4Tl$; M = 513.9 monoclinic; a = 7.50 ± 0.01, b = 9.11 ± 0.01, c = 23.54 ± 0.03Å, β = 94.3 ± 0.3°, U = 1603.9Å^3; space group $P2_1/c$; D_m = 2.14 (by flotation), Z = 4, D_c = 2.13; F(000) = 968; Cu-K_α radiation; μ = 209.

Two axis data: Seven layers on the the a axis and two layers on the b axis giving ≃ 1600 independent, non-zero reflections.

B) Determination and Refinement of the Crystal Structure of $(TlMe_2\ 1,10\text{-phen})ClO_4$

	Structure factor calculation assuming isotropic vibrations: Atoms included	R	Agree. Anal.	Least squares method of refinement: Cycle	Parameters refined	Wtg. scheme	Dist. & Angles	Fourier methods: Type	Atoms located
	Tl,Cl					Unit Weights		Patterson	Tl,Cl
	from Patterson			1	Scalefactor				
A	Tl,Cl	0.189		2	K+X,Y,Z,B, for Tl,Cl	"		Electron Density Map	All atoms of phenan-throline
A	from previous	0.154		3		"			
A	cycle of L.S.	0.145	✓	4		"	✓		
B	Tl,Cl,phen	0.143		5	K+X,Y,Z,B for Tl,Cl and phen. atoms	"			
B	from map					"			
B	Tl,Cl,phen.	0.133		6		"		Electron Density Map	All carbon, nitrogen, oxygen, atoms
B	from L.S.	0.128	✓	7		"	✓		
C	All atoms from map.	0.122		8	K+X,Y,Z,B for all atoms				
C	All atoms from	0.112		9				Electron Density Map around C(15), C(16)	Repositioned C(15),C(16)
C	cycle of L.S.	0.109	✓	10			✓		
D	C(15),C(16) from map	0.105		11	"				
D	Others - L.S.				"				
D	All atoms from L.S.	0.099		12	"				
D		0.093		13	"				
D		0.089	✓	14	"		✓	Difference Synthesis	

Table 4.4c

The Crystal Structure of dimethyl-1,10-phenanthroline thallium perchlorate.

Positional and isotropic vibrational parameters with standard deviations in parenthesis.

	X/a	Y/b	Z/c	U(Å^2)
Tl	0.8513(2)	0.6454(2)	0.1856(1)	0.0242(4)
N(1)	0.7230(37)	0.4109(32)	0.1379(12)	0.031(7)
C(2)	0.6673(61)	0.3012(52)	0.1723(19)	0.056(12)
C(3)	0.6050(65)	0.1580(64)	0.1451(21)	0.069(13)
C(4)	0.6026(67)	0.1448(66)	0.0938(22)	0.072(14)
C(5)	0.6439(69)	0.2556(61)	-0.0079(22)	0.072(15)
C(6)	0.6987(63)	0.3692(61)	-0.0397(20)	0.065(13)
C(7)	0.8027(60)	0.6346(60)	-0.0421(19)	0.061(12)
C(8)	0.8491(59)	0.7576(52)	-0.0161(19)	0.054(11)
C(9)	0.8644(61)	0.7598(54)	0.0435(19)	0.055(12)
N(10)	0.8227(41)	0.6435(43)	0.0764(13)	0.047(8)
C(11)	0.7651(45)	0.5295(39)	0.0475(14)	0.027(8)
C(12)	0.7217(44)	0.3954(36)	0.0801(14)	0.025(8)
C(13)	0.6561(55)	0.2688(48)	0.0520(17)	0.045(10)
C(14)	0.7481(56)	0.5160(48)	-0.0143(17)	0.045(10)
C(15)	0.5983(61)	0.7475(55)	0.1927(19)	0.059(12)
C(16)	1.1172(43)	0.5660(40)	0.1943(14)	0.027(8)
Cl	-0.1350(12)	0.5099(10)	0.3349(4)	0.032(2)
O(1)	0.7750(47)	0.4618(41)	0.3830(15)	0.079(10)
O(2)	0.9045(54)	0.6669(17)	0.3378(17)	0.102(13)
O(3)	1.0383(46)	0.4398(41)	0.3353(14)	0.077(9)
O(4)	0.7619(55)	0.4788(48)	0.2841(17)	0.099(13)

Table 4.4d

The Crystal Structure of dimethyl-1,10-phenanthroline-thallium perchlorate.

Selected bond lengths with their standard deviations.

	Å		Å
Tl - N(1)	2.57 (3)	C(7) - C(14)	1.34 (6)
Tl - N(10)	2.57 (3)	C(7) - C(8)	1.31 (6)
Tl - O(3)'	2.86 (4)	C(8) - C(9)	1.40 (5)
Tl - O(4)	2.89 (4)	C(9) - N(10)	1.36 (5)
Tl - C(15)'	2.13 (5)	N(10) - C(11)	1.30 (4)
Tl - C(16)	2.12 (5)	C(11) - C(12)	1.49 (4)
		C(11) - C(14)	1.46 (5)
N(1) - C(2)	1.37 (5)	C(12) - C(13)	1.40 (5)
N(1) - C(12)	1.37 (4)		
C(2) - C(3)	1.51 (7)	Cl - O(1)	1.43 (4)
C(3) - C(4)	1.22 (7)	Cl - O(2)	1.46 (4)
C(4) - C(13)	1.57 (7)	Cl - O(3)	1.45 (4)
C(5) - C(6)	1.36 (7)	Cl - O(4)	1.41 (4)
C(5) - C(13)	1.42 (6)		
C(6) - C(14)	1.50 (6)		

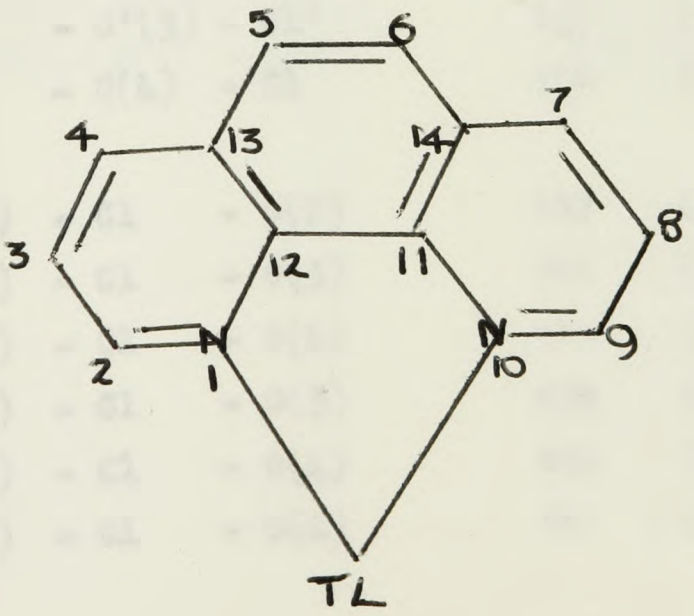

Table 4.4e

Selected bond angles in degrees with their standard deviations (in parentheses).

			°	
N(1)	- Tl	- N(10)	63.6	(1.0)
N(1)	- Tl	- C(15)	95.2	(1.3)
N(1)	- Tl	- C(16)	94.5	(1.3)
N(1)	- Tl	- O'(3)	144.0	(1.0)
N(1)	- Tl	- O(4)	79.3	(1.0)
N(10)	- Tl	- C(15)	94.3	(1.4)
N(10)	- Tl	- C(16)	95.9	(1.4)
N(10)	- Tl	- O'(3)	80.6	(1.2)
N(10)	- Tl	- O(4)	142.6	(1.2)
C(15)	- Tl	- C(16)	168.3	(1.5)
C(15)	- Tl	- O'(3)	82.8	(1.5)
C(15)	- Tl	- O(4)	84.5	(1.5)
C(16)	- Tl	- O'(3)	93.1	(1.5)
C(16)	- Tl	- O(4)	90.9	(1.5)
O'(3)	- Tl	- O(4)	135.8	(1.5)
Tl	- O'(3)	- Cl'	133.	(2)
Tl	- O(4)	- Cl	116	(2)
O(1)	- Cl	- O(2)	112	(2)
O(1)	- Cl	- O(3)	111	(2)
O(1)	- Cl	- O(4)	111	(2)
O(2)	- Cl	- O(3)	105	(2)
O(2)	- Cl	- O(4)	110	(2)
O(3)	- Cl	- O(4)	111	(2)

		o
Tl	- N(1) - C(2)	118 (2)
Tl	- N(1) - C(12)	120 (2)
Tl	- N(10) - C(9)	124 (2)
Tl	- N(10) - C(11)	122 (2)
N(1)	- C(2) - C(3)	118 (4)
C(2)	- C(3) - C(4)	119 (5)
C(3)	- C(4) - C(13)	124 (5)
C(4)	- C(13) - C(5)	124 (4)
C(4)	- C(13) - C(12)	113 (3)
C(13)	- C(5) - C(6)	119 (4)
C(5)	- C(6) - C(14)	122 (4)
C(6)	- C(14) - C(11)	118 (3)
C(6)	- C(14) - C(7)	125 (4)
C(14)	- C(7) - C(8)	122 (4)
C(7)	- C(8) - C(9)	119 (4)
C(8)	- C(9) - N(10)	124 (4)
C(9)	- N(10) - C(11)	113 (3)
N(10)	- C(11) - C(12)	117 (3)
N(10)	- C(11) - C(14)	126 (3)
C(11)	- C(12) - N(1)	116 (3)
C(11)	- C(12) - C(13)	120 (3)
C(12)	- N(1) - C(2)	122 (3)

Table 4.4f

Structure factors for $[TlMe_2 1,10\text{-phen}]ClO_4$

l	Fo	Fc
h= 0 , k= 0		
2	132	-142
4	64	-62
6	361	334
8	332	-323
10	117	97
12	71	63
14	179	-168
16	160	147
18	62	-61
20	41	-33
22	100	104
24	62	-76
26	41	43
h= 0 , k= 1		
1	84	-95
2	106	114
4	188	-213
5	138	-135
6	176	180
7	99	102
8	27	-17
9	66	58
10	142	-137
11	117	-109
12	189	183
13	137	137
14	112	-112
15	74	-75
16	33	-26
17	40	-38
18	108	104
19	114	118
20	104	-108
21	98	-96
22	46	47
h= 0 , k= 2		
0	33	-20
1	217	-251
2	35	-30
3	89	84
4	53	-54
5	113	102
6	35	-24
7	220	-239
8	69	64
9	205	214
10	46	-46
11	47	-44
13	115	-108
14	38	34
15	147	160
16	62	-60
17	113	-122
18	52	43
21	60	65
22	35	-41
23	81	-104
25	60	75
h= 0 , k= 3		
1	131	131
2	86	78
3	278	-270
4	107	-106
5	188	212
6	90	82
7	88	-80
9	121	-131
10	64	-66
11	182	183
12	79	81
13	136	-130
14	47	-46
17	79	91
18	48	48
19	99	-114
21	46	57
h= 0 , k= 4		
0	156	-140
1	147	135
2	140	125
4	56	48
5	87	-76
6	82	-72
7	77	67
8	183	172
9	82	-69
10	110	-100
11	25	20
13	46	43
14	95	95
15	52	-48
16	117	-124
17	72	66
18	105	100

l	Fo	Fc
20	35	27
22	84	-90
23	45	47
24	71	84
h= 0 , k= 5		
1	50	43
2	118	-109
3	85	-79
4	176	171
5	27	26
6	136	-118
9	36	-31
10	153	137
12	158	-146
14	71	67
18	111	-112
20	85	94
22	38	-40
h= 0 , k= 6		
0	140	138
1	131	125
2	100	-101
3	47	-36
4	33	-25
5	59	-53
6	106	103
7	113	102
8	125	-117
9	104	-96
10	55	47
11	33	32
12	54	40
13	54	52
14	93	-82
15	83	-86
16	60	60
17	69	67
h= 0 , k= 7		
1	51	-54
3	97	95
5	124	-121
7	65	55
9	49	50
11	111	-113
13	107	109
h= 0 , k= 8		
0	89	100
1	109	-122
2	35	-3
5	58	53
6	52	57
7	107	-111
8	65	-69
9	79	87
13	46	-44
14	42	-45
h= 0 , k= 9		
2	64	78
4	75	-91
6	60	65
h= 0 , k= 10		
0	61	-87
2	43	53
h= 0 , k= 11		
2	23	-42
3	41	-62
4	37	54
5	37	60
h= 1 , k= 0		
-24	66	-80
-20	120	115
-18	129	-128
-16	96	91
-12	81	-73
-10	227	247
-8	162	-166
-6	74	69
-4	122	116
2	35	27
4	194	-171
6	271	[illegible]
8	188	-121
10	157	-140
12	172	171
14	233	-224
16	90	71
18	92	72
20	167	-167
22	104	94
26	44	[illegible]
28	61	72
h= 1 , k= 1		

l	Fo	Fc
-24	51	47
-23	48	50
-22	96	-85
-21	106	-103
-20	95	91
-19	86	73
-16	97	-81
-15	139	-128
-14	173	164
-13	130	129
-12	105	-102
-11	84	-79
-9	118	-118
-8	182	174
-7	180	183
-6	193	-198
-5	182	-162
-4	85	79
-3	22	14
2	220	241
3	60	48
4	116	-120
5	49	46
6	58	-58
7	41	-36
8	176	172
9	105	102
10	189	-179
11	72	-57
12	59	58
13	52	40
14	57	49
15	38	35
16	110	-119
17	68	-65
18	107	103
19	58	57
20	44	-43
22	34	-33
24	70	77
25	53	53
26	59	-66
27	33	-43
h= 1 , k= 2		
-25	84	-92
-23	48	47
-19	119	-109
-18	63	53
-17	157	154
-16	69	-55
-15	72	-70
-13	88	-75
-12	76	69
-11	183	178
-10	80	-75
-9	189	-191
-7	63	63
-6	92	79
-5	83	84
-4	143	-136
-3	210	-225
-2	93	100
-1	191	227
0	53	44
1	73	-67
2	130	-135
3	85	-90
4	87	82
5	189	219
6	36	-29
7	194	-220
9	62	68
10	27	27
11	126	127
13	168	-185
14	29	26
15	126	123
19	94	-90
21	107	115
23	61	-69
h= 1 , k= 3		
-23	97	-89
-22	44	-47
-21	95	93
-19	49	-50
-18	34	-36
-17	95	-83
-16	64	-57
-15	111	108
-14	84	69
-13	144	-142
-12	99	-89
-11	87	79
-9	96	92
-8	102	87
-7	[illegible]	-172
-6	112	-99
-5	190	176

l	Fo	Fc
-4	80	69
-3	93	-87
-2	41	-32
-1	69	-52
0	41	-41
1	170	205
2	105	105
3	183	-228
4	106	-106
5	27	35
6	30	-32
7	115	118
8	79	79
9	206	-227
10	76	-63
11	135	145
12	28	28
14	30	34
15	101	-99
16	37	-34
17	160	169
19	74	-77
h= 1 , k= 4		
-20	44	-48
-19	69	55
-18	135	142
-17	44	-43
-16	98	-86
-14	45	42
-12	132	122
-11	89	-77
-10	178	-189
-9	99	90
-8	112	109
-7	50	-42
-5	30	-27
-4	199	-198
-3	125	123
-2	221	237
-1	107	-94
0	112	-92
1	44	37
2	81	-82
3	78	79
4	176	168
5	104	-101
6	124	-125
7	99	88
8	112	103
10	43	38
11	79	-75
12	115	-119
13	80	73
14	78	77
15	66	-64
16	99	-93
18	45	-48
19	60	60
20	62	68
21	51	-55
22	70	-75
24	33	36
h= 1 , k= 5		
-22	84	92
-20	77	-82
-17	35	-31
-16	112	110
-14	119	-120
-12	107	107
-8	145	-139
-7	28	19
-6	160	159
-5	38	29
-4	135	-128
-3	52	-41
-2	42	-36
-1	45	36
0	94	162
2	213	-200
3	48	-36
4	102	93
5	50	34
6	42	34
8	143	-134
9	46	-43
10	170	169
11	51	39
12	83	-82
14	39	-45
16	100	115
17	66	55
18	103	-115
h= 1 , k= 6		
-20	51	45
-19	62	61
-18	67	-67
-17	88	-93

l	Fo	Fc
-16	49	48
-15	40	40
-12	68	-64
-11	115	-108
-10	100	89
-9	124	119
-8	66	-61
-7	40	-30
-5	80	-65
-4	69	68
-3	137	131
-2	108	-97
-1	114	-101
0	100	87
3	88	78
4	95	-89
5	137	-125
6	138	123
7	112	81
8	98	-85
11	80	-75
12	111	108
13	82	85
14	91	-93
15	63	-56
18	50	41
19	37	49
20	68	-70
21	57	-62
22	49	58
23	37	40
h= 1 , k= 7		
-21	59	-81
-19	53	52
-15	108	-103
-13	118	117
-11	66	-55
-9	76	-77
-7	144	145
-5	130	-129
-1	103	83
0	38	-28
1	168	-163
3	122	120
7	100	-84
9	125	138
11	80	-76
15	61	63
17	73	-86
19	57	59
h= 1 , k= 8		
-11	75	73
-10	48	48
-9	89	-87
-3	118	-100
-2	63	-58
-1	126	121
0	63	43
3	53	-49
4	45	-46
5	109	100
6	80	68
7	109	-95
8	53	-52
11	55	55
12	50	55
13	87	-91
14	62	-65
15	63	68
h= 1 , k= 9		
-14	79	82
-12	61	-60
-8	89	85
-6	108	-104
-4	55	54
0	108	-104
1	34	33
2	93	91
3	39	-42
8	74	81
9	41	-38
10	66	-74
h= 1 , k= 10		
-4	65	-75
-2	86	56
0	42	-49
4	67	73
6	63	-78
h= 2 , k= 0		
-22	93	[illegible]
-20	165	[illegible]
-18	106	-101
-16	36	-33
-14	166	159
-12	153	-159

l	Fo	Fc
-10	105	95
-8	95	86
-6	189	-190
-4	126	125
-2	79	-76
0	228	-224
2	37	35
4	155	-162
6	124	128
8	51	39
10	170	-154
12	211	194
14	97	-84
16	67	-64
18	131	141
20	117	-116
24	39	47
26	80	-96

h= 2 , k= 1

l	Fo	Fc
-24	65	70
-23	45	52
-22	71	-69
-18	95	74
-17	62	53
-16	133	-119
-15	92	-81
-14	86	87
-13	75	70
-11	38	28
-10	99	-97
-9	176	-173
-8	172	172
-7	151	154
-6	136	-133
-5	67	-60
-4	37	-34
-3	37	-38
-2	76	93
-1	274	275
0	309	-336
1	83	-98
2	20	29
3	17	12
4	49	57
5	128	139
6	176	-193
7	145	-142
8	168	180
9	39	37
10	31	-30
11	39	37
12	82	-83
13	94	-97
14	120	129
15	87	89
16	90	-93
17	40	-37
19	37	-36
20	46	48
21	60	64
22	80	-90
23	35	-39
24	48	59

h= 2 , k= 2

l	Fo	Fc
-21	102	101
-19	123	-129
-17	50	56
-15	93	91
-14	31	-25
-13	188	-185
-12	74	65
-11	161	158
-10	54	-52
-9	30	-35
-8	26	-15
-7	162	-167
-6	57	51
-5	184	197
-4	82	-77
-3	131	-125
-2	49	54
-1	67	62
0	33	-33
1	126	137
2	78	-73
3	200	-203
4	82	79
5	160	166
8	58	-50
9	137	-150
10	60	52
11	155	166
13	114	-110
16	39	31
17	103	104
19	112	-126
21	61	65
25	55	-71

l	Fo	Fc
-23	99	-102
-21	52	45
-19	77	74
-18	49	43
-17	161	-147
-16	68	-61
-15	126	119
-11	110	-103
-10	52	-42
-9	189	189
-8	89	74
-7	117	-112
-6	39	-18
-5	38	26
-4	33	28
-3	156	150
-2	97	97
-1	232	-226
0	90	-78
1	149	122
2	85	77
3	40	34
4	61	55
5	108	-108
6	86	-84
7	181	177
8	96	93
9	127	-133
10	32	-26
12	47	-49
13	98	98
14	74	67
15	112	-124
17	110	105
21	66	-76
23	84	96

h= 2 , k= 4

l	Fo	Fc
-22	58	57
-20	72	-83
-19	59	51
-18	62	59
-14	88	-85
-13	81	70
-12	153	148
-11	76	-69
-10	137	-124
-9	33	35
-8	29	-27
-7	44	37
-6	133	143
-5	123	-116
-4	224	-221
-3	107	98
-2	126	121
0	46	41
1	74	-72
2	198	-185
3	109	103
4	198	183
5	100	-97
6	103	-97
7	35	38
8	81	-93
9	79	79
10	156	160
11	89	-112
12	95	-126
13	55	62
16	58	69
17	62	-71
18	97	-122
19	37	54
20	41	57

h= 2 , k= 5

l	Fo	Fc
-18	110	-109
-16	110	119
-14	95	-94
-10	160	159
-8	178	-189
-6	86	80
-4	47	36
-3	39	35
-2	205	-191
0	214	188
2	93	-92
4	94	-89
6	146	142
8	152	-152
10	54	56
12	59	57
14	104	-112
16	102	118
18	37	-41
20	49	-48
22	74	87

h= 2 , k= 6

l	Fo	Fc
-22	44	-51
-21	49	-53
-20	76	80
-19	62	71
-18	64	-64
-14	99	102
-13	83	88
-12	99	-101
-11	91	-77
-10	36	39
-9	43	32
-8	70	60
-7	57	58
-6	118	-111
-5	117	-123
-4	85	76
-3	102	94
0	49	-40
1	100	-89
2	95	84
3	141	127
4	99	-95
5	100	-91
6	60	50
9	95	86
10	87	-79
11	111	-110
12	85	87
13	59	55
14	42	-43
17	54	-59
18	60	67
19	52	63
20	54	-68
21	29	-33

h= 2 , k= 7

l	Fo	Fc
-17	72	80
-15	82	-90
-13	41	34
-11	37	45
-9	119	-128
-7	139	127
-5	55	-42
-3	65	-59
-2	65	52
-1	186	185
1	161	-139
5	127	112
7	165	-160
9	100	95
13	95	-97
15	95	100

h= 2 , k= 8

l	Fo	Fc
-7	74	-70
-6	59	-57
-5	100	97
-4	53	46
-3	70	-78
1	65	67
2	42	38
3	75	-78
4	59	-53
5	67	75

h= 2 , k= 9

l	Fo	Fc
-10	54	-66
-9	55	35
-8	93	93
-6	55	-57
-2	95	88
0	106	-111
6	85	-89
8	82	88

h= 2 , k= 10

l	Fo	Fc
-6	53	64
-4	69	-81
-2	44	54
2	73	-81
4	76	87

h= 3 , k= 0

l	Fo	Fc
-24	57	66
-22	76	-102
-20	70	77
-16	122	-120
-14	177	186
-12	112	-112
-10	104	-102
-8	228	236
-6	212	-228
-4	75	71
-2	116	106
0	275	-252
2	214	209
4	55	-47
6	103	-103
8	191	189

l	Fo	Fc
10	124	-118
12	38	40
14	93	92
16	122	-133
18	78	88
22	48	-46
24	65	82
26	48	-67

h= 3 , k= 1

l	Fo	Fc
-21	64	62
-20	84	-83
-19	83	-70
-18	117	107
-17	60	52
-16	66	-64
-14	47	-45
-13	43	-47
-12	104	110
-11	100	97
-10	161	-164
-9	76	-65
-8	57	64
-6	48	43
-5	91	82
-4	156	-146
-3	134	-128
-2	191	214
-1	43	43
0	84	-88
1	36	31
2	90	-96
3	60	-56
4	147	166
5	129	133
6	149	-160
7	125	-133
8	63	60
10	100	106
11	101	105
12	104	-119
13	126	-139
14	114	114
15	67	62
18	60	-60
19	79	-88
20	84	101
21	64	70
22	49	-56

h= 3 , k= 2

l	Fo	Fc
-21	101	98
-18	55	-44
-17	112	-104
-15	139	148
-14	44	-41
-13	129	-123
-11	42	33
-9	147	160
-7	193	-206
-6	42	34
-5	127	137
-1	162	-187
0	34	8
1	191	242
2	55	-48
3	120	-124
4	28	37
5	74	-73
7	151	162
8	62	-51
9	170	-188
10	77	73
11	74	70
13	53	48
15	106	-104
16	49	48
17	117	120
18	51	-34
19	72	-57

h= 3 , k= 3

l	Fo	Fc
-19	116	111
-18	64	57
-17	103	-95
-15	48	49
-13	106	97
-12	67	57
-11	184	-185
-10	44	-44
-9	145	136
-5	138	-144
-4	47	-46
-3	209	227
-2	85	77
-1	143	-150
0	51	-38
2	31	-32
3	146	162
4	108	101

l	Fo	Fc
5	145	-157
6	56	-52
7	96	100
8	35	22
9	48	39
11	113	-117
12	81	-90
13	107	100
15	77	-72
19	71	77
21	67	-76

h= 3 , k= 4

l	Fo	Fc
-24	60	-68
-23	39	47
-22	77	84
-18	46	-43
-16	115	94
-15	70	-65
-14	111	-100
-13	64	66
-12	58	49
-10	51	49
-9	84	-63
-8	128	-117
-7	93	82
-6	139	121
-5	68	-67
-4	50	-44
-2	63	-59
-1	58	47
0	144	130
1	97	-96
2	147	-135
3	87	69
4	70	60
6	60	54
7	64	-55
8	171	-167
9	90	82
10	130	139
11	42	-49
14	63	-69
15	64	60
16	129	140
17	51	-60
18	67	-74

h= 3 , k= 5

l	Fo	Fc
-20	73	75
-18	120	-115
-16	51	55
-12	132	-127
-11	61	-48
-10	169	156
-9	59	40
-8	70	-71
-6	65	-48
-5	67	-62
-4	188	188
-3	62	57
-2	167	-151
0	37	37
2	107	92
3	43	36
4	165	-152
6	133	126
8	100	-42
12	127	130
14	76	-77

h= 3 , k= 6

l	Fo	Fc
-17	53	56
-16	86	-80
-15	71	-70
-14	82	80
-13	64	61
-12	64	-61
-10	45	-34
-9	70	-69
-8	128	113
-7	92	80
-6	119	-102
-5	79	-73
-4	42	43
-2	63	52
-1	51	44
0	143	-128
1	125	-122
2	111	98
3	104	77
6	90	-67
7	62	-57
8	94	87
9	115	104
11	64	-54
14	45	39
15	63	61
17	69	-78
18	40	44

l	Fo	Fc
-13	70	-63
-11	109	100
-9	76	-75
-5	71	65
-3	125	-111
-1	127	108
3	90	-80
5	136	125
7	109	-99
11	74	86
13	110	-109
15	54	59

h= 3 , k= 8

l	Fo	Fc
-15	70	73
-14	58	61
-13	64	-71
-12	46	-42
-9	73	67
-8	70	60
-7	114	-100
-6	84	-77
-5	71	71
-1	94	-87
0	75	-71
1	88	86
2	64	54
3	51	-59
7	77	75
8	49	51
9	74	-82

h= 3 , k= 9

l	Fo	Fc
-5	41	-38
-4	69	-72
-3	47	44
-2	79	87
4	71	74
6	77	-79

h= 3 , k= 10

l	Fo	Fc
0	60	74
2	64	-75

h= 4 , k= 0

l	Fo	Fc
-20	45	-52
-18	104	98
-16	106	-110
-14	57	63
-12	42	39
-10	161	-164
-8	177	182
-6	85	-92
-4	81	-80
-2	223	202
0	223	-212
2	70	69
4	114	114
6	227	-245
8	165	183
12	131	-140
14	140	162
16	81	-90
20	70	80
22	69	-86
24	34	48

h= 4 , k= 1

l	Fo	Fc
-20	93	-95
-19	79	-70
-16	59	60
-15	95	91
-14	126	-125
-13	125	-128
-12	117	116
-11	71	68
-10	48	-44
-9	59	55
-8	107	-101
-7	136	-135
-6	158	157
-5	120	119
-4	113	-114
-3	77	-65
-2	52	52
-1	75	-75
0	127	131
1	72	81
2	113	-122
3	115	-112
4	125	135
5	57	54
8	93	-95
9	57	-60
10	115	125
11	79	87
12	87	-96
13	56	-53

APPENDIX V

PROGRAMME TITLE

Intensity Statistics

Computer programme written in C203 autocode for use on English Electric KDF9 computer.

PURPOSE

To examine the statistical properties of reciprocal space for any compound with triclinic, monoclinic or orthorhombic space groups (except Fddd and Fdd2). The theory of the different steps is included in the Discussion (page 39). A one-step programme to carry out the following operations:-

1) Read in reflections interpolating between the maximum and minimum reflections of any row line to find accidental absences. Store F^2, $\sin^2\theta$, multiplicity, corrected for symmetry number for each reflection, omitting reflections where $\sin\theta < \lambda/a_{min}$ (a_{min} is the shortest axis length) and where the symmetry number is known (these are stored separately) (see Page 39).

2) Calculate K (overall scale factor) and B (overall temperature factor) from a Wilson plot (using least-squares fitting of a straight line) (see Page 191).

3) Correct all stored F^2 values for thermal vibration and scattering factor fall-off with $\sin\theta$ using either the K and B calculated in Section '2' or alternatively input values.

4) Calculate $\langle F^2 \rangle$ and compare with value for reflections in zones of

reciprocal space with unknown symmetry number to give evidence of mirrors or rotors in the crystal.

5) Calculate the Wilson ratio.

6) Construct tables of probabilities and cumulative probabilities of $\underline{z} = F^2/\Sigma$ (see Page 45).

7) Calculate 'theoretical' and 'observed' second and third moments for all possible space groups (see Page 47).

FLOW DIAGRAM

1) Read cell dimensions and wavelength, λ, Calculate R_{ij}'s, and value of λ/a_{min}.

2) Read information of systematic absences, zones in reciprocal space with high symmetry number, and zones with unknown symmetry number (p).

3) Read halve-directives for calculation of multiplicities (m).

4) Read names and number of atoms. Read the number and value of points in sin θ/λ for which values of scattering factors are given. Read values of scattering factor at each of these points for each atom type.

5) Read number of space group tests for theoretical higher moment calculations. For each read in type of higher moment calculation, number and type of atoms in general positions, and special positions with one, two or three fixed positional parameters. For the last type read type of reflections to be analysed separately.

6) Read next reflection, $\underline{h}$, $\underline{k}$, $\underline{l}$ and $\underline{F}^2$. Go to 8 if data ended. Reflections are read with $\underline{l}$ the fastest running index, starting with

its minimum value for particular h and k values. Calculate and store F^2/p, $\sin^2\theta$, m and q (a pointer giving information about type of reflection with respect to atom in a fixed spacial position, if q = 0, then no such spacial position) for accidental absences (with intermediate l values) and observed reflections. Go to 7 if p is known. If symmetry number is not known definitely, store separately. Go to 6.

7) Update totals of number of reflections, the number interpolated, the multiplicity corrected F^2 and sin θ (stored in 20 equal ranges of $\sin^3\theta$). Go to 6.

8) Store end sign. If temperature factor B read, go to 14.

9) Calculate mean value of F^2 for mean value of sin θ for reflections in each of the 20 ranges.

10) Calculate $\sum_{j=1}^{N} f_j^2$ for each of the 20 mean values of sin θ .

This involves interpolation between 'f' values for given $\sin\theta/\lambda$ values. This was achieved by a method recommended by Dr. J. S. Rollett in 'Computing Methods in Crystallography', Page 42.

Given n+1 values of 'f' at points $\sin(\theta_i)$, the value of f at sin θ is given by

$$f(\sin\theta) = \sum_{i=0}^{n} \alpha_i(\sin\theta)\, y(\sin\theta_i)$$

where $\alpha_i(\sin\theta) = \prod_{j\neq i} (x-x_j) / \prod_{j\neq i} (x_i-x_j)$

11) Calculate number of reflections possible in each range, N_o

Calculate $\ln\left[\langle F^2\rangle / \sum_{j=1}^{N} f_j^2\right] = L$

12) Print out for each of 20 $\sin^3\theta$ ranges, $\langle \sin\theta \rangle$, number of reflections interpolated, total number of reflections (N_1), $\langle F^2 \rangle$ and $(N_1/N_o)^2 \equiv W$ and L.

The penultimate figure can be used as a measure of the reliability of any point on the graph.

13) Fit a least squares straight line to the relationship between L and $\langle \sin\theta \rangle^2/\lambda^2 \equiv S$.

Now $L = \ln K - 2Bs$

Observations of L and S will not obey this equation exactly. Thus

$\ln K - 2Bs - L_i = e.$

The best fit will be such that $M = \sum_{i=0}^{20} we^2$ is minimised with respect to B and lnK

Thus at the minimum

$$\frac{dM}{dB} = \sum_{i=0}^{19} -w_i s_i \left[\ln K - 2Bs_i - L_i \right] = 0$$

and $$\frac{dM}{d\ln K} = \sum_{i=0}^{19} w_i \left[\ln K - 2Bs_i - L_i \right] = 0$$

whence

$$\ln K = \frac{\sum_{i=0}^{19} w_i s_i \sum_{i=0}^{19} w_i s_i L_i - \sum_{i=0}^{19} w_i L_i \sum_{i=0}^{19} w_i s_i^2}{\sum_{i=0}^{19} w_i \sum_{i=0}^{19} w_i s_i^2 - \sum_{i=0}^{19} w_i s_i \sum_{i=0}^{19} w_i s_i}$$

$$B = 0.5\,\frac{\sum_{i=0}^{19} w_i L_i \sum_{i=0}^{19} w_i s_i - \sum_{i=0}^{19} w_i s_i L_i \sum_{i=0}^{19} w_i}{\sum_{i=0}^{19} w_i \sum_{i=0}^{19} w_i s_i^2 - \sum_{i=0}^{19} w_i s_i \sum_{i=0}^{19} w_i s_i}$$

The terms $\sum_{i=0}^{19} w_i s_i$, $\sum_{i=0}^{19} w_i$, $\sum_{i=0}^{19} w_i s_i^2$, $\sum_{i=0}^{19} w_i s_i L$, $\sum_{i=0}^{19} w_i L_i$

are accumulated and substituted in the equations above to allow the derivation of K and B.

Print K and B.

14) Calculate $\sum_{i=0}^{N} g_j^2$ for the $(n+1) \sin\theta / \lambda$ points.

$$\sum_{j=1}^{N} g_{j\theta}^2 = \sum_{j=1}^{N} f_{j\theta}^2 \exp\left(-2B \sin^2\theta / \lambda^2\right)$$

Calculate $\sum_{j=1}^{N} g_{j0}^2 / \sum_{j=1}^{N} g_{j\theta}^2 = c_0$ for the $(n+1)$ points.

This is a scattering factor and temperature factor correction.

15) Read $F^2/_p$, b = 1/m, q, and sin θ for reflection of group in which the symmetry factor is known. If end sign, go to 18. Interpolate to find correction factor, c, at sin θ using method in 10. Apply correction. If $q > 0$, go to 17.

16) Add to current totals to $bF/\sqrt{p}$, $bF^2/_p$, $bF^4/_{p^2}$ and $bF^6/_{p^3}$, and count reflection. Go to 15.

17) Accumulate different totals as in 16 for reflections of different 'q'. Go to 15.

18) Calculate mean values $\langle I \rangle$, $\langle I^{\frac{1}{2}} \rangle$, $\langle I^2 \rangle$, $\langle I^3 \rangle$. Store.

Go to 20.

19) Calculate mean values as in (18) for each group reflections.

20) Clear 100 registers.

21) Read I from general store. Go to 26 if end sign. Calculate

$z = \frac{I}{\langle I \rangle}$.

Keep 20 registers kept for accummulating N(z) (for N(z) cumulative plot). These are for z = 0(0.1) 1.9. Add b to each register with z greater than z_{obs}.

22) Keep 30 registers for accumulating number of reflections within $z \pm 0.05$ for values of z increasing by 0.05. This is for P(z) plot. Add 10b to relevant totals.

23) Keep 30 registers for accumulation numbers reflections within $z \pm 0.05$ for values of $\sqrt{z}$ increasing by 0.05. This is for P(F) plot. Add 10b to relevant totals.

24) Keep 20 registers for accumulating N(F) for the cumulative N(F) plot, for values of $\sqrt{z}$ of 0(0.1)1.9. Add 'h' to all registers in z greater than $\sqrt{z}_{obs}$.

25) Add b to general total (T).

Go to 21.

26) Divide the number of reflections for each value of z or z in each of the above procedures by T.

Print values of N(z) at 20 values of z

Print values of P(z) at 30 values of z

Print values of P(F) at 30 valees of $\sqrt{z}$

Print values of N(F) at 20 values of $\sqrt{z}$

27) Print Wilson ratio $\langle\sqrt{I}\rangle^2/\langle I\rangle$

Print $\langle I\rangle$

28) Go to 31 if no theoretical second and third moments required.

29) For higher moment test, calculate $\sum_{j=1}^{N} f_j^2$, $\sum_{j=1}^{N} f_j^4$ and $\sum_{j=1}^{N} f_j^6$ for general and different types of special position, and calculate theoretical $\langle I\rangle$, $\langle I^2\rangle$ and $\langle I^3\rangle$ for each of these. Calculate for separate groups of reflections if special position requires this.

30) Substitute in expressions given on page 48 to give $\langle I\rangle$, $\langle I^2\rangle$ and $\langle I^3\rangle$ for whole structure. Print out observed and theoretical second and third moments for this test.

Go to 29, if another test is required.

31) End if no reflections of unknown symmetry number.

32) Read location of group of reflections of unknown symmetry number.

Go to 34 if end sign.

33) Read I, $\sin^2\theta$ and h. Interpolate to find correction factor, c, and apply this. Accumulate total of h and hI. Go to 33.

34) Calculate $\langle I\rangle = \sum bI/\sum b$.

Print $\langle I\rangle$

Go to 32 if further group of unknown symmetry number.

END.

APPENDIX

1) PROGRAMME TITLE

E calculation.

PURPOSE

To calculate normalised structure factors, E, given by

$$E^2 = F^2/p \sum_{j=1}^{N} f_j^2$$

INTRODUCTION

The strategy of this simple programme is apparent from the flow diagram. The programme was written in C203 autocode for the KDF9 computer.

FLOW DIAGRAM

1) Read scale factor K and overall isotropic vibrational factor, B.

2) Read information defining body or face centres, screw axes, glide planes, mirror and rotors.

3) Read cell dimensions and wavelength of radiation. Calculate R_{ij}'s.

4) Read in number of different types of atom in the unit cell, the number of each type of atom, the values of $\sin\theta/\lambda$ for the scattering factors, and the values of the scattering factors at those points.

5) Calculate $\sum_{j=1}^{N} f^2_j$ for $\sin\theta/\lambda$ points.

6) Multiply $\sum_{j=1}^{N} f^2_j$ by $\exp\left[-B\sin^2\theta/\lambda^2\right]/K$.

7) Go to 11, if data ended.

Read h, k, l, F^2 for the next reflection and calculate sin

8) Interpolate to get correct value of $\sum_{j=1}^{N} f^2_j$ for reflection.

9) Calculate symmetry number, p, for reflection.

10) Calculate E. Print indices and E. Go to 7.

11) End.

2) PROGRAMME

Tangent Formula Refinement.

PURPOSE

To refine phases using the tangent formula

$$\tan \alpha_{\vec{h}} = \frac{\left\langle |E_{\vec{k}}|\ |E_{(\vec{h}-\vec{k})}|\ \sin\left[\alpha_{\vec{k}} + \alpha_{(\vec{h}-\vec{k})}\right]\right\rangle}{\left\langle |E_{\vec{k}}|\ |E_{(\vec{h}-\vec{k})}|\ \cos\left[\alpha_{\vec{k}} + \alpha_{(\vec{h}-\vec{k})}\right]\right\rangle}$$

for orthorhombic space groups.

INTRODUCTION

The programme divides naturally into three parts. The first concerns the storage of the data, the second the Σ_2-listing and the calculation of the right hand side (R.H.S.) and the third, the selection of phase to be used in the subsequent cycle of refinement. The programme has been written in C203 autuocode, modified so that all available store of the KDF9 computer can be used as direct access variables. This modification of C203 autocode was made by O. J. R. Hodder.

The second section is the most time consuming part and has been written in KDF9 User Code. The author is grateful for the useful discussion with O. J. R. Hodder concerning the strategy of this part of the programme. In the third part, the method adopted in a programme developed by M. J. Adams has been closely followed. This programme was designed specifically for insulin which has a hexagonal space group. The storage of data and Σ_2-listing in the latter programme are achieved by a completely different method which offers no possibility of generalisation.

The programme will now be described.

Part I. Storage of data

It is convenient to store the data for the R.H.S. and L.H.S. separately.

For the L.H.S., three words were used for each reflection. The programme input specifies the lowest $E_{\vec{h}}$ value needed for the R.H.S. in any cycle. The reflections with $E_{\vec{h}}$ greater than this value are stored in order of their input. Two words (48 bits each) were used to store the indices, $|E_{\vec{h}}|$ and $\alpha_{\vec{h}}$ for each reflection. A third word was kept clear to store calculated values of $|E_{\vec{h}}|$ and $\alpha_{\vec{h}}$.

For the R.H.S., only $|E_{\vec{h}}| \sin \alpha_{\vec{h}}$ and $|E_{\vec{h}}| \cos \alpha_{\vec{h}}$ need be stored and these are easily packed into one word. The programme calculated the maximum value of $\underline{h}_1$, and the maximum values of $\underline{h}_2$ and $\underline{h}_3$ for each value of $\underline{h}_1$. A function defining storage location of each allowable reflection in terms of its indices for half of reciprocal space is then

computed so that none of the store is wasted, and the values of $|E_{\vec{h}}|\sin\alpha_{\vec{h}}$ and $|E_{\vec{h}}|\cos\alpha_{\vec{h}}$ are stored in the relevant location for all reflections for which $_{h}$ is available. For this, $\alpha_{\underline{h}_1,\bar{\underline{h}}_2,\bar{\underline{h}}_3}$, $\alpha_{\underline{h}_1,\bar{\underline{h}}_2,\underline{h}_3}$ and $\alpha_{\underline{h}_1,\underline{h}_2,\bar{\underline{h}}_3}$ are generated using class tests.

Part II. $\sum_2$-listing and calculation of R.H.S.

As this part is very time consuming, several different methods were investigated.

The storage of R.H.S. for half the reciprocal sphere, of course, involved the storage of interdependent information but the use of this larger storage area is compensated by the greatly increased speed of calculating the R.H.S. Phases of reflections in the other half of reciprocal space are easily derived from $\alpha_{\underline{h}_1\underline{h}_2\underline{h}_3} = -\alpha_{\underline{h}_1\underline{h}_2\underline{h}_3}$.

Two techniques may be used in the $\sum_2$-listing. Both of these are considerably accelerated if the indices of $\vec{h}$, i.e., the reflections stored on the L.H.S. are all positive. The generalisation of the programme to include monoclinic space groups involves the inclusion of conditional jumps which considerably reduce the speed of the programme, and thus separate programmes have been written. This programme concerns orthorhombic space groups.

Both techniques involve the systematic coverage of the reflections stored for the R.H.S. with reflections $\vec{k}$, the calculation of $(\vec{h} - \vec{k})$ and the checking that the reflection with indices $(h - k)$ lies within the area of reciprocal space for which reflections are stored. If $\vec{k}$ is initially set at $\underline{k}_1\max, \underline{k}_2\max, \underline{k}_3\max$, the reciprocal space can be

explored by decreasing $\underline{k}_3$, until $\underline{k}_3$ is again equal to $\underline{k}_{3max}$, and then decrease $\underline{k}_2$ and so on. The first technique would be to have a conditional jump on the value of $\vec{k}$, and a further conditional jump on the value of $(\vec{h} - \vec{k})$. In fact, a second technique which is to calculate the number of values of $\underline{k}_3$ for a fixed set of $\underline{k}_1$ and $\underline{k}_2$ which are inside the area of stored reciprocal space and gives values of $(\vec{h} - \vec{k})$ also obeying this condition is simpler. The number of values for an orthorhombic system is the smallest of $[2\underline{k}_{3max} + 1]$ and $[\underline{k}_{3max} + (\underline{h}_3 - \underline{k}_3)_{max} + 1 - \underline{h}_3]$. A similar calculation is made for the number of values of $\underline{k}_2$. The programme then cycles through the reciprocal space without any conditional jumps on the values of indices. New values of the number of cycles must obviously be calculated for each value of $\underline{k}_1$, the number of values of which are calculated in a similar way.

Obviously only reflections with stored values of $|E|\sin\alpha$ and $|E|\cos\alpha$ can be included in R.H.S. calculation, and the presence of a value must always be tested.

Finally, the above survey includes pairs of values of $\vec{k}$ and $(\vec{h} - \vec{k})$ which are the same. The nomenclature of $\vec{k}$ and $(\vec{h} - \vec{k})$, of course, can be reversed, so that only half the values of $\vec{k}$ need be investigated.

When a pair has been identified, the values of $|E|\sin\alpha$ and $|E|\cos\alpha$ for reflections $\vec{k}$ and $(\vec{h} - \vec{k})$ are added to totals of

$$|E_{\vec{k}}|\sin\alpha_{\vec{k}}|E_{(\vec{h}-\vec{k})}|\cos\alpha_{(\vec{h}-\vec{k})} + |E_{\vec{k}}|\cos\alpha_{\vec{k}}|E_{(\vec{h}-\vec{k})}|\sin\alpha_{(\vec{h}-\vec{k})} \text{ and}$$

$$|E_{\vec{k}}|\cos\alpha_{\vec{k}}|E_{(\vec{h}-\vec{k})}|\cos\alpha_{(\vec{h}-\vec{k})} - |E_{\vec{k}}|\sin\alpha_{\vec{k}}|E_{(\vec{h}-\vec{k})}|\sin\alpha_{(\vec{h}-\vec{k})}$$

Part III. Calculation of phase to be used in next cycle

When all the possible relationships in the Σ_2-listing have been investigated, the calculated value of $\alpha_{\vec{h}}$ and also of $|E_{\vec{h}}| = \left[\cos^2 \alpha_{\vec{h}} + \sin^2 \alpha_{\vec{h}}\right]^{\frac{1}{2}}$ are stored in the third word kept available for each reflection included in the L.H.S.

This is repeated for all reflections of the L.H.S., and sums of E_{obs} and E_{calc} are calculated. From these a scale for E_{calc} is computed at the end of a cycle of tangent formula refinement, and the E_{calc} values are rescaled. The values of E_{calc} and α_{calc} are then systematically examined. If E_{calc} is less than 0.4, the original value of α_h is used in the subsequent cycle. If the phase shift is greater than 120° but E_{calc} is less than one, the original value is used for the phase. If the phase shift is less than 120° and the value of E_{calc} is greater than 0.4, the value of the phase used in the subsequent cycle of refinement is a weighted mean computed from:-

$$= \frac{E_{calc}\,\alpha_{calc} + \alpha}{E_{calc} + 1}$$

An R-value is computed for the cycle from

$$\Sigma(E - E_{calc})/\Sigma E$$

In following cycles the minimum value of the normalised structure factor for the L.H.S. may be altered.

Flow chart for tangent formula refinement programme

1) Read cell dimensions and wavelength of radiation used.

2) Go to 3 if no maximum indices $[\underline{h}_1, \underline{h}_2, \underline{h}_3]$ for each reciprocal lattice layer given. Read $\underline{h}_{1max}$, and $\underline{h}_{2max}$, $\underline{h}_{3max}$ for allowed value of $\underline{h}_1$. Go to 4.

3) Read maximum sin θ value for data. Calculated maximum values of $\underline{k}$ and $\underline{l}$ allowed for each allowed value of $\underline{h}$.

4) Read number of cycles of tangent formula refinement, n, and the minimum value of E to be included on left-hand side in each cycle.

5) Read in class tests and the relationship of $\alpha_{\underline{h}_1\bar{\underline{h}}_2\bar{\underline{h}}_3}$, $\alpha_{\bar{\underline{h}}_1\underline{h}_2\underline{h}_3}$, and $\alpha_{\underline{h}_1\underline{h}_2\bar{\underline{h}}_3}$, the phases of the equivalent reflections for $\alpha_{\underline{h}_1\underline{h}_2\underline{h}_3}$ for each class test.

6) Read in data (a) $\underline{h}_1,\underline{h}_2,\underline{h}_3$, $E_{h_1h_2h_3}$ and phase $\alpha_{h_1h_2h_3}$ where phase is known (b) $\underline{h}_1,\underline{h}_2,\underline{h}_3$, $E_{h_1h_2h_3}$ where phases is not known.

7) Calculate area of store needed, one word (48 bits) for each $\vec{\underline{h}}$ for half of the reciprocal space lying within the maximum allowed indices. Calculate expression relating storage location for reflection, $\underline{h}_1,\underline{h}_2,\underline{h}_3$ with the values of $\underline{h}_1$, $\underline{h}_2$ and $\underline{h}_3$.

8) Go to 10 at end of data.

For next reflection, $\underline{h}_1,\underline{h}_2,\underline{h}_3$, check that indices are within maxima. Generate $\underline{h}_1$, $\underline{h}_2$, $\underline{h}_3$; $\underline{h}_1$, $\underline{h}_2$, $\underline{h}_3$; $\underline{h}_1$, $\underline{h}_2$, $\underline{h}_3$ with requisite phases using class tests. Calculate $E_{\underline{h}_2,\underline{h}_2,\underline{h}_3}\cos(\alpha_{\underline{h}_1,\underline{h}_2,\underline{h}_3})$ and $E_{\underline{h}_1,\underline{h}_2,\underline{h}_3}\sin(\alpha_{\underline{h}_1,\underline{h}_2,\underline{h}_3})$ for each of the four equivalent reflections. Pack the cosine and sine terms together for each reflection, and store in the appropriate location.

9) For reflection $\vec{\underline{h}}$, go to 8 if $E_{\vec{h}}$ is less than E_{min} for L.H.S. in any cycle.

Store $\underline{h}$, $E_{\vec{h}}$ and $\alpha_{\vec{h}}$.

10) Set E_{min} for current cycle.

11) Read from store the value of next $\vec{\underline{h}}$, $E_{\vec{h}}$ and $\alpha_{\vec{h}}$ for L.H.S.

Go to 11 if $E_{\vec{h}} < E_{min}$ for current cycle.

For $\vec{k}$, set $\underline{k}_1$ as $\underline{k}_{1max}$, the maximum value of the first index.

12) Go to 22, $(\underline{h} - \underline{k})_1 > \underline{k}_1$.

Fetch $\underline{k}_{2max}$ and $\underline{k}_{3max}$. Set $\underline{k}_2$ and $\underline{k}_3$ equal to these.

Calculate $(\underline{h} - \underline{k})_1$.

Fetch $(\underline{h} - \underline{k})_{2max}$.

Calculate $\left[(\underline{h} - \underline{k})_{2max} + \underline{k}_{2max} + 1 - \underline{k}_2\right]$

and $\left[2\underline{k}_{2max} + 1.\right]$

Put n_2 equal to the minimum of these.

Fetch $(\underline{h} - \underline{k})_{3max}$.

Calculate $\left[(\underline{h} - \underline{k})_{3max} + \underline{k}_{3max} + 1 - \underline{k}_3\right]$

and $\left[2\underline{k}_{3max} + 1.\right]$

Put $\underline{n}_3$ and $\underline{n}_1$ equal to the minimum of these.

Go to 18 if $(\underline{h} - \underline{k})_1 = \underline{k}_1$.

13) Calculate $(\underline{h} - \underline{k})_2$.

14) Read $\left|E_{\vec{k}}\right| \cos \alpha_{\vec{k}}$ and $\left|E_{\vec{k}}\right| \sin \alpha_{\vec{k}}$.

If no value stored go to 15.

Calculate $(\underline{h} - \underline{k})_3$.

Read $\left|E_{(\vec{h} - \vec{k})}\right| \cos \alpha_{(\vec{h} - \vec{k})}$ and $\left|E_{(\vec{h} - \vec{k})}\right| \sin \alpha_{(\vec{h} - \vec{k})}$.

If $(\underline{h} - \underline{k})_1$ is negative read values for Friedel pair.

If no value stored go to 15.

Update relevant totals for R.H.S. If $(\underline{h} - \underline{k})_1$ is negative include contributions relevant to $-\alpha_{(\vec{h} - \vec{k})}$

15) Decrease $\underline{n}_3$ by 1, go to 16 if $\underline{n}_3 = 0$

Decrease k_3 by 1, go to 14

16) Put $\underline{k}_3 = \underline{k}_{3max}$, set $\underline{n}_3 = \underline{n}_1$.

Decrease $\underline{n}_2$ by 1, go to 17 if $\underline{n}_2 = 0$.

Decrease $\underline{k}_2$ by 1, go to 13.

17) Decrease $\underline{k}_1$ by 1, go to 12.

18) Calculate $(\underline{h} - \underline{k})_2$.

Go to 22, $(\underline{h} - \underline{k})_2 > \underline{k}_2$.

19) Read $|E_{\vec{k}}| \cos \alpha_{\vec{k}}$ and $|E_{\vec{k}}| \sin \alpha_{\vec{k}}$.

If no value is stored, to to 20.

Calculate $(\underline{h} - \underline{k})_3$.

If $(\underline{h} - \underline{k})_2 = \underline{k}_2$, and $(\underline{h} - \underline{k})_3$ $\underline{k}_3$, go to 22.

Read $E_{(\underline{h} - \underline{k})} \cos \alpha_{(\underline{h} - \underline{k})}$ and $E_{(\underline{h} - \underline{k})} \sin \alpha_{(\underline{h} - \underline{k})}$

If no value is stored go to 20.

Update relevant totals for R.H.S.

20) Decrease $\underline{n}_3$ by 1, go to 21 if $\underline{n}_3 = 0$.

Decrease $\underline{k}_3$ by 1, go to 19.

21) Set $\underline{k}_3 = \underline{k}_{3max}$, set $\underline{n}_3 = \underline{n}_1$.

Decrease $\underline{k}_2$ by 1, go to 18.

22) Go to 23 if [denominator (A) + numerator (B)] > 0.01.

Put E_{calc} and α_{calc} equal to zero.

Go to 24.

23) Calculate $\alpha_{hkl} = \tan^{-1} B/A$.

Calculate $\left[A^2 + B^2\right]^{\frac{1}{2}} = |E_{calc}|$

24) Update relevant totals for $|E_{calc}|$ and $|E_{obs}|$

Print indices of reflections, $|E_{obs}|$, α_{obs} and α_{calc}.

Print shift or phase and $|E_{calc}|$

Print shift of phase and E_{calc}.

Store α_{calc} and E_{calc}.

Go to 11 if data for L.H.S. not ended.

Calculate scale for E_{calc} from the sums of E_{calc} and E_{obs}.

Print scale.

Rescale all values of E_{calc}.

25) Go to 28 if data ended.

Read next reflection for L.H.S. from store.

Update totals for $[E - E_{calc}]$ and E.

Go to 25, if $E_{calc} < 0.4$.

Go to 27, if $[\alpha - \alpha_{calc}] > 120$.

Put $= \dfrac{E_{calc}\,\alpha_{calc} + \alpha}{E_{calc} + 1}$

26) Store new values for L.H.S.

Modify R.H.S.

Go to 25.

27) If $E_{calc} < 1$, go to 25.

Set $\alpha = \alpha_{calc}$.

Go to 26.

28) Print $\Sigma(E - E_{calc})/\Sigma E$.

If correct number of cycles have not been completed, go to 10.

Print tape for all reflections $\underline{h}_1$, $\underline{h}_2$, $\underline{h}_3$, E and α if known.

End.

REFERENCES

1) C. M. Harris and R. S. Nyholm, J. Chem. Soc., 1956, 4375.

2) J. A. Brewster, C. A. Savage and L. M. Venanzi, J. Chem. Soc., 1962, 1548.

3) G. A. Mair, H. M. Powell and L. M. Venanzi, Proc. Chem. Soc., 1961, 170.

4) E. L. Muetterties and R. A. Schunn, Quart. Rev., 1966, XX, 245.

5) L. Pauling, "The Nature of the Chemical Bond", Cornell University Press, 1939.

6) R. Daudel and A. Bucher, J. Chem. Phys., 1945, 42, 6.

7) J. W. Linnett and C. E. Mellish, Trans. Far. Soc., 1954, 50, 665.

8) R. J. Gillespie, J. Chem. Soc., 1963, 4679.

9) F. Basolo and R. G. Pearson, "Mechanisms of Inorganic Reactions", J. Wiley and Son, 1958.

10) J. Donohue and A. Caron, Acta Cryst., 1964, 17, 663.

11) F. A. Cotton, T. G. Dunne, and J. S. Wood, Inorg. Chem., 1956, 4, 318.

12) R. D. Cramer, R. V. Lindsey, C. T. Prewitt and V. G. Stolberg, J. Amer. Chem. Soc., 1965, 87, 658.

13) J. B. Wilford, Private Communication.

14) T. L. Blundell, Part II Thesis, Oxford 1965.
B. T. Kilbourn, T. L. Blundell and H. M. Powell, Chem. Comm., 1965, 444.

15) A. S. Kasenally, J. Chem. Soc., 1965, 5343.

16) G. J. Ballhausen and C. Klixbull Jørgensen, Kgl. Danske Videnskab. Selskab Mat. Fys. Medd., 1954, 29 (No. 14).

17) G. A. Mair, H. M. Powell and D. E. Henn, Proc. Chem. Soc., 1960, 415.

18) J. W. Collier, F. G. Mann, D. G. Watson and H. R. Watson, J. Chem. Soc., 1964, 1803.

19) N. A. Bailey, J. M. Jenkins, R. Mason and B. L. Shaw, Chem. Comm., 1965, 237.

20) A. T. Phillip, Private Communication.

21) C. M. Harris, R. S. Nyholm and D. J. Phillips, J. Chem. Soc., 1960, 4379.

22) P. R. H. Aldeman, P. G. Owston and J. M. Rowe, J. Chem. Soc., 1962, 668.

23) A. Pignedoli and G. Peyronel, Gazzetta, 1962, 92, 745.

24) L. Sacconi, P. Nannelli, N. Nardi and U. Campigli, Inorg. Chem., 1965, 4, 943.

25) L. M. Venanzi, J. Chem. Soc. (A), 1967, 540.

26) P. J. Wheatley, J. Chem. Soc., 1964, 3718.

27) P. J. Wheatley, J. Chem. Soc., 1964, 2206.

28) T. N. Polynova and M. A. Porai-Koshits, J. Struct. Chem., 1961, 2, 445.

29) T. N. Polynova and M. A. Porai-Koshits, J. Struct. Chem., 1960, 1, 146.

30) I. R. Beattie and P. A. Gockling, J. Chem. Soc., 1965, 3860.

31) M. J. Buerger, "X-ray Crystallography", J. Wiley & Son, 1962.

32) "International Tables for X-ray Crystallography", Vol. II, (Kynoch Press, Birmingham, 1959).

33) B. T. Kilbourn, "D. Phil Thesis", Oxford, 1965.

34) E. N. Maslen, Private Communication.

35) W. R. Busing and H. A. Levy, Acta Cryst., 1957, 10, 180.

36) R. H. B. Mais, "D. Phil Thesis", Oxford, 1964.

37) A. F. Wells, "Structural Inorganic Chemistry", Clarendon Press, Oxford, 1962.

38) J. S. Rollett, W. C. Hamilton and R. A. S. Sparks, Acta Cryst., 1965, 18, 129.

39) A. J. C. Wilson, Nature, 1942, 150, 152.

40) D. Rogers, Private Communication.

41) A. J. C. Wilson, Acta Cryst., 1949, 2, 318.

42) A. J. C. Wilson, Acta Cryst., 1950, 3, 258.

43) R. Strinivasen, Acta Cryst., 1960, 13, 388.

44) D. C. Phillips, D. Rogers and A. J. C. Wilson, Acta Cryst., 1950, 3, 398.

45) F. Foster and A. Hargreaves, Acta Cryst., 1963, 16, 1124.

46) M. J. Buerger, "Vector Space", J. Wiley and Son.

47) H. Lipson and W. Cochran , "The Determination of Crystal Structures", G. Bell and Sons Ltd., London, 1966.

48) G. Sim, Acta Cryst., 1958, 11, 123.

49) G. Sim, Acta Cryst., 1959, 12, 813.

50) Y. Okaya, Y. Saito and R. Pepinsky, Phys. Rev., 1955, 98, 1857.

51) R. Pepinsky and Y. Okaya, Proc. Nat. Acad. Sci. U.S., 1956, 42, 286.

52) W. N. Lipscomb, J. Chem. Phys., 26, 713.

53) G. N. Ramachandran and S. Raman, Acta Cryst., 12, 957; S. Raman, Acta Cryst., 12, 964.

54) G. N. Ramachandran and S. Raman, Curr. Sci., 1956, 25, 348.

55) A. F. Peerdeman and J. M. Bijvoet, Acta Cryst., 9, 1012.

56) J. W. Moncrief and W. N. Lipscomb, Acta Cryst., 1966, 21, 322

57) J. Karle and H. Hauptman, Acta Cryst., 9, 635.

58) J. Karle and H. Hauptman, Acta Cryst., 11, 264.

59) G. A. Mair, Seventh International Congress, I.U.C., 1966, 10, 25.

60) R. Strinivasen, Acta Cryst., 14, 1163.

61) E. N. Maslen, Acta Cryst., 1963, 16, 703.

62) F. R. Ahmed and D. W. J. Cruickshank, Acta Cryst., 1953, 6, 385.

63) S. F. Darlow, Acta Cryst., 1960, 13, 683.

64) W. R. Busing and H. A. Levy, Acta Cryst., 1964, 17, 142.

65) G. J. Arai, J. Rec. Trav. Chim., 1962, 81, 307.

66) R. E. Rundle, J. Amer. Chem. Soc., 1954, 76, 3101.

67) G. G. Sumner, H. P. Klug and L. E. Alexander, Acta Cryst., 1964, 17, 722.

68) N. A. Bailey, M. R. Churchill, R. Hunt, R. Mason and G. Wilkinson, Proc. Chem. Soc., 1964, 401.

69) O. S. Mills and G. Robinson, Proc. Chem. Soc., 1964, 187.

70) W. G. Sly, J. Amer. Chem. Soc., 1959, 81, 18.

71) L. F. Dahl et al., J. Chem. Phys., 1957, 26, 1750.

72) K. Manan, D. Phil Thesis, Oxford, 1965.

73) M. J. Bennett and R. Mason, Nature, 1965, 205, 761.

74) J. A. Ibers, Ast. Amer. Cryst. Assoc., 1965, B10.

75) M. Ciampolini, Inorg. Chem., 1966, 5, 35.

76) T. L. Blundell and H. M. Powell, Autumn Meeting of the Chemical Society, 1966.

77) T. L. Blundell, H. M. Powell and L. M. Venanzi, Chem. Comm., 1967, 763.

78) J. A. Bertrand and D. L. Plymale, Inorg. Chem., 1966, 5, 879.

79) G. Dyer and L. M. Venanzi, J. Chem. Soc., 1965, 2771.

80) D. L. Stevenson and L. F. Dahl, J. Amer. Chem. Soc., 89, 3424.

81) E. G. Cox, A. J. Shorter and W. Wardlow, J. Chem. Soc., 1938, 1886.

82) H. M. Powell and D. M. Crowfoot, Z. Krist., 1934, 87, 370.

83) G. H. W. Milburn and M. R. Truter, J. Chem. Soc., 1967, 648.

84) D. Grdenic, Quart. Rev., 1965, XIX, 303.

85) T. L. Blundell and H. M. Powell, Chem. Comm., 1967, 54.

86) M. J. Norgett, J. H. M. Thornley and L. M. Venanzi, J. Chem. Soc., 1967, 540.

87) J. S. Rollett, "Computing Methods in Crystallography", 1965, Pergamon Press, Oxford.